Organisation subcellulaire et remobilisation métabolique durant la sénescence chez le colza : effets des stress abiotiques

C. Sorin

THÈSE / UNIVERSITÉ DE RENNES 1
sous le sceau de l'Université Européenne de Bretagne

pour le grade de

DOCTEUR DE L'UNIVERSITÉ DE RENNES 1

Mention : Biologie

Ecole doctorale Vie-Agro-Santé

présentée par

Clément Sorin

Préparée aux unités de recherche :
TERE-Technologie des équipements agroalimentaires, Irstea
IGEPP-Institut de Génétique, Environnement, et Protection des Plantes, INRA, Université de rennes 1, Agrocampus Ouest.

Subcellular modification and nutrient remobilization during *Brassica napus* leaf senescence: effects of abiotic stresses.

Thèse soutenue à Rennes le 10/12/2014

devant le jury composé de :

Henk Van As
Professor Université de Wageningen / r*apporteur*
Thierry SIMONNEAU
Directeur de recherches INRA / *rapporteur*
Olivier LEPRINCE
Professeur Agrocampus Ouest / e*xaminateur*
François GASTAL
Directeur de recherches INRA / *examinateur*
François MARIETTE
Directeur de recherches Irstea / directeur de thése
Alain BOUCHEREAU
Professeur Université de Rennes 1 / directeur de thése
Laurent LEPORT
Maitre de conférence Université de Rennes 1/ invité
Maja MUSSE
Chargé de recherches / *invitée*

Remerciements

Je souhaite tout d'abord remercier mes encadrants Maja et Laurent ainsi que mes directeurs Alain et François pour leur soutient tout au long de cette thèse. Merci à Maja et Laurent pour le temps et l'attention qu'ils m'ont consacrés (même le mercredi). Merci à Alain et François d'avoir su trouver dans leur emploi du temps surchargés le temps pour moi lorsque j'en avais besoin. Dans le contexte particulier de cette thèse (deux équipes, RMN que je ne connaissais pas…) la très bonne entente de l'équipe encadrante et sa disponibilité a été essentielle.

Je remercie toute l'équipe RCA pour son accueil et son soutien. Merci à Francoise (Leprince) et Anne-Marie pour l'aide apportée dans les broyages et les dosages et merci aux autres (Laurie, Solène, Sophie…) qui maintenaient une bonne ambiance dans le labo durant ces manips. Merci aussi à Carole, Françoise (Le Caherec), et Marie-Françoise pour les discussions qui m'ont aidées pour la rédaction des articles et surtout pour leur aide avant et pendant le congrès de Versailles.
Je remercie toute l'équipe de serristes de l'IGEPP pour leur aide et les très nombreux colzas (presque 200) qu'ils ont cultivés pour mes expériences. Merci à Laurent pour sa patience avec mes fiches de vœux. Je remercie en particulier Patrick pour sa bonne humeur et l'aide apportée sur plusieurs expérimentations (mesures SPAD, PSII, suivi plantes, Phytotron…)
Merci à tous ceux que j'ai croisé en pause-café ou dans les couloirs et qui participent à la bonne ambiance générale.

Je remercie toute l'équipe IRM-food en commençant par Melodica pour toute l'aide apportée en début de thèse quand je découvrais le labo et la RMN. Merci à Dominique et Mireille de d'avoir toujours été présents dès qu'un problème se présentait dans mes manips(ou mes traitements) et ce même lorsque j'étais moi-même le problème. Je remercie aussi Corinne qui a participé à mes comités de thèse, Sylvain qui m'a aidé pour les traitements d'images, Amina pour son efficacité, Julie qui m'a supporté, Brigitte qui m'a ouvert lorsque j'oubliais mon badge (souvent donc), Marie-Christine et Asma pour leur aide administrative, à Michel pour sa capacité à créer des outils sur demande… Merci à tous, même ceux avec qui je n'ai pas travaillé directement (Stephane, Guylaine, Tiphaine, Yves, David, Armel..) pour votre soutien et votre camaraderie.
Merci aussi à toutes les personnes de l'unité GERE et d'ACTA avec qui j'ai sympathisé pendant les pause ou les activités (Julie, Patricia, Christine, Eric…)

Merci à toutes les personnes de plateformes extérieures qui ont participés à ce travail, et en premier lieu Brigitte BOUCHET et Camille ALVARADO de la plateforme BIBS. Merci à Muriel Escadillas du CRMPO et Gael BOURBOUZE du CRT. Merci à Pierre-Antoine Eliat pour son aide lors des essais IRM sur feuille.
Merci aussi à l'administration de l'université et de VAS pour leur aide tout au long de cette thèse, ainsi qu'à Françoise HENNION pour avoir été ma tutrice.

Merci bien entendu à tous les doctorants, postdocs ou assimilés (Lucas) pour leur amitié dans et en dehors du labo. Merci à tous les doctorants du bureau du fond, ceux qui sont partis : Benjamin et Carole et ceux qui sont restés : Berline, Pascal, Séverine, Anne-Sophie et Alexandre. Merci à tous pour les conversations, pas toujours scientifiques, les fous rire et les nombreuses plantes qui égayaient

le bureau. Merci aussi à celles et ceux qui n'avaient pas la chance d'être dans notre bureau (Aurore, Clément, Maxime…)
De même je souhaite remercier les doctorants partis trop tôt de l'Irstea : Souad, Cécile, Delphine et Yannick. Grace à la soutenance Cecile j'ai appris beaucoup sur les pates feuilletées et grâce à celle de Delphine énormément sur les bulles dans le fromage et en dépit de leurs sujets d'étude je suis content de les avoir rencontrés. Yannick, tes grognements contre windows, la qualité et le capitalisme manquent dans le bureau, tes affiches de Dave beaucoup moins.
Merci à tous les autres avec qui j'ai joué au basket presque régulièrement, Sam, Lucas, Diemer, Julien, Anthony, Jordan, Etienne, Cyril, Lionel, Nicolas, Guillaume et Ruzica. Et à ceux avec qui j'ai bu des coups régulièrement, presque les mêmes auxquels s'ajoutent Faustine et Axelle.
Un grand merci à tous les stagiaires qui ont participés directement (Noémie) ou non (Jocelyn, Jeanne, Solène, David…) à cette thèse.

Je souhaite aussi profiter de ces remerciements pour rendre hommage à Papi Jean qui aurait été très fier de me voir devenir docteur. Un grand merci à papi et mamie Joseph dont les repas et conversations à Sion-le- mines m'ont souvent rechargé les batteries. Merci à mes parents et à mes sœurs de m'avoir soutenu et encouragé. Merci en plus à Marine et Fabrice de m'avoir hébergé au début de ma thèse.

Merci à mes amis qui m'ont soutenu qu'ils soient en thèse (Marco, Pascal, Faustine, Laure…) ou non (Jé, Flo…) Je souhaite finir ces remerciement par mes amis proches, qui bien que souvent loin et très peu au courant du déroulement de ma thèse m'ont permis de me changer les idées, merci à JF, Chloé, Chouk, Denis, Sarah, Yo, Camille et Kevin. Un merci particulier à Delphine qui n'hésite pas à venir de Londres à ma soutenance.

Abreviation list

ABA: ABscissic Acid

ACC: AminoCyclopropaneCarboxylate

ACBP3: Acyetyl Coenzyme A Binding Protein

APOD: Ascorbate PerOxyDase

ARR2: Arabidopsis Response Regulator

AS: Asparagine Synthétase

CAT: CATalase

CHL: CHLorophyllase

CND41: Chloroplast Nucleotid DNA-binding protein

CPMG: Carr Purcell Meiboom Gill

DGAT1: DiacaylGlycerol AcylTransferase

EIN: Ethylene INsensitive

ETR: Ethylene Resistant

FID: Free Induction Decay

GDH: Glutamate DesHydrogénase

GS: Glutamine synthase

HR: Hypersensitive Reaction

IDL: Individually Darkened Leaves

MEM: Maximum Entropy Method

MST: MonoSaccharid Transporter

NAE: Nitrogen Assimilation Efficiency

NCC: Non fluorescent Chlorophyll Catabolite

NiR: Nitrate Reductase

NUE: Nitrogen Use Efficiency

NUpE : Nitrogen Uptake Efficiency

NUtE : Nitrogen Utilization Efficiency

OLD: Onset of leaf Death

PAO : PolyAmine Oxydase

PCD : Programmed Cell Death

PSII : Photosystem II

WSCP: Water Soluble Chlorophylle binding Protein

RCB: RuBisCO Containing Bodies

RCC: Red Chlorophylle Catabolite

RMN: Resonance Magnetique Nucléaire

ROS: Reactive Oxygen Species

RuBisCO: Ribulose 1, 5 Bisphosphate Carboxylase Oxygenase

SAG: Senescence Associated Gene

SGR: Stay GReen

SOD: SuperOxyde Dismutase

SUT : SUcrose Transporter

TAG : TriAcylGlycerol

TABLE OF CONTENT

INTRODUCTION

INTRODUCTION

Brassica napus (oilseed rape) represents a major renewable resource for food (edible oil, proteins for animals) and non-food uses (green energy, lubricant…). That crop is the third main oil crop worldwide (58.5 Mt in 2011) and the first in Europe and France (19Mt and 5,2Mt respectively) (www.fao.org) Over the last 30 years, that production has increased 5-fold overall world (10-fold in Europe). The world oilseed production will be faced to an increasing demand in the next thirty years catapulted by a combination of factors, including an increasing demand due to higher consumption for edible oils in emerging countries (China and India), the development of the biofuels industry and also increasing needs for green chemistry. That crop plays thus a major role in French economy; more oilseed rape is also a major source of income for the breeding and seed production sectors (France is the second seed exporter in the world) (www.fao.org). In a context of limited to no increasing cultivated surfaces, a significant increase in yield for oilseed rape is essential to fulfill the above-mentioned requirements for the production of vegetable oils.

Oilseed rape production has a fundamental dependence on inorganic N that is one of the most expensive nutrients; indeed N fertilization is the main expense for farmers and represents 1/2 of the energetic cost at the production level (Singh, 2005). More, the culture is a serious concern regarding N loss in the field, giving rise to soil and water pollution by nitrate leaching, as well as air pollution by greenhouse gas emissions. The greenhouse gas emissions for French oilseed rape crop production have reached around 3.2 Mt eq. CO_2 and nitrate content of ground water is still high (> 50 mg/L) in many areas of intensive agricultural production where oilseed rape is cultivated (Cetiom).

Nitrogen use efficiency (NUE) is defined as the grain yield obtained per unit of available N for the crop, including soil N from mineralization and N applied from fertilization. NUE is the product of two components: nitrogen uptake efficiency (NUpE), the proportion of available soil N that is absorbed by the crop, and nitrogen utilization efficiency (NUtE), the grain (or oil) yield obtained per unit of N absorbed by the crop. To improve sustainable oilseed production through limiting N fertilizer input, it is therefore necessary to grow oilseed rape genotype with higher NUE that can remove the nutrient applied to soil efficiently (higher NUpE), and further assimilate, recycle and store nutrients to produce high quantities of high quality seeds (higher NUtE).

Although with a high NUpE, NUE in modern grown oilseed rape varieties is quite low, around 15 kg seed/kg fertilizer N, compared to other crops (e.g. more than 35 kg/kg for wheat, and more that 40 kg/kg for barley) (Singh, 2005). Increasing NUE of the oilseed rape varieties could allow achieving either current yields with lower N input or higher yields with current N supply, both of which will reduce the cost and the environmental impacts (soil, water and air pollution) of this crop. Most

of the research concerning the NUE-related traits at the plant or crop levels, has been done on cereals (wheat, maize, barley) while little work has been performed on oilseed rape(Diepenbrock, 2000). Therefore, the RAPSODYN project (funded by the French National Research Agency (ANR); program "Investments for the Future"), assembling several public and private partners, ambitions to insure long-term competitiveness of the oilseed rape production through improvement of the oil yield and reduction of nitrogen inputs during the crop cycle. A part of this project is the study of NUtE with special attention on NRE (N remobilization efficiency) during leaf senescence in order to fully understand all processes involved in the remobilization of nutrients (especially N) from senescing tissue to growing organs. Indeed, low NRE of oilseed rape is a major cause of low NUE, and the aim of the present study is to contribute to a better understanding of cellular and molecular processes operating in leaf tissues during senescence progression to deliver putative targets for breeding. Senescence is a highly regulated process implying numerous genes, hormones and enzymes (Lim et al., 2007), and all these aspects have been more or less described in model plant species. Although more and more molecular candidates are being highlighted, leaf tissue and sub-cellular organization changes operating during senescence is still poorly understood as a major nutrient resource for C and N recycling. Leaf structure has been commonly studied through microscopy (Wuyts et al., 2012). However, the recent progress in the use and the interpretation of NMR relaxometry signal demonstrated the potentialities of that method for accessing water repartition at the cell level. This should give us precious information on leaf structure; as structure is modified with development the NMR signal can be a reliable marker of leaf developmental state. The NRE being a character hardly quantifiable such indicator would be very useful for breeding. The present study focuses on leaf structure modifications provoked by remobilization processes during senescence; despites the known consequences of remobilization (plasts disappearance for example) the structural impact of senescence has yet not been described and the link between structure and remobilization is unknown.

The present manuscript relates the main results obtained in this thesis carried out as part of acollaboration between two scientific groups (UR TERE; IRSTEA and UMR IGEPP, INRA-Agrocampus Ouest-Université de Rennes 1). It was funded by the Brittany region for the salary and partly on operating funds from RAPSODYN program. The first part (in French) describes the state of art about the biochemical and genetic knowledge on leaf senescence. As that process is highly regulated numerous studies focus on phytohormones and genes regulation, and because it implies remobilization of cell constituents, several degrading and export processes have been described. The work has been focused on abiotic stresses impact on leaf structure, so these aspects have also been detailed. Indeed, the important role of nitrogen in oilseed rape crop and its impact on leaf senescence in *Brassica napus* is also reviewed. Because it's a major stress worldwide, impact of water stress on leaf senescence is also described. The last part focuses on the knowledge acquired on leaf structure and described precisely the work already done on plant product through NMR.

A material and method section assembled all the technical procedure used during this study.

The first chapter presents the structural impact of natural senescence on leaf structure. A related publication entitled "*Structural changes in senescing oilseed rape leaves at tissue and subcellular levels monitored by Nuclear Magnetic Resonance relaxometry through water status*" published in Plant Physiology is inserted. That paper highlights the leaf hydration accompanying leaf senescence and describes precisely the modifications of the leaf structure through the analysis of the NMR relaxometry signal. The chapter also includes a second publication entitled: "*Assessment of nutrient remobilization through structural changes of palisade and spongy parenchyma in oilseed rape leaves during senescence*" published in Planta that completes the description of leaf structure modifications during senescence. This kinetic work goes further in the study of senescence, than the leaf rank comparison of the first paper, confirming the pattern of evolution of NMR signal during leaf senescence. The study also highlights the accuracy of NMR relaxometry signal to determinate the leaf physiological and developmental age.

The second chapter focuses on the impact of abiotic stresses on the structure of leaves from plants grown under field-like conditions in relation with the NRE. The Nitrogen deficiency is studied in the publication entitled "*Nitrogen deficiency impacts cell and tissue leaf structure with consequences on senescence and nutrient remobilization efficiency in Brassica napus"* submitted to the journal Plant Science. The study describes the leaf structure modifications during senescence on two oilseed rape genotypes chosen for their different tolerance to N-stress and grown under optimal and N-stress conditions. This gives us new information about the link between NRE and leaf structure. The last part of this chapter presents unpublished work centering on the impact of water stress on the leaf modifications occurring during senescence. The aim was to describe and understand tissue and cellular structure modifications impacting leaf during senescence of plants submitted to water stress.

These two chapters are integrated into a general discussion that takes stock of the work done at the critical elements found in the literature. The main elements of conclusions and the prospects for this work come close this document.

ETAT DE L‘ART

Introduction

La sénescence foliaire est un processus le plus souvent associé au vieillissement de la feuille et dont l'un des effets les plus spectaculaires est la dégradation des pigments chlorophylliens (Hoertensteiner, 2006). Ce processus est notamment à l'origine de l'apparition des couleurs variées des feuilles en automne chez les espèces pérennes. Il s'agit d'un phénomène développemental strictement ordonné, contrôlé et obligatoire, initié par divers facteurs internes, comme l'âge de la feuille, la balance nutritionnelle ou hormonale, ou des facteurs environnementaux (Lim et al., 2007). Au moment du vieillissement des tissus foliaires, la feuille mature non sénescente est une feuille source assurant la remobilisation des photosynthétats vers les organes puits (organes en croissance ou de stockage). Dans la feuille en sénescence, le maintien du statut d'organe source dans des tissus qui perdent peu à peu leur capacité d'autotrophie, est alors assuré par la dégradation et la remobilisation de nutriments à partir des composants structuraux. L'étape ultime de la sénescence est la mort de la feuille. Nooden *et al.* (1997) ont décrit la sénescence foliaire en trois étapes principales, une étape d'initiation, une étape associée à la dégradation et la remobilisation des composants cellulaires et une étape finale correspondant à la mort cellulaire.

L'objet principal de l'étude est le tissu foliaire. Quelques éléments d'organisation structurale de ces tissus seront décrits en premier de manière à pouvoir cerner plus précisément, à l'échelle du mésophylle, comment la sénescence est initiée et évolue. A ce jour, il n'a pas été décrit de progression différenciée du processus de sénescence au sein des différents parenchymes, alors que ces tissus ont des vocations physiologiques propres dans la feuille.

La phase d'initiation de la sénescence est caractérisée par les changements d'expression de nombreux gènes (BuchananWollaston, 1997). Elle peut être influencée par des facteurs de l'environnement mais aussi par des facteurs internes. Dans la présentation des mécanismes du processus de sénescence foliaire, le rôle des différentes hormones impliquées dans l'initiation ainsi que les modifications d'expression des gènes associées sont décrits ici (Quirino et al., 2000; Buchanan-Wollaston et al., 2003; Lim et al., 2003).

La deuxième étape de la sénescence, c'est-à-dire le démantèlement cellulaire et la remobilisation des constituants vers les organes puits est, chez les espèces de grande culture notamment, une étape particulièrement importante dans l'établissement du rendement final. En effet la feuille représente l'une des principales réserves de carbone et d'azote mobilisables par la plante. La dégradation des constituants cellulaires implique, en fonction de leur nature biochimique, des mécanismes variés présentés dans cette partie. Au niveau cellulaire, les plastes sont plus particulièrement étudiés dans la mesure où la majeure partie des protéines et des lipides remobilisables de la feuille (RuBisCO notamment, mais aussi un grand nombre de protéines membranaires) y est localisée. La dégradation de ces constituants fait intervenir de nombreuses enzymes comme les protéases et les lipases ainsi que

des mécanismes complexes de transit de ces constituants dans la cellule, en situation d'autophagie. Les molécules exportables issues de ces processus de dégradation sont ensuite transportées, par voie phloémique, spécifiquement suivant leur nature (sucres, acides aminés, acides organiques, peptides,…) vers les organes puits. La phase ultime de la sénescence foliaire correspondant à la dégénérescence et à la mort de la cellule implique également des phénomènes de dégradations qui sont présentés dans cette première partie.

Ces informations mécanistiques sont de nature à fournir des indicateurs spatiaux et temporels de la progression de la sénescence foliaire applicables au repérage des différentes phases et au suivi de ces étapes critiques du développement (Wu et al., 2012). Un bilan est établi des indicateurs fréquemment rapportés dans la littérature et généralement utilisés comme repères moléculaires, physiologiques ou phénologiques de la sénescence foliaire.

L'effet des facteurs environnementaux sur la sénescence a été abondamment documenté, notamment l'effet de deux contraintes majeures en agriculture, le stress hydrique et les carences nutritionnelles (Andersen et al., 1996; Malagoli et al., 2005; Masclaux-Daubresse et al., 2008). La production du colza nécessite un apport important en fertilisants azotés, avec des conséquences économiques et environnementales qui peuvent s'avérer pénalisantes. Dans le contexte actuel de réduction de ces engrais, il apparaît opportun de caractériser les effets potentiels d'un stress nutritionnel et les processus physiologiques inhérents qui peuvent concourir à une meilleure valorisation des ressources assimilées. Le stress hydrique, temporaire ou durable, survient fréquemment lors d'un cycle de production et pénalise la croissance et le développement. Il interfère avec les capacités de nutrition minérale (azotée notamment) et contribue à des ajustements importants du métabolisme de la plante. Le contrôle exercé par ces contraintes isolées ou combinées sur l'induction et la progression de la sénescence a des conséquences sur l'efficience d'utilisation des nutriments. Nous rapporterons quelques-uns des effets exercés par les stress abiotiques sur la régulation de la sénescence foliaire en particulier.

La relaxométrie par Résonance Magnétique Nucléaire (RMN) est une technique donnant accès à l'état et à la compartimentation de l'eau dans une matrice. Cette méthode a déjà été appliquée pour la caractérisation de diverses matrices végétales. Après un rappel des mécanismes de relaxation dans les produits biologiques, des exemples d'application aux végétaux sont donnés. Il faut noter que dans la littérature seul un nombre limité de travaux portant sur l'étude des organes foliaires par RMN sont disponibles.

1-Changements structuraux et ultra-structuraux au cours de la sénescence

La structure foliaire est complexe et dépend aussi bien de l'organisation et de la taille des tissus mais aussi de paramètres cellulaires comme la taille des cellules, l'élasticité de la paroi… La cellule en elle-même possède une structure complexe dépendant de la taille et des caractéristiques des organites qu'elle contient ainsi que de la composition et les propriétés de la paroi.

1.1 Au niveau tissulaire

Au sein de la feuille, différents tissus sont organisés pour la réalisation de la photosynthèse, l'absorption et le rejet d'O_2, de CO_2 et d'eau, et les échanges en nutriments avec le reste de la plante. Les cellules épidermiques constituent une barrière protégeant les autres cellules, et en créant une atmosphère propre à l'intérieur de la feuille permettent de réguler le flux transpiratoire par l'intermédiaire des stomates. Ce rôle essentiel des stomates explique que ces cellules restent fonctionnelles jusqu'aux derniers stades de la sénescence et que l'épiderme soit le dernier tissu à être impacté par la sénescence (Keech et al., 2007). Le parenchyme palissadique, constitué de cellules chlorophylliennes densément réparties, est supposé être le siège principal de la photosynthèse, tandis que le parenchyme lacuneux, moins dense, réalise les échanges gazeux avec le milieu extérieur (Nardini et al., 2010). Ces différents tissus, interconnectés, sont reliés aux tissus conducteurs, constitués par les cellules conductrices du xylème et du phloème afin de réaliser les échanges d'eau et de nutriments (Turgeon and Wolf, 2009). L'export des nutriments se déroulant jusqu'à la fin de la sénescence, les tissus conducteurs ne sont pas dégradés et leur structure ne change pas. Cependant le parenchyme palissadique, siège de nombreuses dégradations au cours de la sénescence, devrait subir plus de modifications ; en effet en raison de son rôle supposé dans la photosynthèse ce tissu devrait être plus touché par la remobilisation. Ce phénomène n'a cependant pas été décrit dans la littérature. En effet la structure foliaire a été décrite de manière très précise chez de nombreux arbres (Castro-Diez et al., 2000) et chez certaines plantes modèles comme le tabac (Radochova et al., 2000), le riz (Inada et al., 1998) et Arabidopsis (Wuyts et al., 2012). Cependant il n'existe que très peu d'études portant sur des modifications des différents tissus de la feuille mature, la plupart étudiant l'impact d'un stress hydrique ou de l'ozone. Ainsi Wuyts et al. (2012) ont prouvé chez Arabidopsis qu'en réponse à la lumière et à la disponibilité de l'eau, différents génotypes ont été impactés différemment en terme de modifications au niveau de la taille des cellules et de l'épaisseur des tissus. Les changements de tailles et la mort des cellules provoqués par l'ozone spécifiquement sur les cellules du parenchyme lacuneux ont aussi été étudiés (Günthardt-Goerg et al., 2000; Al Sahli et al., 2013).

1.2 Au niveau cellulaire et subcellulaire

De la même manière que pour les tissus, peu d'études portent spécifiquement sur la structure des cellules (Martinez et al., 2007; Wuyts et al., 2012) et aucune parmi elles sur les changements

structuraux au cours de la sénescence. Pourtant la dégradation des plastes pendant la sénescence, très bien décrite (Ghosh et al., 2001; Wada and Ishida, 2009), modifie surement la structure de la cellule. De plus, la vacuole a une forte activité lytique pendant la sénescence et pourrait servir en plus de lieu de stockage transitoire des produits de dégradation des constituants cellulaires (Otegui et al., 2005). Ainsi la composition de la vacuole devrait être fortement impactée par la remobilisation. La vacuole étant à l'origine de la turgescence cellulaire, ces modifications devraient aussi impacter la structure cellulaire. En plus de la paroi (Martínez and Guiamet, 2014), le cytosquelette est aussi dégradé lors de la sénescence (Keech, 2011). Ces déterminants principaux (plaste, vacuole, paroi cytosquelette) étant impactés par la sénescence la structure cellulaire est certainement modifiée.

2-Mécanismes de la sénescence foliaire

2-1 Initiation

L'initiation de la sénescence est finement contrôlée et peut être influencée par de nombreux facteurs internes et externes. Cette étape est particulièrement importante car l'initiation de la sénescence dans la feuille marque notamment le début du déclin de l'activité photosynthétique et une sénescence précoce peut donc impacter le rendement. Les facteurs abiotiques et biotiques influençant la sénescence et particulièrement son initiation sont nombreux et sont résumés dans la Figure1. Comme la plupart des phases de développement et de croissance des tissus et des organes végétaux, la sénescence foliaire, notamment dans sa phase d'initiation, est sous le contrôle des phytohormones.

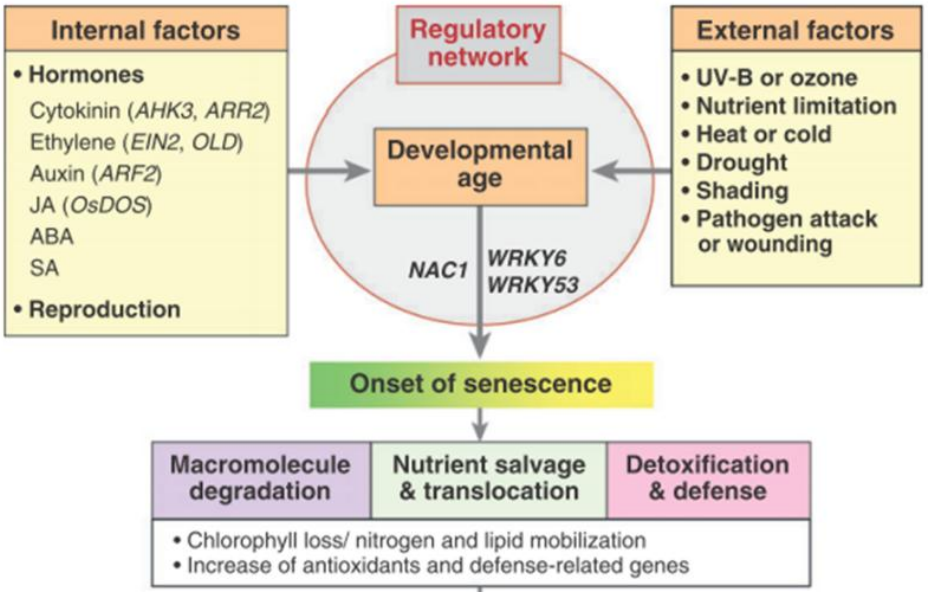

Figure 1 : Schéma représentatif des différents facteurs externes et internes influençant l'initiation de la sénescence (d'après Lim *et al*, (2007)).

2-1-1 Rôles des différentes phytohormones dans l'initiation de la sénescence

Les hormones végétales sont nombreuses et chacune possède en général une action complexe et interactive. Plusieurs hormones interviennent dans la régulation de l'initiation et de la progression de la sénescence (figure 2) au travers d'activités activatrice ou répressive (Sarwat et al., 2013).

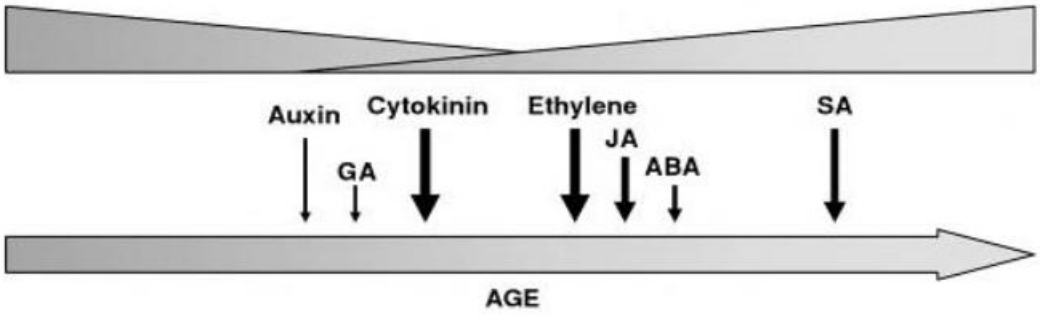

Figure 2 : schéma représentatif des différentes hormones impliquées dans la régulation de la sénescence. Avec l'âge les effets des régulateurs négatifs de la sénescence (Auxine, acide Giberillique (GA) et cytokinines) diminuent tandis que les effets des enzymes provoquant la sénescence augmentent.

Les cytokinines ont un rôle essentiel dans la physiologie de la plante notamment dans le contrôle de la prolifération cellulaire, de la ramification, de la synthèse des chlorophylles et de la sénescence. En effet, leur capacité à ralentir la progression de la sénescence foliaire a été démontrée depuis longtemps (Back and Richmond, 1969; Aharoni et al., 1975). La concentration en cytokinines diminue dans une feuille sénescente, en adéquation avec la sous-expression des gènes de leur synthèse et la sur-expression des gènes de dégradation (Buchanan-Wollaston et al., 2005). Chez des transformants de tabac surexprimant les gènes de synthèse des cytokinines la sénescence foliaire est ralentie (Wingler et al., 1998). De manière générale, la voie de signalisation des cytokinines, telle que décrite chez *Arabidopsis thaliana* passe par la perception du signal hormonal au niveau de récepteurs de type histidine kinases (AHKs) provoquant une cascade de phosphorylation activant des facteurs de transcription. Les mécanismes restent encore peu connus mais il semble qu'un des trois récepteurs aux cytokinines d'*Arabidopsis*, AHK3/ORE12, jouerait un rôle majeur. Ce récepteur agirait sur la phosphorylation d'ARR2 (*Arabidopsis* response regulator 2) qui induirait ou réprimerait d'autres gènes. Brenner *et al* (2005) ont mis en évidence, chez *Arabidopsis*, 71 gènes surexprimés et 11 sous-exprimés en réponse directe aux cytokinines, bien que ces gènes ne soient pas tous inversement contrôlés lors de la diminution de la concentration des cytokinines accompagnant la sénescence, indiquant l'intervention d'autres facteurs (van der Graaff et al., 2006). Par ailleurs, un rôle des sucres dans le mécanisme de régulation de la sénescence par les cytokinines a été proposé en lien avec la démonstration que l'inhibition d'une invertase pariétale, impliquée dans le chargement des sucres dans le phloème, annulait l'effet retardateur des cytokinines sur la sénescence (Lara et al., 2004).

L'éthylène joue un rôle important dans différents phénomènes développementaux comme la maturation du fruit ou la sénescence des fleurs. Des enzymes de la voie de biosynthèse de l'éthylène comme l'ACC synthase (AminoCyclopropaneCarboxylate synthase) et l'ACC oxydase sont activées dans les feuilles sénescentes (van der Graaff et al., 2006). Il a été montré chez *Arabidopsis* que les ACC synthase sont nombreuses et finement régulées aussi bien de manière spatiale que temporelle (Tsuchisaka and Theologis, 2004). De plus des mutants d'*Arabidopsis*, éthylène-résistant 1 (*etr1*) et éthylène-insensitive 2 (*ein2*), affectés respectivement dans la perception de l'éthylène et dans la transcription du signal, présentent un phénotype de sénescence retardée (Oh et al., 1997). Ceci met en évidence un rôle d'accélérateur de la sénescence de l'éthylène bien qu'il ne semble ni nécessaire (les feuilles des mutants *ein 2* et *etr1* sénescent) ni suffisant (les mutants surproduisant l'éthylène ne présentent pas de sénescence accélérée) à la sénescence (Jing et al., 2002). Le gène *old1* (onset of leaf death 1) est exprimé en fonction de l'âge du tissu et le mutant *old*1 présente un phénotype de sénescence accéléré chez Arabidopsis. Une exposition à l'éthylène accélère encore l'entrée en sénescence des mutants *old1*. Il apparaît donc que *old1* régule négativement l'intégration de la voie l'éthylène dans la sénescence foliaire. Ceci expliquerait en partie le fait que seules les feuilles âgées présentent une induction de la sénescence en réponse à l'éthylène (Grbic and Bleecker, 1995), alors que des feuilles non mâtures sont insensibles. En début de sénescence (quand les effets des hormones régulant positivement la sénescence diminuent) les tissus foliaires sont sensibles à l'éthylène seulement pour un temps donné (appelé sénescence dépendante de l'éthylène). A ce moment la sénescence est encore réversible, mais passé un stade, la sénescence est irréversible, l'éthylène n'a plus d'effet (sénescence indépendante de l'éthylène) et d'autres hormones comme l'acide abscissique (ABA) et l'acide salicylique (AS) entrent en jeu.

L'ABA est une phytohormone qui régule la réponse de la plante à différents stress environnementaux mais contribue également à contrôler certains évènements de développement comme la germination de la graine et la croissance cellulaire (Gubler et al., 2005; Zhao et al., 2014). Il a été démontré que l'application exogène d'ABA provoque la sénescence et l'abscision des feuilles (Zeevaart and Creelman, 1988). De plus lors de la sénescence, la concentration en ABA augmente (He et al., 2005; van der Graaff et al., 2006), et trois gènes majeurs de la voie de synthèse de cette phytohormone (NECD, AAO1, AAO3) sont surexprimés dans les feuilles en sénescence. On retrouve aussi des niveaux élevés de cette hormone dans les feuilles de plantes soumises à des stress connus pour accélérer la sénescence foliaire comme les stress hydrique ou thermique (Guo and Gan, 2005). Cependant les mécanismes exacts de régulation de la sénescence par l'ABA restent encore inconnus. L'application exogène d'ABA provoque une surexpression de plusieurs gènes SAGs (Senescence Associed Genes) dans les feuilles âgées (Zhang et al., 2012) parmi lesquels SAG13. Ce gène fait partie de la sous-famille A des PP2C (Protein ser/thr Phosphatase 2C) et est impliqué dans la régulation de l'ouverture des stomates. L'augmentation de la concentration en ABA induit, en plus de la fermeture des stomates, l'expression de gènes liés aux activités antioxydantes comme la superoxyde dismutase

(SOD), l'ascorbate peroxydase (APOD), et la catalase (CAT). Ces enzymes jouent un rôle dans la détoxification des ROS (Reactive Oxygen Species), produites en grande quantité pendant la sénescence (Zimmermann and Zentgraf, 2005), notamment lors du démantèlement des plastes. L'ABA pourrait donc exercer des fonctions régulatrices de la gestion des dommages lies aux dégradations cellulaires.

L'acide salicylique (AS) est une phytohormone majeure de la réponse de la plante aux bio-agressions. Cependant cette enzyme semble aussi avoir un rôle dans la sénescence, indépendemment de toute attaque de pathogène. En effet la concentration en AS est quatre fois plus importante dans les feuilles sénescentes que dans les feuilles matures chez Arabidopsis. De plus l'expression de nombreux gènes SAG (PR1a, chitinase, et SAG12) durant la sénescence est considérablement réduite chez les mutants défectueux dans la biosynthèse et la voie de signalisation de l'AS (*npr1* et *pad4*) (Morris et al., 2000). D'autres indices comme la sénescence accélérée des feuilles chez les mutants surexprimant ACBP3 (Acyetyl Coenzyme A Binding protein) liée à l'AS (Xiao et al., 2010), l'induction par l'AS de facteurs de transcription (WRKY70, WRKY53) ayant des rôles importants dans la sénescence (Besseau et al., 2012) ou encore le retardement du jaunissement des feuilles chez les mutants produisant peu de AS, indiquent un rôle important de cette hormone dans le retardement de la sénescence mais les mécanismes en restent inconnus.

L'auxine est impliquée dans de nombreux aspects du développement de la plante. Les enzymes de biosynthèse (TSA, AO1, NIT1-3) de l'auxine sont surexprimées pendant la sénescence et le niveau d'auxine augmente dans les feuilles sénescentes. De plus les mutants d'*Arabidopsis arf2* (Auxin Respons Factor) présentent une sénescence foliaire retardée (Ellis et al., 2005). L'application d'auxine exogène provoque une diminution de l'expression des gènes SAG. Le rôle exact de l'auxine durant la sénescence reste inconnu mais son interaction avec l'éthylène pour activer l'abscission de la feuille est bien documentée (Brown, 1997).

L'application foliaire de MeJa (Methyl-jasmonate), un précurseur du jasmonate, induit une perte de chlorophylles, une baisse de l'activité photosynthétique, et l'activation de gènes SAG (SEN4, SEN5, et γVPE) (Xiao et al., 2004). De plus, plusieurs gènes surexprimés lors de la sénescence foliaire sont aussi induits par le jasmonate (He et al., 2002). Il semble donc que le jasmonate puisse être sollicité pour induire la sénescence.

Les polyamines sont des molécules, parmi lesquelles la spermine, la spermidine, la cadavérine et la putrescine sont présentes chez tous les êtres vivants et ont de nombreux rôles au sein des plantes (Bouchereau et al., 1999) notamment dans la PCD (Kusano et al., 2008). La diminution de la quantité de polyamines dans les feuilles sénescentes laisse supposer un rôle inhibiteur de ces molécules sur la sénescence. L'application d'inhibiteurs de la voie de biosynthèse de polyamines sur des feuilles de rosier accélère la sénescence, alors que l'application de spermidine la ralentit fortement (Sood and

Nagar, 2008). Une étude chez la laitue a mis en évidence que l'effet retardant de la spermidine sur la sénescence pouvait être médiée par l'action de transglutaminases (Serafini-Fracassini et al., 2010).

2-1-2 Les gènes impliqués dans de la sénescence

L'initiation et les différentes étapes de la sénescence passent par l'activation et la répression de nombreux gènes. Les premières études sur ce sujet ont porté essentiellement sur des mutants de sénescence, mais dans les années 2000, les progrès de la génomique et le séquençage complet du génome d'*Arabidopsis* ont permis une identification fonctionnelle des gènes impliqués dans les mécanismes de sénescence.

L'analyse fonctionnelle a démontré que beaucoup de ces gènes codaient des protéines impliquées dans la synthèse, la dégradation ou la réception de phytohormones. Ainsi, 96 gènes codant des facteurs de transcription ont été identifiés comme surexprimés lors de la sénescence foliaire chez *Arabidopsis* (Buchanan-Wollaston et al., 2005). Parmi les facteurs de transcription de la famille WRKY (la plus importante), AtWRKY53 a été révélé pour son rôle important dans le contrôle de la sénescence foliaire (Zentgraf et al., 2010). Il contribuerait à réguler des événements précoces de la sénescence. Des mutants KO pour ce facteur de transcription présentent une sénescence ralentie, alors que les mutants de surexpression présentent une sénescence accélérée (Besseau et al., 2012) . Une cartographie comparée de l'expression des gènes d'une feuille soumise à un stress et d'une feuille sénescente montre de nombreuses similarités. Par exemple sur les 43 gènes surexprimés lors de la sénescence, 28 le sont aussi lors de différents stress biotiques et abiotiques (froid, et sècheresse notamment)(Chen et al., 2002).

Une autre fraction importante des gènes sollicités lors de la sénescence foliaire correspond aux enzymes et différentes protéines attachées au fonctionnement photosynthétique et associées aux processus de dégradation des macromolécules et de remobilisation des nutriments.

-Les gènes SAG (Senescence Associated Genes)

Un grand nombre de gènes surexprimés durant la sénescence, appelés SAG (senescence associated genes), ont été isolés chez de nombreuses espèces de plantes. La plupart des gènes SAGs ont été révélés grâce aux analyses de type microarray (Quirino et al., 2000; Buchanan-Wollaston et al., 2003; Lim et al., 2003). Certains de ces gènes codent des facteurs de transcription, ou des composants de la transduction et de la perception des signaux (Ellis et al., 2005; Guo and Gan, 2005; Besseau et al., 2012). D'autres gènes SAG codent des proteines de la synthèse et la régulation des phytohormones mais aussi des enzymes impliquées dans les processus de remobilisation. Le mieux décrit est le gène SAG12 codant une Cys-protéase qui présente un profil d'expression typique lors de la sénescence foliaire, et qui, contrairement à de nombreuses autres enzymes SAG, est surexprimée uniquement pendant la sénescence.

-Les gènes SGR (Stay-Green)

Les mutants stay-green (*sgr*) sont caractérisés par le maintien de la couleur verte des feuilles en comparaison avec une plante sauvage au même stade de développement. Ces mutants présentent un retard dans l'initiation ou la progression de la sénescence foliaire. Ils sont classés en deux catégories : les mutants fonctionnels, qui conservent une activité photosynthétique, et les mutants non-fonctionnels pour lesquels le maintien de la couleur verte n'est pas associée à la conservation de cette activité (Hoertensteiner, 2009). La plupart des mutants stay-green non fonctionnels sont, de par leur mutation, incapables de dégrader la chlorophylle. Ainsi bien que vertes les feuilles de ces mutants ne font pas ou peu de photosynthèse. Certaines protéines SGR sont impliquées dans le désassemblage des complexes chlorophylles/apoprotéines sur le Photosystème II (PSII) (Oh et al., 2000), ce qui est la première étape de la dégradation de la chlorophylle. L'étude des mutant *sgr* a permis d'approfondir les connaissances à propos des mécanismes de dégradation de la chlorophylle et d'autres phénomènes impliqués dans la sénescence (KingstonSmith et al., 1997; Rampino et al., 2006; Horie et al., 2007).

2-2 Dégradation et remobilisation des constituants cellulaires.

La fonction principale de la sénescence est de recycler des nutriments métaboliques, accumulés, sous différentes formes biochimiques, pendant la croissance et la maturation, en éléments exportables et réutilisables à distance par les organes puits. La remobilisation se caractérise donc par la dégradation des différents constituants cellulaires (protéines, chlorophylles, polysaccharides, lipides, acides nucléiques …) puis l'évacuation de catabolites vers les éléments phloémiens. Les constituants de la cellule sont dégradés par différents mécanismes en fonction de leur nature et de leur localisation cellulaire. Ces mécanismes se mettent en place durant la deuxième phase de la sénescence. Les chloroplastes qui occupent de 10% à 15% du volume du mesophylle représentent généralement la majeure partie du carbone et de l'azote remobilisables de la feuille. Les structures mitochondriales et nucléaires sont dégradées tardivement lors de la progression de la sénescence (Makino and Osmond, 1991)

2-2-1 Chloroplastes

Lors de la sénescence, les chloroplastes subissent des destructurations graduelles (Figure 3) qui les transforment en gérontoplastes. Cette transition débute par le gonflement du stroma et le décompactage des thylacoïdes granaires. Les constituants des thylacoïdes sont dégradés de manière différente en fonction de leur nature (chlorophyllienne, lipidique, protéique…). Ces dégradations provoquent la baisse d'activité des photosystèmes II (PS II) (Ghosh et al., 2001). La déstructuration de l'appareil photosynthétique génère l'accumulation des ROS qui contribuent généralement à la mise en place de systèmes de détoxification. Au stade gérontoplaste, les différents constituants de la machinerie photosynthétique sont très dégradés et le plaste n'est plus capable de photosynthèse.

Les thylacoïdes sont grandement dégradés et de nombreuses gouttelettes lipidiques sont visibles dans ces organites. Sa déstructuration ultime demeure non élucidée même si certains auteurs suggèrent une implication de l'autophagie (Wada and Ishida, 2009).

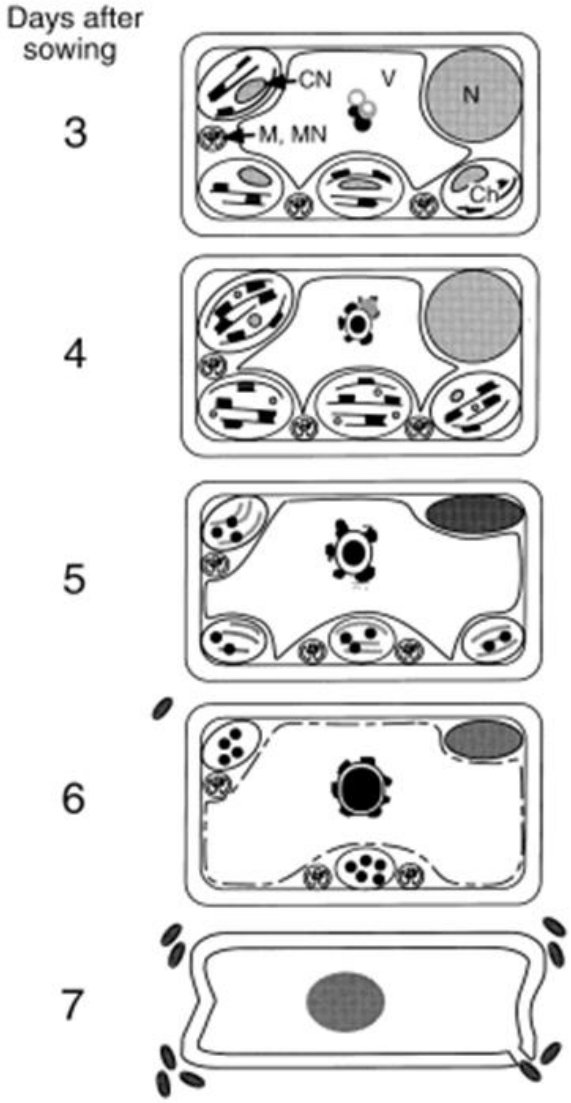

Figure 3 : Schéma des différentes étapes de la dégradation du chloroplaste au sein de la cellule dans les cotylédons (d'après Inada et al, (1998)).

2-2-2 Dégradation des chlorophylles

Au niveau macroscopique, la sénescence est caractérisée principalement par un jaunissement progressif des feuilles dû à la dégradation des chlorophylles dans les chloroplastes (Figure 4).

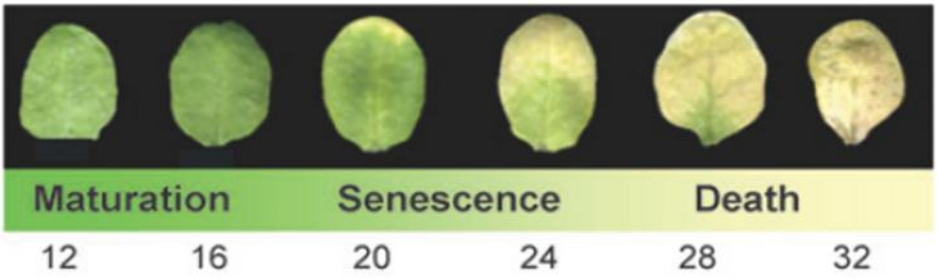

Figure 4 : feuilles d'Arabidopsis âgées de 12 à 32 jours après émergence (d'après Lim *et al* (2007))

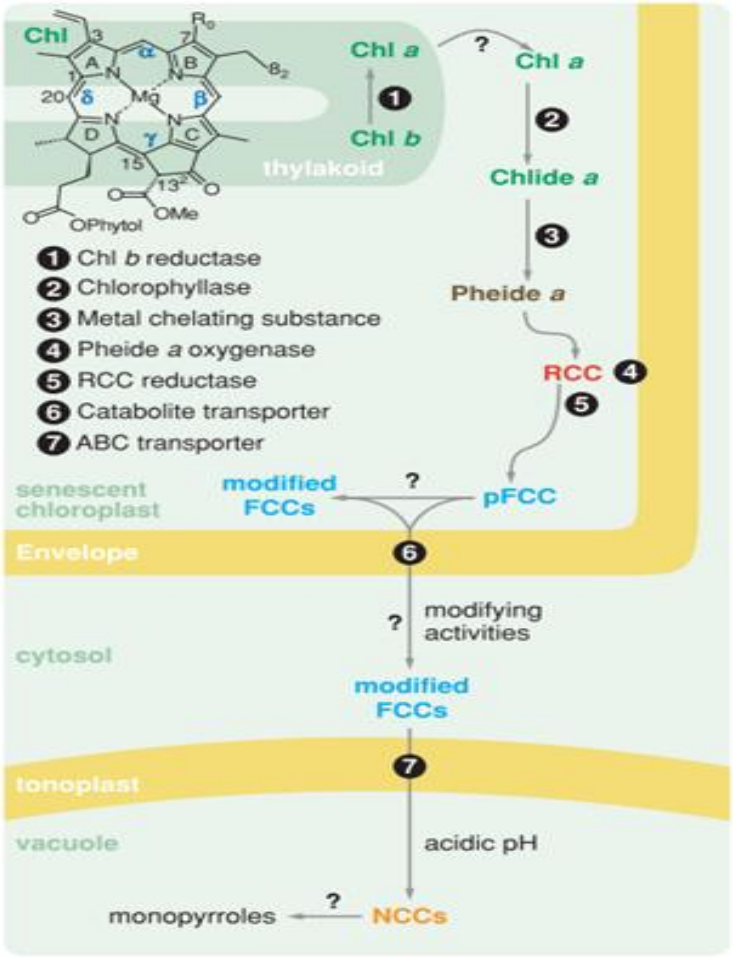

Figure 5 : Représentation schématique de la voie de dégradation de la chlorophylle (d'après Hortensteiner (2006))

La dégradation des chlorophylles se fait à travers plusieurs étapes dont les premières se déroulent majoritairement dans le plaste et mettent en jeu de nombreuses enzymes (Hoertensteiner, 2006) (Figure 5). Les chlorophylles a et b sont des pigments dont le squelette de base est un noyau tétrapyrrolique de chlorine (un dérivé de la famille des porphyrines) au centre duquel est complexé un ion magnésium (Mg^{2+}). Elles s'agrègent aux antennes collectrices des photosystèmes, et captent les photons pour transmettre l'énergie au premier accepteur de la chaine de transport des éléctrons photosynthétiques.

La voie de dégradation des chlorophylles commence par leur désassemblage des aprotéines dans les photosystèmes. Si les chlorophylles ne contiennent en moyenne que 2% de l'azote foliaire, leur dégradation joue un rôle important dans la remobilisation de l'azote chloroplastique dans la mesure où leur libération préalable conditionne la dégradation ultérieure des apoprotéines. L'étape suivante de la dégradation des chlorophylles est une dephytylation (détachement de la queue phytol) qui convertit la chlorophylle en phytol et chlorophyllide. Cette réaction est catalysée par la chlorophyllase (CHL), une enzyme située sur la membrane des plastes, ce qui permet une séparation physique entre cette enzyme et ses substrats (chl*a* mais aussi chl*b* et la phéophytine). Le Mg^{2+} de la chlorophyllide est ensuite libéré par l'action de différentes enzymes, formant ainsi du phéophorbide a, un pigment de couleur brune. Il est ensuite clivé, toujours dans le plaste, par l'action d'une oxygénase, la PAO (Polyamine oxydase), qui produit différentes molécules nommées RCC (Red Chl Catabolite). Ces RCC subissent ensuite une cascade de dégradation impliquant diverse enzymes jusqu'à être tranformés en pFCC (fluorescent chlorophyll catabolites). Ces catabolites sont transférés de manière ATP- dépendante dans la vacuole où le pH acide catalyse leur conversion en NCC (non fluorescent chlorophyll catabolite). Plusieurs indices semblent indiquer une régulation fine de la dégradation des chlorophylles notamment au niveau transcriptionnel ; ainsi chez *Arabidopsis* la

quantité des ARNm codant l'enzyme CHL1 augmente fortement lors d'un traitement au MeJa et la quantité des ARNm codant la PAO augmente pendant la sénescence. Ces deux enzymes sont aussi induites lors d'un stress impliquant une blessure afin de détoxifier la chlorophylle libre. Il est intéressant de noter que chez les mutants déficient en PAO ce n'est pas le pheide *a* qui s'accumule mais la chl toujours liée aux apoprotéines, ce qui démontre un rétrocontrôle. Que ce rétrocontrôle agisse au niveau des protéases (responsables de la séparation chl/apoprotéines) ou de la CHL n'a pas encore été élucidé.

Le catabolisme des chlorophylles, ainsi que la dégradation des membranes des thylacoïdes, qui se déroulent durant la sénescence libèrent des ROS (Zimmermann and Zentgraf, 2005) qui sont très toxiques pour la cellule et qui accélèrent la sénescence. Or une dégradation trop rapide (induites par les ROS) du plaste serait incomplète et ne permettrait pas la remobilisation optimale de ces constituants. Ces dégradations s'accompagnent donc généralement d'une augmentation de l'activité des enzymes détoxifiantes tels que les peroxydases et les catalases (Lin and Kao, 1998; Zimmermann and Zentgraf, 2005).

2-2-3 Amidon

L'amidon est une forme de stockage transitoire du carbone dans les feuilles. Chez *Arabidopsis thaliana*, un modèle a été proposé pour la voie de dégradation de l'amidon pendant la phase nocturne (non photosynthétique) : la β-amylase, responsable de la dégradation de l'amylopectine ainsi que des glucanes linéaires en maltose serait l'enzyme la plus active, contrairement à l'isoamylase, enzyme de débranchement formant des glucanes linéaires à partir de l'amylopectine. L'enzyme DPE1 (D-enzyme platidiale) permet de dégrader ces glucanes en glucose. Le maltose et le glucose seraient alors les formes d'exportation du stroma vers le cytosol. D'autres enzymes peuvent aussi intervenir de façon moins importante, comme l'α-amylase. Cependant, il n'est pas démontré que ce mécanisme de dégradation de l'amidon soit impliqué (Zeeman et al., 2007) durant la sénescence. En effet, il est possible que cette baisse de la teneur en amidon soit associée à une baisse de l'activité photosynthétique, stoppant l'accumulation diurne d'amidon et réduisant la capacité de reconstitution du stock dégradé pendant la nuit.

2-2-4 Protéases

Dans la feuille, l'azote se trouve majoritairement dans les acides aminés qui constituent les protéines. La plus grande partie de ces protéines est dans le plaste, sous forme de protéines solubles dans le stroma comme la RuBisCO ou sous formes de protéines membranaires comme les apoprotéines. La remobilisation de l'azote nécessite donc une dégradation des protéines par des protéases en acides aminés exportables vers les organes puits. Cette remobilisation protéique, au cours de la sénescence des feuilles, a été particulièrement étudiée chez des espèces d'intérêt agronomique comme le riz (Liu et al., 2008), le blé (Roberts et al., 2011), l'orge (Ruuska et al., 2008), le soja (Otegui et al., 2005), et le colza (Tilsner et al., 2005; Desclos et al., 2009). Chez *Arabidopsis*, 826

gènes codant des protéases ont été identifiés (Figure 6). Elles ont des fonctions et des localisations différentes, par exemple la vacuole, les RCB (RuBisCO Containing Bodies) et les autophagosomes.

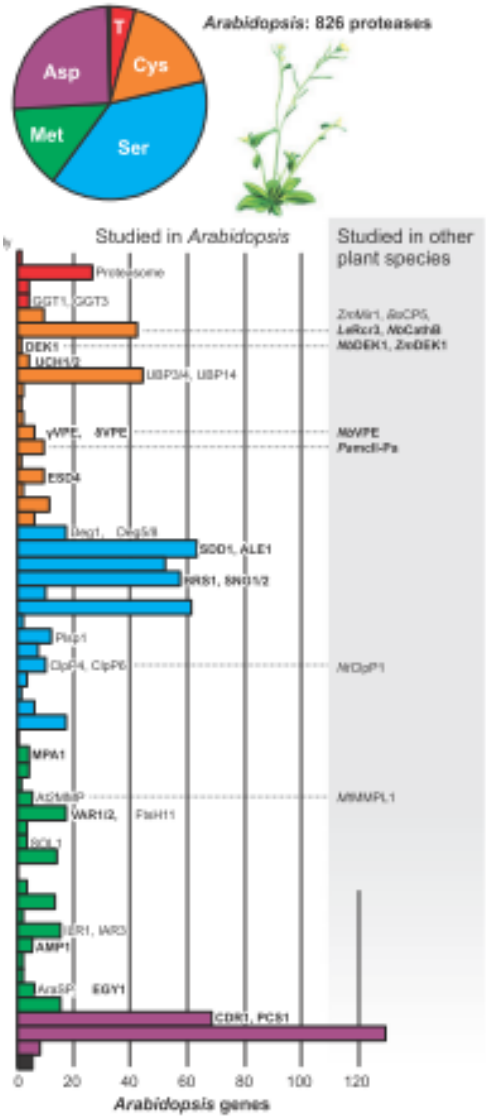

Figure 6 : Différentes protéases chez Arabidopsis (d'après van der Hoorn (2008))

Lors des premiers stades de la sénescence, la dégradation des protéines impliquerait tout d'abord celles accumulées dans le stroma (en particulier la RuBisCO). Des études protéomiques ont révélé que les protéases de type FtsH sont fortement exprimées au début de la sénescence. Les protéases FtsH (famille M41) sont des métalloprotéases membranaires ATP-dépendantes avec un domaine de liaison au zinc (Wagner et al., 2012). Parmi les 12 protéases FtsH, 9 sont chloroplastiques avec un rôle bien connu dans la différenciation des plastes et la dégradation de certaines protéines dans le cycle de réparation du photosystème II (Nixon et al., 2010) ainsi que dans la dégradation des protéines des antennes collectrices (LHCII) chez *Arabidopsis* (Zelisko and Jackowski, 2004). Par conséquent, l'induction spécifique de protéases chloroplastiques FtsH suggère que les protéines associées aux membranes des thylakoïdes sont également dégradées au début de la sénescence des feuilles dans le colza.

La protéolyse ubiquitine-dépendante est le mécanisme majeur de dégradation sélective des protéines cytoplasmiques et nucléaires dans toutes les cellules eucaryotes. Elle est impliquée dans le cycle de vie de la cellule pour dégrader les protéines imparfaites et celles nécessitant un rapide turn-over. Ce mécanisme fonctionne en deux étapes ; l'étiquetage de la protéine cible par l'ajout d'un polymère d'ubiquitine (ubiquitinylation), puis sa dégradation par le protéasome 26S. Ce dernier dégrade les protéines ubiquitinylées en peptides de 3 à 23 acides aminés, qui sont ensuite hydrolysés en acide aminés par d'autres enzymes, les principaux acides aminés exportés étant la glutamine et l'asparagine. L'ubiquitinylation correspond à une cascade de réaction dont la dernière est catalysée par une ubiquitine protéine-ligase appelée E3. Certains gènes codant un constituant d'une enzyme E3, comme ore9, sont connus pour agir sur la sénescence. En effet chez les mutants d'*Arabidopsis ore9*, la sénescence est ralentie. Des analyses par microarray montrent une surexpression du gène ore9 lors de

la sénescence foliaire chez le tabac (Woo et al., 2001). Ces résultats soutiennent une implication de la protéolyse ubiquitine-dépendante au cours de la sénescence foliaire. Cependant d'autres mécanismes participent à la dégradation des protéines lors de la sénescence foliaire. En correspondance avec la dégradation de la RuBisCO, la concentration de CND41 (Chloroplast Nucleotid DNA-binding protein) augmente dans les feuilles sénescentes d'*Arabidopsis* et de tabac (Kato et al., 2004; Kato et al., 2005; Kato et al., 2005). Cette enzyme joue un rôle important dans la dégradation de la RuBisCO, bien que les mécanismes n'aient pas encore été totalement élucidés. L'hypothèse que la dégradation de la RuBisCO soit initiée par les effets délétères des ROS a été proposée (Feller*et al*., 2008), la protéase de type aspartique CND41 n'agissant *in vivo* que sur de la RuBisCO partiellement dégradée (Kato et al., 2004). La suite de la dégradation se déroule dans la vacuole après un transport de type autophagique dans des petites vésicules appelées RCB (Rubisco Containing Body). D'autres études ont mis en évidence le rôle de la protéase CND41 dans la dégradation de la RuBisCO chez le colza (Diaz et al., 2008), sans pour autant déterminer le lieu exact (plaste ou RCB) de l'action de cette enzyme.

2-2-5 Lipides

Une grande partie du carbone de la cellule chlorophyllienne est sous forme lipidique. Les lipides membranaires, notamment dans les plastes, consituent une source importante de carbone durant la sénescence. La dégradation des membranes dans les chloroplastes est un symptôme précoce de l'initiation de la sénescence et entraîne une augmentation de la perméabilité membranaire et des pertes d'ions, et est associée à une diminution de l'activité des protéines membranaires.

D'une façon générale, les membranes cellulaires sont affectées par la sénescence de la façon suivante : pendant la vie de la cellule, le phénomène de bourgeonnement cellulaire (ou « blebbing ») permet de libérer, à partir des membranes, des particules lipido-protéiques qui sont remplacées par des lipides et protéines néoformés (Brehelin and Kessler, 2008). Les particules sont formées de phospholipides, diacylglycérols, triacylglycérols, ainsi que de lipides et protéines dégradés. Les lipides dégradés sont enfermés dans des gouttelettes de phospholipides qui sont acheminées vers la vacuole afin d'y être recyclées. Ceci permet, dans les tissus foliaires, d'assurer le maintien de l'intégrité et des fonctions membranaires par le « turn-over » des lipides et protéines constitutifs. Lors de la phase de sénescence, ce phénomène de bourgeonnement diminue. Les lipides et protéines dégradés sont donc de moins en moins éliminés des structures membranaires. En parallèle, la sénescence induit la synthèse d'enzymes de dégradation des lipides et protéines membranaires, ce qui favorise encore la présence de molécules dégradées dans la membrane. Le taux de lipides à acides gras polyinsaturés diminue, ces lipides étant préférentiellement affectés par les enzymes induites par l'état de sénescence. L'augmentation de la concentration en catabolites lipidiques dans les membranes conduit à une séparation de phase des lipides membranaires. La membrane, initialement liquide-cristalline, forme des plages d'acides gras sous forme de « gel ». Ceci entraîne donc au final une perte de la compartimentation de l'eau et des solutés (Thompson et al., 1997; Thompson et al., 1998).

Les lipides de stockage sont des triacylglycérol (TAG), composés de trois acides gras estérifiés lié à une molécule de glycérol particulièrement représentés dans le cytosol des graines oléagineuses, et stockés dans de petites vésicules de 0.5-0.2 µm de diamètre (corps gras ou liposomes). Dans les feuilles d'*Arabidopsis*, la quantité de TAG est importante lors de la sénescence (13% en masse), au niveau des plastoglobules, alors qu'elle est beaucoup plus faible dans les jeunes tissus (2%). Les plastoglobules sont des vésicules lipoprotéiques de petit diamètre (50-100 nm)(Figure 7) (Brehelin et al., 2007) et c'est sous forme de TAG au sein de ces plastoglobules que les lipides sont remobilisés lors de la sénescence. La composition en acides gras de ces TAG suggère qu'ils proviennent en majorité de la transformation des galactolipides des membranes chloroplastiques (Lee et al., 2001). La de-estérification des acides gras des galactolipides est due à une ou plusieurs galactolipases. Il a été rapporté qu'une de ces enzymes, LIP1, était induite lors de la sénescence (Kim et al., 2001). L'étape finale de formation des TAG est due à la DGAT1 (diacaylglycerol acyltransferase), dont le gène est aussi surexprimé pendant la sénescence.

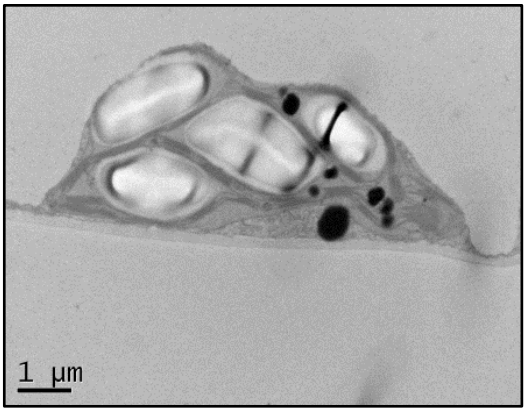

Figure 7 : Image de microscopie électronique d'un chloroplaste d'une feuille de colza

Les plastoglobules sont associés à tous les types de plastes, et ont un rôle à la fois dans le développement des thylacoïdes et dans le stockage temporaire des lipides mais aussi dans la réponse à certains stress comme une carence en azote (Gaude et al., 2007). Lors de la sénescence le nombre et la taille des plastoglobules augmentent ce qui est associé au désassemblage des thylacoïdes (Brehelin and Kessler, 2008). L'hémimembrane qui forme les plastoglobules est en contact avec celle d'un autre plastoglobule et/ou à la membrane des thylacoïdes (Austin et al., 2006) ce qui créé un réseau permettant la circulation des métabolites lipidiques. En plus des lipides, ces vésicules contiennent différentes protéines : des enzymes impliquées dans la biosynthèse et le métabolisme des lipides, mais aussi dans le métabolisme des isoprénoïdes, des protéines de structure, et des protéines capables de lier les chlorophylles a et b. Des études récentes montrent qu'un catabolite issu de la dégradation de la chlorophylle, le phytol, est incorporé à des acides gras, les FAPEs (Fatty acid Phytyl Esters) afin de

contenir ses effets toxiques (détergent). Le phytol est produit en grande quantité par la dégradation de la chlorophylle lors de la sénescence et les FAPEs s'accumulent dans les plastoglobules (Gaude et al., 2007). Ces éléments supposent une implication de ces vésicules dans le mécanisme de dégradation de la chlorophylle (principalement pendant la sénescence) en plus de son rôle dans la dégradation des lipides des membranes internes.

La peroxydation des lipides provoque une augmentation des ROS et en particulier des radicaux libres, ce qui provoque des dégâts aux protéines membranaires (Thompson et al., 1997). Les peroxysomes sont de petits organites des cellules eucaryotes qui ont pour fonction principale la détoxification cellulaire. Les glyoxysomes (Figure 8) sont des peroxysomes spécialisés contenant les enzymes de la voie du glyoxylate en plus des enzymes peroxysomales comme la catalase et la flavine oxydase. Comme les peroxysomes, les glyoxysomes sont capable de réaliser la β-oxydation des acides gras, mais alors que les peroxysomes ne peuvent que transformer les acides gras à longue chaine en acide gras à chaine moyenne ; les glyoxysomes peuvent dégrader entièrement les acides gras en acetyl Coenzyme A. Cette molécule est ensuite transformée en succinate via le cycle de glyoxylation, le succinate ainsi formé peut ensuite être utilisé par le cycle de Krebs dans les mitochondries.

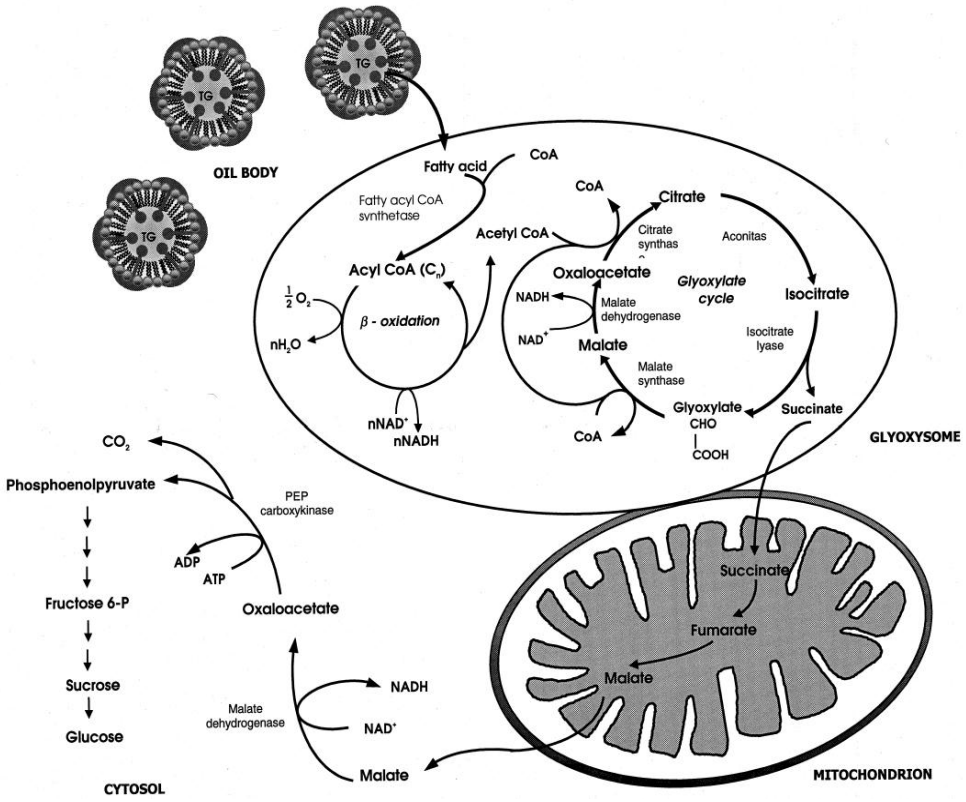

Figure 8 : Représentation schématique de la voie du glyoxylate (d'après Thompson *et al* (1998))

2-2-6 Autophagie

L'autophagie est un phénomène commun aux eucaryotes qui est caractérisé par la formation d'autophagosomes. Ces vésicules incorporent tout ou partie d'organelles (ou du cytoplasme) qui sont ensuite transférés vers la vacuole (le lysosome pour la cellule animale) où ils seront lysés. Chez les plantes les protéines sont partiellement ou totalement dégradées dans les lysosomes. Les lysosomes se dirigent ensuite vers la vacuole, avec laquelle ils fusionnent, ce qui permet la destruction finale des protéines restantes par les hydrolases vacuolaires (Chen and Yu, 2013). Des études chez les levures ont mis en évidence de nombreux gènes ATGs (Autophagy related genes). Par homologie de séquences, de nombreux ATGSs ont été clonés chez *Arabidopsis* et l'analyse des mutants *atg* (knock out) pour de ces gènes, ont permis de mieux comprendre ce phénomène (Chung, 2011). Il apparaît que, chez les plantes, l'autophagie joue un rôle important pendant la sénescence et participe à la remobilisation des nutriments, particulièrement chez les plantes carencées en nutriments (Guiboileau et al., 2012). En effet de nombreux gènes ATGs sont surexprimés pendant la sénescence foliaire et particulièrement lors d'une carence azotée. Des études montrent l'implication de l'autophagie dans la dégradation des chloroplastes indépendamment de celles de certains de ses constituants comme la chlorophylle (Wada and Ishida, 2009; Izumi et al., 2010). La plupart des expériences ont été réalisées sur des IDL (Individually Darkened Leaves)(Yoshimoto et al., 2004; Guiboileau et al., 2012). Cette méthode consiste à provoquer une sénescence artificielle en mettant la feuille à l'obscurité, le plus souvent en la recouvrant de papier aluminium. Bien que cette méthode mime la sénescence naturelle elle semble provoquer un sénescence plus « agressive » (Wada and Ishida, 2009). Les études sur des IDL ont cependant permis de mettre en évidence le rôle des processus d'autophagie dans le recyclage des composants du plaste (Izumi et al., 2010), voir du plaste entier (Wada and Ishida, 2009). Certains autophagosomes sont spécialisés, comme les RCBs qui contiennent majoritairement des produits de dégradation de la RuBisCO. Ces autophagosomes sont formés à partir d'un stromule (prolongement tubulaire de membranes chloroplastiques). D'autres vésicules, comme les SAV, constituées d'une simple membrane contrairement aux autophagosomes, participent également à la dégradation des constituants cellulaires. Les SAV (senescence associated vacuoles) sont des petites vésicules (0.5-0.7 µm) constituées d'une simple membrane provenant des plastes. Elles sont présentes tout au long du développement de la feuille mais leur nombre augmente fortement lors de la sénescence. Ces vésicules ont un pH légèrement supérieur à celui du stroma et possèdent une forte activité protéolytique. Bien qu'elles aient une activité lytique, ces vésicules sont différentes des autophagosomes de par leur taille et la composition de leurs membranes. Lors du fonctionnement du chloroplaste dans une feuille non sénescente, ces vésicules permettent d'assurer la dégradation indispensable au turn-over des protéines. Pendant la sénescence, ces vacuoles accumulent notamment une Cys-protéase typique de la sénescence foliaire : SAG12 (Otegui et al., 2005). De plus, la mise en évidence de grandes sous-unités de la RuBisCO et de la glutamine synthétase chloroplastique (GS2) dans ces vésicules confirme le rôle

de ces vésicules dans la dégradation protéique et la remobilisation associées à la sénescence (Martinez et al., 2008).

2-2-7 Export vers les organes puits

La dégradation des composants cellulaires décrite dans la partie précédente correspond à la première étape de la remobilisation, la seconde étant l'export des molécules obtenues vers les organes puits de la plante. Afin de transporter et d'échanger les nutriments entre les différents organes, les plantes supérieures possèdent deux systèmes de vaisseaux : le xylème et le phloème. Le phloème est constitué de cellules vivantes (contrairement au xylème) qui forment des tubes criblés (Turgeon and Wolf, 2009). Chez les plantes, la principale forme de transport du carbone réduit est le saccharose partiellement remplacé chez certaines espèces, par des polyols (sorbitol, mannitol) ou des oligosaccharides comme le raffinose ou le stachyose (Lalonde et al., 2004). Le transport des produits de dégradation des constituants cellulaires au sein de la feuille et en direction du phloème se fait de manière passive à travers les plasmodesmes (voie symplasmique) ou de la paroi (voie apoplastique). Les produits sont ensuite chargés dans le phloème, les mécanismes de chargement/déchargement du phloème, *via* des cellules compagnes, sont complexes et mettent en jeux de nombreux transporteurs spécifiques.

Les sucres

Chez les plantes les sucres sont le plus souvent transportés sous forme de disaccharides et principalement le saccharose. Le saccharose est formé dans le mésophylle des organes photosynthétisants et il se déplace vers le phloème, situé dans les nervures, par un mouvement symplastique *via* les plasmodesmes jusqu'au lieu de chargement dans le phloème. Le chargement du saccharose dans le phloème se fait par l'intermédiaire de transporteurs spécifiques. Il existe de nombreux transporteurs de sucres (Bush, 1999), cependant l'entrée dans le phloème se fait principalement grâce à des co-transporteurs H+/saccharose, les transporteurs SUT (Sucrose Transporter). Ces transporteurs ont une structure commune constituée de 12 domaines inter-menbranaires et les extrémités N et C terminales située dans le cytosol (Stolz et al., 1999). Le séquençage du génome d'*Arabidopsis* et du riz a permis de mettre en évidence respectivement 9 et 5 membres de cette famille, dont plusieurs sont surexprimés dans les feuilles les plus âgées. Des monosaccharides, résultants notamment de l'action des invertases pariétales sur le saccharose, peuvent aussi être chargés dans le phloème grâce à des MST (MonoSaccharid Transporter). De plus l'action des invertases, de la paroi des cellules compagnes, sur le saccharose, permet d'orienter le gradient de saccharose qui dirige le transport symplastique à travers le mésophylle (Lohaus and Fischer, 2002).

L'azote

Plusieurs études ont étudié la remobilisation de l'azote chez *Arabidopsis* et chez le colza et ont démontré que la majorité de l'azote des graines provenait de la remobilisation foliaire (Malagoli et al., 2005; Diaz et al., 2008). Comme expliqué précédemment, l'azote remobilisé provient en majorité des

plastes, principalement de la RuBisCO (Gregersen et al., 2008) et chez la plupart des plantes, l'azote organique est transporté sous forme d'acides aminés. L'augmentation de la quantité d'ARNm codant des protéases vacuolaires au cours de la sénescence indique que le processus de dégradation des protéines se termine dans la vacuole avant l'export hors de la cellule. Ce transport se fait par le phloème et, contrairement aux sucres, également via le xylème (Okumoto et al., 2002). Comme le métabolisme de l'azote est très compartimenté à l'intérieur de la cellule, il existe de nombreux transporteurs différents d'acides aminés ; ainsi le génome d'*Arabidopsis* contient 53 gènes codant des transporteurs putatifs d'acides aminés. Certains transporteurs de type AAP (Amino Acid Permease) sont exprimés dans les tissus vasculaires où ils assurent le chargement dans le phloème de nombreux acides aminés, par un mécanisme proton (ou sodium) dépendant (Lalonde et al., 2004). Plusieurs enzymes impliquées dans le métabolisme de l'azote et induites spécifiquement lors de la remobilisation ont été identifiées (Masclaux et al., 2000; Buchanan-Wollaston et al., 2005). Les plus importantes semblent être : la glutamine synthétase cytosolique (GS1), la glutamate déshydrogénase (GDH) et l'asparagine synthétase (AS)(Masclaux-Daubresse et al., 2008). Le recyclage et l'assimilation de l'azote au cours du développement d'une feuille se déroule majoritairement au sein des chloroplastes, en effet c'est dans les plastes qu'est localisée la réduction des nitrites (par l'action de la NiR) et l'assimilation de l'ammonium (via le cycle GS/Gogat impliquant la GS2 chloroplastique). Du fait du désassemblage des chloroplastes lors de la sénescence, et donc la dégradation de ces enzymes, d'autres mécanismes sont mis en œuvre pour recycler l'azote. Le mécanisme proposé est une forte synthèse de glutamine pour l'export grâce à l'action de GS1 néosynthétisée (Masclaux-Daubresse et al., 2010). Chez le blé une corrélation positive a été mise en évidence entre l'action de cette enzyme et la quantité d'azote remobilisée des feuilles vers les graines (Kichey et al., 2007). L'activité de cette enzyme associée à celle de la GDH est un facteur déterminant de l'efficience de la remobilisation de l'azote (Masclaux-Daubresse et al., 2010).

2.3 Phase terminale

La sénescence est un processus développemental, contrôlé par l'âge, qui se termine par la mort cellulaire. En fin de sénescence dans une cellule du mesophylle, les gérontoplastes sont peu nombreux et la plupart des membranes sont abimées par l'action délétère des ROS qui s'autoalimentent. Chez certaines espèces comme c'est le cas chez le colza, les dernières étapes menant à la mort cellulaire sont parfois interrompues par l'abscission de la feuille. Mais lorsque cette étape se déroule jusqu'à son terme, les mitochondries, les parois et les noyaux sont partiellement ou totalement dégradés (Thompson et al., 2000; Noodén, 2004). La PCD (Programmed Cell Death) est un processus d'autodestruction cellulaire très finement contrôlé au niveau génétique. Lors de la sénescence, la vitesse de mort cellulaire est plus lente que lors d'autres types de PCD où il n'y a pas nécessairement de remobilisation de métabolites (lors de la réponse de type hypersensible (HR, hypersensitive

reaction) en résistance à des pathogènes par exemple)(van Doorn, 2005). Cependant, la mort cellulaire lors des derniers stades de la sénescence présente tout de même des traits caractéristiques de la PCD comme la destruction contrôlée de la vacuole, la condensation de la chromatine et la destruction de l'ADN. Il semble qu'au sein de la feuille les différents types cellulaires ne meurent pas en même temps et que les cellules épidermiques restent plus longtemps actives que celles du mésophylle (Keech, 2011). Une comparaison de l'expression globale des gènes lors de la mort cellulaire naturelle et celle provoquée par une carence nutritive a été réalisée à partir de suspensions cellulaire d'Arabidospis (Buchanan-Wollaston et al., 2005). Cette étude a mis en évidence des voies différentes menant à la mort cellulaire dans les deux cas, prouvant que bien que proches, la PCD provoquée par la sénescence naturelle et celle induite par un stress étaient différentes.

L'apoplaste est un compartiment largement sollicité lors des étapes de la sénescence. En effet, en plus de contenir la paroi qui structure les cellules, l'apoplaste est impliqué dans la reconnaissance des signaux (notamment hormonaux), la remobilisation des nutriments et l'induction de la mort cellulaire. L'apoplaste est constitué d'une matrice protéique fluide appelée fluide apoplastique, formant un compartiment continu extracellulaire qui permet une communication de cellule à cellule (Sattelmacher, 2001). Delannoy *et al*, (2008) ont listé 46 protéases présentes dans l'apoplaste des feuilles d'*Arabidopsis* parmi lesquels 8 seraient surexprimées durant la sénescence. De plus, les transporteurs de la membrane plasmique sont surexprimés pendant la sénescence (van der Graaff et al., 2006) ce qui laisse supposer un important mouvement de molécules entre le cytosol et l'apolaste. Des études chez le tabac ont mis en évidence des changements de composition du protéome du fluide apoplastique en réponse à un stress salin. Ainsi une accumulation de chitinases et de protéines associées au transport lipidique dans l'apoplaste a été démontrée (Dani et al., 2005). Ces enzymes font aussi partie de celles surexprimées pendant la sénescence (Yoshida et al., 2001). D'autres enzymes présentes dans l'apoplaste comme la lipase Glip1 impliquée dans la réponse à une infection fongique (Oh et al., 2005) présentent une surexpression de leur gène pendant la sénescence (Winter et al., 2007).

Le rôle de l'apoplaste dans le déclenchement de la PCD en réponse à une attaque de pathogène est documenté (Delannoy et al., 2008) cependant son rôle lors de la sénescence n'a pas encore été démontré. De manière générale, la PCD induite par les réactions hypersensibles (HR) lors d'une attaque de pathogène est mieux comprise que celle se produisant dans les derniers stades de la sénescence. Lors d'une attaque de pathogène, la PCD est induite notamment par un burst oxydatif dû à la dégradation de polyamines dans l'apoplaste (Takahashi and Kakehi, 2010) et la sécrétion de certaines molécules comme la cathepsine B (Gilroy et al., 2007). Cependant, ceci n'est pas prouvé dans le cas de la sénescence, bien que la dégradation des chlorophylles et des membranes génèrent une quantité importante de ROS. En plus de son rôle possible dans le déclenchement de la PCD, il a été démontré chez Arabidopsis que plusieurs enzymes dégradant les parois cellulaires (β-glucosidase) sont surexprimées lors de la diminution de la photosynthèse (Mohapatra et al., 2010), suggérant que la

paroi cellulaire des cellules de la feuille est dégradée au cours de la sénescence. Ces auteurs ont suggéré que les polysaccharides liés à la paroi cellulaire peuvent être une source de sucres pendant la phase tardive de la sénescence.

3 Marqueurs de l'évaluation de la sénescence foliaire

La progression de la sénescence des feuilles est généralement évaluée par différents indicateurs physiologiques, biochimiques ou moléculaires tels que le jaunissement des feuilles, des changements de teneurs en chlorophylle et en protéines (Levey and Wingler, 2005), des changements d'expression de certains gènes (Gombert et al., 2006). L'utilisation selon les études de différents indicateurs, associés à des étapes différentes de la sénescence, rend la comparaison des résultats souvent compliquée.

3-1 Marqueurs physiologiques

Le jaunissement de la feuille étant la conséquence la plus remarquable de la sénescence, la quantité de chlorophylles est régulièrement utilisée comme marqueurs de l'avancement de la sénescence (Otegui et al., 2005; Zhang et al., 2012) bien que la précision de cet indicateur reste critiquable. Dans le cas de carences, ce paramètre est encore moins précis, ainsi Gombert *et al*., (2006) ont mis en évidence que deux feuilles de plantes cultivées sous différents régimes azotés présentaient une quantité de chlorophylles identique bien qu'elles soient d'âge très différent.

L'activité dépendante de la sénescence de certaines enzymes comme des peroxydase (Abeles et al., 1988) ou des RNAse (Taylor et al., 1993) peut aussi être utilisée pour mesurer la progression de la sénescence, cependant ces mesures sont lentes, destructives et peu précises.

La mort cellulaire en fin de sénescence s'accompagne de la dégradation de la membrane plasmique et du relargage d'ions qui peut être facilement mesuré (Woo et al., 2001) cependant cet indicateur très précis n'est utile qu'à la toute fin de la sénescence.

3-2 Marqueurs moléculaires

Le profil d'expression particulier (surexpression ou répression spécifiquement associées à la sénescence) de certains de ces gènes peut permettre un balisage précis des différentes phases de progression de la sénescence. Ainsi la surexpression du gène SAG12 (et SAG13) est régulièrement repérée dans les feuilles (Guiboileau et al., 2010). A l'inverse le gène Cab, codant une apoprotéine liée

aux chlorophylles, est réprimé lors de la sénescence foliaire (Gombert et al., 2006), comme de nombreux gènes du métabolisme primaire. Ces gènes ont été proposés comme marqueurs pour identifier la transition source/puits dans une feuille sénescente.

4 Impact d'un stress abiotique sur la sénescence foliaire

Comme décrit précédemment, c'est durant la sénescence que se déroule la remobilisation dont l'efficacité détermine fortement le rendement final chez les plantes de grandes cultures. Les facteurs environnementaux contribuent largement à réguler l'initiation et la progression de la sénescence et les processus de recyclage des ressources. Les stress abiotiques, dépendamment de leur nature, leur amplitude, leur fréquence, leur durée, sont pour la plupart inducteurs de phénomènes de vieillissements accélérés des tissus qui peuvent s'apparenter au processus de sénescence

.

4-1 Stress Hydrique

Un des rôles de l'eau au sein de la plante est le transport des solutés à longue distance dont le principal moteur est l'évapotranspiration. L'eau contribue également au maintien de la turgescence, à de nombreuses réactions chimiques, à la transmission de la chaleur… De manière générale, l'eau se déplace des racines vers les feuilles, ces échanges impliquent qu'un gradient de potentiels hydriques décroissants existe également des racines vers les organes aériens et l'air extérieur. Le cycle de l'eau au sein de la plante est majoritairement contrôlé au niveau de la feuille ou l'ouverture/fermeture des stomates permettent de maintenir le potentiel hydrique dans les lacunes. Le stress hydrique diminue fortement les rendements agronomiques et les prévisions climatiques suggèrent que les épisodes de sécheresse dans le monde seront de plus en plus fréquents (Cook et al., 2007).

La feuille est l'organe de la plante trésréactif aux conditions environnementales et sa structure joue un grand rôle dans les relations hydriques (Aasamaa et al., 2005). En utilisant la particularité nutritive de certains insectes qui ne se nourrissent que du contenu du parenchyme palissadique, Nardini *et al.* (2010) ont mis en évidence le fait que le contrôle des relations hydriques au sein des tissus foliaires se fait par le parenchyme lacuneux. Ils ont démontré que quel que soit la quantité de parenchyme palissadique détruite la résistance hydraulique ne changeait pas.

Différentes adaptations anatomiques, physiologiques, moléculaires sont susceptibles de contribuer à la résistance/tolérance au stress hydrique (Baerenfaller et al., 2012). Chez de nombreuses espèces adaptées à des climats très chauds, la cuticule foliaire est très épaisse afin de minimiser la transpiration non contrôlée, et le stress hydrique peut induire chez certaines plantes la modification de la composition et de la quantité de ces cuticules. Au niveau structural, une diminution de la taille des

cellules du parenchyme lacuneux chez *Phaseolus vulgaris* a été décrite en réponse à un stress hydrique (Martinez et al., 2007) et la contraction des cellules est souvent associée à une meilleure tolérance au stress hydrique (Lecoeur et al., 1995). Cependant, une augmentation de la taille des cellules du parenchyme lacuneux a été observée dans la feuille d'olivier cultivé en condition limitante en eau (Guerfel et al., 2009). Afin de maintenir la turgescence nécessaire au bon fonctionnement de la cellule un ajustement osmotique est nécessaire (Chimenti et al., 2012). Ainsi de nombreuses molécules sont produites, aussi bien des osmolytes permettant de faciliter l'entrée et la rétention de l'eau (Ingram and Bartels, 1996) que des molécules protectrices des macromolécules (Martínez et al., 2008). Parmi ces molécules, la proline est considérée comme un des osmoprotectants majeur (Naidu et al., 2000; Szegletes et al., 2000), son accumulation permettant à la fois l'ajustement osmotique (Albert et al., 2012), la régulation du potentiel redox de la cellule et la détoxification des ROS. Le stress hydrique est, en effet, généralement générateur de ROS (Jaspers and Kangasjarvi, 2010; Miller et al., 2010) et différentes enzymes de détoxification sont nécessaires à leur contrôle. Un lien est établi entre les régulations mises en œuvre au cours de la sénescence foliaire et certaines réponses observées en réaction au stress hydrique. Il a notamment été montré chez le tabac, puis par la suite chez d'autres espèces, que la manipulation génétique du métabolisme des cytokinines pouvait non seulement contribuer à retarder l'avènement de la sénescence foliaire (effet « stay green ») mais contribuait également à renforcer la tolérance des plantes au stress hydrique (Munne-Bosch and Alegre, 2004).

4-2 Nutrition azotée : cas du colza

En phase de croissance végétative, la majeure partie de l'azote et des nutriments minéraux est concentrée dans les organes foliaires (Makino and Osmond, 1991; Schulze et al., 1994) . En dépit de sa bonne capacité à absorber l'azote minéral, le colza (*Brassica napus* L.) est caractérisé par une faible efficience d'usage de l'azote (NUE) et seulement 50% de l'azote absorbé par la plante est présent dans les graines à la récolte (Schjoerring et al., 1995). Alors qu'il faut globalement 6,5 Kg d'azote pour produire un quintal de graines de colza, 3 et 2,2 Kg sont nécessaires pour produire l'équivalent de blé et de tournesol respectivement (Singh, 2005). Une grande partie de l'azote stocké dans la graine de colza sous forme de protéines provient de processus de remobilisation de l'azote organique des parties végétatives (Malagoli et al., 2005). Tout au long du cycle végétatif puis reproducteur de la plante, les organes foliaires sénescent puis chutent avec des teneurs résiduelles en azote organique qui restent parfois élevées (jusqu'à 3% de la matière sèche (Rossato et al., 2001)). L'amélioration de la NUE du colza est nécessaire pour concilier impact environnemental réduit, objectif de haut rendement en qualité et quantité et bilan énergétique optimisé. Fonctionnellement, la NUE (Figure 9) peut être subdivisée en deux grandes composantes: efficacité d'absorption de l'N (NUpE) et l'efficacité d'utilisation de l'N (NUtE). Cette dernière composante complexe intégre les processus d'assimilation (NAE), de stockage et de recyclage ou de remobilisation de N (NRE). Plusieurs études menées en

conditions contrôlées ou sur le terrain (Malagoli et al., 2005; Tilsner et al., 2005; Gombert et al., 2006) ont démontré que que la faible NUE observée pour le colza est en partie attribuable à une NRE modérée. L'élaboration du rendement final en grain est largement dépendante de la mise en place du couvert végétal et de la biomasse végétative. La sénescence séquentielle mise en œuvre au cours de cette phase contribue ainsi à ré-allouer des ressources entre les tissus végétatifs sources et les jeunes feuilles en croissance. Il a été montré que l'élimination de 50% de feuilles de la rosette donne lieu à une importante diminution (-30%) du rendement (Noquet et al., 2004). Les approches transcriptomiques ont révélé l'induction de nombreux transporteurs d'oligopeptides au cours de remobilisation de l'N dans les feuilles sénescentes de colza (Karim et al., 2005). Il semble que la faible NRE associée à la sénescence séquentielle pourrait ne pas être due à une limitation de l'export des acides aminés mais est principalement liée à une hydrolyse incomplète des protéines foliaires (Noiraud et al., 2003; Tilsner et al., 2005). En utilisant une technique de marquage ^{15}N et l'élaboration d'un modèle mathématique de la remobilisation,, Malagoli *et al.* (2004) ont montré, par simulation, que la teneur en protéines ou le rendement en grain pouvait être améliorés d'environ 15% grâce à l'optimisation de la NRE pendant les stades végétatifs. Parallèlement, au cours de la dernière décennie, quelques études ont cherché à améliorer la NUE du colza *via* l'optimisation des caractéristiques de fonctionnement racinaire (NUpE) (Schulte auf'm Erley et al., 2007). Des approches transgéniques ont aussi démontré que l'amélioration de la NAE à travers la sur-activation d'enzymes impliquées dans le processus d'assimilation de l'N (alanine aminotransférase, l'asparagine aminotransférase) peut conduire à des améliorations tout à fait significatives de la NUE (Good and Beatty, 2011). Néanmoins, dans un contexte de réduction des intrants azotés, l'optimisation de la NRE par la feuille est probablement l'un des principaux leviers pour améliorer sensiblement la NUE du colza.

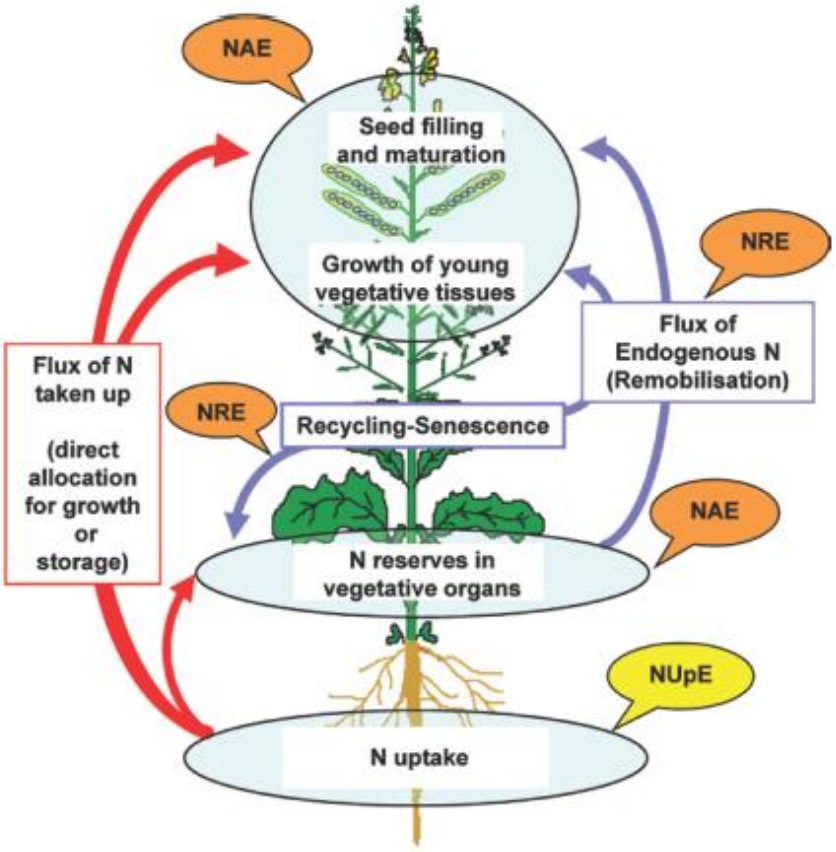

Figure 8 : Schéma représentatif des flux d'azote et des différentes composantes de la NUE chez le colza (Avice and Etienne, 2014)

Un stress azoté, chez le colza, induit et accélère la sénescence des feuilles agées. En effet, certaines études réalisées aussi bien sous serre (Gombert et al., 2006; Etienne et al., 2007) qu'au champ (Gombert et al., 2010) ont montré que des plantes carencées en azote présentaient une sénescence précoce des feuilles les plus âgées qui contribuerait à prévenir ou limiter la pénurie dans les tissus les plus jeunes. Ces études ont permis de mettre en lumière le rôle des protéases et des inhibiteurs de protéases dans le contrôle de la sénescence, notamment en situation de nutrition azotée limitante. Notamment, la protéine BnD22 (*Brassica napus* Drought induced protein 22 kDa) exerçant à la fois un rôle d'inhibiteur de serine-protéase et une fonction de WSCP (Water Soluble Chlorophyll Protect) est plus abondante dans les tissus jeunes et d'autant plus que la plante est carencée en azote en lien étroit avec le ralentissement de la sénescence. Les WSCP sont des protéines se complexant avec les chlorophylles pour les protéger notamment lors de la sénescence (Horigome et al., 2007). Des études ont démontré que BnD22 et d'autres WSCPs sont accumulées dans les jeunes feuilles en réponse à divers stress abiotiques et pourraient contribuer à assurer une gestion optimisée des stocks d'azote organique disponibles dans les tissus en situation de contrainte (Satoh et al., 2001; Desclos et al., 2009).

5 L'étude des végétaux par résonance magnétique nucléaire

La relaxomètrie RMN (Résonance Magnétique Nucléaire) à bas champ est une technique permettant de mesurer le signal de relaxation (retour à l'équilibre après excitation par une séquence d'impulsions magnétiques spécifiques) des spins des protons soumis à l'action d'un champ magnétique. Ce signal est fait de deux composantes : la composante longitudinale, ou relaxation spin-réseau T_1, provoquée par l'interaction des spins avec l'environnement et la composante transversale, ou relaxation spin-spin T_2, due à l'interaction entre les spins (figure 9). Les valeurs des temps de relaxation T_1 et T_2 et l'intensité du signal sont influencées respectivement par la mobilité et la quantité de protons. Le temps de relaxation sont également influencés par les échanges de protons entre les molécules.

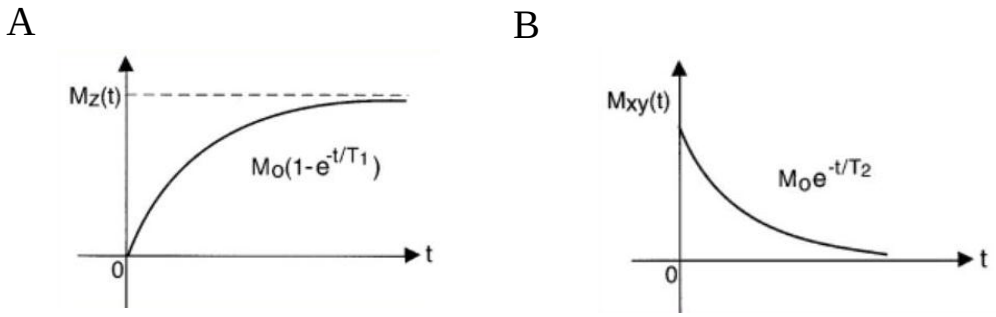

Figure 9 : schéma représentatif des deux composantes de relaxation du signal RMN, la relaxtion spin-réseau (A) et la relaxatiuon spin-spin (B)

Le signal de relaxation T_2 décroit comme une exponentielle dont l'intensité dépend de la quantité de protons dans le tube et la vitesse d'amortissement dépend du temps de relaxation. Dans les systèmes hydriques, le temps de relaxation de l'eau va dépendre de la composition de la phase aqueuse et de la structure des molécules contenues dans cette phase aqueuse, mais aussi de la microstructure de la matrice. Par exemple, dans un système binaire composé d'eau et de protéines, il est possible de distinguer quatre types de protons avec des temps de relaxation différents : les protons de l'eau dite « libre » (sans interactions avec les protéines), les protons de l'eau d'hydratation des protéines, les protons échangeables des protéines (groupement -OH, -NH2, -SH...) et enfin les protons non échangeables des protéines (protons des chaines carbonées). Lorsque les temps de relaxation sont longs par rapport à la vitesse des échanges chimiques entre les différentes populations de protons échangeables, et si les échanges de molécules d'eau par diffusion entre l'eau « libre » et l'eau d'hydratation sont rapides, alors le signal de relaxation sera décrit par deux exponentielles différentes. La première correspondra à la relaxation des protons non-échangeables des protéines et l'intensité de l'exponentielle sera proportionnelle à la quantité de protéine. La deuxième exponentielle sera

caractérisée par un temps de relaxation « moyen » qui sera la somme de différentes vitesses de relaxation $1/T_2$ pondérées par les proportions de chaque type de protons :

$$1/T_{2\ obs} = P_a/T_{2a} + P_b/T_{2b} + P_c/T_{2c}$$

avec P les populations des différents types de protons. a) : les protons de l'eau libre b) : les protons de l'eau d'hydratation des macromolécules et c) : les protons échangeables des macromolécules. L'intensité à l'origine de cette exponentielle sera donc proportionnelle à la quantité d'eau (libre et hydratation) et la quantité de protons échangeables des protéines.

Du fait de l'échange chimique entre les protons échangeables des protéines et les protons de l'eau, ceci entraine une forte diminution de la relaxation de l'eau sans nécessairement réduire la mobilité intrinsèque de la molécule d'eau. Ainsi, tout changement de mobilité de ces molécules non-aqueuses entrainera par voie de conséquence une diminution du temps de relaxation de l'eau. Ce mécanisme confère une propriété à l'eau d'être une sonde des changements de mobilité des molécules avec lesquelles l'eau interagit.

Les phénomènes décrits sont valables pour un milieu homogène, c'est-à-dire un milieu pour lequel les molécules d'eau peuvent sondées l'ensemble des environnements du fait d'un coefficient de diffusion élevé et donc d'une diffusion rapide. Par contre, si le milieu devient hétérogène de sorte que l'eau n'a pas le temps (ou la possibilité) de diffuser entre les différents environnements, alors le signal sera multi-exponentiel. Ceci est observé dans le cas de gel présentant des poches d'eau. Pour un tel système le signal de relaxation sera tri-exponentiel, avec une exponentielle pour les protons non-échangeables, une exponentielle pour la fraction d'eau dans le gel et une exponentielle pour la fraction d'eau contenue dans les poches d'eau.

Cette situation est classiquement observée dans les tissus végétaux. Les signaux de relaxation multi-exponentiels obtenus dans ce cas sont expliqués par les limites à la diffusion entre les différents compartiments hydriques et sont souvent attribuées aux différents compartiments de la cellule végétale (Hills et al., 1990; Ratcliffe, 1994). De plus, du fait de l'organisation et de la composition des différents compartiments les protons de l'eau de la paroi, des chloroplastes, de la vacuole... ne relaxent pas avec les mêmes temps de relaxation. Les mécanismes décrits précédemment affectent la relaxation T_1 et T_2, mais du fait de la plus grande sensibilité des T_2 à la composition de chaque compartiment, ce dernier est plus souvent utilisé pour étudier les états hydriques des végétaux (Snaar and Van As, 1992).

Dans la plupart des tissus végétaux la composante du signal RMN ayant le T_2 le plus long et l'amplitude la plus importante, est généralement associée à l'eau de la vacuole. En plus de la composition et de la nature des solutés, le T_2 sera influencé par la taille de la vacuole et la perméabilité membranaire (Van As, 2007). Une grande vacuole favorisera des temps de relaxation élevés, tandis qu'une petite vacuole présentera des temps de relaxation faible. Tous les solutés n'influencent pas le

signal de l'eau de la même manière; le T_2 moyen de la feuille de blé est par exemple corrélé négativement à la concentration de protéines et ceci est dû en partie aux échanges de protons entre protéines (Nagarajan et al., 2005). D'autres solutés tels que les ions paramagnétiques comme Mn^{2+} par exemple modifient drastiquement ce signal (Bacic and Ratkovic, 1984) en raison uniquement de leur moment magnétique électronique très élevé. En effet cet ion affecte le signal de relaxation des protons de l'eau avec laquelle il est en interaction (la valeur du T_2 diminue). Les importants progrès sur l'attribution des autres composantes du signal RMN ont été réalisés grâce à l'utilisation de cet ion ; Snaar *et al*, (1992) ont décrit le signal de relaxation T_2 en trois exponentielles dans les tissus de pomme. Une composante avec un T_2 proche d'1 seconde et qui représente 75% du signal, une deuxième avec un T_2 de 190ms et 16% du signal et la dernière avec un T_2 de 30 ms. En appliquant du Mn^{2+} sur les tissus, ils ont observé les variations des différents T_2. En partant du modèle simple où les ions manganèse vont tout d'abord diffuser dans l'espace intercellulaire, puis dans le cytosol et ensuite dans la vacuole les auteurs ont pu attribuer chacune des composantes du signal RMN à un compartiment. En effet, ils ont tout d'abord observé une forte diminution des T_2 de la composante ayant un T_2 de 30 ms, avant stabilisation. La composante avec un T_2 initial autour de 190ms présente elle aussi une forte diminution du T_2 mais qui commence plus tardivement après l'application de manganèse. La dernière composante à être modifiée par le manganèse est la composante vacuolaire. Ainsi, sur la base de ces cinétiques de variation des T_2, ils ont proposé les attributions suivantes : la composante la plus courte serait celle de la paroi (eau extracellulaire), la composante avec un T_2 de 190 ms serait l'eau dans le cytosol et la composante ayant un T_2 plus long serait l'eau de la vacuole. Cette étude a été réalisée sur le parenchyme des fruits de pommes où les cellules sont relativement homogènes, cependant il ne faut pas perdre de vue que dans d'autres échantillons végétaux ces différentes exponentielles peuvent également être associées à une hétérogénéité cellulaire. Ainsi le mésophylle d'une feuille est composé de différents parenchymes très hétérogènes en termes de quantité d'air, d'eau ou même de volume cellulaire ; on peut donc s'attendre à un signal RMN différent entre ces parenchymes. Dans ce cas, les composantes du signal RMN ne seraient plus attribuées aux différents compartiments hydriques au sein des cellules, mais à des compartiments hydriques de même nature mais de volume ou de composition différents du fait de l'hétérogénéité cellulaire entre tissus (Qiao et al., 2005). Par exemple deux temps de relaxation peuvent être identifiés si l'hétérogénéité de taille de cellules est suffisamment large pour entrainer des T_2 différents en fonction de la taille des vacuoles, dans ce cas le signal RMN sera caractérisé pas deux composantes vacuolaires.

Le signal RMN permet donc de mesurer la quantité et l'état de l'eau dans les différents compartiments d'un tissu végétal et même si l'attribution précise des composantes du signal à chaque compartiment fait encore l'objet de débats, la sensibilité de la relaxation RMN à l'hétérogénéité au sein de la cellule ou du tissu en fait un indicateur très sensible pour étudier la structure et/ou la composition cellulaire des tissus végétaux et mesurer l'impact de la croissance, du développement et

de l'environnement sur ces structures a fortiori si le statut hydrique est perturbé. La RMN a ainsi régulièrement été appliquée à l'étude de la réactivité aux stress abiotiques chez les végétaux. Par exemple Mc Cain *et al*., (1990) a étudié la nature du signal RMN de feuilles issues de plants de pomme de terre cultivés dans un milieu très riche en manganèse. Cette démarche a permis de mettre en évidence que l'accumulation de Mn^{2+}, lors d'un fort excès, se faisait majoritairement dans les vacuoles des vieilles feuilles. Les résultats semblent différents de ceux décrits précédemment car il n'y a pas eu d'application directe de manganèse sur le tissu mais bien un prélèvement racinaire et un stockage dans la vacuole contrôlé. Des études RMN portant sur les effets et la tolérance au stress hydrique ont été menées sur les feuilles de certaines espèces comme le blé (Gambhir et al., 1997) par exemple. Ces études ont consisté à comparer le signal RMN des feuilles de variétés, ayant des comportements différents lors d'un stress hydrique ou à évaluer les effets du stress sur la répartition et l'état de l'eau dans la cellule. Bien que moins souvent utilisés, les T_1 ont aussi permis de mettre en évidence sur une feuille l'effet du froid (Kaku, 1993) ou de la déshydratation (Kaku and Iwayainoue, 1990) démontrant une relation linéaire entre le T_1 et le contenu en eau entre 75 et 95% de teneur en eau. Par ailleurs la stabilité des membranes au sein des végétaux peut être étudiée par RMN. En effet, les changements d'état voire la déstructuration de ces dernières provoquent des changements dans la compartimentation de l'eau et des solutés (Raison et al., 1980) et par voie de conséquence des modifications des coefficients de diffusion de l'eau et du signal RMN correspondant. Par exemple, l'état des membranes lipidiques au sein de la cellule est très influencé par la température et lorsque celle-ci est trop élevée, les membranes se déstructurent libérant ainsi tous les constituants du compartiment (Schreiber and Berry, 1977). Cette altération des membranes peut être détectée à travers le relargage d'ions (Marcum, 1998) mais provoque aussi une diminution brutale du T_2 de l'eau qui passe de 120 ms à 44°C à 85ms à 48°C dans des feuilles de blé (Maheswari et al., 1999). Il est à signaler qu'avant cette température critique (entre 30°C et 42°C), le T_2 diminue légèrement avec l'augmentation de la température. Ce type d'étude a aussi permis de caractériser la déshydratation de feuilles de poirier (Larher et al., 2009) ou l'effet de la congélation chez la carotte (Hills and Nott, 1999), ou la pomme (Hills and Remigereau, 1997). L'étude des T_1 a aussi permis de mettre en évidence les effets d'un stress biotique sur la feuille. En effet les galles, provoquées par différents insectes, allongent le T_1 des tissus foliaires proches chez différents arbres (*Machilus, Zelkova* et *Cinnamomum*)(Kaku and Iwayainoue, 1990).

Plusieurs études RMN ont été également appliquées à l'analyse des graines et ont mis en évidence un lien entre le signal RMN, la viabilité (Krishnan et al., 2004), le pouvoir germinatif (Krishnan et al., 2004) mais aussi l'impact de stress abiotiques sur la graine en développement. Ainsi Krishnan *et al*., (2014) ont observé à partir de maïs cultivé en condition de stress azoté, une diminution du T_2 de la troisième composante, la plus importante du signal, dans le grain au cours du remplissage. Le T_2 de cette composante diminue de 420 à 360ms entre les plantes carencées et non carencées. De la même manière, un stress hydrique provoque un changement de compartimentation de l'eau dans les graines de soja en développement (Krishnan et al., 2014). Il est important de souligner à ce stade que

l'attribution du signal de relaxation dans le cas des graines est plus complexe que dans celui des feuilles ou des tissus fortement hydratés. En effet dans le cas des graines, la présence de polysaccharides, de protéines et de lipides peut aussi être à l'origine du comportement multi-exponentiel de la relaxation. Pour ce type de tissu, le comportement multi-exponentiel est donc expliqué à la fois par une hétérogénéité de répartition hydrique mais aussi par la composition complexe de la matrice.

Les études citées précédemment impliquaient la mise en œuvre de prélèvements destructifs au sein des feuilles ou des tissus limitant ainsi la réalisation d'études dynamiques et cinétiques. Néanmoins, les avancées techniques ayant permis la création d'appareils de RMN avec des aimants dits de surface ; il est aujourd'hui possible de réaliser des mesures par simple contact, non dégradant, avec la feuille. Cette démarche est illustrée par les travaux de Capitani *et al* (2009) qui montrent des variations des temps de relaxation en fonction de l'état hydrique de la feuille de différentes espèces. Ces mesures sont encore peu précises notamment en raison de l'hétérogénéité du champ magnétique de l'aimant de surface. Le perfectionnement de tels appareils laisse espérer des mesures précises directement *in situ* dans les prochaines années. Des aimants ont déjà été conçus afin de permettre la mesure de signal des tiges de *Ricinus cummunis* directement sur des plantes en croissance (Peuke et al., 2006)mettant en évidence des changements dans le signal RMN des vaisseaux conducteurs en réponse à un stress hypothermique. Très récemment, des aimants portables ont été appliqués au même type de mesure et ont été testés avec succès sur *Phaseolus vulgaris* et *Populus nigra* (Windt et al., 2006). Enfin l'utilisation de l'Imagerie par Résonance Magnétique dans le cas des tissus végétaux présentent des perspectives très intéressantes. Sardans et al,. (2010) ont réussi à suivre la progression spatiale de la déshydratation d'une feuille de chêne (Figure 12) mettant en évidence son caractère basipète. Cependant si l'IRM donne une cartographie des temps de relaxations, la spectroscopie RMN fournit un signal permettant une analyse plus fine de la matrice étudiée.

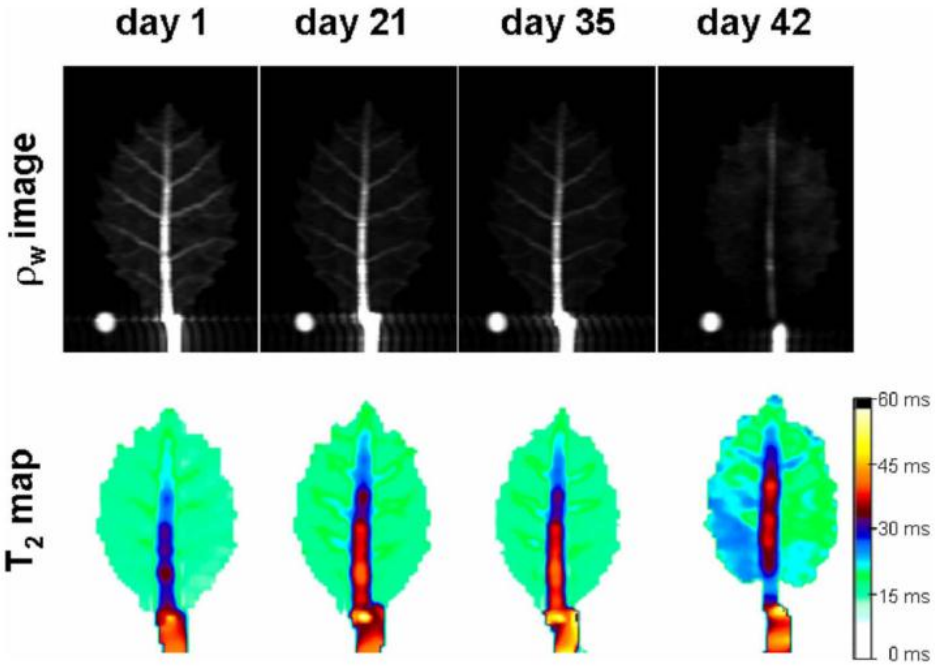

Figure 12: Images de la densité des protons **(ρ_w)** et carte des T_2 dans des feuilles de chêne à différents temps après l'arrêt d'arrosage d'après (Sardans et al., 2010)

MATERIALS AND METHODS

Material and Method

The description of materials and methods of the different chapters have been presented in the same paragraph, except when different protocols were used. In this case, the heading of the text is followed by the mention of the concerning chapter as indicated below:

1: Chapter 1; a : Musse et al, 2013; b : Sorin et al 2014

2: Chapter 2; a : Nitrogen depletion; b : Water stress

Plant material and sampling

Plant material, experimental design and growth conditions[1a]

About 100 seeds of oilseed rape Brassica napus L., genotype Tenor, were individually weighed and the 45 most homogeneously sized seeds selected. Each working day for 3 weeks, 3 seeds were sown in individual containers filled with a growing medium (FALIENOR 9226-6F2) containing 65% light peat, 20% dark peat and 15% perlite. Three-week-old seedlings were individually planted into two-liter pots filled with the same growing medium and grown in a growth cabinet for 5 weeks (fig 1 A). Plants were watered throughout the growing period, with a fertilizing solution (Liquoplant bleu) used at 3‰ and irrigation was adjusted to the evaporation-transpiration rate of the pots. The growth cabinet conditions were 14hr daylight (at 200 µmol photons m-2 s-1) and 10hr dark (relative humidity: 75/90 %; temperature: 20/18 °C).

Sixteen of the forty-five plants (P-1 to P-16) were selected (1 out of every 3 plants analyzed) in order to obtained homogeneous plants with a wide range of leaf development status, characterized by non-destructive measurement of chlorophyll content.

Direct measurements of leaf water status were performed in an additional experiment on the plants grown in same conditions as described above. For these measurements, 10 seeds were sown, 6 three-week-old seedlings were individually planted and thereafter 4 plants were selected (P-17 to P-20).

Sampling [1a]

For the sixteen plants selected (P-1 to P-16), leaf tissues were collected from six leaves (four senescing leaves, one mature and one young leaf) for NMR measurements, and microscopy studies were performed on the same leaves as for NMR analysis but for only five plants (plants P-1, P-5, P-6, P-10 & P-11). Starch was quantified for all leaves from all fifteen plants, and molecular analyses were performed for all leaves from five plants (plants P-1, P-6, P-11, P-12 & P-13).

Six leaf discs of 8 mm in diameter were cut from the limb tissue for the NMR experiment. In order to obtain homogeneous tissues, discs were taken from each side of the central vein as close as possible to the vein by avoiding lateral nervures. Discs were then placed in NMR tubes which were closed with a 2-cm long Teflon cap to avoid water loss during measurements.

For microscopy studies, 18 leaves from five plants were analyzed. About 30 1-mm² leaf samples per leaf were taken with a small punch around the discs used for NMR analysis. The leaf samples were immediately fixed in a solution of 2.5% m/v glutaraldehyde and 2% m/v paraformaldehyde in 0.1 M phosphate buffer, pH 6.8.

For starch quantification and for gene expression, two sets of 20 leaf discs (diameter of 8 mm) were collected from all leaves near the location where NMR and microscopy were performed, then frozen in liquid nitrogen and stored at 80° C.

For the direct measurements of leaf water status, 5 leaves (leaf ranks 1, 2, 4, 6 and 8) were selected from each plant (P-17 to P-20). Prior to leaf water status measurements, NMR measurements were performed on all selected leaves.

Plant material, experimental design and growth conditions [1b]

About 10 seeds (homogenous weight) of oilseed rape, *Brassica napus* L., genotype Tenor, were sown in individual containers filled with a growing medium (FALIENOR 9226-6F2) containing 65% light peat, 20% dark peat and 15% perlite. Four sowings (series S-1, S-2, S-3, and S-4) were undertaken at one-week intervals. The 8 most homogenous three-week-old seedlings of each series were individually planted into four-liter pots filled with the same growing medium and grown in a growth cabinet for five (t1) to twelve (t8) weeks (Figure1 B). The 32 plants used for this experiment were watered throughout the growing period, with a fertilizing solution (Liquoplant bleu) used at 3‰ and irrigation was adjusted to the evaporation-transpiration rate of the pots. The growth cabinet conditions were 14hr daylight (at 200 µmol photons m-2 s-1) and 10hr dark (relative humidity: 75/90%; temperature: 20/18°C).

Sampling [1b]

For all series, one plant was taken each week for 8 weeks (week1 to week 8) and all the leaves for each plant were numbered according to their rank (L-1 for the first leaf after the cotyledon).

Six to ten leaf discs of 8 mm in diameter were cut from the limb tissue for the NMR measurements to sample similar tissue weights. In order to obtain homogeneous tissues, discs were taken from each side of the central vein as close as possible to the vein and avoiding lateral nervures. Discs were then placed in NMR tubes which were closed with a 2-cm long Teflon cap to avoid water loss during measurements. Leaf discs were also collected for microscopy studies from selected plants

and leaf ranks,. The rest of the leaf limb was frozen in liquid nitrogen and kept at -20°C to be subsequently ground and freeze-dried for starch quantification.

For microscopy studies, mesophyll tissues were collected from series 4 (S-4) plants, from three leaves (leaf ranks 4, 6, and 8) at three times (weeks 3, 4, and 5). Five bands 3-millimeters wide and 1-centimeter long were taken perpendicularly to the central vein. In order to confirm our vacuolar volume approximation, in the first plant five bands were also collected alongside the central vein. After sampling, the fixative solution (phosphate buffer 0.1 mol. L-1 p H 7.4 (PB), 3% (w/v) glutaraldehyde) was infiltrated into the leaf tissues using 10 cycles of depressurization with a vacuum pump (5 min of low pressure in each cycle). Samples were returned to the same fixative solution for 24 h at 4°C and then were washed in PB and dehydrated in a graded series of increasing concentrations of ethanol (50, 70, 90 and 100% v/v). Samples were kept in pure ethanol for 12 h at 4°C.

Plant material, experimental design and growth conditions [2a]

Twenty oilseed rape seeds (homogenous weight) of each Aviso and Express genotype were sown in individual containers filled with a growing medium (FALIENOR 9226-6F2) containing 65% light peat, 20% dark peat and 15% perlite. Eight homogenous three-week-old seedlings of each genotype were individually planted into four-liter pots filled with the same growing medium and grown in a growth chamber. Growth chamber conditions were 14hr daylight (at 200 µmol photons m-2 s-1) and 10hr dark (relative humidity: 80 %; temperature: 22°C/17°C). After three weeks in the growth chamber, the newest leaf of each plant was tagged and referred as the tag 0. Plants were then progressively submitted to a six-week vernalization period (4°C). At the end of this period, the conditions were progressively returned to the initial values. The initial quantity of N available in each pot was assumed to be around 180 kg.ha-1. At the end of the vernalization period control plants were supplied with nitrogen by three inputs of NH4NO3 (one each week) in order to reach 240 kg.ha-1 . The N deficient plants did not received any supplementary N. Leaves were sampled four weeks after the end of the vernalization period, at the beginning of N starvation.

Sampling [2a]

All measurements were performed on the five oldest leaves of each plant. Two older and three younger leaves compared to the reference senescing leaf (tag 0) from Aviso and Express plants grown in optimal and nitrogen deficiency conditions were analyzed. All the leaves sampled were immediately imaged in front of a reference in order to determine leaf area.

Plant material, experimental design and growth conditions [2b]

About 80 seeds (homogenous weight) of oilseed rape *Brassica napus* L., genotype Aviso, were sown in individual containers filled with a growing medium (FALIENOR 9226-6F2) containing 65%

light peat, 20% dark peat and 15% perlite. The 72 most homogenous three-week old seedlings of each series were individually planted into four-liter pots filled with the quantity of growing medium. They were grown in a growth cabinet for five weeks. The growth cabinet conditions were 14hr daylight (at 200 µmol photons m-2 s-1) and 10hr dark (relative humidity: 75/90 %; temperature: 20/18 °C). A six weeks vernalization period was applied in the growth cabinet (4°C). All plants used for this experiment were watered throughout the growing period, with a fertilizing solution (Liquoplant bleu) used at 3‰ and irrigation was adjusted to the evaporation-transpiration rate of the pots. Plants were then put in greenhouse condition (relative humidity: 75/80 %; temperature: 24/18 °C) during three to five weeks depending of the sampling time. After three weeks in greenhouse all plants were flowering and the watering was stopped on 56 of them.

Sampling[2b]

For each condition (watered or stressed) eight plants were used at each sampling, four for NMR and physiological measurement (*i. e.* chlorophyll content and yield) and four for hydric parameters measurement (*i. e.* stomatic operture, leaf water and osmotic potential). Stressed plants were sampling 7, 9, 11, 14, 16, and 18 days after the water stop whereas watered plants were sampled only after 9, 16 and 18 days. At each sampling date measurement were performed on the tagged leaf and the three leaf rank under if present.

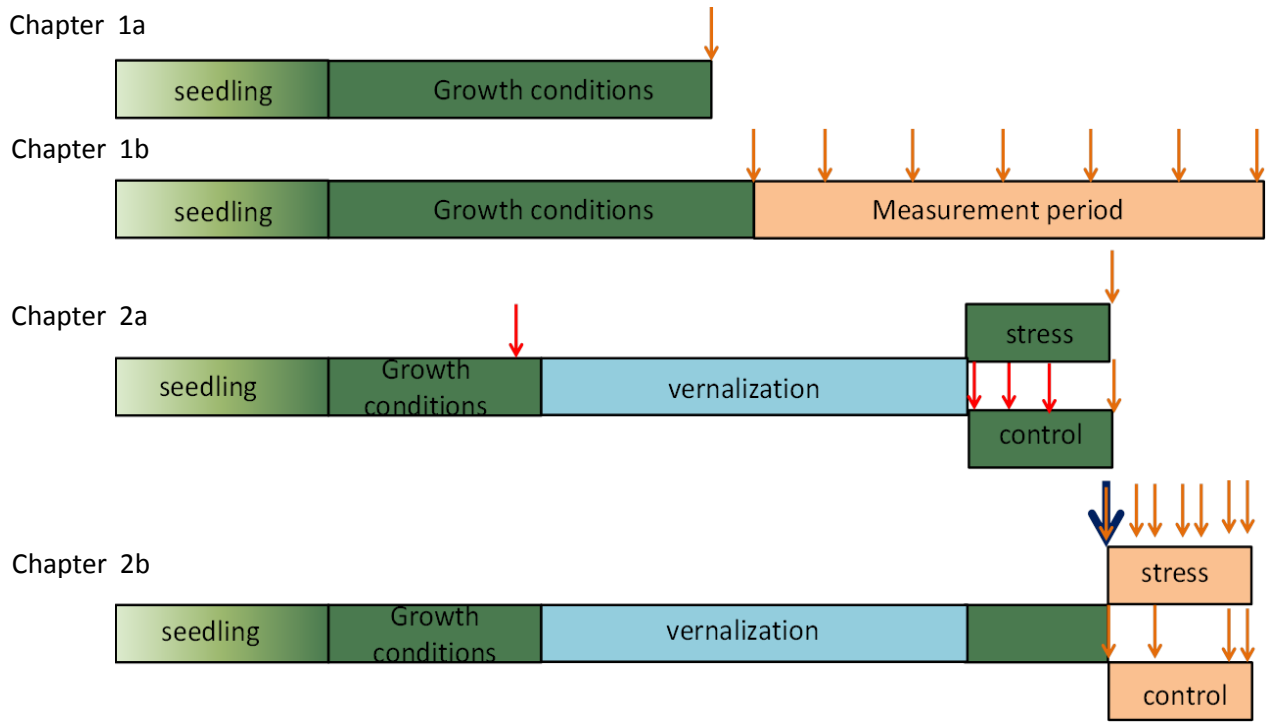

Representative schema of the experimental growth conditions used in the present work. Orange arrow correspond with the sampling date, red arrow to Nitrogen input and Blue arrow correspond with the date of the watering stop.

Dehydration procedure[2b]

Leaves of three different leaf ranks (2, 4, and 6) were taken from four plants grown in the same conditions as present in Figure 1A. Ten leaf discs were sampled on each leaf, and immediately weighted. The ten leaf discs were rehydrated in distilled water for 1h in dark conditions and then weighted before placed in a NMR tube and submitted to two dehydration cycle, each made of 10 minute of slow N-flux in the NMR tube. NMR measurements were performed immediately after sampling, after rehydration and after each dehydration cycle.

NMR Relaxometry

Depending of the leaf size, six to eight discs of 8 mm in diameter were cut from the limb tissue for the NMR experiment. In order to obtain homogeneous tissues, discs were taken from each side of the central vein, as close as possible to the vein and avoiding lateral nervures. Discs were then placed in NMR tubes which were closed with a 2-cm long Teflon cap to avoid water loss during measurements.

NMR Relaxometry measurements were performed on a 20 MHz spectrometer (Minispec PC-120, Bruker, Karlsruhe, Germany) equipped with a thermostatted probe. The temperature was set at 18°C. T_2 was measured using the combined FID-CPMG sequence. The FID signal was acquired from 11 µs to 70 µs at a sampling decay of 0.4 µs. For the CPMG measurements, the 90°-180° pulse spacing τ was 0.1 ms and the signal of a single point at the echo maximum was acquired. Data were averaged over 64 acquisitions. The number of successive echoes recorded was adjusted for each sample according to its T_2. The recycle delay for each sample was adjusted after measurement of the T_1 with a fast-saturation-recovery sequence. The total time of acquisition of data for T_2 (including spectrometer adjustments and T_1 measurement) was about 10 min per sample.

Fitting was performed in two steps: first T_2 relaxation curves from the CPMG data only (after removing the FID signal from the combined FID-CPMG signal) were fitted by Scilab software according to the MEM (Mariette et al., 1996), which provides a continuous distribution of relaxation components without any assumption concerning their number. In this representation, the peaks of the distribution are centered at the corresponding most probable T_2 values, while peak areas correspond to the intensity of the T_2 components. Then, T_2 relaxation curves obtained by the combined FID-CPMG sequence were also analyzed using the Levenberg-Marquardt algorithm which allows a discrete solution for the complete fitting curve according to the equation:

Eq. 1: $$I(t) = I_1 \exp(-t/T_{21})^2 + \sum_{i=2} I_{R0i} \exp(-t/T_{2i}) + offset$$

where I_{R0i} is the relative intensity of the i_{th} exponential at the equilibrium state and T_{2i} the characteristic transverse relaxation time for the i_{th} exponential. The number of terms that best described the relaxation curve was determined by examining the residual plots and the values of the coefficient of determination.

Leaf samples were weighed within the NMR tubes before and after each NMR experiment in order to check possible water loss during the measurements. At the end of the NMR experiments, samples were transferred to laboratory cups and dried in an oven at 103°C[1] for 16h (70°C for 24h[2,3]). The water content (expressed as percentage of fresh matter), dry matter, fresh matter and water masses were calculated. Specific leaf water weight per component (LWWi) was computed according to the equation:

Eq. 2:
$$LWW_i = \frac{I_{R0i}\, x\, m_w}{A}$$

where mw corresponds to water mass of the NMR sample made of six leaf discs in g, A to the area of the discs in m2 and I_{R0i} to the relative intensity of the i_{th} NMR signal component as %.

Physiological and biochemical measurement

Starch quantification [1, 2a]

Starch was quantified according to the method proposed by Smith (Smith and Zeeman, 2006). Starch was extracted from 30 mg dry weight of freeze-dried lamina leaf tissue using 1 mL phosphate buffer (0.2 mol. L^{-1}, pH 6.5) for 20 min at 95°C. The supernatant was collected after centrifugation at 14,000 x g for 5 min at 4°C. The extraction step was repeated twice and the supernatants were pooled. Starch quantification was performed following the manufacturer's recommendations (Sigma, # STA20) after hydrolysis by α-amylase and amyloglucosidase. Starch content was expressed in glucose equivalent after subtraction of free glucose content.

Starch quantification

Water content [1, 2]

Water content (WC) was measured on all leaf discs sampled for NMR relaxometry by weighing before (fresh weight) and after drying (dry weight) in an oven at 103°C[1] for 16h (70°C for 24h[2,3]). WC was expressed as percentage of fresh weight.

CAB/SAG molecular markers [1a]

RNA extraction

Total RNA was extracted from 500 mg fresh weight of frozen lamina leaf tissue. The RNA isolation protocol based on phenol extraction and lithium chloride precipitation was applied as described by Verwoerd *et al.* (1989). The quantity and quality of RNA samples were assessed by spectrophotometry with a NanoDrop ND 1000.

RT-PCR analysis

Total RNA (2 µg) treated with RNase-free DNase I (Fermentas, Thermo Fisher Scientific Inc., Waltham, MA, USA) was reverse transcribed with Moloney murine leukemia virus reverse transcriptase (M-MLV RTase) (Q-BIOgene, MP Biomedicals, Illkirch, France) following the manufacturer's recommendations. PCR reactions were performed using specific primers for *Brassica napus Cab* gene *LHCII type I* (AY288914) (forward primer 5'-GGCAGCCCATGGTACGGATC-3' and reverse primer 5'-CCT CCITCGCTGAAGATCTGT-3'), primers shared by *SAG12-1* (AF089848) (forward primer 5'-GTTTTGTTTAGCCAAAGTCAAACA-3' and reverse primer 5'-CGGCGGAAGATTGGCT-3') and primers designed from *Arabidopsis thaliana EF1α* (X16430) (forward primer 5'-GTTTTGTTTAGCCAAAGTCAAACA-3' and reverse primer 5'-CGGCGGAAGATTGGCT-3'). All the PCRs were performed with Q biogen Taq polymerase for 35 cycles for *EF1α* , 27, 29 and 31 cycles for *SAG12-1* and 22, 24 and 26 cycles for *Cab*. After 5 min at 95°C, RT-PCRs were performed by cycles including 15s at 95°C, 40s at 60°C and 72°C for 1 min, and one cycle at 72°C for 10 min. Products of 183 bp, 587 bp and 290 bp were amplified from *BnEF1α*, *BnSAG12-1* and *BnCab* gene cDNAs, respectively, as verified by sequencing. RT-PCR products were separated by agarose gel electrophoresis. Each PCR product was quantified using image J software and normalized using the intensity of the *EF1α* RNA signal. For all RT-PCR reactions, *EF1α* RNA was used as a cDNA synthesis and amplification control. Relative expressions of *Cab* and *SAG12-1* were determined with reference to the maximum and represented the mean of PCR products obtained after different PCRs with various numbers of cycles.

Chlorophyll content [1, 2]

Before sampling[1] (one day before sampling) [2], relative chlorophyll content per unit of leaf area was determined using a non-destructive chlorophyll meter SPAD (Soil Plant Analysis Development; Minolta, model SPAD-502). Chlorophyll content of each leaf was estimated as an average value of 6 to 8 independent measurements. It has been demonstrated that relative SPAD value depends on chlorophyll content in a linear manner (Monje and bugdee 1992).

Chlorophyll fluorescence yield [1, 2]

Before sampling[1] (one day before sampling) [2], chlorophyll fluorescence yields (Fv/Fm) were measured on all leaves studied using a portable chlorophyll fluorometer (Hansatech Handy PEA). Measurements were carried out near the central vein, after a dark adaptation time of 10 min.

Nitrogen quantification [2a]

Elemental analyses of nitrogen content were performed at the Centre Régional de Mesures Physiques de l'Ouest (CRMPO, University of Rennes 1, Rennes, France) and were obtained by the complete combustion and chromatography method with a FlashEA 1112 CHNS/O analyzer (Thermo Electron Corporation, Thermo Fisher Scientific Inc., Waltham, MA, USA).

Water relations [1,2b]

Water content (WC), relative water content (RWC), leaf water potential (ψ_w) and leaf osmotic potential at that RWC (ψRWC), were measured as described previously (Leport et al., 1999). The turgor pressure (T) was calculated as:

Eq. 6 $$T = \psi_w - \psi RWC$$

The water deficit (WD)[1a] was calculated as:

Eq. 7 $$WD = 1\text{-}RWC$$

Stomatal conductance [2b]

Stomatal conductance was measured on all leaves before sampling using AP4 Leaf Porometer. Depending of the leaf size two to four measurements were realized on each leaf.

Water and Osmotic potential[2b]

Leaf water potential (ψ_w) was determined as the petiole xylem pressure potential using the Scholander-type pressure chamber (Model 1000, PMS Instrument Co., Albany, OR, USA).Leaf osmotic potential (ψ_S) was estimated by measuring osmolality of crushed leaf juice with a freezing-point osmometer (Model 13DR, Roebling, Berlin,Germany).

Electron and light microscopy

Sample preparation[1a]

After sampling, the fixative solution (2% (w/v) paraformaldehyde, 2.5% (w/v) glutaraldehyde) was infiltrated into the leaf tissues using 5 cycles of depressurization with a vacuum pump (15 min of low pressure in each cycle). Samples were replaced in the same fixative solution for 24 h at 4°C. After extensive washing in 0.2 mol. L^{-1} phosphate buffer (PB, pH 6.8), samples were incubated for 60 min in 2% (w/v) tannic acid solution in PB, washed in PB and post-fixed for 90 min with 2% (w/v) osmium tetroxide. Samples were then washed in PB and dehydrated in a graded series of increasing concentrations of ethanol (50, 70, 90 and 100% v/v).

Pure ethanol was then replaced by propylene oxide and samples were gradually infiltrated with increasing concentrations (30, 50, 70 and 100% v/v) of epoxy resin (mixed with propylene oxide) for a minimum of 3 h per step. Samples were left overnight in epoxy resin. Infiltration with DMP30-epoxy resin was continued the next day for 3 h. Samples were finally embedded in a new mix of DMP30-epoxy resin and polymerized at 60°C for 24 h.

Sample preparation[1b, 2b]

Five bands 3-millimeter in wide and 1-centimeter in length were taken perpendicularly to the central vein. After sampling, the fixative solution (phosphate buffer 0.1 mol. L-1 p H 7.4 (PB), 3% (w/v) glutaraldehyde) was infiltrated into the leaf tissues using 10 cycles of depressurization with a vacuum pump (5 min of low pressure in each cycle). Samples were replaced in the same fixative solution for 24 h at 4°C and were then washed in PB and dehydrated in a graded series of increasing concentrations of ethanol (50, 70, 90 and 100% v/v). Samples were kept in pure ethanol for 12 h at 4°C.

For light microscopy, samples stored in pure ethanol were progressively included in an acrylic resin (LRWhite) using a graded series of increasing concentrations of resin solubilized in ethanol (20, 40, 60, 80, and 100 % v/v). Polymerisation was performed at 55°C over 4 days.

For transmission electron microscopy analysis (TEM), ethanol in samples was replaced by propylene oxide by two baths (50 and 100% v/v). Then the propylene oxide was replaced by an epoxy resin (EPON) using the same method (50 and 100% v/v) and the sample was kept for one night at 4°C in an EPON solution. Polymerisation was performed over 1 day at 55°C and 60H at 72°C.

Micrograph acquisition[1,2]

For photonic microscopy, thin sections (500 nm[1a] or 1µm[1b,2]) were cut with a UCT LEICA ultramicrotome and stained with toluidine blue before they were observed with a NIKON Eclipse 80i microscope.

[1a]For transmission electron microscopy analysis (TEM), ultra-thin sections (80 nm) were then cut with a UCT LEICA ultramicrotome, placed on grids post-stained for 60 min with uranyl acetate and then for 20 min with lead citrate and viewed with a JEOL 1400 TEM supplied with a GATAN Orius camera.

[1b]Ultra-thin sections (60 nm) were then cut with an ultramicrotome (LEICA RM 2165),and placed on grids post-stained for 60 min with uranyl acetate. The ultra-thin sections were then examined with a JEOL JEM 1230 transmission electron microscope with an accelerating voltage of 80 kV

Model[1a]

A simplified model similar to that employed by McCain et al (McCain, 1995) was used to interpret microscope images. Our model took into account only the palisade layer and assumed it to be an ordered arrangement of water-filled cells with an ellipsoidal shape. It was also assumed that cell width was equal to cell depth, wall thickness was uniform over the cell and that chloroplasts covered all the inner surface of cell walls while the hyaloplasma contained a negligible water fraction of the cell. As the focus was on the layer that was most affected by senescence, where most of the chloroplasts can be found, the spongy layer was not taken into consideration.

An example of the optical microscope images used for estimation of cell and vacuole dimensions is shown in Figure 1-a-10A. The optical microscope images were also used to measure the perimeter of the cell wall, and its thickness was estimated from MET images (Figure 1-a-10B).

The vacuole ($V_{VACUOLE}$), chloroplast ($V_{CHLOROPLAST}$) and wall (V_{WALL}) volumes were estimated using the model according to following equations:

$$V_{VACUOLE} = 3/4\pi \times 1/8 \times [W_v^2 \times L_V] \quad \text{Eq. 3}$$

$$V_{CHLOROPLAST} = 3/4\pi \times 1/8 \times [(W_C^2 \times L_C)-(W_V^2 \times L_V)] \quad \text{Eq. 4}$$

$$V_{WALL} = 3/4\pi \times 1/8 \times [((W_C + 2W_W)^2 \times (L_C + 2W_W))-(W_C^2 \times L_C)] \quad \text{Eq. 5}$$

where W_C is cell width, L_C cell length, W_V vacuole width, L_V vacuole length, L_W wall length and W_W wall thickness. W_C and L_C do not include the cell wall.

Microscopy images were analyzed using ImageJ software. The images were first manually segmented and quantitative data related to cell structure were then extracted from the two youngest and the two most senescent leaves analyzed. Data were expressed as percentage of the total cell volume in order to compare the evolution of the relative volume of the different compartments with that of the intensity of the different NMR signal components.

Model[1b]

The area (A) of each cell from both parenchyma was measured using image J software. The width (W) of each cell was also measured and the results from samples taken perpendicularly or parallel to the central vein of the same leaves, were compared (see Annexe 1). No difference was observed between the two types of sample, allowing us to estimate the vacuole volume of each cell by multiplying A by W.

Data analysis

Statistical analyses were performed using the Rstudio software package. In order to detect significant differences ($P<0.05$) between different leaf ranks[1a], and between different weeks of sampling[1b], one-factor ANOVA test was applied to all measurements. The multiple range LSD (Fisher's Least Significant Difference) test was used to compare means of the series and correlations[1b,2] were revealed through Pearson's rank correlation coefficient analysis.

Correlation (PCA)[1a]

Principal component analysis (PCA), defined as an unsupervised descriptive multivariate statistics tool, was performed with R software, package *FactomineR*, on the 50 data sets from 11 plants (P-1, P-3, P-4, P-6, P-7, P-8, P-9, P-11, P-13, P-14 and P-15,), consisting of the changes in 10 multivariate data of the six leaves at different leaf ranks (6 to 1). The multivariate data were: chlorophyll, starch and water content, dry matter, $T_{2(comp.1)}$, $T_{2(comp.3)}$, $T_{2(comp.4+5)}$ (weighted average of $T_{2(comp.4)}$ and $T_{2(comp.5)}$), and $I_{0(comp.2)}$, $I_{0(comp.3)}$ and $I_{0(comp.\ 4+5)}$ corrected for the receiver gain and the sample weight.

CHAPTER 1

Cell and tissue modifications during oilseed rape senescence revealed though NMR relaxometry

CHAPTER 1

The first chapter is dedicated to the investigation of the leaf senescence throughout NMR relaxometry. This chapter consists of two publications entitled "*Structural Changes in Senescing Oilseed Rape Leaves at Tissue and Subcellular Levels Monitored by Nuclear Magnetic Resonance Relaxometry through Water Status*" and "*Assessment of nutrient remobilization through structural changes of palisade and spongy parenchyma in oilseed rape leaves during senescence*". Understanding the processes involved in leaf senescence is a major goal for improving oilseed rape NRE. While biochemical and molecular aspects of leaf senescence and processes involved in chloroplast degradation (plast dismantling, senescence associated vacuoles, autophagy,…) have been extensively studied for various species, the structural changes occurring at tissue level are less documented. The purpose of these publications was to demonstrate the sensibility of the T_2 relaxation NMR signal to senescence induced changes at cell and tissue levels. An important aspect of this work was to highlight the relationship between leaf water relations and senescence process. The natural sequential leaf senescence was studied on vegetative plants grown without vernalization, by monitoring leaves according to the leaf rank or age.

Structural Changes in Senescing Oilseed Rape Leaves at Tissue and Subcellular Levels Monitored by Nuclear Magnetic Resonance Relaxometry through Water Status

Maja Musse, Loriane De Franceschi, Mireille Cambert, Clément Sorin, Françoise Le Caherec, Agnès Burel, Alain Bouchereau, François Mariette, and Laurent Leport*

Institut National de Recherche en Sciences et Technologies pour l'Environnement et l'Agriculture, Food Process Engineering Research Unit, F–35044 Rennes cedex, France (M.M., L.D.F., M.C., C.S., F.M.); Université Européenne de Bretagne, 5 Boulevard Laënnec, 35000 Rennes, France (M.M., L.D.F., M.C., C.S., F.L.C., A.Bu., A.Bo., F.M., L.L.); INRA, UMR 1349, Institute for Genetics, Environment and Plant Protection (IGEPP), UMR INRA-Agrocampus Ouest-Université de Rennes 1, 35653 Le Rheu cedex, France (L.D.F., C.S., F.L.C., A.Bo., L.L.); and Microscopy, Rennes Imaging Center, Faculté de Médecine, CS 34317 Rennes cedex, France (A.Bu.)

ORCID ID: 0000-0001-9886-287X (L.L.).

1-a-1 Introduction

The main physiological outcome of leaf senescence is the recycling of organic resources and provision of nutrients to sink organs such as storage and growing tissues (BuchananWollaston, 1997; Hikosaka, 2005; Krupinska and Humbeck, 2008). In crop plants, senescence progresses from the lower older leaves to the younger top leaves. Macromolecular degradation and the mechanism of re-allocation of breakdown products are mediated by up-regulation of senescence-related genes (Lee et al., 2001) in close relationship with both developmental and environmental conditions (Gombert et al., 2010). This leads to remobilization of carbon (C) and nitrogen (N) compounds mostly from plastidial compartments (Martínez et al., 2008; Guiboileau et al., 2012), involving proteolytic activity in plasts, vacuole and cytosol (Adam and Clarke, 2002; Otegui et al., 2005), chlorophyll breakdown (Hoertensteiner, 2006), galactolipid recycling (Kaup et al., 2002) in the plastoglobules (Brehelin et al., 2007) and loading of sucrose and amino acids into the phloem through appropriate transporters (Wingler et al., 2004; Masclaux-Daubresse et al., 2008). In terms of leaf senescence at the cell level where chloroplasts are degraded sequentially, relative organelle volume does not seem to be greatly modified, the vacuole remains intact and in darkness-induced senescence the number of chloroplasts per cell decreases only slightly (Keech et al., 2007). However, major changes in metabolic fluxes and cell water relationships are expected during the senescence program that may be associated with macromolecule catabolism, organic solute synthesis, transport and remobilization and cell structure reconfiguration such as chloroplast evolution to gerontoplast (Hoertensteiner, 2006; Keech et al., 2007; Zhang et al., 2010) through the autophagy process (Wada et al., 2009), accumulation of senescence-associated vacuoles (Otegui et al., 2005) and cell wall degradation (Mohapatra et al., 2010).

The senescent leaves of oilseed rape *(Brassica napus* L.), a major oleiferous crop, generally fall while still maintaining a high N content (about 2.5-3 % (w/w) of the dry matter) (Malagoli et al., 2005). In addition to the environmental impact of this leaking of N out of the plant, the low capacity to remobilize foliar N is associated with a high requirement for N fertilization to meet the potential crop yield (Dreccer et al., 2000). In order to improve the N use efficiency (NUE), new genotypes are being selected for their ability to maintain high yields under limited N fertilization, mainly via improvement of N uptake efficiency and N mobilization from the senescing leaves (Hirel et al., 2007). In Arabidopsis and oilseed rape, N can be remobilized from old to expanding leaves at the vegetative stage during sequential senescence as well as from leaves to seeds at the reproductive stage during monocarpic senescence (Malagoli et al., 2005; Diaz et al., 2008; Lemaitre et al., 2008). Senescence can also be induced by environmental stress such as N starvation (Etienne et al., 2007) or water deficit (Reviron et al., 1992), and propagated from old to mature leaves and delayed in young leaves, suggesting finely tuned high regulation of metabolism at the whole-plant level with consequences for NUE (Desclos et al., 2009). One major challenge to understanding the efficiency of senescence-induced organic resource re-allocation and to highlighting major molecular and mechanistic attributes of nutrient recycling is the monitoring kinetics of the structural re-organization of cell structures. This re-organization will provide nutrients remobilized thought phloem-loading. From a technological and phenotyping point of view, measurement of N remobilization efficiency has already been addressed in crop species and oilseed rape as it is a reliable trait to screen for genetic variability of NUE (Franzaring et al., 2011). However, techniques such as stable isotope feeding are time consuming, destructive and difficult to adapt to large genotype panels. It is therefore important to develop a technique for following changes in water distribution at the cell level in order to understand metabolic reconfigurations occurring throughout senescence.

NMR Relaxometry has been used in several studies to investigate plant cell structure and functioning (Hills and Duce, 1990). The 1H-NMR signal originates almost entirely from water protons because other 1H nuclei in the plant produce much less intense signals as they correspond to molecules that are at a much lower concentration than water. The technique allows measurement of longitudinal (T_1) and transverse relaxation times (T_2) and proton spin density. Water proton relaxation times are related to the rotational and translational mobility of water molecules (Van As, 2007). They are also modified by the mobility and structure of the surrounding macromolecules (i.e. starch, proteins and polysaccharides) through proton exchange (chemical exchange). In plant cells, the water in different cell compartments has different chemical and physical properties, and therefore different bulk T2 values. Moreover, relaxation times are affected by exchange of molecules between different compartments that is determined by water diffusion and therefore by the compartment size and membrane permeability (Van der Weerd et al., 2002). The slow diffusion process between compartments results in multi-exponential behaviour of the relaxation signal. The multi-exponential relaxation reflects water in cell compartments and can therefore be used to study changes in water

distribution and properties at a sub-cellular level and hence be used for estimation of structural and volume transformations in cell compartments. The T_2 relaxation time is more sensitive to small variations in water content and chemical exchange processes than T_1, and is therefore usually preferred. Indeed, differences in T_1 for the different compartments are relatively small, resulting in an averaging effect which results in poor discrimination between water compartments (Van As, 2007).

To date, NMR relaxometry has mainly been used for characterisation of fruit and vegetable tissues and it has been shown to be effective in providing valuable information about cell organization (Sibgatullin et al., 2007). However, although a number of studies have contributed to the interpretation of the NMR results (Snaar and Van As, 1992; Hills and Nott, 1999; Marigheto et al., 2009), this is still not always straightforward as the NMR signal depends both on the nature of the plant tissue and on the NMR measurement protocol. The situation is even more complex in the case of leaves, because leaves contain different tissue types characterized by different cell sizes and structures (Teixeira et al., 2005) and only a few studies involving NMR Relaxometry in leaves have been reported. Changes in T_2 in response to high temperature were investigated in wheat (Maheswari et al., 1999) in order to develop a method for detection of heat injury. McCain et al. (1995) measured the T_2 relaxation time of chloroplast and non-chloroplast water in maple leaves by separating corresponding peaks in an NMR spectrum (McCain, 1995) without taking into account the compartmentalization of non-chloroplast water. Oshita et al.(2006) investigated cell membrane permeability to water in spinach leaves by measuring the T_1 relaxation time of the leaf protoplasts without consideration of the subcellular structure. Qiao et al. (2005) attempted to associate NMR signal components with different chive cells using combined transverse relaxation and restricted diffusion measurements. Finally, Capitani et al. (2009) recently used a portable unilateral NMR instrument to detect the water status of leaves of herbaceous crops, mesophyllous trees and natural mediterranean vegetation under field conditions. Further investigations are therefore necessary to improve leaf characterization by NMR, especially in the attribution of NMR signal components to the tissular and subcellular compartments. Progress in this field would make it possible to use the full potential of non-invasive NMR Relaxometry in plant research and phenotyping.

Using NMR Relaxometry, we describe here the differences in water status which occured at tissue and cellular levels through different leaf ranks of well irrigated oilseed rape plants, from the young leaves at the top of the canopy to the senescing older leaves at the bottom of the plant. The aim of the study was to show that changes that occur in the leaves while senescing can be related to changes in water distribution and cell structure. As these changes are directly linked to the modifications in cell compartment organization, especially those occurring in the chloroplast, vacuole and cell wall due to macromolecule degradation and N and C reallocation processes, this study was designed to contribute to the understanding of these physiological processes.

1-a-2 Results

Changes in physiological traits during leaf development

The whole group of plants grown under homogeneous conditions in a growth cabinet displayed a similar developmental pattern in terms of phenological and physiological status. The different leaf stages (corresponding to leaves of different ages) were collected from eight-week-old plants rank by rank and analyzed for physiological status (Figure 1-a-1).

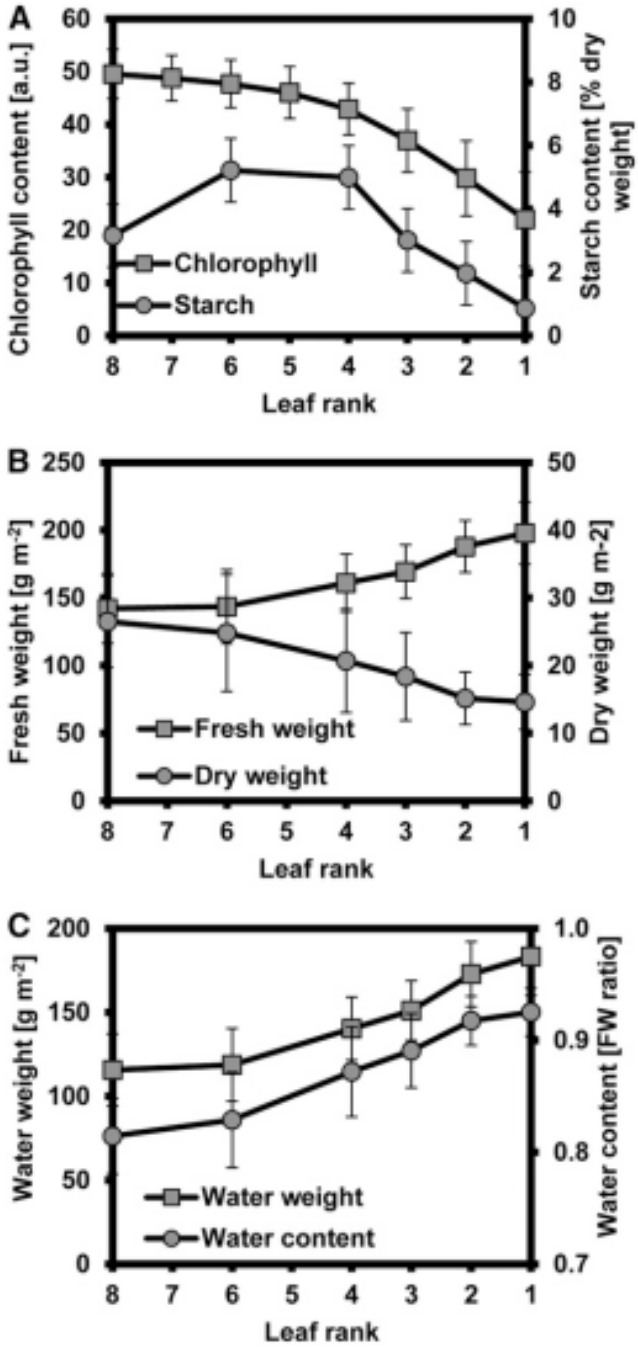

Figure 1-a-1: A) Changes in chlorophyll and starch content, B) fresh and dry weight per leaf area and C) water weight per leaf area and water content in fresh weight ratio in oilseed rape leaves during senescence. Values are means ± standard deviation of sixteen individual plants (P-1 to P-16).

All the individual plants used for measurement had a set of well developed leaves from the youngest green leaves at the top (leaf rank 8) to the yellowish and most senescent leaves at the bottom (leaf ranks 1 and 2). Chlorophyll content, stable from leaf ranks 8 to 6, decreased markedly from leaf rank 4 to 1 (Figure 1-a-1 A). The highest level of starch content was found at around leaf rank 6, again with a decrease in senescing leaves from ranks 4 to 1. Used as global indicators of leaf growth and development, this information ensures the choice of leaf ranks studied through NMR, i.e. rank 8 for younger fully expanded leaves, rank 6 for mature leaves and ranks 4 to 1 for senescing leaves.

Figure 1-a-1 B depicts dry and fresh weights of leaves and Figure 1-a-1 C shows the corresponding water content and water weight data. Dry weight (expressed per m2 of leaf area) decreased from leaf rank 6 to leaf rank 1, whereas a considerable increase in fresh weight and water

content was observed from leaf ranks 6 to 1. The senescence process was clearly associated with hydration (increase in quantity of water per unit leaf area) in leaf tissues whereas dry matter was depleted. This phenomenon was also confirmed in the leaf water status experiment (Figure 1-a-2), in which the increase in water content from the youngest (leaf rank 8) to the oldest (leaf rank 1) leaves was less pronounced but statistically significant. The ANOVA test showed also that differences in leaf water potential and osmotic potential of the youngest (leaf rank 8) and oldest (leaf rank 1) tissues, associated with increase in fresh weight were statistically significant. Turgor pressure, relative water content and water deficit did not change significantly with senescence.

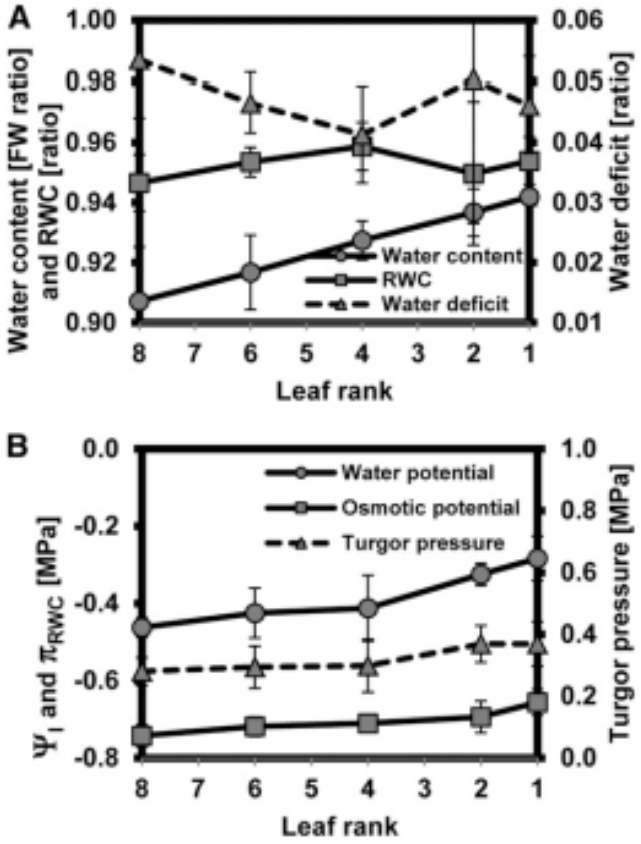

Figure 1-a-2: A) Changes in water content in fresh weight ratio, relative water content (RWC) and water deficit and B) leaf water potential (ψl), leaf osmotic potential (ψRWC) and turgor pressure in oilseed rape leaves during senescence. Values are means ± standard deviation of four individual plants (P-17 to P-20).

Cab/SAG - molecular milestones of leaf development

The physiological characteristics (chlorophyll content, starch deposition & water status) provided a general pattern of leaf development along the plant axis. However, the physiological status of the individual plants studied varied to some extent in terms of leaf development due to growth conditions and heterogeneity of the micro-environment (see standard deviations in Figure 1). In addition, these traits did not make it possible to detect slight physiological variations as the senescence process occurred progressively from one leaf rank to another. In order to evaluate this variability between leaf ranks more precisely, the expression levels of genes previously used to describe the leaf development status of oilseed rape were followed (Gombert et al., 2006). Thus the expression pattern of genes known to be up-regulated (SAG12-1 coding a cysteine protease) or down-regulated (Cab coding a chlorophyll a/b-binding protein) during leaf senescence was established for five plants

throughout the vegetative axes (Figure 1-a-3 A). The concomitant measurement of SAG12 and Cab gene transcript levels provided accurate monitoring of progression of leaf senescence and allowed a theoretical leaf rank to be seen as a critical transition step where the source status took precedence over the sink status (Figure 1-a-3 B). For instance, in the example shown, expressions of Cab and SAG12 were relatively stable from leaf rank 8 to leaf rank 5, while from leaf rank 4 a strong decrease in Cab expression associated with an increase in SAG12 were observed. The theoretical leaf rank differed from plant to plant and was identified in leaf ranks 1 to up to 4 (Table 1). It must therefore be emphasized that, although the plants studied further by NMR displayed homogenous macroscopic phenological traits, individual differences were observed in terms of physiological status of leaves of the same ranks. SAG12/Cab value can be used to target leaves at the same development status, although it does not make it possible to define this status. For example, leaf rank 1 of plant P-1 was comparable to leaf rank 2 of plant P-11 and to leaf rank 3 of plant P-13. In addition, SAG12/Cab results suggested that leaf rank 3 corresponded to a younger leaf in plant P-1 than in plant P-6.

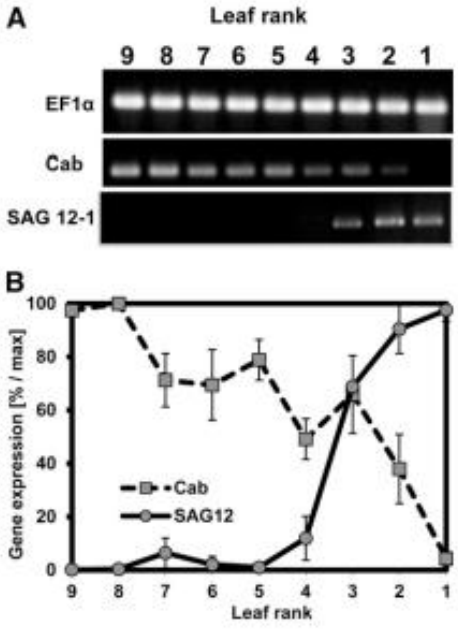

Figure 1-a-3 - Characterization of leaf status in terms of the expression of SAG12 and *Cab* (data from P-13) in oilseed rape leaves during senescence. A) RT-PCR of *SAG12-1* and *Cab* gene expression. *EF1α* was used as a CDNA synthesis and amplification control. B) Determination of the theoretical sink source transition. Cab and SAG12-1 RNA are expressed in percentages related to the maximum (leaf # 8 for Cab and leaf # 1 for SAG12-1).

Table I. *Parameters of leaf water status and senescence and comparison of leaf ranks of different plants of oilseed rape*
The five plants for which critical transition of the *SAG12-Cab* ratio occurred are listed in the second column. Classification of the plants (P-1 to P-16) for which the longest T2 component split into two components is given in the third column.

Leaf Rank	Plants for Which Critical Transition of *SAG12-Cab* Ratio Occurred	Plants for Which Splitting of the Longest T2 Component Occurred
1	P-1	P-1, P-2, P-3
2	P-11, P-12	P-5, P-7, P-8, P-11, P-12, P-14
3	P-13	P-10, P-13, P-16
≥4	P-6	P-6, P-9, P-4, P-15

NMR signal evolution during leaf senescence

The relaxation decay in leaf samples corresponding to the separate CPMG (Carr Purcell Meiboom Gill) data was described by three or four relaxation components depending on developmental stage of the leaf. A typical example of the distribution of transverse relaxation times obtained by the maximum entropy method (MEM) for different development stages is given in Figure

1-a-4, with the peaks centered at the most probable T_2 values and the peak areas representing the intensity of the T_2 components.

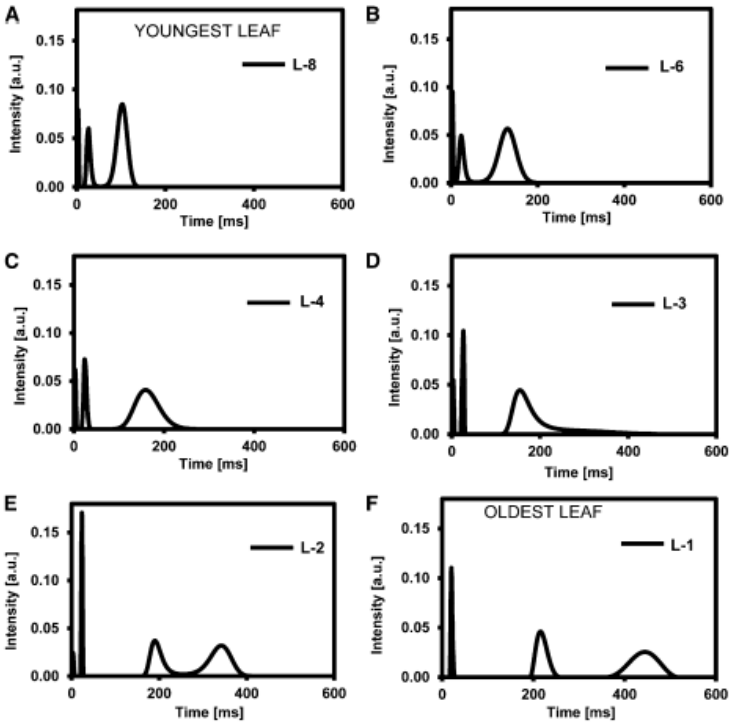

Figure 1-a-4: Transverse relaxation time distribution (MEM) calculated from the CPMG signal for oilseed rape leaves of 6 different leaf ranks (L). Data shown correspond to P-5.

Three components were observed by the MEM method for the youngest leaf analyzed (Figure 4A), with the shortest T_2-component centered at about 3 ms and representing about 8% of the total signal intensity, the intermediate component centered at about 25 ms (19% of the signal intensity) and the longest T_2-component at about 100 ms (73% of the signal intensity). For the example shown, the shortest component remained in the same range of T_2 throughout leaf tissue ageing, until the late senescence stage (leaf rank 1) when it disappeared. The T_2 of the intermediate component was about 20 ms for all measurements, while its relative signal intensity decreased (from 19% to 13%, for leaf ranks 8 and 1, respectively). The T_2 of the longest T_2-component increased from the youngest to the most senescent leaf, starting progressively to split into two components between leaf ranks 3 and 2. Figure 4E shows four distinct components measured at leaf rank 2, with the two longest T_2-components centered at about 190 ms and 340 ms, respectively. Finally, the T_2 values of the two longest T_2-components were about 220 ms and 450 ms, for the late senescence leaf (Fig 4F). The sum of relative signal intensities of the two longest T_2-components increased from 73% to 87% with senescence (for leaf ranks 8 and 1, respectively). The T_2 distribution shown in Figure 1-a-4 was very similar for the sixteen plants analyzed (data not shown). However, some differences were observed between plants with regard to the leaf rank where the split occurred, confirming previously suspected

physiological heterogeneity within leaf ranks. In Table 1, the plants are classified according to the leaf rank at which the longest T_2-component split into two components. It can be seen that the critical transition of the SAG12/Cab ratio (second column) fitted well with the NMR results, for the five plants studied.

The discrete solutions for the complete decay curve (FID+CPMG) obtained by the Levenberg-Marquardt algorithm agreed to a great extent with the MEM results of the separate CMPG curve and in addition provided access to the first component, relaxing at about a few tens of µs (Table 2). The relative intensity of this component ($I_{0(comp.1)}$) decreased during senescence, while its $T_{2(comp.1)}$ seemed to increase only for the most senescent leaf.

Table II. *T2 and corresponding relative intensities for the complete decay curves (FID + CPMG) obtained by the Levenberg-Marquardt algorithm for six oilseed rape leaves presented in Figure 4 (P-5)*

Leaf Rank	Component 1		Component 2		Component 3		Component 4		Component 5	
	I_0	T2	I_0	T2	I_0	T2	I_0	T2	I_0	T2
	%	*ms*	%	*ms*	%	*ms*	%	*ms*	%	*ms*
8	5	0.03	9	2	19	27	66	103	–	–
6	6	0.03	10	3	18	27	66	132	–	–
4	4	0.03	7	2	18	27	71	166	–	–
3	3	0.03	7	3	18	36	72	195	–	–
2	3	0.03	4	1	14	23	32	196	47	341
1	3	0.07	–	–	12	21	36	222	48	448

As previously explained, the NMR signal from vegetable tissue can be attributed mainly to protons from water molecules, characterized by T_2 relaxation times in the range of few ms or more. However, T_2-components relaxing at lower relaxation times (in the range of 10 to 100 µs) in principle correspond to solid matter. In order to check this assumption, the intensity of the first component of the FID-CPMG signal at equilibrium state ($I_{0(comp.1)}$) was correlated with dry matter mass and the sum of the intensities of the other components ($I_{0(comp.2-5)}$) to the water mass. Both relationships (Figure 5) were linear and positive (r^2=0.75 for $I_{0(comp.1)}$ and r^2=0.89 for $I_{0(comp.2-5)}$), and demonstrated that the signal from the first component of the FID-CPMG sequence corresponded to the dry matter and the sum of the signals from the other components to the water, independently of leaf age. In addition, as already explained, the results confirmed that the water and dry matter masses depended on leaf age. The dry matter mass of leaf samples (dry weight per leaf area) and $I_{0(comp.1)}$ for young leaves were relatively high and decreased for mature and senescing leaves, while the water mass and $I_{0(comp.2-5)}$ were highest in the most senescent leaves (ranks 1 and 2) (Figure 1-a-5)

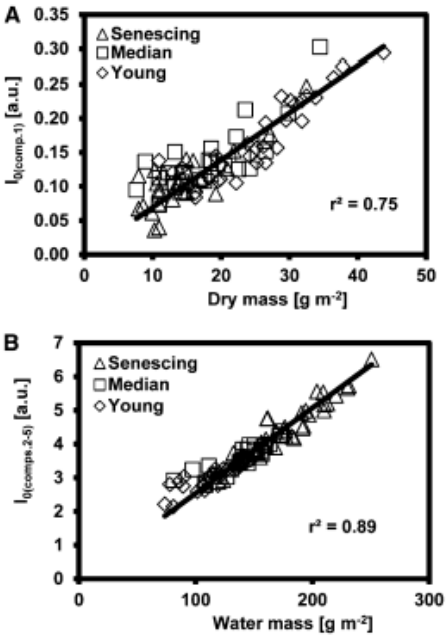

.**Figure 1-a-5** A) Correlations between the intensity of the first components of the FID-CPMG signal assumed to correspond to the solid proton fraction ($I_{0(comp.1)}$) and dry matter mass per leaf area and B) between the sum of the intensity of other components of the FID-CPMG signal assumed to correspond to the water proton fraction ($I_{0(comps.2-5}$) and water mass per leaf area for young (ranks 6 and 8), median (ranks 3 - 5) and senescing (ranks 1 and 2) oilseed rape leaves. Signal intensity was

corrected for the receiver gain. Values correspond to sixteen individual plants (P-1 to P-16).

Figure 1-a-6 shows the relative signal intensities and mean values of T_2 for the sixteen plants studied, expressed in leaf water weight (LWW) for all components, obtained by the Levenberg-Marquardt algorithm. Since the total intensity of components 2 to 5 ($I_{0(comp.2-5)}$) was strongly correlated with total water mass for young to senescent leaves for all plants (Figure 1-a-5 B), variations in water mass related to each component were calculated through leaf development (Figure 1-a-6 A). The results showed that increase in leaf water weight (expressed in water mass per leaf area) of senescing leaves was due to the increase in amount of water associated with components 4 and particularly 5. However, leaf water weight associated with component 3 slightly decreased (Figure 1-a-6 A), while that of component 2 remained unchanged. Note that LWW increase reflected cumulative effects of both increase in signal intensity and water mass.

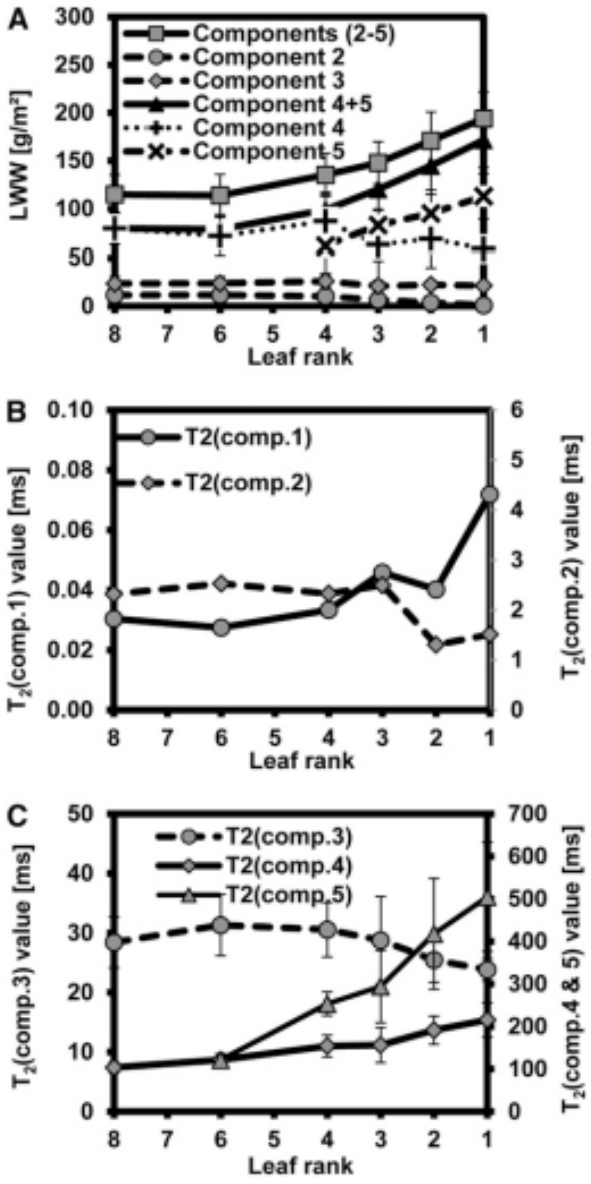

Figure 1-a-6: NMR relaxation parameters of oilseed rape leaves during senescence according to leaf rank. T_2 and corresponding I_0 values for the complete decay curves (FID+CPMG) were obtained by the Levenberg-Marquardt algorithm. A) Water distribution in the water-associated components (2-5) expressed as: $LWW_i = \frac{I_{0i}\, x\, m_w}{A}$, where LWW_i is specific leaf water weight of the i^{th} signal component expressed in g m^{-2}, with m_w water mass per leaf sample used for NMR analysis (in g), A leaf sample area (in m^2) and I_{0i} relative intensity of the i^{th} signal component (as a ratio of total signal of water-associated components (2-5)). B) and C) - Transverse relaxation times. Values correspond to sixteen individual plants (P-1 to P-16).

The overall trend for T_2 of components was the same as in the example given in Table 2. The T_2 of components 4 and 5 increased markedly (Figure 1-a-6 C), which could be related to the increase in the amount of water associated with these components (Figure 1-a-6 A).

Correlation between NMR signal and physiological traits of leaves

Principal Component Analysis (PCA) was performed in order to draw up a general framework of all the variables measured. The first principal component (PC1, 72.8% of total variance) appeared to be mainly assigned with leaf development (Figure 1-a-7 A). First, young leaves (leaf rank 6) were characterized by high levels of chlorophyll and starch content and dry matter (right part of PCA – Figure 1-a-7 B) whereas the most senescent leaves (leaf ranks 1 – 2) were characterized by higher water content (left part of PCA – Figure 1-a-7 B). This is in agreement with the phenomenon of dry weight lost during senescence, associated with chlorophyll and starch breakdown. Moreover, the results demonstrated that this loss of dry weight was correlated with increase in leaf water content and therefore hydration of leaf tissues. Secondly, the high intensities of the second ($I_{0(comp.2)}$) and third ($I0_{(comp.3)}$) components of the NMR signal were associated with the youngest leaves (right part of PCA - Figure 1-a-7 B), whereas the high total intensity of components 4 and 5 ($I0_{(comp.4-5)}$) and the high value of the corresponding $T2_{(comp.4-5)}$ were associated with the most senescent leaves (left part of PCA - Figure 1-a-7 B).

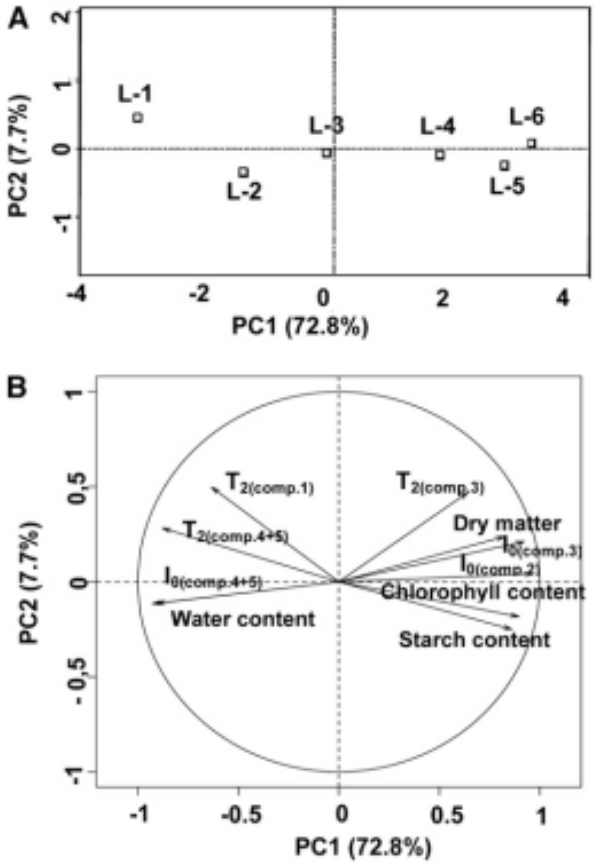

Figure 1-a-7: Principal component analysis (PCA) of 10 multivariate data (chlorophyll, starch and water content, dry matter, $T_{2(comp.1)}$, $T_{2(comp.3)}$, $T_{2(comp.4+5)}$, and $I_{0(comp.2)}$, $I_{0(comp.3)}$ and $I_{0(comp.\ 4+5)}$ corrected for the receiver gain and the sample weight of the six leaves of different 6 leaf ranks (6 to 1) from 11 oilseed rape plants grown in standard conditions. A) Score (L=leaf rank) plots for PC1 and PC2. B) Loading plot on the factorial plane made of the first two principal components (PC1, PC2). PC1 and PC2 axes explain 80.5% of the total variance. Dots are means of up to 11 independent biological replicates.

The Pearson correlation coefficients of the PCA analysis set out in Figure 7 A and B are shown in Table 3.

Table III. *Pearson correlation coefficients of the data presented in Figure 7*
CC, Chlorophyll content; DM, dry matter; SC, starch content; WC, water content.

	CC	DM	$I_{0(comp.2)}$	$I_{0(comp.2)}$	$I_{0(comp.4+5)}$	SC	$T_{2(comp.1)}$	$T_{2(comp.3)}$	$T_{2(comp.4+5)}$	WC
CC	1.00									
DM	0.59	1.00								
$I_{0(comp.2)}$	0.82	0.85	1.00							
$I_{0(comp.3)}$	0.82	0.75	0.89	1.00						
$I_{0(comp.4+5)}$	−0.81	−0.75	−0.85	−0.86	1.00					
SC	0.85	0.61	0.82	0.72	−0.71	1.00				
$T_{2(comp.1)}$	−0.50	−0.45	−0.64	−0.48	0.47	−0.53	1.00			
$T_{2(comp.3)}$	0.49	0.44	0.62	0.68	−0.55	0.46	−0.33	1.00		
$T_{2(comp.4+5)}$	−0.89	−0.57	−0.80	−0.74	0.78	−0.83	0.58	−0.48	1.00	
WC	−0.76	−0.93	−0.92	−0.85	0.83	−0.74	0.52	−0.50	0.75	1.00

Relationship between NMR signal and cell structure

Optical micrographs from young (A-B) and senescent (C-D) leaf tissues are shown in Figure 1-a-8. Four parallel layers of cells can be observed on the images (upper and lower epidermis, palisade and spongy layers). As expected, the palisade layer (PL) was composed of elongated, relatively tightly packed cells arranged in 2 to 3 rows, while the spongy layer (SL) was made up of rounded cells with large intercellular spaces. Moreover, most of the chloroplasts were stuck to the plasmalemma, especially in the palisade mesophyll. The upper and lower monolayered epidermal cells can be easily seen in the images. Both the length and width of the palisade mesophyll cells increased considerably in senescing tissues, whereas those of the spongy mesophyll cells seemed to remain almost unchanged. The number of chloroplasts per cell appeared to remain stable throughout the senescence process, and consequently their relative volume decreased compared to the relative volume of the vacuole. The regular shape of chloroplasts was preserved in most of the senescent leaves studied (Figure 1-a-8 C-D), indicating that the end of the senescence process had not been reached, even for these leaves. Finally, the area of palisade cells of senescent leaves was estimated to be about four times greater than that of the corresponding young leaf tissues.

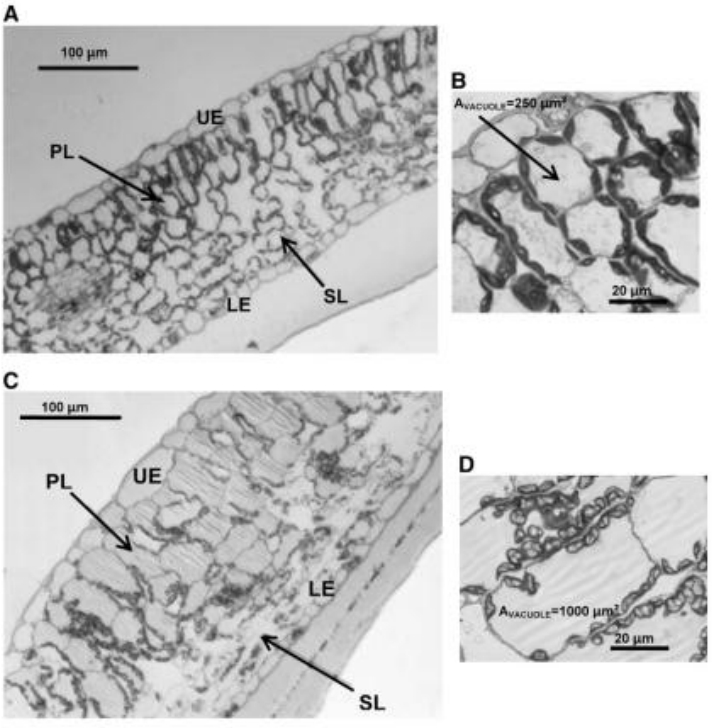

Figure 1-a-8: A) Light micrograph of young oilseed rape leaf tissues, with B) zoom on the palisade cells. C) Light micrograph of senescent oilseed rape leaf tissues, with D) zoom on the palisade cells. PL - palisade layer; SL - spongy layer; UE – upper epidermis and LE – lower epidermis.

Variations in the volume of vacuoles, chloroplasts and cell wall (Figure 1-a-9 A) were estimated (see Materials and Methods, Eqs. 7-9). A considerable decrease in the relative volume of the plastidial

compartment was observed as senescence progressed. In the young leaves the chloroplast volume was roughly estimated to be about 40% of the cell volume, and it dropped to below 20% in the most senescent leaves. In contrast, the size of the vacuole increased from about 55% to almost 80%. Finally, our method did not permit clear detection of variations in cell wall volume, although the results seemed to indicate a minor volume reduction (Figure 1-a-9 A).

Figure 1-a-9 B depicts the relative intensities of the NMR signal components for young and senescent leaves that can be considered as an estimation of water distribution in cell compartments. Similar patterns can be observed in the NMR and the microscopy results, on comparing Figure 9 A and B. For young leaves, the vacuole occupied about 55% of the cell volume, whereas the intensity of components 4+5 was about 65%. The relative vacuole volume for senescing leaves increased to about 80%, and a similar phenomenon was observed for the relative intensity of components 4+5 (~85%). On the other hand, chloroplast volume in young leaves was estimated to be about 40%, decreasing to about 20% in senescing leaves, whereas the relative intensity of the third component decreased from about 20% to about 10%. Finally, cell wall volume was estimated to be about 5% and 3% for young and senescing leaves, respectively, and the relative NMR signal intensity of the second component decreased from 9% to 2% according to leaf maturity.

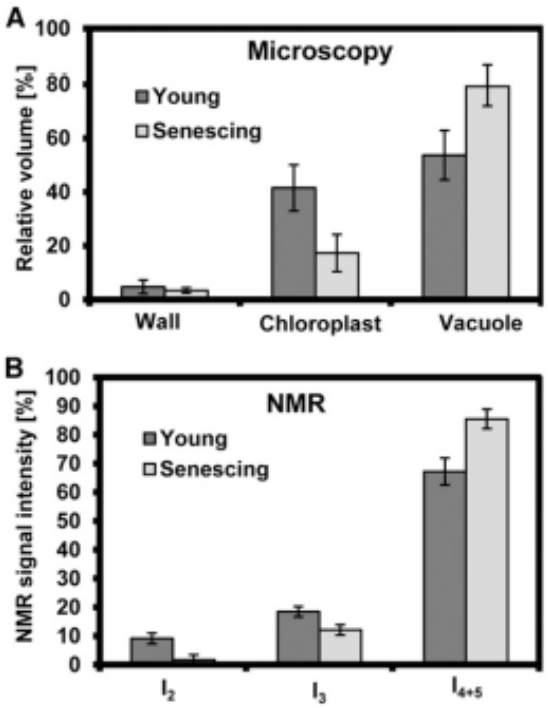

Figure 1-a-9: A) Relative volumes of the cell wall, chloroplasts and vacuole of young (ranks 6 and 8) and senescing (ranks 1 and 2) oilseed rape leaves estimated from the light and electron micrographs, compared to B) the relative NMR signal intensities of liquid components 2, 3 and 4+5 in %. Eighteen leaves of five plants were used for microscopy studies.

It should be noted that the variations in the volumes of vacuoles, chloroplasts and cell wall were estimated roughly, as the spongy layer and the upper and lower epidermal cells occupying the leaf surface were ignored in the analysis. Additionally, exchange of protons between different cell compartments over the biological membranes can affect the relative intensities of different NMR signal components.

Figure 1-a-10: - Light (A) and electron (B) micrographs of oilseed rape leaf cell. W_C - cell width, L_C - cell length, W_V - vacuole width, L_V - vacuole length and W_W - wall thickness.

1-a-3 Discussion

Senescence induced changes at the cell level

The biochemical markers for identification of leaf senescence used in this study have already been described in the literature (Masclaux et al., 2000; Desclos et al., 2008). The decreases in chlorophyll and starch content (Figure 1-a-1) that we observed in senescent leaves were in accordance with the literature (Diaz et al., 2005; Albert et al., 2012). However, although these biochemical traits are relevant to providing a general view of senescence across plant shoots (Gombert et al., 2006), they are not precise enough to be used for comparisons between leaf ranks from different plants. Molecular markers such as SAG12/Cab gene expression (Gombert et al., 2006) provided a more precise description of changes in leaf development (Figure 1-a-3) although handling them is fairly complex.

The senescence process has been well described in several reviews (Thomas and Stoddart, 1980; Buchanan-Wollaston et al., 2003; Lim et al., 2007) and, as far as we are aware, it is commonly accepted that water loss occurs in leaves during senescence (McIntyre, 1987). Decrease in specific leaf dry weight during senescence, reflecting the drain of organic constituents from the leaves to other plant organs has also been described (McIntyre, 1987; Malagoli et al., 2005). In the present study, as expected, a decrease in dry weight was observed for senescing leaves (Figure 1-a-1 B). However, an increase in water content was observed (Figure 1-a-1 C), leading to an increase in total specific leaf water weight. Moreover, the relatively high increase in cell size associated with tissue hydration of leaves during natural senescence was observed (Figures 1-a-8 and 1-a-9). This increase in cell size has not, to our knowledge, been previously reported in the literature. Thomas and Stoddart (Thomas and Stoddart, 1980) described senescing leaves with increasingly vacuolated cells and with a diminishing rim of cytoplasm, but they did not report cell enlargement. Keech et al. (Keech et al., 2007) reported an increase in the perimeter of mesophyll cells of Arabidopsis leaves during senescence induced by dark treatment. The cell enlargement process has been reviewed by Cosgrove (Cosgrove, 1999; Cosgrove, 2005). It occurs prior to cell growth associated with dry matter production and depends on

the ability of the wall to loosen and to undergo stress relaxation. Cell wall extensibility is mediated by several protein factors, especially alpha-expansin expression (Cosgrove, 1999). The consequence of the cell enlargement process is water uptake. This process has not previously been reported in senescing tissues, although alpha-expansin expression has been studied during floral development. It has been linked to an early development stage corresponding to the rapid expansion associated with cell growth, but was also found in senescing floral tissues(Gookin et al., 2003). Finally, Reid and Chen (Reid and Chen, 2008) reported that cell wall loosening also occurred in senescing flower tissues due to degradation of cell wall macromolecules. The results of the present study, i.e. micrographs (Figure 1-a-8) and measurements of water status (Figure 1-a-2), clearly demonstrated that a process of cell enlargement occurred in senescing leaves (especially for palisade cells) and that it was associated with cell hydration. Considering the trend in cell wall volume estimated from the leaf tissue micrographs (Figure 1-a-9) and the observations reported for flower tissues (Reid and Chen, 2007), this process could be explained by degradation of cell wall macromolecules that induces changes in the fibrillar structure of the cell wall and consequently causes water uptake from adjacent tissues. In our study, the slight and consistent increase in water content was associated with a slight increase in leaf water potential and osmotic potential (Figure 1-a-2), probably reflecting tissue hydration. We demonstrated that this variation in leaf water content was not linked to a water stress event as the water deficit remained constant. As the relative water content (RWC, see Eq. 4, Materials and Methods section) that can be expressed as RWC=water content/(turgid weight/fresh weight – dry weight/fresh weight) remained unchanged, water content increase and dry weight decrease, associated with the fresh weight at full turgor increase, suggested an increase in cell wall elasticity. The latter is in agreement with the micrograph observations.

Interpretation of the NMR signal of senescing leaves

The results of previous NMR studies performed on leaves differ from our results, as the NMR signal depends on leaf tissue type and on the measurement and signal processing protocols. For instance, T_2 measurements in wheat leaves (Maheswari et al., 1999) were performed by the CPMG method at the same magnetic field as that used in our study (20 MHz), but with considerably fewer sampling points (250 instead of 6000) and with longer pulse separation (0.5 ms instead of 0.1 ms used in our study) at temperatures from 35 to 58°C. They obtained bi-exponential T_2 decay, with the longer T_2-component of T_2=130-180 ms and I0=65-70% attributed to intracellular water and the shorter component of T_2=40-60 ms attributed to extracellular and hydration water. These two components correspond roughly to the two longest T_2-components measured in our study in relatively young oilseed rape leaves (Table 2). The T_2-component relaxing at 3 ms in oilseed rape leaves was not observed because of the relatively long pulse space, and the very small number of points sampled for the CPMG curve. Finally, in the Maheswari's study, the CPMG decay curve was acquired over 250 ms which was not long enough for reliable fitting of the curve since the baseline was not reached (last

point < 1.4 x T_2-max). On the other hand, Capitani et al. (Capitani et al., 2009) investigated the leaves of several species using a portable unilateral NMR apparatus (18.153 MHz) characterised by an inhomogeneous magnetic field that did not allow measurement of the FID signal and produced shortening of the T_2 values measured. Relaxation decays in the unstressed leaves were described by two- or three-exponential decays with T_2 values of up to 40 ms. This approach has been demonstrated to be promising for application in field conditions, but was not focused on interpretation of the NMR signal. Any comparison with our results thus seems difficult. The results of studies on chive tissues (Qiao et al., 2005) performed at 300 MHz were interpreted at the tissue level; T_2/diffusion peaks were assigned to cells of different tissue types, such as palisade and spongy layers and xylem vessels. The subcellular level was not considered in their study, although in green leaf tissues chloroplasts represent a significant level of cell volume. For instance, in wheat, chloroplasts occupy up to 70% of the surface area of mesophyll cells and approximately 20% of their volume (Ellis and Leech, 1985). In addition, they are believed to have distinct relaxation and diffusion properties (Van As, 2007) due to their small size (about 6 μm in diameter). The results of T_2 measurements obtained in maple leaves at 300 MHz using a different approach (McCain, 1995) differed considerably from those in chive tissue. Chloroplast water was discriminated and its T_2 was surprisingly estimated to be higher than the T_2 of non-chloroplast water.

Except for the last study mentioned, the longest T_2 component is generally associated with vacuolar water (Van As, 2007), because of its relatively high mobility. It usually also has the highest relative intensity, as the vacuole encloses the highest amount of cell water (Teixeira et al., 2005). As explained above, young and mature leaves (leaf ranks 8-3) were characterized in our study by three water-associated components (Figure 1-a-4). According to the literature, the highest T_2 component could be attributed to the vacuole, as it represented about 70% of the total water and had a relatively long T_2 (about 100-200 ms) depending on the leaf rank (Table 2). In senescing leaves, this water fraction was distributed between two NMR components, still representing three quarters of the total water. This could be explained by tissue heterogeneity that was emphasized during senescence. In fact, differentiation in cell morphology between palisade and spongy layers was observed on light micrographs (Figure 8) and showed that cell enlargement occurred only for palisade cells. This heterogeneity of cell size may affect the NMR relaxation times (Van der Weerd et al., 2002) of the two cell types (Qiao et al., 2005), resulting in the increase in T_2 of enlarged palisade cells. Finally, the relative signal intensity of the two longest T2-components and its trend during senescence approximately matched the relative volume of the vacuole estimated from the light micrographs (Figure 1-a-9).

T_2 values of these vacuole-associated components increased during senescence, particularly the T_2 of the fifth component (Figure 1-a-6). This can be explained by increase in vacuole size, according to the sensitivity of T_2 to compartment size (Van der Weerd et al., 2002) and by water influx

induced by senescence. On the other hand, entry of dead-end metabolites of organic component degradation occurring during the senescence process (Buchanan-Wollaston et al., 2003; Wada et al., 2009) could shorten T_2 values through chemical exchange between protons of these metabolites and water protons. However, the latter process seemed to be minor comparing with the effects of water content increase due to rise in water amount in the vacuolar compartment.

The overall results of this study indicated that the third T_2-component could probably be assigned to the plastidial water. Chloroplast volume and its trend during senescence estimated from the micrographs matched well the relative intensity of the third T_2-component (Figure 1-a-9). Covering of the mature cell surface by chloroplasts varies considerably in higher plants, with a total chloroplast area per unit plan area of cell greater than 70% in spinach and as low as 25% in *Nicotiana glutinosa* (Honda et al., 1971). However, as shown by Ellis and Leech (Ellis and Leech, 1985) the chloroplast volume is fairly constant in leaf mesophyll tissue for any given species. Their results demonstrated that chloroplasts represented up to 40% of total cell volume for mature leaves. As the chloroplast dimensions measured (about 6 µm diameter and 2 µm thick) were in agreement with the literature (Ellis and Leech, 1985), their volume can be estimated to be about 50 μm^3, also in accordance with the literature (Zellnig et al., 2010). On the other hand, plastids are distributed as a peripheral monolayer in mesophyll cells (Ellis and Leech, 1985) in the same way as in cells of equivalent size and shape. Their average number may therefore be estimated as about 90 chloroplasts per cell (with an estimated volume of less than 12000 μm^3) and the relative volume to be about 40%. However, this percentage may be slightly overestimated as in species such as wheat there are fewer than 70 chloroplast for cells as large as 1400 μm^2 (Ellis and Leech, 1985). Following the hypothesis that chloroplast water content is about 50%, based on the ratio of the relative volumes of well watered stroma and lipid-enriched thylakoids and plastoglobules (Zellnig et al., 2010) and as the water content increases markedly in the gerontoplast due to the loss of thylakoid membranes, the estimated volume of plastidial water weighed by water content fitted even better the amount of water computed from the NMR signal intensity. The T_2 of the third component has only been reported for maple leaves (McCain, 1995) to our knowledge. Its value in their study was surprisingly high (about 40 ms) considering that measurements were performed at a relatively high magnetic field (300 MHz). The plastid T_2 obtained in the present study (Table 2) was in the same range, although it was measured at 20 MHz. However, in view of the differences in size between plastidial and vacuolar compartments, such plastidial T_2 values appeared to be in agreement with the T_2 found for vacuoles.

Finally, the low T_2 value (Table 2) of the second component (about 3 ms) should correspond to that of water close to macromolecules or to solid surfaces (Van As, 2007), and this component represented about 10% of the cell water (Table 2). Different hypotheses can therefore be proposed for its attribution, such as starch hydration water or cell wall water. Firstly, the T_2 value measured (Mariette et al., 1999; Tang et al., 2000) and the fact that component 2 disappeared in the most

senescent leaves at the same time as the starch suggest that it may correspond to water in starch granules. However, according to Mariette et al. (Mariette et al., 1999), the mass of water enclosed in starch granules per total starch mass is 0.3829 g/g and it was estimated to be 0.3% for leaf rank 6. This is far beyond the relative intensity of component 2. On the other hand, the T_2 values measured (Table 2) may indicate that component 2 corresponds to the water in rapid exchange with cell wall protons according to the attribution proposed for fruit (Sibgatullin et al., 2007). Additionally, the relative water volume enclosed in the cell wall could correspond to the relative NMR signal intensity of component 2 (Figure 9). The fact that the second component disappeared in the most senescent leaves could be explained by cell wall thinning associated with macromolecule degradation.

As demonstrated above, the first component was attributed to dry matter protons. The analysis performed did not allow going into further details. Indeed, the sole organic compound quantified was starch and it represented between 1 and 5% of the dry weight, while dry matter content represented between 20 and 8% of the total weight, depending on the leaf senescence stage. On the other hand, the intensity of the first component relaxing at about 30µs was about 5% of the total FID-CPMG signal.

The PCA analysis (Figure 1-a-7) showed that chlorophyll breakdown and starch degradation were associated with leaf aging. The NMR signal was shown to be able to describe this senescence-induced sub-cellular water redistribution. For instance, the relative intensity of components 4 and 5 ($I_{0(comp.4+5)}$) and the transverse relaxation times ($T2_{(comp.4+5)}$) associated with vacuole water were positively correlated with senescence, describing water entry and vacuole enlargement. On the other hand, the relative intensity of the third component ($I_{0(comp.3)}$) was negatively correlated with senescence, describing the decrease in the relative volume of the chloroplasts.

1-a-4 Conclusion

This study demonstrated that NMR Relaxometry is a powerful technique for monitoring leaf development, as T_2 measurements provide access to the cell structure through sub-cellular water distribution. Applied to a wide leaf panel, this technique was shown to be able to detect slight variations in senescence evolution accurately. Combining NMR with microscopy and physiological characterization throughout the senescence process contributed to understanding of the attribution of NMR signal components. The results represent an important step toward further studies investigating the biological significance of the signal.

One of the main applications of leaf NMR Relaxometry would be in field applications, such as leaf tagging and plant phenotyping. It will be necessary first to investigate the leaf NMR signal in relation to different environmental conditions, such as water or nitrogen depletion. As field applications require portable NMR devices, and this will inevitably weaken the quality of the signal, this aspect should be also evaluated.

One other important application of the proposed technique will be to improve understanding of plant functioning at cell and tissue levels. Changes in the water distribution and cell structure during any physiological process or under abiotic or biotic stress are not directly accessible with currently used techniques and therefore NMR represents a promising and powerful technique for plant investigations.

Acknowledgments

The authors thank Dominique Poulain* for help with the statistical analyses. We also thank the Greenhouse team, particularly Laurent Charlon**, Loic Daniel** and Patrick Rolland**. Finally, we thank Sophie Rolland** for starch analysis, Anne-Marie Gouraud** for molecular analysis and Françoise Leprince** and Patrick Leconte** for sample processing.

* UMR SAS (INRA- AGROCAMPUS OUEST)** IGEPP

Planta
DOI 10.1007/s00425-014-2182-3

ORIGINAL ARTICLE

Assessment of nutrient remobilization through structural changes of palisade and spongy parenchyma in oilseed rape leaves during senescence

Clément Sorin · Maja Musse · François Mariette · Alain Bouchereau · Laurent Leport

1-b-1 Introduction

A leaf goes through different phases during its development, the last being senescence. Senescence is a highly regulated complex process that leads to the death of the tissue. This process has been shown to involve three phases (Nooden et al. 1997). The first phase is regulated by hormones and is characterized by transduction of the senescence signal (from environmental or internal factors) that leads to activation of key genes. The second phase is a degenerative phase corresponding to the disassembly and remobilization of cell components. Remobilization during that phase allows recycling cell nutrients from senescing tissues to growing organs. Finally, the terminal phase corresponds to disorganization of the nucleus, degeneration of the tonoplast and distortion of the cell wall leading to the cell death. Mitochondria remain active until the latest stage of senescence (Sakamoto, 2006). All these events are programmed in order to allow maximal carbon (C) and nitrogen (N) remobilization in correspondence with sink demand. For crop species, the ability of the plant to remobilize nutrients highly impacts seed yield, especially in the current context of fertilizer input reduction. For instance, oilseed rape crop is known to have suboptimal N use efficiency partly due to low leaf organic N recycling performance and inherent important N residual amount in fallen leaves. As nitrogen fertilization has a major impact on oilseed rape production costs and environment quality, low N remobilization efficiency (NRE) has negative economical and agro-ecological consequences. Improving oilseed rape NRE should be a breeding challenge and would therefore necessitate a better understanding of senescence associated nutrient allocation and partitioning processes in leaves especially at the cell structure and organization levels were organites and macromolecules constitute predominant sources for metabolite recycling and sink feeding.

A leaf is constituted of the palisade and the spongy parenchyma crossed by vascular tissues and surrounded by two epidermises. In Brassica napus, the palisade parenchyma consists of regular shaped

cells organized in layers whereas the spongy parenchyma, presenting large intercellular spaces, is less well organized (Castro-Diez et al. 2000). The principal leaf functions are photosynthesis, photorespiration and transpiration. Even if there is no experimental data supporting that, it is currently accepted that photosynthesis is mainly performed by palisade tissue (Nardini et al. 2010) whereas the spongy tissue is known to be involved in gas exchange. Moreover, it has been shown in Acer hippocastanum (horse chestnut) with abaxial position of stomata that the spongy tissue has a major role in the homeostasis of the leaf hydraulic status (Nardini et al. 2010). Although the leaf has often been studied as a homogeneous organ the structural and functional differences described above may suggest different patterns of evolution during development and senescence. It might be expected that palisade and spongy tissues evolve differently in terms of metabolism during senescence possibly leading to different contributions to remobilization process. The question of differential evolution of the palisade and spongy parenchyma during leaf development has not been addressed to date in the literature. The only differential response between leaf parenchyma were revealed by microscopy in plant under water (Bacelar et al. 2006; Martinez et al. 2007) and ozone stresses (Bohler et al., 2013).

As already stated structural modifications due to macromolecules dismantling and recycling in senescing leaves are at the origin of cell compartment disruption, dry matter reallocation and probably water redistribution between compartments. Low field proton Nuclear Magnetic Resonance (NMR) has been used for investigation of cell water compartmentalization in various plant organs (Hills and Remigereau 1997; McCain 1995; van der Weerd et al. 2001). The technique allows measurement of relaxation signals that for highly hydrated plant tissues originate mainly from water. In the case of compartmentalized systems characterized by slow diffusion exchange of water molecules between compartments, relaxation times have a multi-exponential character due to differences in physical and chemical properties of water in different compartments. The relaxation signal is therefore used to study changes in water status and distribution. In most studies, transverse relaxation time (T_2) has been used rather than longitudinal relaxation time (T_1) as it is more sensitive to variations in water properties occurring in plant tissues. The multi-exponential T_2 has mainly been interpreted at a cell level to assign different signal components to principal cell compartments while assuming homogeneity of cells in the sample being examined (Snaar and Van As 1992b). This model was developed for fleshy fruit (Snaar and Van As 1992a) and vegetable parenchyma (Hills and Remigereau 1997). It has also been used for leaf tissues from different plants (Colire et al., 1988; Capitani et al., 2009). Another approach was used by Qiao *et al*. (2006) who considered only heterogeneity of the sample at the tissue level. Musse *et al*. (2013), investigating leaf senescence of Brassica napus, recently drew attention to the fact that both cell compartmentalization and tissue heterogeneity have to be taken into account in the interpretation of the NMR signal. The NMR signal of leaves was shown to be sensitive to the senescence stage and all signal components to be affected by it. The principal signal changes concerned the vacuole-related component that separated into two

components in senescing leaves. An interpretation was proposed associating these changes with a process of cell enlargement and hydration, probably linked to remobilization processes.

The focus of the present study was on changes occurring in vacuole properties, the major place of macromolecules degradation during remobilization, and plast structures that constitute the main N reserve of the leaf, during leaf senescence. NMR measurements and an extended microscopy study were performed to observe changes at both cellular and tissue levels. Light microscopy was used for the quantification of tissue thickness and vacuolar volume, whereas plasts and cell walls were investigated using electronic microscopy. The design of the experiment allowed investigation of natural leaf senescence in a large number of plants grown under controlled conditions through an eight-week kinetics study. This design made it possible to compare different developmental scales commonly used to describe senescence (*i.e.* leaf rank, leaf age and physiological markers). The output of the study was to demonstrate a differential structural and probably functional evolution linked to nutrient remobilization processes of palisade and spongy parenchyma cells in naturally senescent leaves of *Brassica napus*.

1-b-2 Results

Physiological characterization of leaf development

Leaf development was characterized through chlorophyll and starch content, water content and dry weight measurements (Figure 1-b-1). In order to compare leaf pattern of evolution according to the position in the canopy and to time, two approaches were used to present the results:

(i) All leaves were followed during the eight-week measurement period. The eighth rank leaf (LR-8) was chosen for presentation in Figure 1-b-1 (a, b) because it was present on the plant during the whole measurement period (from eight weeks to fifteen weeks).

(ii) All leaves from one plant were analyzed at one measurement time (b, d). The results presented correspond to the ten-week-old plant (third week of measurement period).

Figure 1-b-1 a shows that the chlorophyll content was at its maximum until the sixth week and then decreased to the end of the measurement period. The amount of starch increased until the fifth week of measurement and then started to decrease with ageing and destruction of the photosynthetic pigment. The water content was about 85% of fresh weight in young leaves (Figure 1-b-1 c) and increased during the last three weeks. Dry weight was constant until the sixth week and then decreased slightly. The results of fresh weight measurement (see annexe 2, Supplementary data 1) showed that the increase in water content observed in old leaves was due not only to the decrease in dry weight but also to an increase in the amount of water.

Similar patterns were observed while comparing physiological parameters corresponding to different leaf ranks from the same plant at a given time (Figure1-b-1 b, d) to those from a leaf over eight weeks (Figure 1a, c). This demonstrated that analyzing leaves for the parameters measured in the present study throughout the canopy from old to young leaves can be considered equivalent to studying one leaf during its development.

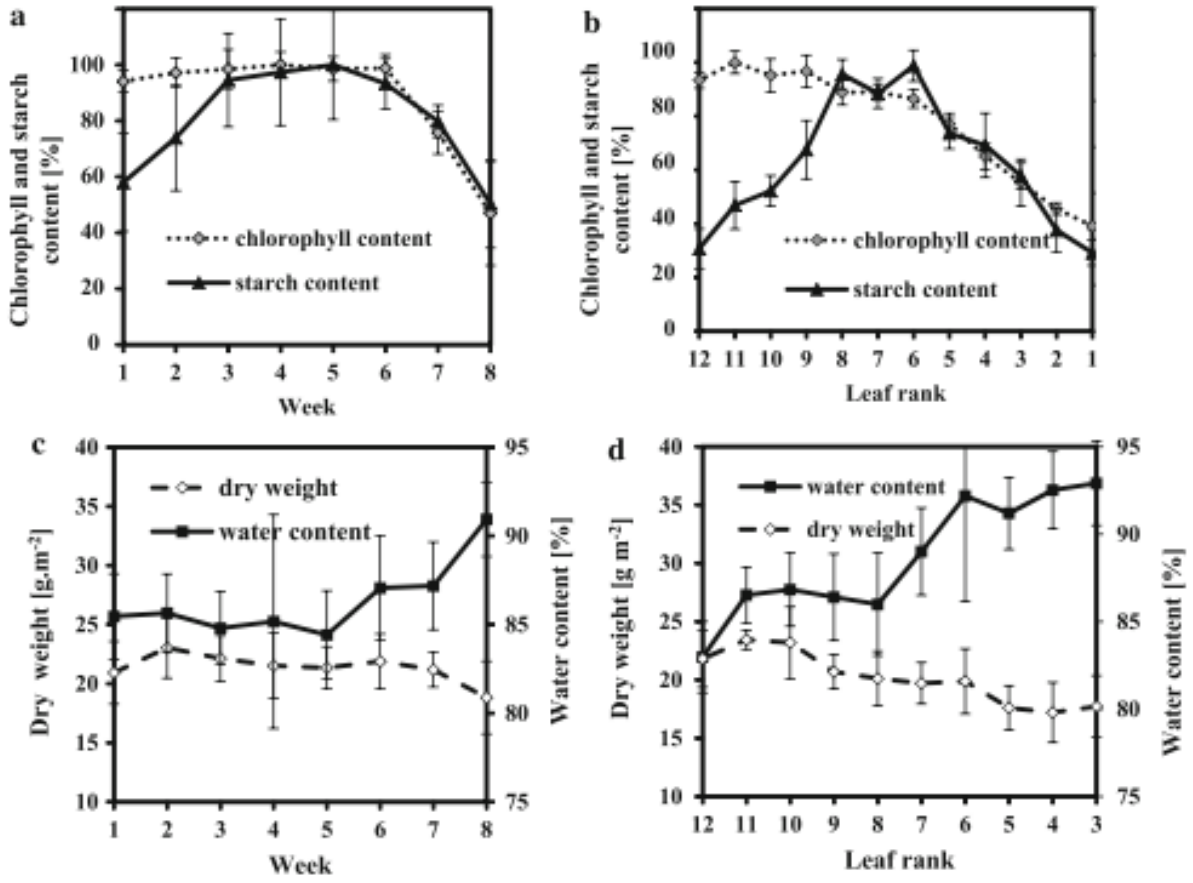

Figure 1-b-1 Changes in chlorophyll and starch content, water content and dry weight during leaf development in oilseed rape. a, c The eighth rank leaf was followed during the eight-week measurement period. b, d All leaves from four plants were analyzed at the third week of the measurement period. The values correspond to averages ± standard deviations of data collected from leaves of four individual plants

NMR characterization of leaf development

Changes in NMR signal were followed throughout leaf development. Figure 1-b-2 presents a continuous distribution of transverse relaxation times obtained by the maximum entropy method (MEM) calculated from the separate CPMG (Carr Purcell Meiboom Gill) data from different leaves. The dotted line represents MEM results for the selected leaf (LR-8) obtained at four different times in the eight-week measurement period. The solid line shows the results for four leaves (LR-10, LR-7, LR-5, LR-3) from one plant at one measurement time (third week). The NMR signal for Brassica

napus leaves is characterized by four or five components, depending on leaf age (Figure 2), the first component corresponding to the solid state protons (not represented in Figure2) and the others to the liquid fraction (Musse et al. 2013). The longest T_2 component attributed to the vacuole (Musse et al. 2013; Van As 2007) represented more than 75% of the leaf water. The T_2 of this component increased with time and started to split into two components in mature leaves (Figure 1-b-2 b). For senescent leaves, two separate vacuolar components were observed (Figure 1-b-2 c) for which T_2 values increased until the end of the measurement period (Figure 1-b-2 d). As for the physiological parameters, Figure 2 shows that the evolution of transverse relaxation time distributions was the same when monitoring one leaf during several weeks and when analyzing leaves throughout the plant axis from old to young leaves at one measurement time.

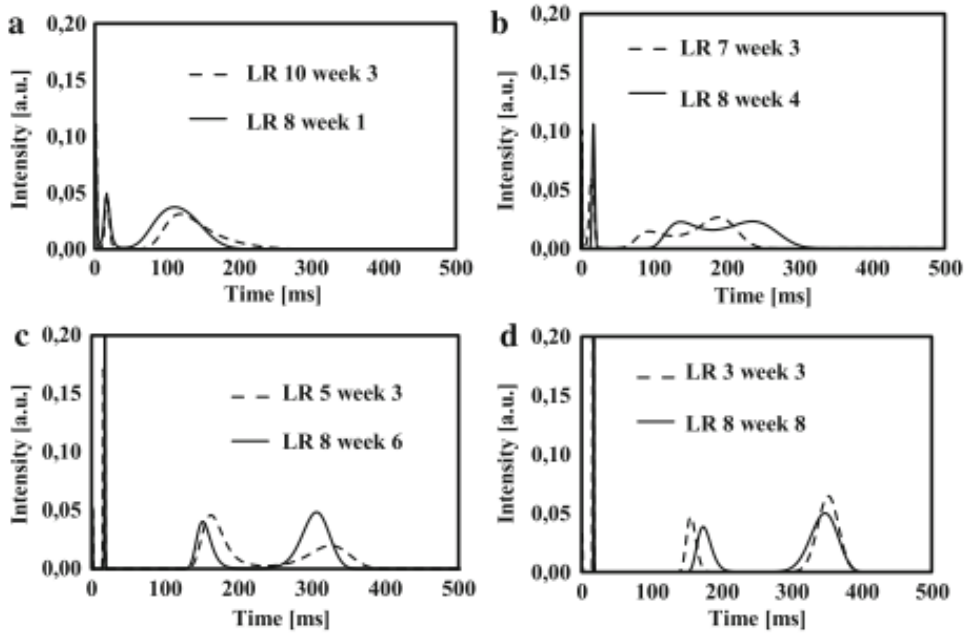

Figure 1-b-2 Transverse relaxation time distribution (MEM) calculated from the CPMG signal for *B. napus* leaves. The dotted line represents results of the selected leaf (LR-8) obtained at four different times (weeks 1, 4, 6 and 8) of the eight-week measurementperiod. The solid line shows results of four leaves (LR-10, LR-7, LR-5, LR-3) from one plant at one measurement time (week 3)

The leaf rank for which the longest T_2 component observed in young leaves separated into two components is represented in Figure 3. The emergence of the new component is from here on referred to as "the split". Both our former study (Musse et al. 2013) and the present results showed that this split was linked to the developmental process of the leaf. Between week 2 and week 7, the leaf rank at which the split occurred increased by one rank each week (Figure 3). During the eight-week measurement period, the number of leaves in which the split occurred represented a constant ratio of 40 - 50% of all the expanded leaves of the plant.

T_2

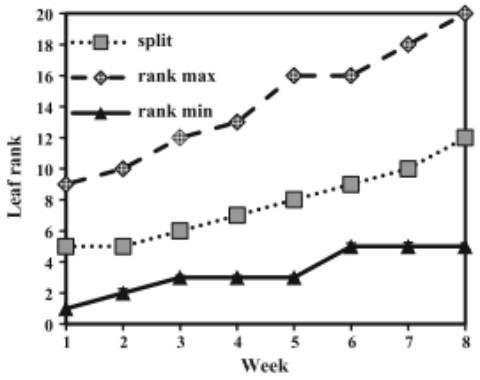

Figure 1-b-3 Leaf rank at which the longest component observed in young leaves split into two components and maximum and minimum leaf ranks of the plant studied from each measurement week. Data shown are the averages (rounded to the whole number) of the four series

The results presented in Figs. 1-b-2 and 1-b-3 show that it was possible to use the split to target leaves at the same developmental stage. In this aim, tag zero was assigned to leaves in which the split had occurred, the subsequent leaf rank was numbered 1, etc. According to this scale, the older the leaf was, the higher its tag, while negative tags represented young leaves. This NMR split scale made it possible to average values from data obtained in leaves at different measurement weeks and from different leaf ranks. These results took into account all 340 leaves from the 32 plants used in this study, giving an overview of leaf development from young to very senescent leaves. The NMR split scale is used in the subsequent Figures.

The discrete solutions for the complete decay curve (FID+CPMG) obtained by the Levenberg-Marquardt algorithm agreed to a great extent with the MEM results of the separate CPMG curve. In addition, the FID provided access to a fast-relaxing component linked to the solid phase protons, with T_2 of a few tens of microseconds and 2-5% of total signal intensity. Component 1 was not further analyzed but the correlation between its intensity and dry weight (see annexe 2, Supplementary data 2) may be valuable in future studies to determine leaf age as the dry weight decreases during senescence (Figure 1-b-1).

For the liquid fraction components, Figure 4 shows the T_2 value and relative intensity of the NMR signal (components 2 to 5) expressed in leaf water weight per leaf area during leaf development obtained by the Levenberg-Marquardt algorithm. The T_2 of component 2 (Figure 1-b-4 a) remained at around 2 ms from the youngest leaves to two ranks before the split occurred (tag -7 to tag -2, according to the split scale). It then decreased progressively until tag +4 and component 2 finally disappeared in older leaves. The T_2 of component 3 was relatively stable, at around 20 ms for young leaves (tag -7 to tag -1) and 16 ms for older leaves (tag +1 to tag +7). The T_2 of component 4 (Figure 4b) was around 100ms for the youngest leaves (tag -7) and progressively reached 200 ms at tag -1. After the split, the two components (4 and 5) had different pattern of evolutions, component 4 increased slightly up to 235 ms (tag +7), while the T_2 of component 5 first increased steadily to 400 ms until the tag +5 and then strongly to 800 ms until tag +7.

Figure 1-b-4 c shows the relative signal intensity expressed in leaf water weight per leaf area (LWWi) in order to present the amount of water associated with each component. The LWW2 remained stable until the disappearance of component 2 (tag +5). The amount of water associated with

component 3 increased slightly during leaf development from 40 g/m2 (tag -7) to more than 50 g/m2 in the oldest leaves. LWW_4 was about 220 g/m2 before the split. At the first appearance of component 5, LWW_5 was 180 g/m2 whereas LWW_4 was around 100 g/m2. It remained around this value after the split whereas LWW_5 increased markedly to 440 g/m2 from tag 0 to tag +6.

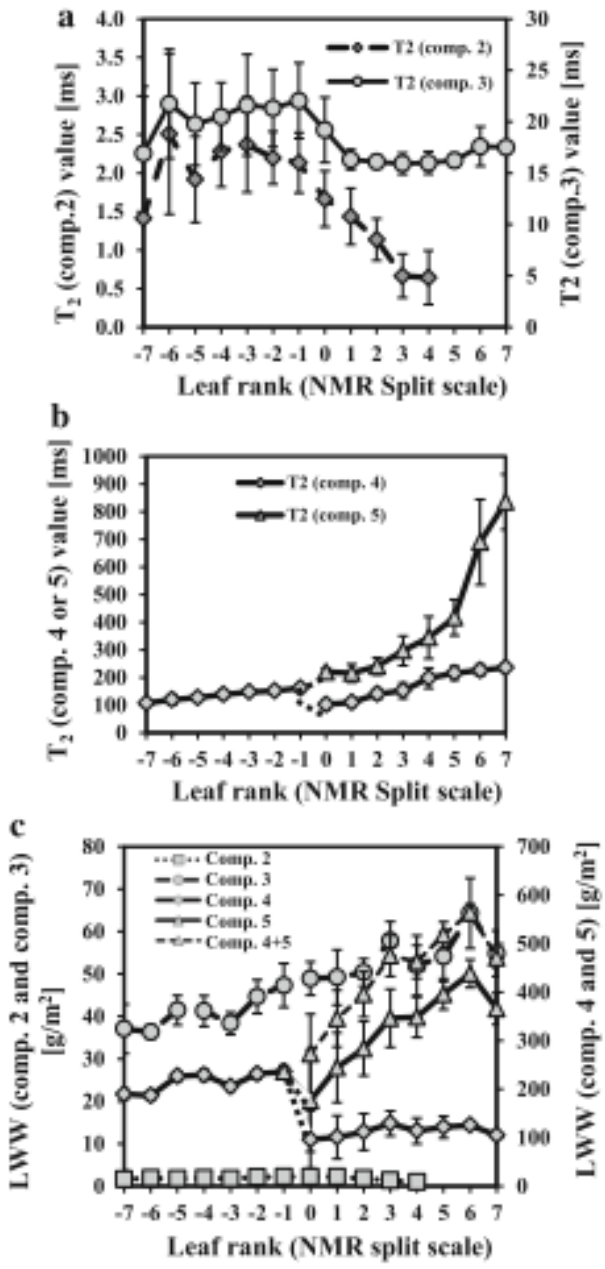

Figure 1-b-4 NMR relaxation parameters of oilseed rape leaves according to the week report to the NMR split scale. Transverse relaxation times of the component 2 and 3 (a) and 4 and 5 (b) in ms and in relation to NMR split scale. c Water distribution in the water-associated components (2–5) expressed as LWW where LWW i is specific leaf water weight of the ith signal component expressed in g m^{-2}. Values correspond to average of 8–16 leaves

In Figure 1-b-5, the physiological parameters are expressed on the NMR split scale. The same patterns for chlorophyll and starch content and can be observed in Figure 1-b-1. By comparing conventional approaches (Figure 1-b-1) and the NMR split scale (Fig 1-b-5) it was demonstrated that the NMR split scale allowed averaging of more data for each point. Indeed, for the representation according to leaf position or leaf age (Figure 1-b-1), number of data averaged for each point corresponded to the number of repetitions (4 in the present study). In contrast, in the case of the representation using the NMR split scale, all leaves from all plants were considered and each point represents an average of 7 to 21 measurements on individual leaves. The number of averaged data depended on the number of leaves with similar NMR signals, without taking into account the characteristics of the experimental design (leaf rank and measurement week). Moreover, the NMR split scale made it possible to extend the range of the development scale, as can be observed in Figure 1-b-5. The NMR split scale therefore makes it possible to reconstruct the pattern of evolution of parameters throughout leaf development by taking into account all the individual leaves studied.

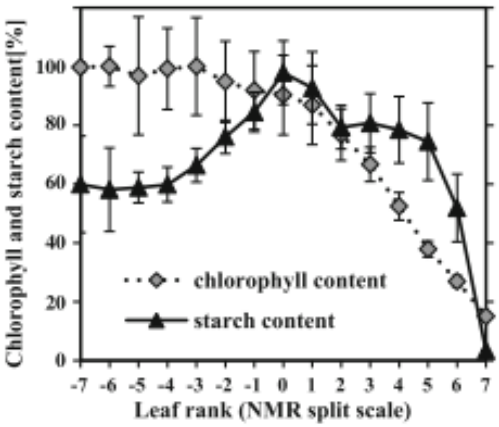

Figure 1-b-5 Chlorophyll content and starch content of oilseed rape leaves expressed as a percentage of the maximum in relation to the NMR split scale. Values are an average of 7–24 results ± standard deviation

Limb structure modifications

Changes in leaf internal structure were characterized by electronic and light micrographs. Figure 1-b-6 represents examples of leaf light micrographs of young (tag -2), mature (tag +2) and senescing leaves (tag +4). The general structure of the leaf remained constant at all stages of leaf development, with upper epidermis, palisade parenchyma, spongy parenchyma and lower epidermis (from top to bottom). However, the tissue differentiation became trickier in senescing leaves (from tag +4) where the structure tended to be less organized. The most obvious structural modification observed between the leaf stages was the increase in leaf thickness with ageing. This was mostly due to enlargement of the palisade cells. The upper epidermis seemed to experience similar swelling to the palisade parenchyma, and the structure of the lower epidermis, that was less affected by ageing, was likely to change in the same way. Another noticeable structural change that can be observed (Figure 1-b-6) was the disappearance of chloroplasts during leaf development. In addition to changes in numbers of chloroplasts, plast structure was also affected by ageing. This is illustrated in Figure 1-b-7 depicting electronic micrographs of plasts at three developmental stages. Chloroplasts had several starch granules in young and mature leaves, well defined thylakoids and few small plastoglobuli (Figure 1-b-7 a). By contrast, in gerontoplasts present in senescing leaves (Figure 1-b-7 b), plastoglobuli were larger and numerous. A few thylakoids were observed, but not stacked as in chloroplasts, and no starch granules were visible. Gerontoplasts were found mainly in senescent leaves, although a few of them were observed in mature leaves. In the final stage of development (corresponding to the oldest leaves (Figure 1-b-7 c)) plasts were constituted of relatively large lipid droplets surrounded by an envelope. These plast were not detectable by light microscopy because they were rare and because toluidine blue is known specifically to stain starch in the plast.

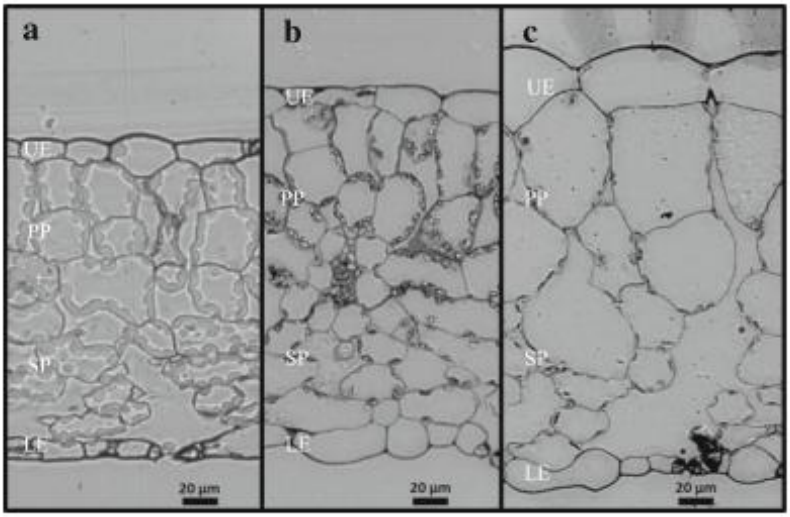

Figure 1-b-6 Light micrographs of cross sections of oilseed rape leaves at three typical developmental stages: young (tag -2) (a), mature (tag+2) (b) and senescent (c) (tag +4). UE upper epidermis, PP palisade parenchyma, SP spongy parenchyma, LE lower epidermis

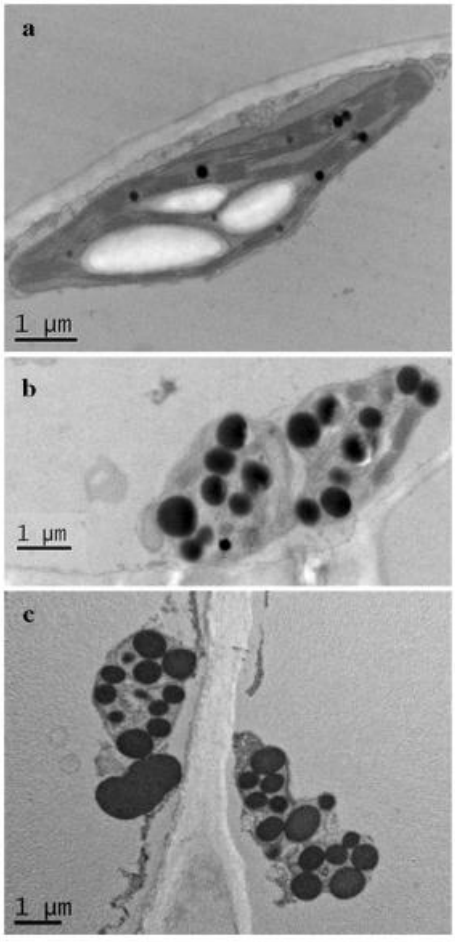

Figure 1-b-7 Electron micrographs of plasts from oilseed rape leaves: a chloroplast from young (tag +2) and mature leaves; b gerontoplast from a senescent leaf (tag +4) and (c) plasts in final developmental stage present only in the oldest leaves (tag +5)

Changes of parenchymal structure

The structural modification of leaf tissues seen in Figure 1-b-6 is presented in Figs. 8. The average vacuolar volume of palisade parenchyma cells increased markedly (Figure 1-b-8), while that of spongy parenchyma remained around 0.3 mm3. Leaf thickness increased from around 250 µm to 320 µm, mainly due to an increase in the palisade parenchyma (from 100 µm to 160 µm). The thickness of the spongy parenchyma remained at around 100 µm. Each epidermis presented a slight increase in thickness.

Note that, as mentioned earlier in Materials and Methods section, measurements of the area and width of the vacuole on the samples taken perpendicularly and parallel to the central vein confirmed that vacuole depth and width can be considered as identical, validating the model for volume estimation based on micrograph observations (see annexe 1).

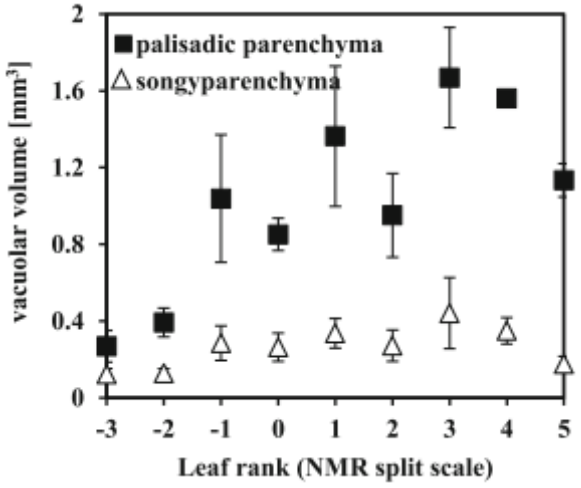

Figure 1-b-8 Vacuole volume of the cells of different parenchyma of the oilseed rape leaf. Each measurement is an average of at least 40 cells of four different images

Figure 1-b-9 depicts the percentage of the leaf cross section occupied by each tissue according to the NMR split scale. In order to approximate vacuolar water at the tissue level, internal spaces and plasts were removed from the representation. The volume of epidermis cells represented about 15% of the leaf tissues and therefore contributed to the NMR signal. Due to their irregular shape, the volume of epidermis cells could not be estimated from micrographs. However, an increase in both upper and lower epidermis thickness was observed, indicating similar evolution of these tissues to that of palisade parenchyma, i.e. in accordance with the hydraulic designs proposed in leaves by Zwieniecki (Zwieniecki et al. 2007). We therefore supposed that the fifth component of the NMR signal reflected epidermis vacuoles in addition to the palisadic parenchyma vacuoles. In consequence, the volumes occupied by epidermis and palisade cells were pooled for comparison with NMR results (Figure 1-b-9).

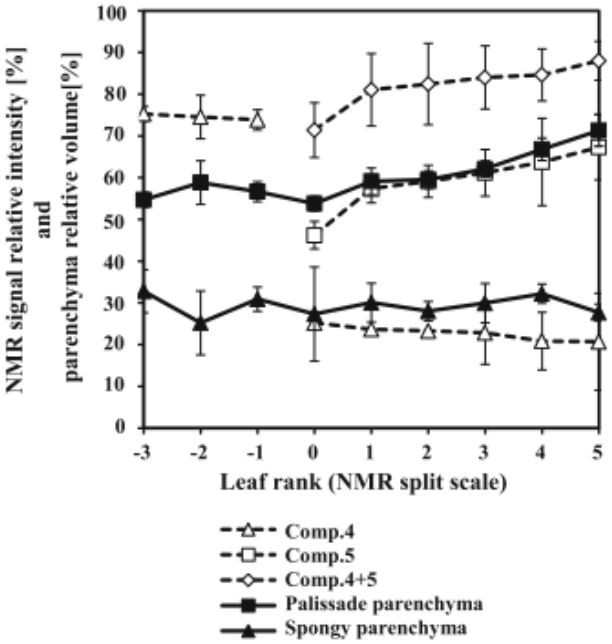

Figure 1-b-9 NMR signal intensity of the fourth (white triangle) and fifth components (white square) and both components (white diamond) expressed as percentage of the total NMR signal intensity and in relation to the split. Relative volume of spongy parenchyma (black triangle) and relative volume of palisade parenchyma and epidermis (black square) measured on light micrographs of oilseed rape leaf cross sections and presented in relation to the split and expressed as percentage of the whole limb volume. Each point represents the average of measurements from 4 to 10 images (from at least three different leaves)

For comparison with the vacuolar water changes measured from micrographs, the percentages of the total intensity of components 4, 5 and 4+5 are represented on the same graph. The results showed an increase in volume of palisade and epidermis tissues whereas the spongy parenchyma remained constant. At the same time, the relative intensity of the fifth component increased, while that of the fourth remained almost constant. The latter indicated that the fourth component might be related to vacuoles of spongy parenchyma cells while the fifth component might correspond to those of the palisade parenchyma cells.

1-b-3 Discussion

Differential structural changes of leaf parenchyma throughout leaf senescence

As described in the introduction, leaf parenchyma have different functions that may lead to different patterns of evolution during senescence. The major limitations for studying functions of each parenchyma separately are technical; for example, there is no easily available technique that allows differential evaluation of biochemical traits at the tissue level. In C3 plants, like oilseed rape, only structural differences between parenchyma have been analyzed in detail, due to the fact that they are visible microscopically. Microscopic studies of leaf tissue structure have mostly focused on the impact of water stress in Arabidopsis (Wuyts et al. 2012), peas (Martinez et al., 2007), olive trees (Bacelar et al. 2006) and horse chestnut trees (Nardini et al. 2010). The impact of ozone has also been measured at the tissue level by measuring leaf tissue thickness of different woody plant species, because of the

well-known gas exchange role of spongy cells (Günthardt-Goerg et al. 2000). The results reported have shown significant differences between species in response to such stress, in terms of size and structure of parenchyma.

The different patterns of evolution of palisade and spongy cell volumes (Figure 1-b-8) reported here could be explained by the specialized functions attributed to each type of parenchyma. In view of their major role in photosynthesis (Nardini et al. 2010), palisade cells would be more impacted by the nutrient remobilization process associated with plast dismantling, especially in terms of change in solute composition of the vacuole that is the major site of degradation of different molecules during senescence (Otegui et al. 2005). The increase in palisade cell volume corresponding to leaf hydration (Figure 1-b-1) could be explained by cell wall loosening probably together with lowering of vacuolar osmotic potential. For instance, it has been shown on Arabidopsis that several cell wall degrading enzymes (β-glucosidase) are enhanced by decline in photosynthesis (Mohapatra et al. 2010), suggesting that cell wall degradation occurs in the leaf cells during senescence. These authors suggested that polysaccharides bound to the cell wall that remains intact even during the late phase of senescence may be a possible source of sugar. On the other hand, spongy cells, that have a major role in the leaf's hydraulic status (Nardini et al. 2010), are believed to regulate water status during senescence.

As a matter of fact water content was shown to increase in oilseed rape leaves during senescence (Figure 1-b-1 c and d), in accordance with findings previously reported by Musse *et al.* (2013). This increase is due to loss of dry weight that materializes remobilization of cell materials (Diaz et al. 2008) and to leaf hydration. This hydraulic characteristic was revealed by both micrographs and the increase in fresh weight observed during senescence progression (see Annexe 2, Supplementary data 1). The water entry is at the origin of the slight increase of the intensity of the signal corresponding to the vacuole and probably of the increase in T_2. In mature leaves (tag 0), the fifth component appeared as a result of the split in the fourth component. This is supported by the fact that the sum of the LWW of two longest T_2 components in mature and senescing leaves (Figure 1-b-4) represented a continuation of the pattern of LWW of the fourth component in young leaves. After the split, the LWW and the T_2 of the fourth component continue to increase slightly, and both parameters of the fifth component markedly increased. As discussed by Musse et al. (Musse et al. 2013), the significant increase in the T_2 of the fifth component is probably due to several phenomena. First, the water influx, at the origin of cell enlargement combined with decreased dry weight, probably induced a dilution of vacuole solutes. This phenomenon was in part counterbalanced by the increase in solute concentration due to degradation processes occurring during senescence (Otegui et al. 2005). Secondly, the increase in cell volume had an impact on the T_2 value because of the sensitivity of T_2 to compartment size (van der Weerd et al. 2001). The trends of components 4 and 5 were linked to the observations from the light microscopy, showing clear tissue differentiation (Figure 1-b-8). Indeed, the

vacuolar volume of the palisade cell increased markedly, whereas such changes did not occur in spongy cells. The variations in palisade vacuole volume measured in the present study (from 0.4 mm3 (tag -2) to 1.6 mm3 (tag 4)) affected the T_2 values of the fifth component. A linear relationship between the relaxation rate ($1/T_2$) and the sum of the inverse of the cell compartment radii has been demonstrated in maize and pearl millet by van der Weerd *et al*. (2001), implying constant permeability of the compartment membrane and the same solute composition of vacuole. However, the linear relationship could not be applied to the results of the present study because of the changes in the vacuole composition and because there was no evidence that tonoplast permeability did not vary during leaf development. The sudden increase in T_2 of the fifth component at the very end of senescence (tag +6 and +7) and the high value of standard deviation of the measurements (Figure 1-b-4) may be linked to active dismantling of the tonoplast of some the palisade cells just before their death. Indeed, the water enclosed in the vacuoles may then spread over the entire symplast compartment. In spongy cells the volume measured on micrograph changed very slightly during senescence compared to palisade cells and was in agreement with changes in signal intensity. The slight increase in the T_2 of the fourth component was probably due to the same mechanisms in young leaves. The relatively small changes in LWW and vacuole volume in this tissue fits well with the spongy cell supposed role in the homeostasis of the leaf hydraulic status. Comparison of the relative intensity of the fourth and fifth components with the volume occupied by the two parenchyma (Figure 1-b-9) demonstrated the attribution of the fourth component to the spongy parenchyma vacuoles and of the fifth component to the palisade parenchyma and epidermis vacuoles.

Note that several authors have postulated that leaves lose water during senescence (McIntyre 1987; Zhang et al. 2012). It was shown by Zhang et al. (2012) that detached senescent Arabidopsis leaves lose water faster than mature leaves. However, there is no abscission of the leaf in Arabidopsis, unlike *B. napus*, and dead leaves of Arabidopsis remain fastened to the plant while drying. Zhang *et al.* (2012) also showed that the abscissic acid level is greater in senescent leaves, indicating that stomata are closed. A decrease in stomatal conductance with aging has already been highlighted in *B. napus* (Albert et al. 2012). Moreover, guard cells live longer than leaf parenchyma cells (Gotow et al., 1988) and are able to control water flux in leaves until the final senescence stage.

In the present study, the focus was on the T_2 components associated with the vacuole. However, certain results suggested putative attribution of the other components of the NMR signal. The third signal component of young leaves (tag -3), relaxing at about 20 ms (Figure 1-b-4) and representing about 15% of the water signal, has previously been linked to the plasts (Musse et al. 2013). Such attribution was supported here by comparison with the results of quantitative analysis of light micrographs, showing that plasts occupied about 13% of leaf tissue volume. However, while following senescence to its final stage, as performed here, the results showed that this component was still detected when plasts had disappeared on light micrographs. Consequently, the third T_2 component in

senescing leaves probably originates, in addition to the plastidial water, from other proton pool relaxing at a similar relaxation rate. Several phenomena resulting from plast degradation could be at the origin of the formation of proton pools. One phenomenon may correspond to the proliferation of small vesicules such as senescent associated vacuoles (Avice and Etienne 2014; Otegui et al. 2005) and RuBisCo containing bodies (Hoertensteiner 2006). These lytic compartments have dimensions in the same order of magnitude as plasts. The second phenomenon may correspond to the proliferation and increase in size of the plastoglobuli (Brehelin et al. 2007) clearly observed on the micrographs (Figure 1-b-3), resulting from the thylakoid membrane remobilization. Note that first and second order vascular tissues were successfully avoided by the sampling procedure; however, a few third and all fourth order vascular tissues were present in leaf samples used for NMR experiments. The contribution of these tissues to the NMR signals, and especially to the third component remains to be evaluated.

The second T_2 component, relaxing at about 3 ms and representing about 2% of the water signal, has been attributed to apoplastic water and to a lesser extent to water inside starch granules (Musse et al. 2013). Our microscopy results (see annexe 2, Supplementary data 4) are in agreement with the literature (Mohapatra et al. 2010), where it was suggested that an increase in cell wall elasticity due to its thinning can be linked to the decrease in intensity and T_2 of this component just before it disappeared. Moreover the disappearance of the second component corresponded to the loss of the plast integrity, and starch granules within them.

Changes in physiological indicators of C and N remobilization throughout leaf senescence

Plasts contain 75% to 80% of total leaf nitrogen (Makino and Osmond 1991) and high amount of lipids (Thompson et al. 1998). They are thus the major source of nutrients remobilized during senescence. Plast dismantling, characterized by chlorophyll breakdown, is generally measured in terms of chlorophyll loss (BuchananWollaston 1997; Otegui et al. 2005). The chlorophyll content was shown to be constant in young and photosynthetically active leaves and to decrease slowly with ageing and plast dismantling (Ghosh et al. 2001). Our results (Figure 1-b-1 a) are in accordance with these results and those of former studies (Inada et al. 1998; Lim et al. 2007; Otegui et al. 2005), demonstrating that the chlorophyll degradation is an early event in senescence. Chlorophyll content, as measured here, was a good indicator of the general plast status but did not make it possible to access information about specific tissues changes. This question was addressed through light microcopy. The light micrographs showed that plast degradation started with a decrease in volume and was followed by a reduction in number, in accordance with results obtained on darkened leaves (Ghosh et al. 2001; Inada et al. 1998; Keech et al. 2007). Despite the higher density of plasts observed in palisade

parenchyma and the different functions attributed to leaf tissues, plast disappearance was concomitant in both parenchyma. This could indicate that the degradation mechanisms are similarly regulated.

Electron microscopy was shown to be complementary to light microscopy as it allowed the investigation of plast structure. Electron micrographs (Figure 1-b-7) showed typical young chloroplast presenting well organized thylakoids and starch granules demonstrating plast functionality (Parthier, 1988). Plastoglobuli, that are responsible for membrane replacement (Brehelin et al., 2007), were not numerous at this age. Gradual chloroplast shrinkage and transformation into gerontoplasts was clearly visible in our images (Figure 1-b-7 b) showing only a few membranes that were stacked and larger and more numerous plastoglobuli. The process described above is characterized by the disintegration and remobilization of thylakoid membranes through plastoglobuli (Thompson et al., 1998, Keech et al. 2007), leading to the accumulation of these plastoglobuli in the plast. The last stage of plast dismantling, corresponding to the oldest leaves studied (Figure 1-b-7 c), was characterized by large plastoglobuli without remaining thylakoids, surrounded by the plastidial envelope. As far as we are aware, this ultimate stage of plast dismantling has not been described in the literature to date, probably because plast evolution through senescence has mainly been studied on darkened leaves (Keech et al. 2007; Wada and Ishida 2009). Dark treatment is known to induce intracellular degradation more aggressively than natural ageing (Wada and Ishida 2009), and it probably enhanced the autophagy remobilization processes. Despite evidence of autophagy of whole plasts during senescence (Guiboileau et al. 2012; Wada and Ishida 2009), the presence of plasts at that late stage therefore demonstrated that they were not all dismantled through autophagy. This may be linked with the suboptimal nutrient remobilization observed in *Brassica napus* leaves during senescence.

Plasts contain an important part of the leaf carbon in the starch granules. Starch content (Diaz et al. 2008; Wada and Ishida 2009) is another common parameter used to monitor senescence. Masclaux *et al.* (2000) proposed that for tobacco leaves studied according to leaf rank, the onset of decrease in starch content represents the source/sink transition. Their results also showed a decrease in dry matter associated with remobilization during senescence. The latter phenomenon was observed in the present study (Figure 1-b-1 b and d) and was at the origin of the decrease in the intensity of the first NMR signal component, demonstrating that NMR signal could be used as indicator of remobilization activity.

While the link between tissue-specific structural modifications and efficiency of nutrient remobilization remains unknown, it is clear that the senescence-associated processes of cell enlargement and tissue hydration occurring in palisade layer may have an impact on this efficiency. Even if the cell hydration seems not to have an impact on plast disappearance, with no difference observed in terms of plast density evolution between the two parenchyma layers, one may expect differences in term of cell metabolism between the two layers that remain to be investigated.

Using parenchyma differentiation on NMR signals as a developmental marker

Investigation of leaf senescence requires knowledge of the developmental stage of the leaves studied. This stage can be determined more or less accurately via parameters such as leaf rank or leaf age, chlorophyll content, gene expression, etc. During plant development, new leaves appear at the top of the plant and leaf senescence progresses from the bottom to the top of the canopy (Masclaux et al. 2000). It should be noted that the progression of senescence is acropetal (Avice and Etienne 2014) in the leaf limb and that this phenomenon was taken into account in the sampling procedure.

In crop plants, such as oilseed rape, wheat, rice and tobacco, leaf rank scale is commonly used to present physiological results (Mae and Ohira, 1981; Masclaux et al., 2000). Presentation of the results according to leaf rank and measurement week showed that leaf rank is a good criterion for monitoring natural senescence. Another approach is to tag leaves according to the time of appearance and to follow their development. If the analysis method is destructive, different plants are necessary for such analysis. However, both approaches necessitate averaging values of leaves from different plants, and are susceptible to variability because leaves from different plants of the same leaf rank or time of appearance are not necessarily of the same physiological status, even from plants grown in controlled conditions.

Chlorophyll content is also commonly used to determine physiological status as it represents a simple, non-destructive method (Otegui et al. 2005; Zhang et al. 2012). However, this method cannot be used to discriminate between young and mature leaves with the maximum of chlorophyll. Moreover, Gombert et al. (2006) demonstrated that chlorophyll content was not a precise parameter to determine physiological status of a leaf. For instance, in the case of nitrogen deficiency, the same chlorophyll content was measured in leaves from stressed and control plants of different developmental status. Our results also showed that the method used for measurement of chlorophyll content was not suitable for determining the senescence stage of very old leaves, characterized by the absence of plasts on micrographs but still with chlorophyll content of around 10% of maximum (Figure 1-b-5).

Similarly, starch content seems to be overvalued in old leaves. Indeed, various authors have detected small amounts of starch in old leaves where the photosynthesis apparatus has clearly been dismantled (Diaz et al. 2008; Masclaux-Daubresse et al. 2008). Our results in old leaves (tag +5 and more) also showed a small amount of starch whereas no plasts were visible on light microscopy.

Another common approach to determine the physiological status of a leaf has been to use the expression of two genes, sag12 (senescence associated gene 12) that is unregulated during senescence and cab (chlorophyll a/b binding protein) that is downregulated during senescence (Gombert et al. 2006). The cross-over between in the expression of these genes was proposed as the onset of

senescence. While the method is helpful to determine a specific leaf status at the cross-over, it is less clear before and after this cross-over and the method remains time consuming.

Finally, the approach using individually darkened leaves (IDL) allows control of the beginning of senescence and therefore better monitoring of plast dismantling occurring in late senescence (Keech et al. 2007). However, it may induce intracellular degradation more aggressively than natural ageing (Wada and Ishida 2009).

As described above, all the methods commonly used have specific defects. The main limitations are related to insufficient method accuracy and the limited sensitivity of the parameter selected in specific developmental ranges. In contrast, NMR signals for oilseed rape leaves were found to be very sensitive to the developmental stage over a very wide period of time. The major modification of the NMR signal is the splitting of the last T_2 component of young leaves, reflecting differences in the pattern of evolution of palisade and spongy tissues. NMR measurement protocol was associated with signal analysis based on two different approaches (MEM and Levenberg-Marquardt) providing in this way a robust method for split estimation. The split appeared to be an essential stage in leaf development, and its progression in the canopy (Figure 1-b-3) was constant (about one leaf rank per week). When using the split for tagging, the changes in the NMR signal throughout the entire development process became highly reproducible (Figure 1-b-4). Physiological parameters occurring according to the split scale (Figure 1-b-5) validated this approach. Moreover, the split scale allowed accurate presentation of the results over a wide range of developmental stages.

In view of the high reproducibility of the NMR signal shown in this study, it should be possible to use all the parameters in the NMR signal to identify the age of an individual leaf. As the method described is based on the differences in the pattern of evolution of palisade and spongy tissues in Brassica napus under specific experimental conditions, the general character of the method should be further evaluated. Indeed, this would require the acquisition of a NMR database for specific experimental conditions and other species, and would be an important step in leaf characterization compared to current methods based on metabolic indicators (chlorophyll, starch content) that require measurement of kinetics.

1-b-4 Conclusion

In this study, different patterns of evolution of the palisade and spongy parenchyma of Brassica napus leaves during development were revealed, associated with leaf thickening due to cell enlargement and tissue hydration. The NMR signal was shown to be sensitive to tissue modifications, and an original interpretation was therefore proposed taking into account both cellular compartmentalization and heterogeneity at the tissue level. The experimental design of the study made it possible to follow structural and physiological changes in leaf during natural senescence, up to its

ultimate stage, where late stage of gerontoplasts was revealed. The link between tissue-specific structural modifications and the efficiency of nutrient remobilization remains unknown; however, the results highlighted the importance of considering the complexity of the tissue structure while studying leaf functioning. Finally, it was also shown that the structural changes can be used instead of long-time measurements of kinetics in order to monitor leaves according to their developmental status. In the current context of fertilization reductions and climatic changes, occurrence of nitrogen depletion and water deficit is expected to increase. One interesting outcome of the present study would therefore be to see how leaf structural modifications and nutrient remobilization during senescence are impacted by these abiotic stresses.

Acknowledgements

We thank the Regional Council of Bretagne for financial support. We also thank the Genetic Resources Center (BrACySol, BRC, UMR IGEPP, INRA Ploudaniel, France) for providing the seeds of the Tenor variety. We thank our colleagues of the Biopolymers, Structural Biology platform, INRA Nantes, France for their help and support with TEM studies. We thank Mireille CAMBERT (IRSTEA) for her assistance with NMR measurements, Françoise LEPRINCE for starch analysis, and Patrick LECONTE and the greenhouse team (IGEPP) for technical support with plant management.

CHAPTER 2

How leaf structure modifications, linked to remobilization processes during senescence, are impacted by abiotic stress.

Chapter 2

The second chapter focuses on the impact of abiotic stresses on the senescence induced leaf structure changes and the link between these changes and the nutrient remobilization. The studies were performed on plants during the regrow period following the vernalization, in order to simulate field conditions. The two main abiotic stresses, i.e. nitrogen deficiency and water stress were applied. The results of the study concerning moderate N stress was presented in the paper entitled *"Nitrogen deficiency impacts cell and tissue leaf structure with consequences on senescence and nutrient remobilization efficiency in Brassica napus"* submitted to Plant Science. The chapter also includes the results of the work focusing on the impact of water stress on leaf structure.

2. a) Nitrogen deficiency impacts cell and tissue leaf structure with consequences on senescence and nutrient remobilization efficiency in *Brassica napus*

Abstract

Improvement of Nitrogen Use Efficiency (NUE) is a major goal for several crop plants, especially *Brassica napus*. Indeed, the low NUE in this crop results in negative economic and ecological consequences (Singh, 2005). The low NUE of oilseed rape is mainly due to low remobilization of nitrogen from vegetative parts to growing organs (Malagoli et al., 2005). Remobilization of leaf nitrogen takes place during senescence (Avice and Etienne, 2014), a process known to strongly modify cell and tissue structure (Sorin et al., 2014). This study focused on the impact of moderate N depletion (180kg/ha instead of 240kg/ha) on both these structural modifications and nutrient remobilization. Two genotypes (Aviso and Express) with different tolerance of nitrogen depletion were studied. Structural modifications of leaf cells and tissues were investigated through NMR relaxometry and light microscopy, while the remobilization efficiency of the genotypes was evaluated through amounts of nitrogen in leaves. Lower tolerance of N depletion was associated with lower nutrient remobilization and fewer structural modifications. The results showed that leaf structure modifications monitoring during senescence could be used to select a genotype with high nitrogen remobilization efficiency.

Keywords: oilseed rape; leaf senescence; NMR Relaxometry; NUE; microscopy

2-a-1 Introduction

Brassica napus is a worldwide crop with numerous uses in food, feed and non-food products (biofuel, lubricants, etc). Its production has increased more than five-fold over the last thirty years (www.fao.org). Nitrogen (N) fertilization is one of the highest costs of oilseed rape production (Singh, 2005). Conventional crop management practices requires the use of relatively high amounts of N fertilizers, (from 150 to 300 kg of N ha^{-1}) to ensure an optimum yield (Rathke et al., 2006). Whatever the rate of N fertilization, the oilseed rape N harvest index is low compared to cereals (Dreccer et al., 2000) and despite a good capacity for N absorption, less than 50% of the nitrogen absorbed by the plant is present in the seeds at harvest (Schjoerring et al., 1995). Oilseed rape is known to have low nitrogen use efficiency (NUE) mainly due to low N remobilization efficiency (NRE) during sequential leaf senescence, as reported in several studies performed under field or control conditions (Malagoli et al., 2005; Tilsner et al., 2005; Gombert et al., 2006). The remobilization processes associated with senescence in this crop species are not maximal and can lead to high amounts of residual organic nitrogen in falling leaves. In addition, this low remobilization performance during sequential senescence strongly impacts on agronomic potential and final yield (Noquet et al., 2004). Its low NRE therefore affects oilseed rape production both economically and environmentally (Singh, 2005). Some studies have focused on improving other components of the NUE, e. g. nitrogen uptake efficiency (NupE) (Schulte auf'm Erley et al., 2007) and nitrogen assimilation efficiency (NAE) (Good and Beatty, 2011). However, NRE improvement has been considered a major target in the current context of input reduction, in order to maintain oilseed rape yield (Kessel and Becker, 1999; Berry et al., 2010; Miro, 2010) .

Senescence processes have been shown to be highly gene regulated (Buchanan-Wollaston et al., 2003) and former studies have demonstrated that several genes are involved in nitrogen metabolism (Horst et al., 2003). A high NRE should fit with optimum rate of N recycling, including dismantling of plasts and other organits (Martínez et al., 2008). These dismantling processes affect all constituents of the internal leaf structure, *i. e.* plasts, cell vacuoles and cell wall. Plasts represent around 15% of the volume of oilseed rape leaves and are the main source of N and C. They are dismantled and disappear during senescence. Vacuoles, representing the main site of macromolecule degradation during senescence, are also highly affected by remobilization in terms of operating (Otegui *et al.*, 2005). Moreover, the vacuolar structure of oilseed rape leaves has also been shown to be modified during senescence and significant changes in the tissue structure have been reported (Sorin et al., 2014). Indeed, the cell wall is degraded during natural senescence and leaf water content increases, leading to an increase in cell size, especially in the palisade parenchyma. The low NRE of oilseed rape during the vegetative stages might not be due to a limitation of the amino acid transport to the phloem but seems to be related to incomplete hydrolysis of proteins (Noiraud et al., 2003; Tilsner et al., 2005). The regulation and efficiency of the degrading enzyme and autophagy process during senescence has been extensively studied (Sakamoto, 2006; Martinez et al., 2008) highlighting the upregulation of numerous

proteases (Gombert *et al.*, 2006). NRE is determined during senescence and that process can be strongly impacted by environmental conditions. Indeed, water or nitrogen deficiency have been shown to accelerate leaf senescence and thus reduce NRE (Albert et al., 2012).

Senescence and remobilization efficiency have also been studied through the biochemical changes occurring in the case of nitrogen deficiency (Albert et al., 2012). Nevertheless, few studies have revealed the structure modifications occurring during senescence and no information is available on the effects of nitrogen deficiency on the leaf structure. The precise link between remobilization performance and structural changes remains to be clarified. Revealing cellular and tissular modifications can be of a great interest for selection for efficient remobilization of leaf nutrients during sequential leaf senescence. These modifications can be finely evaluated by low field proton Nuclear Magnetic Resonance (NMR), that has been used for investigation of cell water compartmentalization in various plant organs (Hills and Remigereau, 1997; van der Weerd et al., 2001; Duval et al., 2005; Musse et al., 2010). Recently, NMR signal has been used to reveal cell and tissue structure modifications in *Brassica napus* leaves during senescence (Sorin et al., 2014).

The aim of the study presented here was to investigate the effects of nitrogen deficiency on tissue and cell structure modifications and nutrient remobilization processes occurring in oilseed rape during senescence. Two genotypes of oilseed rape were studied: The Aviso genotype was chosen because it is known to be adapted to nitrogen depletion (Bouchet et al.) and the Express genotype was chosen because it is more affected by N stress (Rathke et al., 2006). Plants were grown in a controlled environment reproducing at best field conditions and submitted to moderate N deficiency. Leaves of plants of both genotypes were sampled during stem elongation, a period in which remobilization from senescing organs is important. Indeed, several studies have shown that leaves at this stage can be considered the major contributors of N to the seeds (Noquet et al., 2004; Malagoli et al., 2005). Leaf structure modifications were revealed by low field NMR and light microscopy. The physiological status of leaves was characterized through chlorophyll and water content, and N quantification was used to assess remobilization progress.

2-a-2 Results

Characterization of leaf senescence

As described in Materials and Method, the measurements were performed on the five or six oldest leaves. Rank 0 corresponded to the last leaf appeared on each plant before the beginning of the vernalization period, thus positive ranks corresponded to leaves appearing during vernalization when the nitrogen depletion begin for N-stressed plants. For both genotypes, nitrogen stress induced earlier leaf fall compared to well fed plants, as can be seen in Figures. 2-a-1 to 2-a-4 depicting the physiological characteristics of the leaves

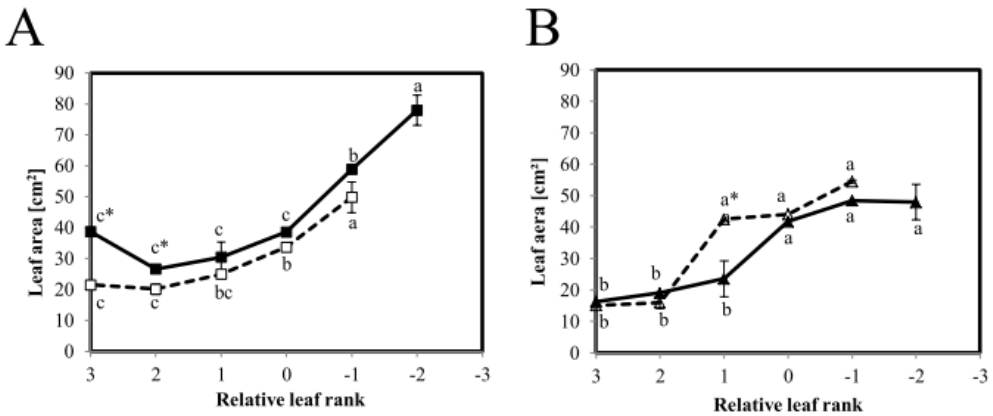

Figure 2-a-1: Area of the oldest leaves of twelve-weeks old plants of two genotypes of oilseed rape, Aviso (A) and Express (B), grown in two conditions: control (solid line) and nitrogen deficiency (dotted line). Each data point corresponds to the average of four repetitions. Relative leaf rank 0 corresponds to the last leaf appearing before vernalization.

Figure 2-a-1 depicts the total area of the leaves studied. A global decrease in the leaf area was observed from the oldest to the youngest leaves, Aviso (Figure 2-a-1 A) having larger leaves than Express (Figure 2-a-1 B). Overall, there was no difference between leaf areas of control and N-stressed plants, except that the youngest leaves were larger in control Aviso plants (Figure 2-a-1 A). The impact of nitrogen deficiency on photosynthesis was evaluated through both chlorophyll content and chlorophyll fluorescence yield (Figure 2-a-2).

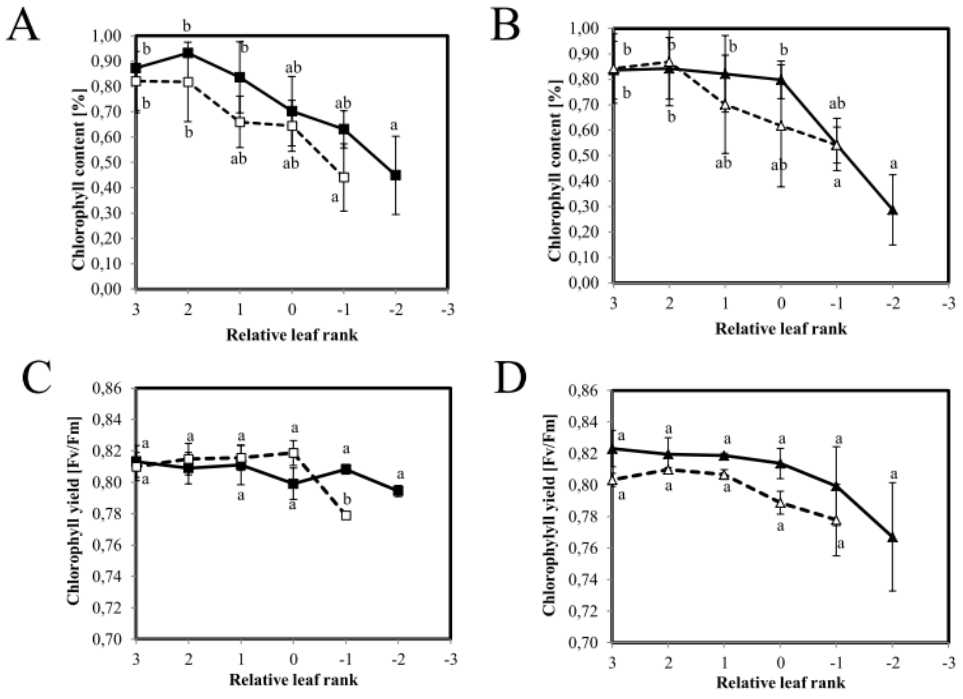

Figure 2-a-2: Chlorophyll content (A, B) and yield (C, D) of the oldest leaves of twelve-weeks old plants of two oilseed rape genotypes, Aviso (A, C) and Express (B, D), grown in two conditions: control (solid line) and nitrogen deficiency (dotted line). Each data point corresponds to the average of four repetitions. Relative leaf rank 0 corresponds to the last leaf appearing before vernalization.

As expected, all plants presented a decrease in chlorophyll content with ageing. Nitrogen depletion induced an emphasized decrease in chlorophyll content (Figure 2-a-2 A, B) in all leaves of the Aviso plants, while this trend was less marked for Express leaves. Chlorophyll yield remained stable for all the Aviso leaves studied

whatever N treatment (Figure 2-a-2 C). In contrast, chlorophyll yield decreased slightly with both age and nitrogen treatment in leaves from the Express genotype (Figure 2-a-2 D). Dry matter per leaf area decreased according to leaf age in Aviso, and remained stable in Express leaves. Nitrogen depletion had a different impact on dry matter per leaf area in the two genotypes investigated, with a reduction in Aviso and a rise in Express plants.

Water content (Figure 2-a-3 C and D) in the youngest leaves (rank 3 to rank 1) in the Aviso plants grown in both optimal and low nitrogen conditions was relatively low (around 70% of fresh weight), and it increased with leaf age to 85% for the oldest leaves studied. Water content remained constant and clearly distinct between treatments in Express leaves at around 80% for control and 70% for stressed leaves.

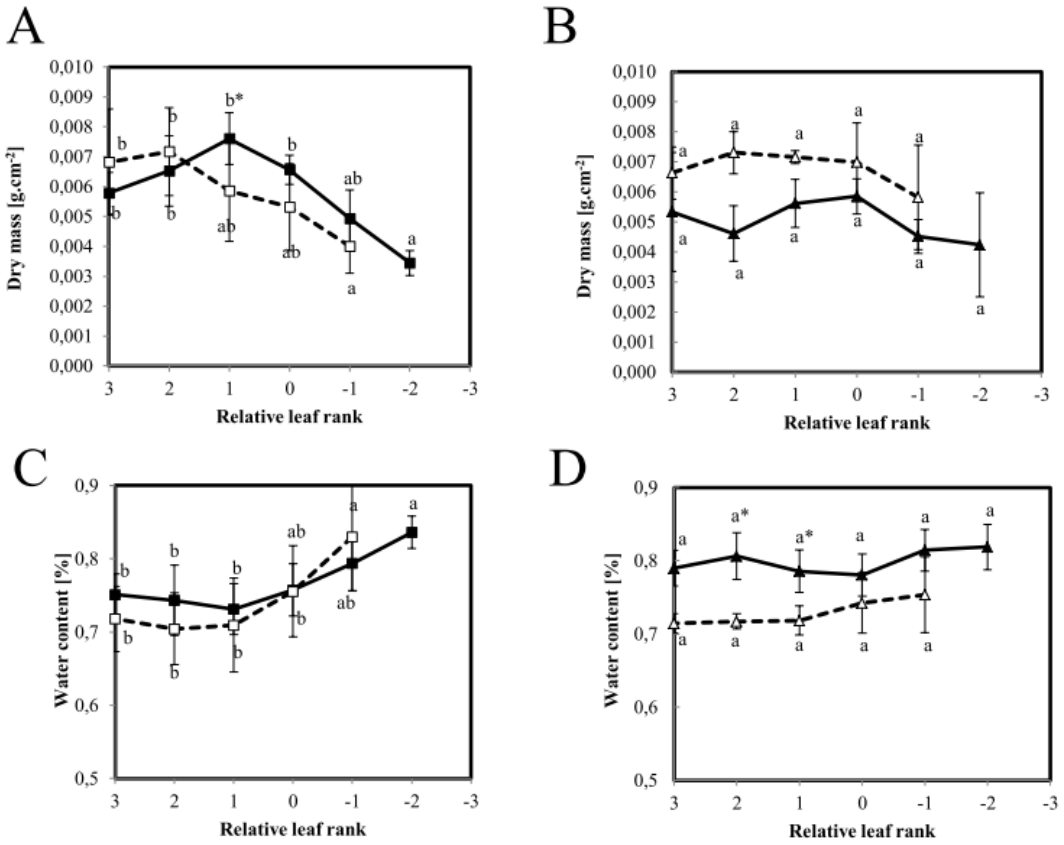

Figure 2-a-3: Dry mass per disc (A, B) and water content (C, D) of the oldest leaves of twelve-weeks oilseed rape plants of two genotypes, Aviso (A, C) and Express (B, D), grown in two conditions: control (solid line) and nitrogen deficiency (dotted line). Each data point corresponds to the average of four repetitions. Relative leaf rank 0 correspond to the last leaf appearing before vernalization.

Characterization of nitrogen depletion

Figure 2-a-4 shows the N content measured in leaves from control and stressed plants of both genotypes. For Aviso, the amount of N was higher in leaves of rank 3 and 2, indicating that all mineral N supplemented at the onset of the stem elongation was preferentially driven in young organs. On the other hand, N content was clearly reduced in the oldest leaves (rank -2).

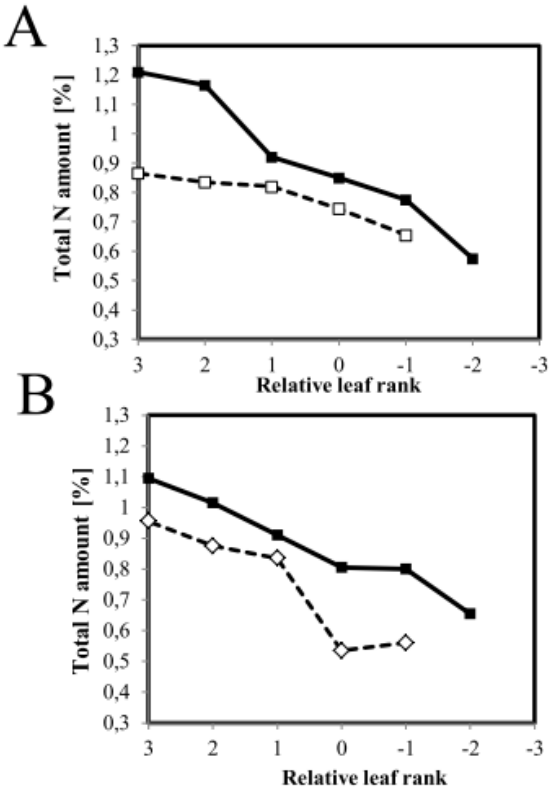

Figure 2-a-4: Total amount of Nitrogen in leaves from Aviso (A) and Express (B) genotypes in control (solid line) and N deficiency (dotted line) conditions. Each data point corresponds to the average of three technical repetitions made on two biological repetitions.

The difference between treatments was visible in young leaves (positive ranks), the N content being noticeably lower in leaves from stressed plants, in accordance with the absence of N fertilization at the beginning of the stem elongation period. The evolution of N content measured in control Express leaves was very similar to that of leaves from control Aviso leaves. As in Aviso plants, N content was lower in stressed plant leaves compared to control leaves, emphasizing the difference between N treatments.

Structural modifications

Figure 5 shows an illustration of light micrographs of different leaf ranks from control and N-stressed Aviso plants. Palisade parenchyma consisted of three to four layers of regular-shaped cells, while spongy parenchyma was characterized by less organized structure. Very slight differences in leaf thickness and vacuole volume were observed on the control leaf micrographs between the youngest and oldest leaves studied from plants grown in both control and stressed conditions. Epidermis tissues were very thin and covered with a relatively thick wax layer. As expected, intercellular spaces were mainly present in spongy parenchyma leaves from control plants, although some were observed in palisade parenchyma, as reported by Evans and Voncaemmer (1996).

More surprisingly, significantly increased numbers of large intercellular spaces, estimated from micrographs, were observed in both palisade and spongy parenchyma, in leaves from stressed plants compared to control leaves (Figure 2-a-6 A). The effect of N depletion seemed to be more enhanced with ageing. The same trends were observed for the Express plants, but to a lesser extent (Figure 2-a-6 B). Chloroplasts were visible in all leaves and did not significantly differ in number whatever the leaf age, indicating that in the conditions of the present study the senescence process was far from being completed even in the oldest leaves studied.

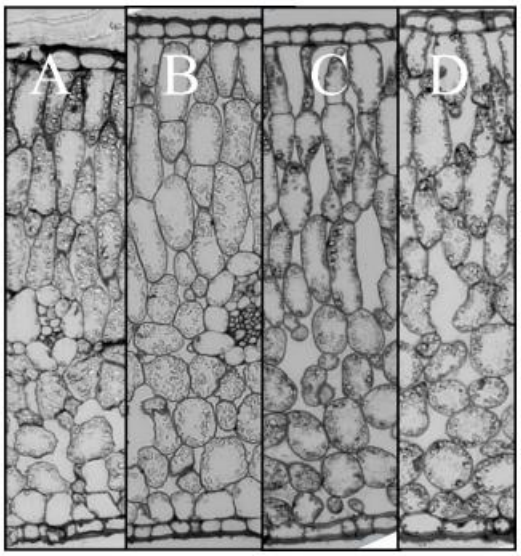

Figure 2-a-5: Micrographs of cross sections from the two oldest leaves of Aviso genotype in both conditions. A: control condition rank -1 ; B: Control condition rank -2; C: N- condition rank 0; D: N- condition rank -1.

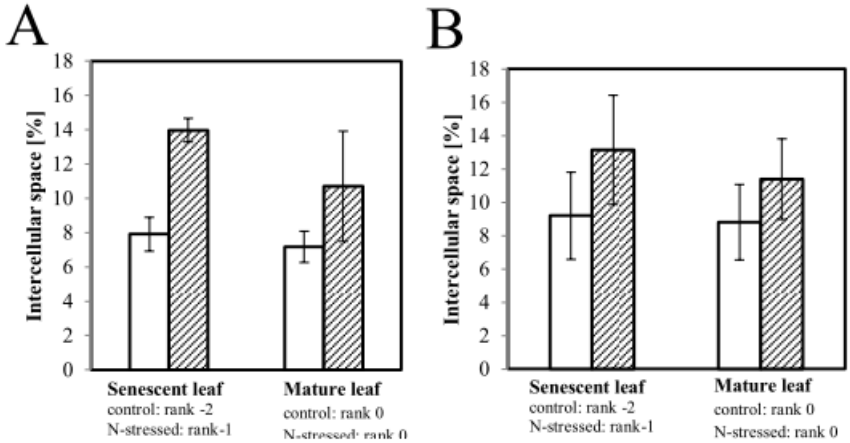

Figure 2-a-6: Percentage of intercellular space in mesophyll of Aviso (A) and Express (B) leaves from plants grown in control (white) and N deficiency conditions (hatched)

The distribution of vacuolar volume in all cells of both the palisade and the spongy parenchyma of Aviso leaves is presented in Figure 2-a-7. (A, C, E, G). The results indicated that in the majority of cells the vacuolar volume of rank 1 leaf (Figure2-a-7 A) was centered at about 0.35 mm^3. With ageing (leaves of rank -2, Figure 2-a-7 C), the distribution of vacuolar volume was wider, indicating an increase in the number of large cell, associated with structural changes in leaf tissues. The same trend was observed in leaves from control (Figure 2-a-7 A, C) and N-depleted plants (Figure 2-a-7 B, D). Figure 2-a-7 (B, D, F, H) depicts a continuous distribution of water NMR transverse relaxation times obtained from the same leaves as presented in Figure 2-a-7 A-D. Three components, relaxing at around 2, 12, and 100 ms, were observed for the mature leaves (rank 1) of plants grown in both conditions (Figure 7 B and D). The longest T_2 component attributed to the vacuole (Van As, 2007; Musse et al., 2013) represented more than 75% of the leaf water. The T_2 of this component split into two components in the oldest leaves analyzed (Figure 2-a-7 F and H), resulting into two separate vacuolar components, as already described (Sorin et al., 2014).

The relatively homogeneous distribution of vacuole volumes found in youngest leaves studied (Figure 2-a-7 A and C) may be associated with a single vacuole-associated NMR signal component (Figure 2-a-7 E and G). On the other hand, enlargement of some cells from both parenchyma observed in senescing leaves (Figure 2-a-7 B and D) was in agreement with the splitting of the longest T_2 NMR signal (Figure 2-a-7 F and H).

It is of note that, in addition to the water NMR signal components, a fast relaxing component was measured associated with the protons from dry matter, relaxing at around 0.03ms. This represented about 5% of the total signal intensity, and the intensity of this component decreased with ageing as the dry mass of the leaf decreased.

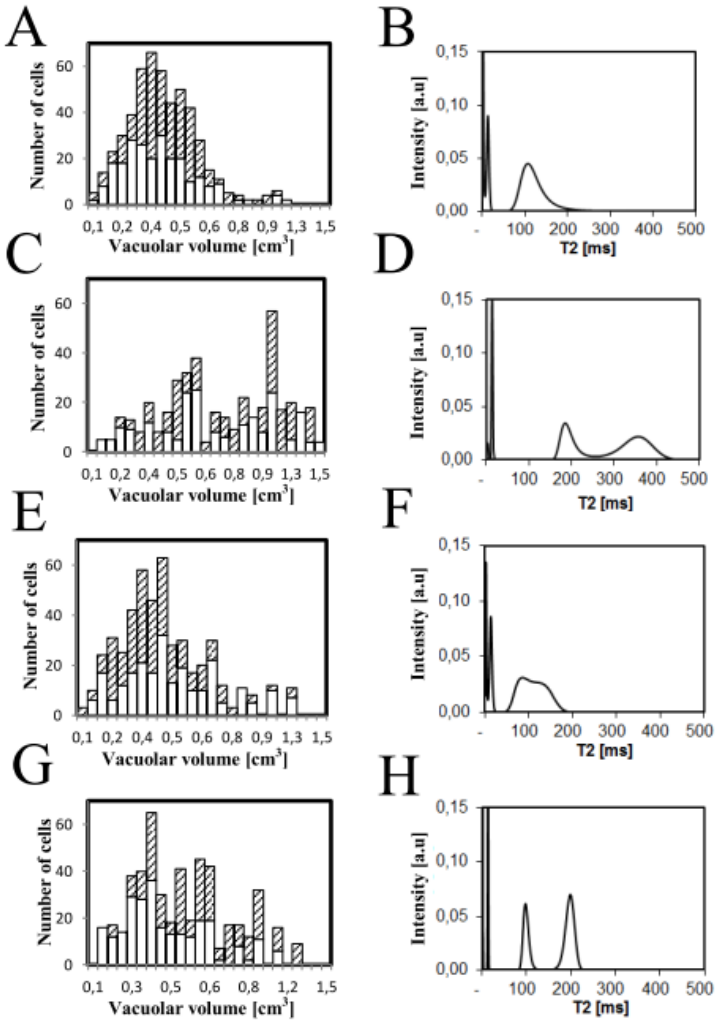

Figure 2-a-7: Vacuolar volume distribution (A, C, E, and G) and transverse relaxation time distribution (B, D, F, H) of the two oldest leaves of an Aviso plant in control (A, B, C, D) and N deficiency conditions (E, F, G, H). A and B correspond to rank -2, C and D to rank -1, E and F to rank 0 (in stressed condition) and G and H to rank -1 (in stressed condition).

Figure 2-a-8 shows the T_2 values of the water-associated NMR signal (components 2 to 5) during leaf ageing for control and stressed plants of both Aviso and Express genotypes. In both cases, the fourth NMR signal component was about 100 ms in higher leaf ranks (rank 3 to rank 0). In control plants, the signal then started to increase and split for the oldest leaves studied (rank -2) as observed

on Figure 7. Nitrogen depletion accelerated the appearance of the fifth NMR signal component for Aviso, whereas in Express leaves no differences were observed between N conditions (Figure 8 A, B). The T_2 of the third component remained stable for both genotypes and both conditions (Figure 8 C, D). The second component disappeared in the oldest leaves (rank -2) of Aviso control plants, while it was observed for all leaves of control Express plants (Figure 2-a-8 F). Moreover, the pattern of evolution of the T_2 of this second component differed between conditions. In Aviso plants, several leaves presented a higher T_2 than control leaves, whereas there were no significant differences in Express plants.

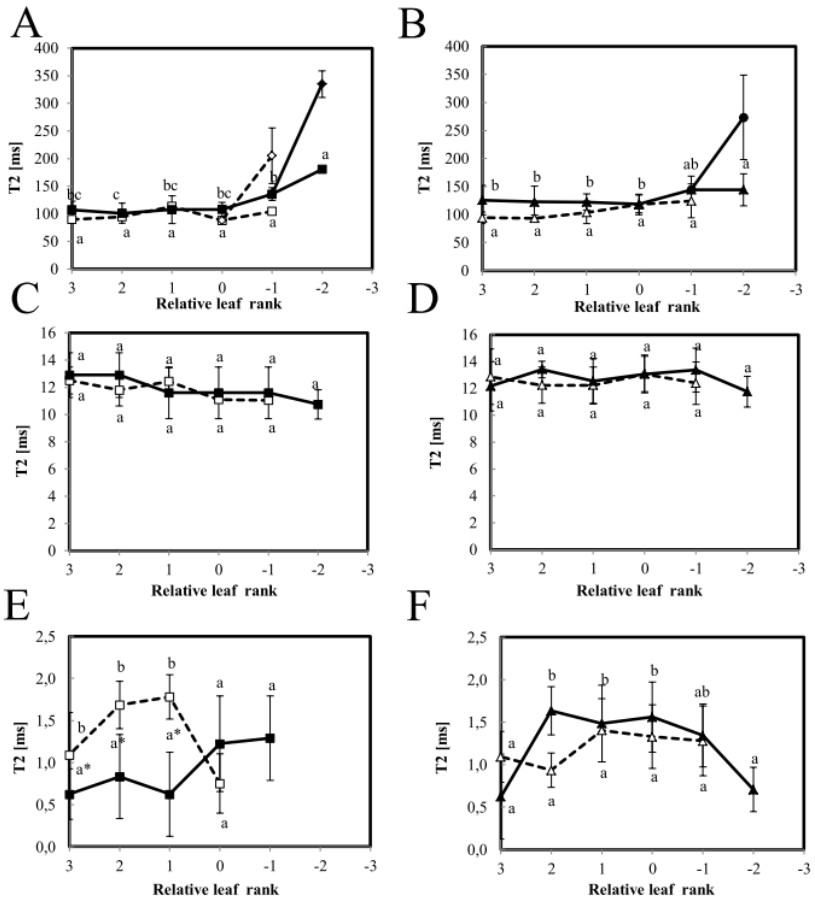

Figure 2-a-8: T_2 of leaves from Aviso (A, C, E) and Express (B, D, F) genotypes in control (solid line) and N deficiency (dotted line) conditions. Fourth and fifth components of the NMR signal are presented in A and B, the third in C and D and the second in E and F.

Figure 2-a-9 represents the amount of water corresponding to the different components of the NMR signal of leaves (LWW) according to rank in Aviso and Express plants. For both genotypes, the LWW of the fourth component of control plants increased very slightly, ranging from about 1.2 g/m^2 in young leaves to 1.5 g/m^2 in senescing leaves. In the oldest leaf (rank -2), the LWW of both fourth and fifth components, generated by the split, was around 1.5 g/m^2, and about two thirds of this water was associated with component 5. The LWW value of the third component was almost constant for all leaf ranks and genotypes and for both N treatments. The LWW values of the second component were stable at around 0.2 g/m^2 in the youngest leaves in Aviso plants. The LWW decreased in the leaves

when the split occurred, reaching zero in the oldest leaves. The same evolution was observed in Express plants but to a lesser extent. The N treatment did not affect the values in Aviso plants whereas in a slight increase in LWW was observed for all leaves of the Express plants.

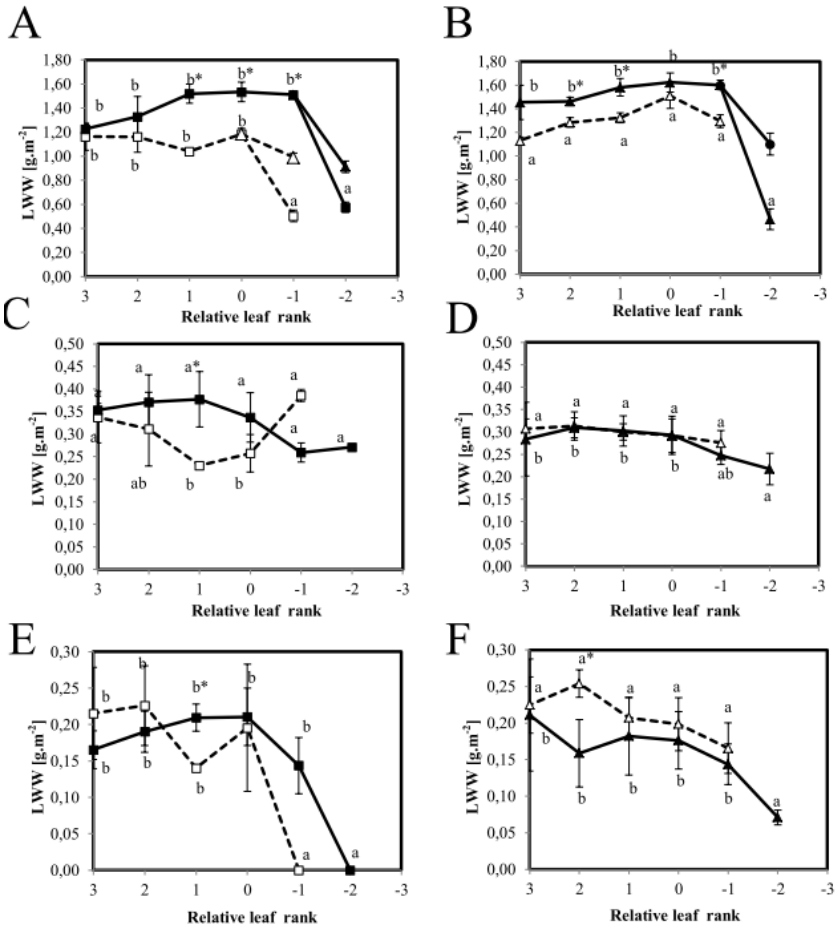

Figure 2-a-9: LWW (expressed in g.m^{-2}) of leaves from Aviso (A, C, E) and Express (B, D, F) genotypes in control (solid line) and N deficiency (dotted line) conditions. Fourth and fifth components of the NMR signal are presented in A and B, the third one in C and D and the second component E and F

2-a-3 Discussion

Phenological and physiological impact of moderate nitrogen deficiency

The 30% reduction of N fertilization applied in the present study was conducted in such a way as to correspond to the reduction in N input under field conditions envisaged in the context of near future sustainable oilseed rape production (Singh, 2005). As shown through the several parameters measured, this relatively moderate nitrogen fertilization clearly impacted plants in terms of phenological and physiological traits. Indeed, for both genotypes, in accordance with previous observations, a reduction in number of leaf ranks was observed in stressed plants, corresponding to a disturbance of plant development (Gombert et al., 2006; Masclaux-Daubresse et al., 2008; Albert et al., 2012). In the case of Aviso genotype, nitrogen depletion may also have impacted on the growth of

young leaves, as already reported in the literature (Bouchet et al.). The other physiological parameters measured, *i. e.* water content, dry matter and indicators of photosynthesis performance (chlorophyll fluorescence yield and content) were not significantly impacted by N depletion, indicating that the study was focused on an early phase of nitrogen deficiency. Indeed, these parameters are known to be strongly affected by long-term N stress (Gombert et al., 2006). Moreover, the measurements were performed at the onset of post-vernalization regrowth when, on the basis of their physiological status, oldest leaves seemed to fall before completing the senescence process. The results of physiological measurements showed expected rank to rank senescence pattern (decrease in chlorophyll content and dry mass) in both genotypes, clearly indicating that the sampling procedure allows to follow remobilization process from its beginning to the leaf falling. In addition to the physiological impact, the effects of N stress were also observed on phenological and final yield characteristics (data not shown). Indeed, N stress induced a delay in flowering time and a reduction in biomass production and seed yield measured on plants conducted until maturity and harvest time (data not shown).

Structural modifications provoked by N deficiency

The palisade parenchyma in oilseed rape leaves consists of regular shaped cells organized in layers, whereas the spongy parenchyma is less well organized and presents large intercellular spaces (Castro-Diez et al., 2000). These two predominant tissues are surrounded by epidermis cells and covered by cuticles. Two palisade cell layers were reported in a previous study performed on oilseed rape of the Tenor genotype grown under non-vernalized conditions(Sorin et al., 2014). These results differed from those of the present study in which three to four layers were observed. Interestingly such structural differences may be due to the effects of the increase in cell division stimulated by vernalization (Manupeerapan et al., 1992) and/or to genotypics differences. The increase in leaf thickness associated with leaf ageing observed here was lower than expected from previous studies (Sorin et al., 2014). It could be attributed to the fact that the senescence process was incomplete under the present conditions, as mentioned above. Further, this phenomenon could also be associated to hardening phenomenon provoked by the vernalization step; a relatively thick cuticle observed on the micrographs probably limited the enlargement of the palisade layer. One other interesting point was that the epidermis cells were small and their size did not vary with leaf ageing, in contrast to earlier results (Sorin et al., 2014). These results highlight the strong impact of growth conditions on leaf structure and confirm the importance of taking these conditions into account when studying remobilization efficiency.

The fact that the amount of leaf water (LWW in g/m^2) in Aviso was significantly lower in N-stressed plants than in control plants, whereas the water content was the same, could be explained by a reduction in dry weight due to remobilization of cell material. Indeed, an increase in the relative percentage of leaf intercellular spaces from 8% to 14% induced by N starvation was estimated from micrographs. In addition, while in control plants intercellular spaces were observed mainly in spongy

parenchyma as expected, these spaces were present in the whole mesophyll of leaves from stressed plants. The same phenomenon, but to a lesser extent, was observed for Express leaves. The increase in the amount of intercellular space could be attributed to the loss of cell-cell adhesion due to decrease in cell wall binding, as observed in fleshy fruits (Redgwell et al., 1997). Indeed, N depletion acting on the synthesis of proteins could be at the origin of lower enzymatic activities of apoplastic proteins. Moreover, different studies have reported that, despite the absence of differences in terms of cellulose and hemicellulose, nitrogen depletion clearly decreased the amount of lignin (Wilson and Mannetje, 1978; Murozuka et al., 2014), and that different cell wall expansin genes are upregulated in reponse to such stress (Scheible et al., 2004).

The results of previous studies demonstrated the sensitivity of the NMR signal to both cell and tissue modifications in oilseed rape leaves during senescence, An interpretation has been proposed taking into account both cellular compartmentalization and heterogeneity at the tissue level. Sorin *et al*. (Sorin et al., 2014) demonstrated that the splitting of the last NMR signal component measured in mature leaves (component 4) into two components was due to massive enlargement of palisade cells during senescence linked to increased water content. The results of the present study indicated that splitting of the NMR component was associated with an increase in vacuole volume of a relatively large number of cells not only distributed in the palisade parenchyma but also in the spongy parenchyma (Figure 2-a-6). It appeared that, under the experimental conditions of the present study, the senescence-associated structural modifications did not result in the same tissue reorganization. Nevertheless, the developmental-induced changes in cell structure were clearly revealed by the NMR signal, confirming that the relaxation signal can be used as a senescence progression indicator under different environmental conditions.

Absence of variations in the third NMR signal component with leaf ageing generally attributed to plasts (Musse *et al.,* 2013) observed for both genotypes and conditions was in accordance with the preservation of plast integrity estimated by physiological parameters and micrographs. This was contrasted with findings reported in the literature (Ghosh et al., 2001; Sorin et al., 2014), where most of the plasts disappeared at the end of senescence. The difference was probably due to the fact that leaves fell before complete senescence in the specific conditions of the present study.

The relationship between the decrease in dry mass due to ageing and remobilization processes and changes in the signal intensity of the first component confirms previous findings, indicating that the dry matter signal can be used as a reliable indicator of relative leaf age (Musse et al., 2010).

Genotype differences in terms of response to N deficiency

The two genotypes used in the present study were chosen for their different behaviors when submitted to N starvation. The final yield components (dry matter production (DM) and seed yield (SY)) showed that they were similar in control conditions (DM 15-16 g/plant, SY 3-3.5 g/plant), while

noticeable differences were observed for plants submitted to N depletion. Indeed, DM decreased by about 30% and 35% for Aviso and Express plants, respectively. The differences between genotypes were even more pronounced for SY, with a decrease of about 37% and 48%, for Aviso and Express plants, respectively. The yield data confirmed greater ability of Aviso plants to adapt to N starvation. This adaptation could not be linked to more effective photosynthesis by Aviso plants during the measurement period but the hypothesis of a better photosynthesis rate after this period cannot be ruled out. The ratio between seed yield and plant dry matter showed more effective nutrient remobilization by Aviso in the situation of nitrogen deficiency. Indeed, this ratio, nearly the same for both genotypes under control conditions , decreased from 21±2% to 19±3% for Aviso and to 17±2% for Express. These results are in agreements with those obtains in a study comparing ten oilseed rape genotypes where it was reported that the maintain of leaf biomass production in low nitrogen conditions was related to a high increase in NRE for Aviso, more efficient than in Express (Girondé *et al.* in prep.).

The differences in the response to N deficiency between the genotypes studied in terms of remobilization efficiency were consistent with structural leaf tissue evolution observed during the experimental period *i. e.* the re-growth period just after vernalization step. First, the micrographs showed a greater increase in the relative volume fraction of intercellular spaces induced by N deficiency with ageing in Express plants compared to Aviso plants (Figure 2-a-6). This is probably at the origin of the lower water content of stressed Express leaves. On the other hand, in Aviso leaves water content did not seem to be affected by N deficiency and increased with leaf ageing, as previously reported (Musse et al., 2013). Secondly, the vacuolar component of stressed Aviso leaves split in the oldest leaves analyzed, whereas this was not the case for Express. As the splitting of the fourth NMR signal component has been shown to be an early event of leaf senescence (Sorin et al., 2014), its absence indicates that either the senescence process was interrupted by leaf fall or it proceeded differently. This hypothesis was supported by the fact that the pattern of the second NMR signal component was different from expected pattern; indeed it was expected to disappear at the end of natural senescence (Musse et al., 2013) but was still observed in the leaves just before falling.

According to Martinez and Guiamet (2014), the leaf apoplast has a major role in both cell structure (cell wall) and nutrient remobilization through numerous apoplastic enzyme activities. Moreover, several authors (Wilson and Mannetje, 1978; Murozuka et al., 2014) have reported that apoplast composition is modified in response to nitrogen depletion. One hypothesis is that nitrogen depletion affects the apoplast composition of the two genotypes in different ways. This could explain both the changes in leaf tissue structure and the different remobilization efficiency.

This study demonstrated that both the pattern of leaf structure evolution during senescence and the remobilization process in oilseed rape are affected by N depletion. Both phenomena occurred although the physiological parameters were only slightly affected. The differences between the two genotypes indicated that there is probably a link between the modification of leaf tissue structure and nutrient remobilization efficiency during senescence. One step has therefore been taken towards

understanding the mechanisms of nutrient remobilization. Further studies should focus on the chemical properties of the apoplast and the cell wall composition and on understanding its role in leaf ageing. This should elucidate the mechanisms explaining the link between leaf structure changes and remobilization process during senescence.

ACKNOWLEDGEMENTS

We acknowledge the Regional Council of Bretagne for financial support. This study was a part of the RAPSODYN project. We also thank the Genetic Resources Center (BrACySol, BRC, UMR IGEPP, INRA Ploudaniel, France) for providing the seeds of the Aviso and Express varieties. We thank our colleagues atthe Biopolymers, Structural Biology platform, INRA Nantes, France for their help and support with TEM studies. We thank Mireille CAMBERT (IRSTEA) for her assistance with NMR measurements, Sylvain CHALLOIS for assistance in image processing, Patrick LECONTE (IGEPP) for plant management and phenotyping and Françoise LEPRINCE for technical assistance. We thanks GERE (Gestion environementale et traitement biologique des déchets) for loaning us light microscope.

2. b) Leaf tissue modification in response to water stress in oilseed rape leaves during senescence

2-b-1 Introduction

Drought is one of the most important environmental factors limiting the growth and productivity of field crops (Blum, 1996; Cattivelli et al., 2008). Previsions about expected global climatic changes indicate that the periods of drought will be more frequent and severe in the near future. Oilseed rape is one of the major oil crops and has numerous uses (food, feed, biofuel…). In this species water deficiency has been shown to provoke a significant loss of grain yield and the depreciation of all yield components (Andersen et al., 1996; Norouzi et al., 2008). This reduction of yield is linked to a decrease in plant height and shoot growth ratio (Norouzi et al., 2008). In addition, drought induces a decline of seed oil content (Tesfamariam et al., 2010) and changes of lipid composition (Bouchereau et al., 1996).

In response to drought, plants can set up different physiological processes in order to reduce water loss(Silva et al., 1999; Serraj and Sinclair, 2002; Rivero et al., 2007). The effect of water stress and plant reactivity was shown to depend on multiple factors such as drought intensity and duration, growth and developmental stages of the plant, genotype and overall conditions of nutrition and culture management (Norouzi et al., 2008; Albert et al., 2012). In response to drought, stomata play a major role in the regulation of transpirational water loss through guard cells (stomatal aperture) functioning and/or leaf stomatal density (Schroeder et al., 2001; Nilson and Assmann, 2007; Kim et al., 2010). Transpiration is also controlled by the lipidic and hydrophobic plant cuticle, which coats the aerial plant surfaces. Cuticle therefore reduces overall transpirational water loss and optimizes drought tolerance by delaying the onset of cellular dehydration during prolonged water deprivation (Chaves et al., 2003; Lu et al., 2012). At the cellular level, numerous metabolic changes occur in response to water stress. In order to maintain cell turgor and functions, some compatible osmolytes are produced and accumulated. In oilseed rape, one of the major osmolytes, proline (Larher et al., 1993; Trotel et al., 1996), seems to fulfill multiple roles of osmoregulation, osmoprotection, redox buffering and nitrogen status management (Albert et al., 2012).

Leaf structure has a major role in the plant water status homeostasis (Aasamaa et al., 2005) and is consequently strongly affected by drought (Netto et al., 2000; Correa de Souza et al., 2011). Using the feeding particularity of some insects that eat only the palissade parenchyma of the leaf, Nardini et al (2010) highlighted the role of spongy parenchyma in the control of the leaf water status,. A decrease in spongy cells size has also been described in response to water deficit in *Phaseolus vulgaris* (Martinez et al., 2007) and associated to a better tolerance to drought (Lecoeur et al., 1995). In

addition, in some olive tree species, large spongy cells were shown to provide better tolerance to plant grown under limiting water conditions (Guerfel et al., 2009). Among the few studies concerning modifications of leaf tissue structure by water stress none was performed on *Brassica napus*.

The aim of the present study was to determine the effects of water deficit on senescence-induced leaf structural modifications in oilseed rape. Since senescence has already been shown to be related to major structural perturbations of leaf tissues in links with nutrient remobilization processes towards sink tissues (see chapter 2a), putative interference of drought stress response with regular developmental processes are under focus. Our previous works also proved that changes in leaf structure can be revealed through NMR relaxometry (see chapter 1) and that this method allows the characterization of different water pools in leaf tissues. Therefore stress impacts were revealed using low field NMR and light microscopy, while the physiological status of leaves was characterized through chlorophyll content and chlorophyll fluorescent yield and water status. An experiment was done in a growth chamber under controlled conditions (see Material and Methods).

Before the experiment introduced above, a preliminary experiment was performed on detached leaf discs submitted to dehydration process. The aim was to obtain the leaf NMR signal changes induced by water stress under simplified and well controlled experimental conditions. Indeed, such experimental design made it possible to quantify the effect of water loss only without effect of the physiological modifications induced during water stress.

2-b-2 Results

Dehydration of detached leaf discs

The investigation was performed on senescing leaves; the NMR signal was therefore characterized by five T_2 components. An example of T_2 distribution is shown in Figure 2-b-1 A. As described in Material and Method section, before applying the dehydration process the discs were soaked into distilled water to insure optimum water content. The T_2 distribution obtained from leaf discs after rehydration is depicted in Figure 2-b-1 (A, B, C, and D). After the rehydration step an increase in the fourth and fifth components was observed. This indicates that vacuoles filled up in order to reach the full turgor. At the intermediate step of dehydration process t2 (10 min), the T_2 value clearly decreased for both the fourth and fifth signal components (Figure 2-b-1 C), while at the end of desiccation stress treatment, only four T_2 components were observed (Figure 2-b-1 D). Figures 2-b-1 E and F represent the intensity of vacuolar components, expressed in Leaf Water Weight (LWW_4, LWW_5 and LWW_{4+5}) and the total water of the leaf (LWW_{2-5}). The LWW_{2-5} increased slightly at t1 and then decreased after t2 and t3. The difference between LWW_{2-5} and vacuolar LWW (LWW_{4+5}) remained unchanged during the experiment, and LWW_2 and LWW_3 were not affected (Figure 2-b-1

F), indicating that changes in total water impact mostly vacuolar components. More precisely, the results showed that these changes principally occurred for the fourth component (LWW_4). Finally, an interesting result was the disappearance of the fourth NMR signal component at the last measurement point (Figure 2-b-1 D, E). Note that the first component, linked to the dry matter of the sample, did not change for excised leaf tissue under our experimental conditions (data not shown).

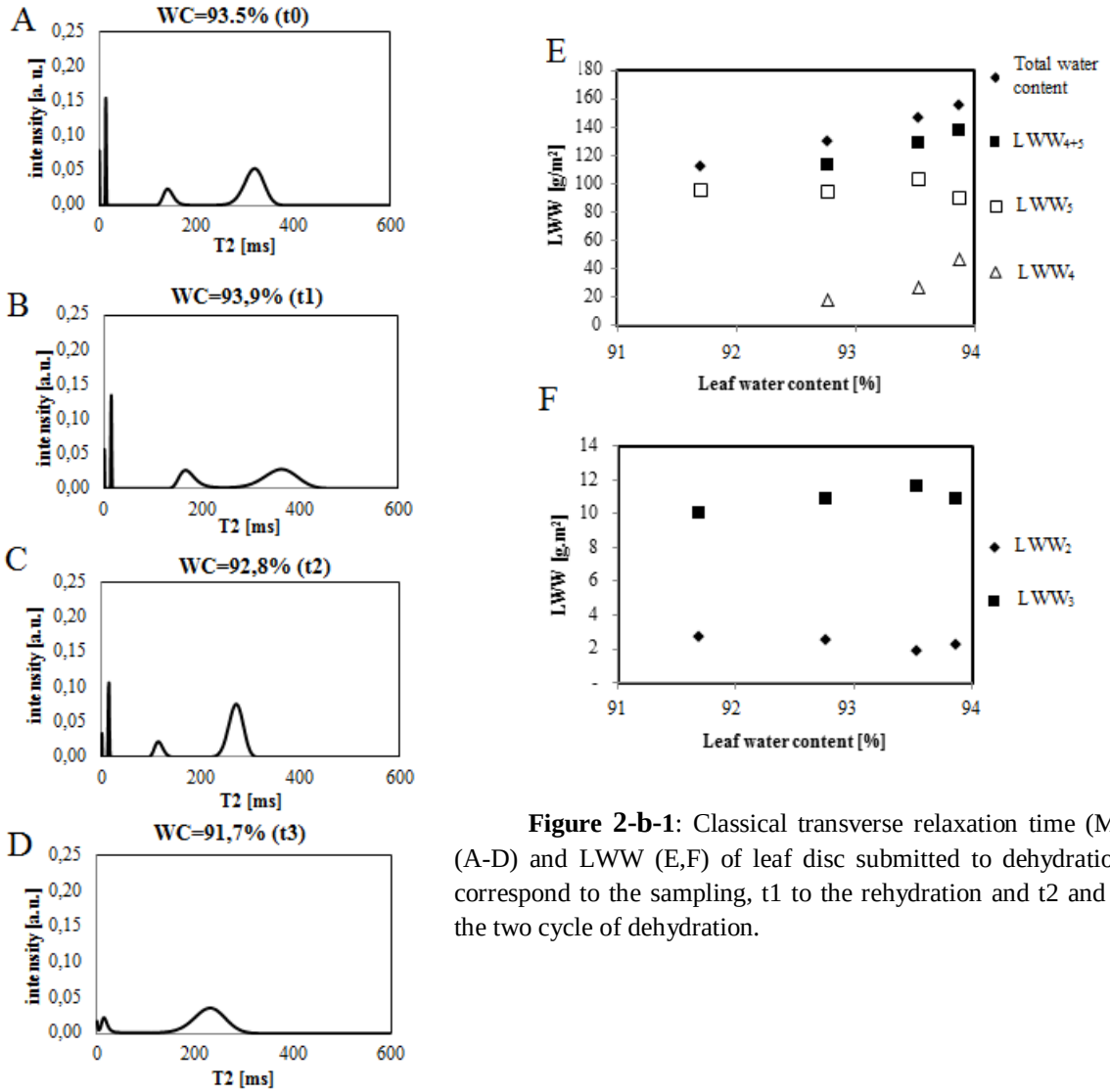

Figure 2-b-1: Classical transverse relaxation time (MEM) (A-D) and LWW (E,F) of leaf disc submitted to dehydration. t0 correspond to the sampling, t1 to the rehydration and t2 and t3 to the two cycle of dehydration.

Water stress applied to whole plants

Figure 2-b-2 presents the evolution of the soil water content during the measurement period. When the water content of the control soil was kept constant at 70% of the maximum field capacity during the whole measurement period, it experienced an approximately linear decrease from 70% to 30% of the maximum field capacity under stress conditions.

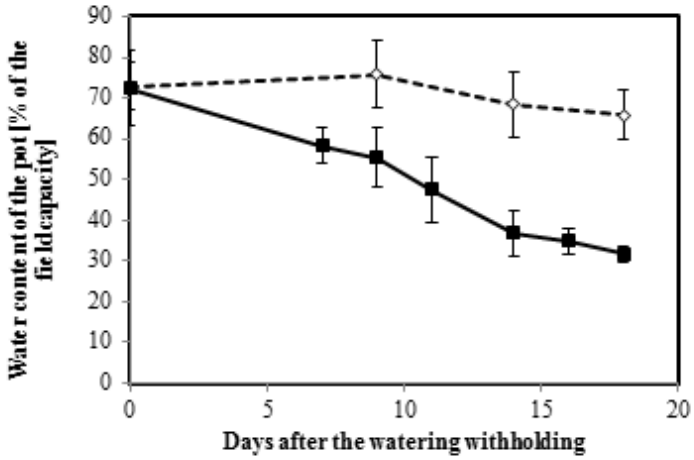

Figure 2-b-2: Water content in the soil express in % of the field capacity during the experiment period for both control (dotted) and stressed (full) conditions. Each point corresponds to the average of eight values

The youngest leaf of each plant was tagged at the end of the vernalization period and measurements were performed on this leaf (leaf rank 4) and the three older leaves below (leaf ranks 1, 2 and 3). Figures 2-b-3 and 2-b-4 depict the physiological and water parameters (chlorophyll content, chlorophyll fluorescence yield, stomatal conductance, water content and relative water content) measured in leaf 4 as an example. For both conditions, the chlorophyll content varied between 30 and 45 a. u. during the first 16 days and fell to 5 a. u. 18 days after watering withholding. However, the chlorophyll content tended to be slightly lower in stressed plants than in control ones. The chlorophyll fluorescence yield remained at its maximum value during the first 17 days under both conditions (Figure 2-b-3 B). On the latest measurement day, it was at 50% of the maximum value in stressed leaves whereas it remained unchanged in control ones. The data registered on leaves 1, 2 and 3 were in accordance to the results presented.

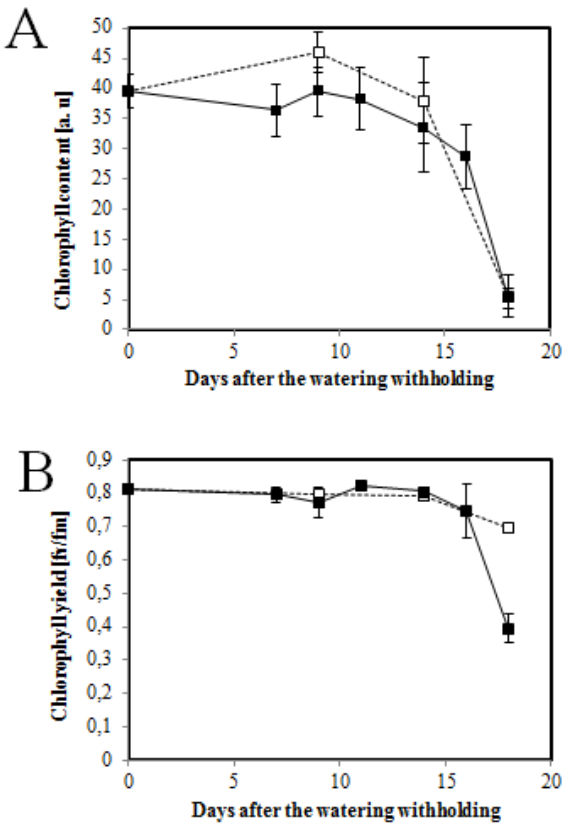

Figure 2-b-3: Chlorophyll content (A) and yield (B) of the leaf during the experiment period for both control (dotted) and stressed (full) conditions.

In control plants, the leaf stomatal conductance did not change until the 9th day, while it was very low at the last two measurement points (Fig 4A). In stressed plants, stomatal conductance was impacted by water deficiency only one week after the watering withholding. It remained stable during few days and reached its minimum value of about 5 mol H_2O/m^2 at day 14. The stomata then remained closed up to the end of the measurement period. Under both conditions, the leaf water content (B) remained constant at around 80% during the two first weeks. It then increased to 85% in control plants whereas it

decreased to 70% in stressed plants. The relative water content (RWC) remained stable around 95% until the end of the experimentation on the control leaf. At the opposite, under stress conditions the RWC started to decrease after the eleventh day and dropped to about 60% at the last measurement day

Leaf water potential (ψ_w), leaf osmotic potential (ψ_s) and associated turgor pressure (T) characteristics of the leaf 4 are presented in Figure 2-b-5. Under well-watered conditions, all parameters remained constant, at around -0.3 MPa for ψ_w, -0.8 MPa for ψ_s and about 0.5 MPa for T, during all the measurement period. In drought-stress leaves, ψ_w started to decrease from the ninth day, first slowly until the eleventh day and then drastically to reach its final value of about -1.2 MPa (Figure 2-b-4 A) at the fourteenth day. In contrast, ψ_s decreased continuously from -0.8 MPa to above -1.2 MPa (Figure 2-b-4 B). The turgor pressure computed from ψ_w and ψ_s showed that up to the eleventh day, the stressed leaf was able to maintain turgor constant by adjusting its water relations while from the fourteenth day, the leaf turgor was lost. Note that the two last points for the stressed leaf were obtained on two or three leaves (instead of four) because some of the leaves analyzed were too dehydrated for accurate measurements of water potential.

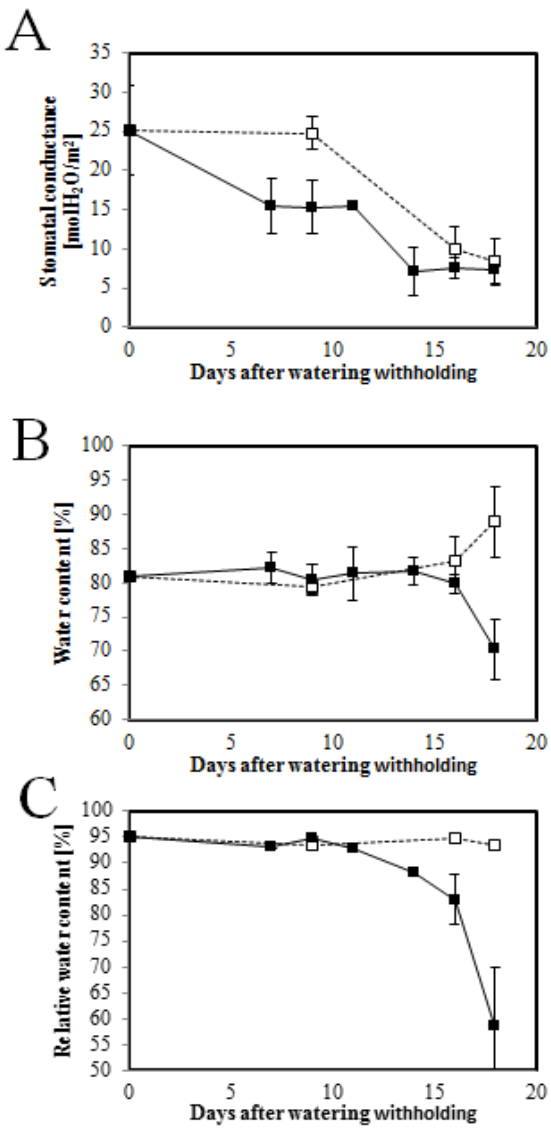

Figure 2-b-4: stomatal conductance (A) water content (B) and RWC (C) of the leaf during the experiment period for both control (dotted) and stressed (full) conditions.

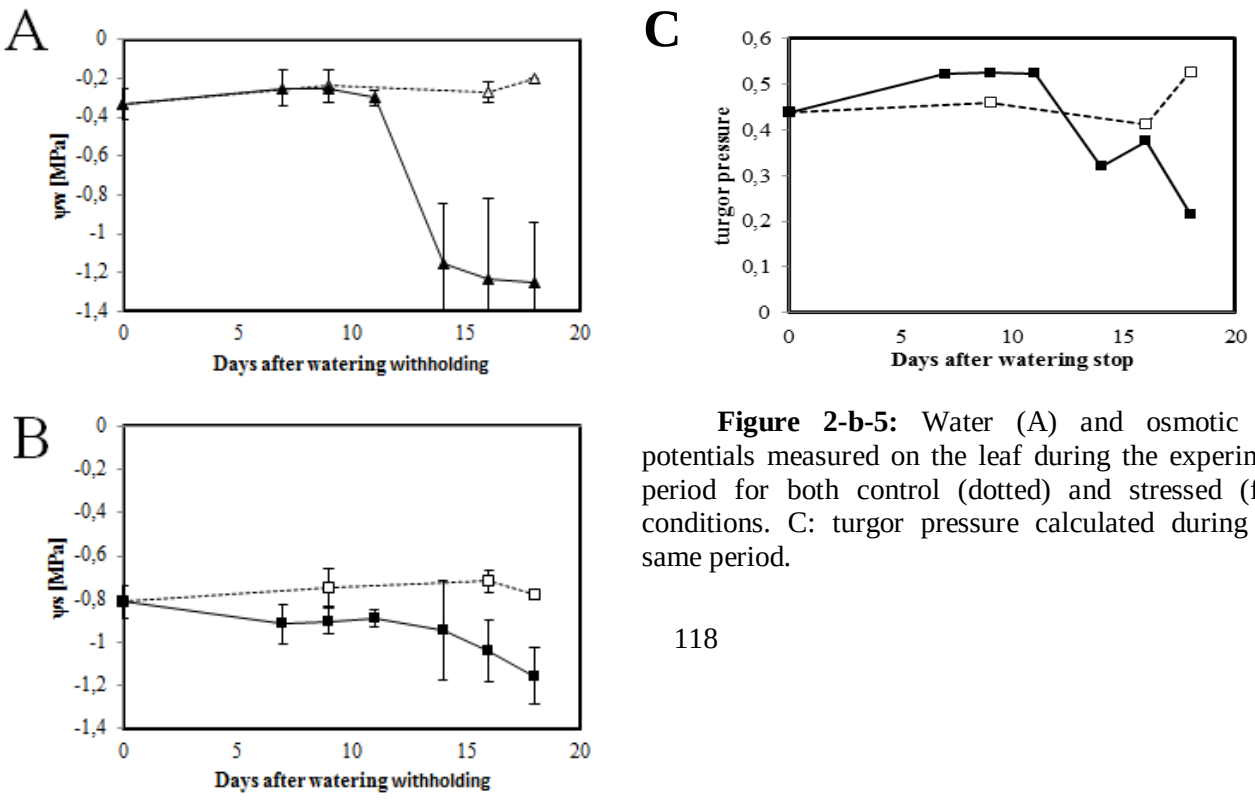

Figure 2-b-5: Water (A) and osmotic (B) potentials measured on the leaf during the experiment period for both control (dotted) and stressed (full) conditions. C: turgor pressure calculated during the same period.

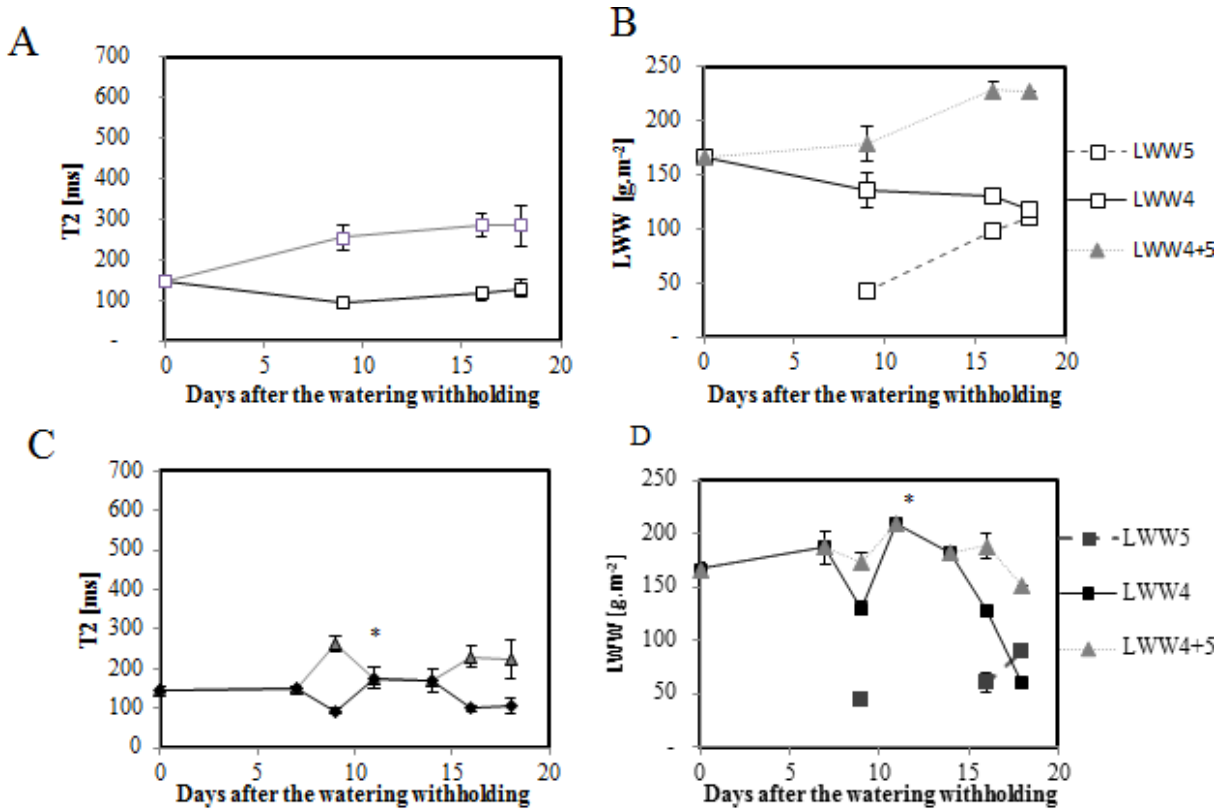

Figure 2-b-6: Evolution patterns of T_2 (A, C) and LWW (B, D) of vacuolar components (of the NMR signal) of the fourth leaf during the experiement for control (A, B) and stressed (C, D) conditions. * represents the data points were only two repetitions were averaged

At the beginning of the measurements, the NMR signal of the leaf 4 consisted of four components, the fourth one characterizing by a T_2 of 150ms and representing the major part (70%) of the signal intensity (Figure 2-b-6). As expected, under control condition this component split into two components at the end of the first week, according to the senescence induced structural changes as described in the first chapter. At this point, the fourth component was characterized by a T_2 of 100ms whereas the fifth one had a T_2 of more than 250ms and the ratio LWW_5/LWW_4 was around 0.4. This result differs from the results of our previous study in which the LWW_5 was always higher than LWW_4. Between the ninth and the sixteenth day, the T_2 and LWW of both components increased slightly and T_2 remained unchanged until the end of the experiment. From the sixteenth to the eighteenth day, LWW_4 decreased, while LWW_5 increased to reach almost the same value. As under control conditions, the fourth NMR signal component of stressed leaves split one week after the beginning of the measurements. From this point, the evolution pattern was complex, with the lack of the fifth component between the eleventh and fourteenth days. Note that at the eleventh day only two of the four repetitions were in this configuration, while for two other repetitions the components five was present. This indicate that each plant have its own developmental kinetic and that NMR is enough

precise to separate two leaves considered as biological replicates. The vacuole-associated water amount expressed by LWW_{4+5} remained constant from the first to the sixteenth day. During this period, in leaves in which the split occurred, the LWW_5/LWW_4 was about 0.35. At the last measurement point, the total vacuole-associated water (LWW_{4+5}) decreased noticeably which was consistent with the drop of the relative water content. It is important to observe that this decrease was due only to the changes in the intensity of the fourth component.

The fourth and fifth vacuole-associated NMR signal components presented considerable differences between the leaves of different ranks (ages), in both T_2 and intensity terms (Figure 2-b-7). As expected, at the first measurement point, the split occurred for the leaves of low leaf ranks (1 and 2) and T_2 of the fifth components was higher in the older leaf. During the experiment, T_2 of the fifth component decreased, indicating that the stress effects overweighed the expected senescence induced T_2 changes. This effect was more pronounced for older leaves. The surprising result concerning the highest LWW_4 compared to LWW_5 observed for the leaves 4 was also observed for leaf 3 whereas leaf 1 presented the expected pattern of evolution. However, at the first measurement point water distribution tended to the expected ratio according to the leaf appearance date expressed in leaf rank (Figure 2-b-7). For example, the LWW_5/LWW_4 was about 1.5 and 4, for the leaf ranks 2 and 1, respectively.

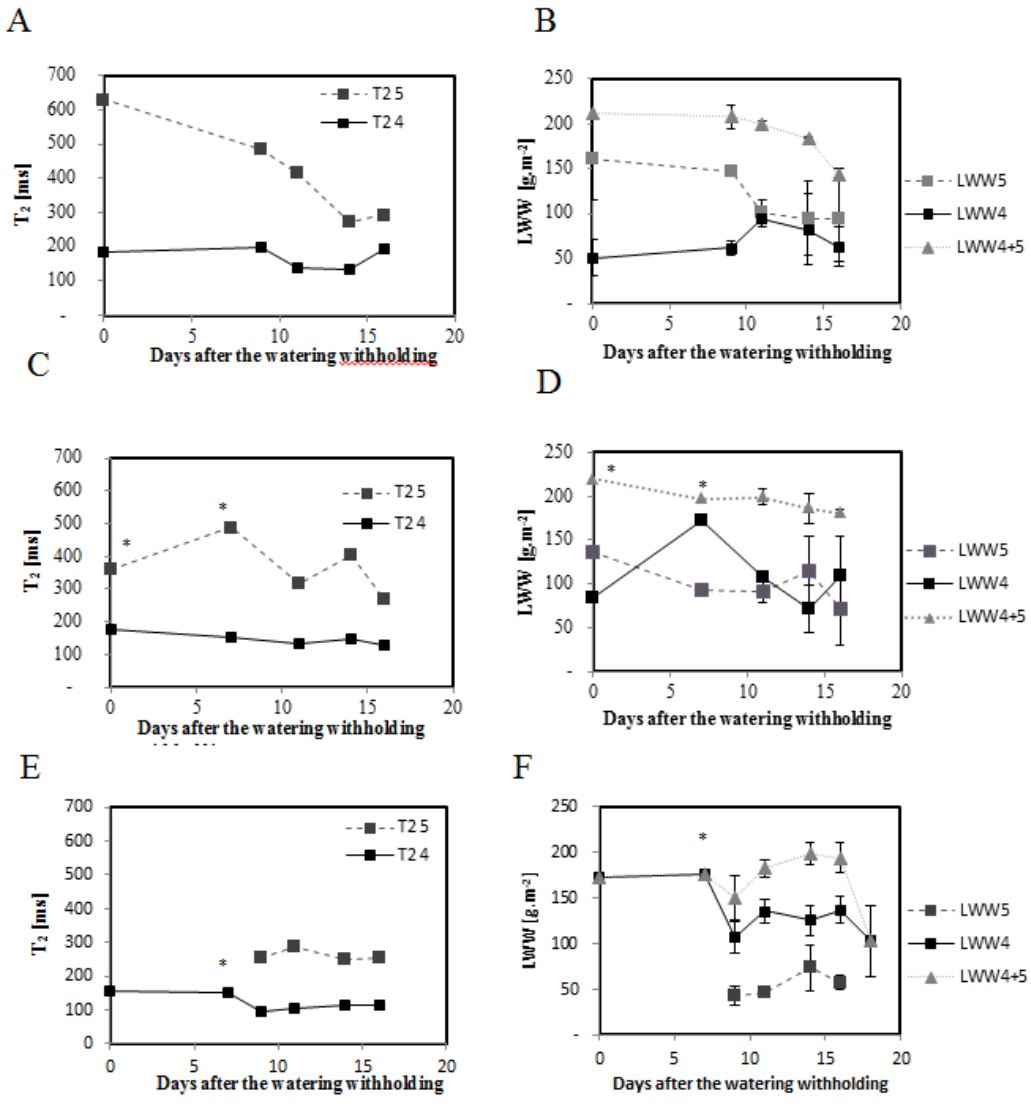

Figure 7: Pattern of evolution of T_2 (A, C, E) and LWW (B, D, F) of vacuolar components (of the NMR signal) of stress leaves 1 (A, B); 2 (C, D) and 3 (E, F) during all the experiement. * represents the data points were only two repetitions were averaged.

The third NMR signal component was not impacted by the stress. In opposite, the second component disappeared in control leaves 19 days after the beginning of the watering stop, whereas it was still present under stressed conditions (data not shown).

2-b-3 Discussion

Dehydration of detached leaf discs

Plants used for the dehydration of the detached leaves can be compared to the plants analyzed in the first chapter, as the same genotype and growing conditions were used. According to this study, the fourth NMR signal component was associated to vacuoles of the spongy parenchyma whereas the fifth component was linked mainly to palisade vacuoles. Results (Figure 2-b-1) showed that the dehydration treatment applied in our experiment affected more strongly spongy parenchyma than other tissues. Indeed, LWW_5 remained almost unchanged during the experiment, while LWW_4 increased during the rehydration period and then decreased until disappearance at the end of the dehydration treatment. On the other hand, T_2 of both vacuolar components decreased during the dehydration treatment indicating the changes in the status of the vacuolar water. The $T_{2(5)}$ decrease cannot be explained by the compartment size variation as LWW_5 remained constant; this indicates that T_2 changes were due to another phenomenon. In the specific experimental conditions applied in this study, the T_2 decrease can hardly be attributed to solute accumulations so we assume that the modification of the T_2 can be explained by the stress induced on the membrane permeability.

Water stress applied to whole plants

In this experiment, water stress was applied after the vernalization period during active growth renewal and highly efficient remobilization processes associated to the onset of the monocarpic senescence. A decrease of 36% of the final seed yield (data not shown) was observed and indicated that, this remobilization process was most likely affected by the water stress. The choice of the leaf ranks allowed following the senescence up to nineteen days after the watering withholding for the youngest leaves studied.

In well irrigated plants, the age associated stomata closure observed here (Figure 2-b-4) was in accordance with the results reported by (Zhang and Outlaw, 2001; Albert et al., 2012). In water-stressed plants, the acceleration of the stomatal closure (Figure 4 A) allowed transpiration control and consequently slowed down the water loss, as described by (Jordan et al., 1975). The leaf cuticle also plays an important role in transpiration limitation (Jenks et al., 1994; Riederer and Schreiber, 2001),

additionally to the physical protection of leaf tissues. It has been shown that an increase of cuticle thickness improves drought tolerance in the case of water deficit (Cameron et al., 2006; Kosma et al., 2009). If the quantification of the cuticle was in the present study impossible, the slight increase in dry weight (data not show) in stressed leaf could be partly attributed to cuticle thickening.

It is well known that additionally to water flux control, the stomatal closure impacts photosynthesis through the control of gas exchanges (Kim et al., 2010). In the present study, the photosynthetic apparatus, as far as measurements are a relevant expression of functionality, was not impacted by the water deficit until the last measurement day. The relative slow response of chlorophyll content to water deficit indicated that it was not a good indicator of the leaf water balance management (Martinez and Guiamet, 2004), as already reported for plants under another abiotic stress (Gombert et al., 2006). The decline of the chlorophyll content in leaves from both well watered and stressed plants (Figure 3 A) was associated to chloroplasts dismantling (Wada and Ishida, 2009) corresponding to onset of senescence. In contrast, the chlorophyll fluorescence yield, revealing the efficiency of Photosystem II, appeared to be a better indicator of water stress as it was able to discriminate between water treatments at the last measurement day (Figure 2-b-2 B). That marked decrease in photosystem II activity may be due, in stressed conditions to a less-controlled chloroplast dismantling.

The water relations at the leaf scale were estimated through different parameters such as water content, RWC, water and osmotic potentials. Due to the leaf senescence (see chapter 1a), the water content increased at the end of the measurement period in control leaves (Figure 4), while for the stressed plants, the water loss induced by the treatment prevailed over this phenomenon. RWC was shown, as expected from the literature (Quick et al., 1992), to be the most appropriate measure of the physiological consequence of cellular water deficit, as independent of the changes in dry matter associated to the leaf age and development.

The leaf water potential is a common parameter used for description of leaf water status of plant submitted to drought (Ehrler et al., 1978; Matin et al., 1989; Jongdee et al., 2002). In the present study, the measurement of this parameter (Figure 2-b-5 A) indicated that the stressed plant were affected relatively late (from the eleventh day), although stomatal closure (Figure 4A) indicated that plants started to respond to water deficit earlier (from the seventh day). This delay corresponded to a period of cell adaptation to water stress expressed by a slight osmotic adjustment (around 0.15 MPa, estimated from the Figs. 2-b-4 C and 2-b-5 B), allowing cells to maintain positive turgor pressure (Bartlett et al., 2012). Indeed, in response to drought stress numerous molecules are synthetized and accumulated in order to adjust cytoplasmic and vacuolar osmotic potential (Ingram and Bartels, 1996) but also to protect structure and macromolecules (Szegletes et al., 2000). Proline metabolism is most likely activated under these conditions as a frequently described metabolic adjustment in response to osmotic stress in oilseed rape (Trotel et al., 1996; Gibon et al., 2000; Hatzig et al., 2014). After the

eleventh day, the three parameters reflecting tissue integrity (Figure 2-b-5) indicated that leaf tissues lost their capacity to counteract the effect of stress. At the last day of measurement, ψ_w, ψ_s and T (Figure 5) together with the tissue dehydration described through cell water relations (Figure 2-b-4 B-C) seems to indicate the loss of membrane integrity.

Note that the physiological and water parameter patterns of evolution of leaf 4 are representative of the impact of water stress on the other leaves studied.

At the beginning of the experiment, NMR signal measured in leaves of different ranks varied as expected from previous experiments (see chapter 1). Indeed, the fifth component was observed only in older leaves (ranks 2 and 1), with the associated T_2 value higher for the rank 1 and LWW_5 higher than LWW_4 and both observations linked to leaf ageing phenomena. In opposite, when the split of the fourth NMR signal component occurred in the youngest leaf studied (rank 4) under control conditions, the water distribution differed from the expected result. Indeed, LWW_4 was higher than LWW_5 during the almost whole measurement period, reflecting changes in leaf tissue structure probably due to the vernalization effects. Indeed, the effects of cold temperatures on leaf parenchyma structure have already been described for wheat (Dornbusch et al., 2011) and beet (Sakr and Almaghrabi, 2011). However, these structural leaf changes induced by cold temperature seem to be reversible in relatively short time. This is consistent with the evolution patterns of $LWW_{4\ and\ 5}$ of the leaf of rank 4 at the advanced development stage under control conditions (Figure 2-b-6 B). Moreover, previous study on vernalized oilseed plants (see chapter 2a) did not show these cold temperature effects on water distribution between LWW 4 and 5 as leaves analyzed were all expanded before vernalization, comparing to the present study. Note that differences in leaf tissue structure of the leaves of low (1) and higher ranks (2-4) were probably emphasized by the fact that the leaf 1 was already developed before the beginning of the vernalization.

The opposite effects of leaf senescence and water stress on leaf water status make the interpretation of the NMR signal complex. In leaf 4, strongly affected by cold temperatures, it seems that the variation in the number and characteristics of NMR signal components (4 to 5) was due to both vernalization effect and water stress. As observed for detached leaf discs experiment only LWW_4 decreased in stressed plants at the last measurement point when RWC dropped drastically. This is probably explained by the specific role of the spongy parenchyma in leaf water relations (Nardini et al., 2010). Note that except for the oldest leaf (rank 1), other leaves presented similar NMR signal changes when submitted to water stress. In the oldest leaf (rank 1), the water stress induced reduction in LWW_5 corresponded to the loss of water of the highly hydrated palisade cells associated to the advanced senescence.

DISCUSSION AND PERSPECTIVES

Discussion and Perspectives

The aim of the present work was to investigate oilseed rape leaf structure modifications associated with senescence process and to seek whether these structural changes could be analyzed in relation with remobilization process when plants are submitted to environmental constraints in order to improve crop yield. Nitrogen and water use efficiency improvement are especially under concern. To do so, NMR relaxometry method making it possible to measure changes in cell water distribution associated with these structural changes, was evaluated. The NMR signal has been described in the literature as operable to characterize cell water status and structure when used on plant organs such as fruits and leaves from different species (Snaar and Van As, 1992; Gambhir et al., 1997; Hills and Nott, 1999). In these studies, performed mostly on fruit samples, the attribution of the different T_2 components to different cell compartments was proposed. In the present work, an original model for the T_2 relaxation component attribution taking into account both cell compartmentalization and heterogeneities at tissue level has been proposed. From this first result three main goals were pursued. It was first proposed to use the NMR relaxometry of the leaf tissue as an accurate minimally invasive technology to follow the different phases of development especially the differents steps of senescence associated to metabolic remobilization processes and nutrient recycling. The second objective was to demonstrate that leaf structure followed through the NMR relaxometry could be affected by growth conditions and environmental stress. The third and final goal was to infer that leaf structural evolution monitored by NMR relaxometry could be linked to nutrient remobilization and water use efficiencies, so that NMR leaf signal could be used for phenotyping and genetic improvement of these traits for oilseed rape production.

1-NMR signal component can be attributed to different cellular (or tissular) compartments

In different plant tissues investigated through NMR *i.e.* seeds (Krishnan et al., 2004), fruit (Musse et al., 2010), and leaf (McCain and Markley, 1989), the NMR T_2 signal was shown to be multi-exponential. According to the literature, the multiple components of this signal correspond to cell compartments. However, the actual attribution remains complex as the T_2 relaxation depends on the tissue studied and on the experimental parameters used. Moreover, in plant tissues there are, at the cell level, many different proton pools, *i. e*. vacuoles, cell wall, plasts and other organits and in the case of the leaf, different tissues have also to be taken into account (parenchyma, vessels,…). Their size and organization, and thus the NMR relaxation, depend on the plant studied (species and genotype) and environmental conditions. The exact attribution of NMR signal components is essential in order to fully understand the physiological processes operating.

The present work has highlighted that *B. napus* leaf senescence is accompanied by an increase in water content associated with an increase in cell hydration. Indeed, it was demonstrated that, additionally to the decrease in the dry weight of the leaf due to the cell material remobilization (Avice and Etienne, 2014), the water content also increases due to water entry in the leaf. The evolution of water content during leaf senescence is subject of debate. It is generally assumed that the leaf senescence is characterized by water loss (McIntyre, 1987; Zhang et al., 2012). Results presented here indicate that the cell death happens when the leaf hydration is at its maximum. Indeed, the marked increase in T_2 of the fifth signal component at the end of senescence has been associated with the tonoplast dismantling, demonstrating that when the senescence is complete, cell death happens before leaf abscission and drying. Water content can thus be an indicator of leaf age in mature and senescent leaves, and its correlation to the NMR signal intensity of the CPMG signal components (2 to 5) could be used to easily approach its value. In the present work, whatever the experimental condition, we demonstrated that the intensity of the CPMG was correlated to the water content of the sample. Surprisingly, the relation between T_2 and water content was less clear.

Several NMR and MRI studies have focused on the relation between T_2 and water content. Hills and Remmigereau (1997) found no difference in the major longest relaxing T_2 components from apple fruit despite a loss of 10% in water content (slow drying). Mariette *et al*. (1999), observed after gently drying of samples of apple parenchyma (9% of water loss) a decrease in all relaxation times components (from 1200 ms to 550 ms for the longest one). In leaves of different Azalea species, Kaku *et al*., (1992) reported different species-dependent linear correlations between T_1 values and water content. As a noticeable point, in plant matrice T_1 and T_2 have similar behavior. In the present work changes in water content whether increase during natural senescence or decrease during water stress, impact mostly vacuolar compartments, which correspond to **the longest T_2** component in most plant

matrices. Nevertheless, taking into account all leaves studied in the present work, although higher water content generally fitted with higher vacuolar T_2 component values it has been not possible to correlate water content to T_2 values. For example, choosing 80% of water content as reference depending of leaf age and growth conditions, the T_2 value changed from 90 to 150 ms. That means that when water changes are gentle (unlike dehydration) T_2 is more influenced by leaf structure and physiology than by water content, and the relationship between T_2 and water content is only observed for a small variation of the cellular water.

Van der Weerd *et al*, (2001) have revealed though MRI measurements, a linear relationship linking T_2 value and the associated compartment size (expressed in sum of the inverse of cell radii along the x, y and z axis) in stem of two cereal species. This relation supposes a similar composition of the compartment (here vacuoles) and a similar permeability of the membrane surrounding the compartment. Measurement of cell size and NMR relaxation were in our study performed on leaves of different ages grown under different nutritional regimes, these conditions being known to impact both vacuole composition (Otegui et al., 2005) and tonoplast permeability (Schussler et al., 2008). The latter can explain why, although T_2 increased with cell size, the relationship linking both these parameter was not linear. Regarding all data, the compartment size seems to influence T_2 value more than water content does. During physiological process like senescence others parameters have to be taken into account, such as vacuole composition which remain very difficult to estimate experimentally and tonoplast permeability, a parameter that can be measured through NMR diffusion relaxometry as shown by Sibgatullin *et al*., (Sibgatullin et al., 2007).

Our approach combining NMR and microscopy revealed, not only tissue ageing differentiation, but allowed also to attribute the two longest T_2 components to vacuoles of two different cell types. The attribution of the last component of the NMR relaxation distribution was assigned to vacuolar compartments decoupled into two proton populations during the onset of leaf senescence. Each of them was attributed to either spongy or palisade parenchyma because of potential heterogeneous hydration of these two tissues.

In our experimental conditions, the **third NMR T_2 component** was characterized by a T_2 around 20 ms and an intensity representing around 15% of the total leaf water content. Based on the T_2 value and the fact that in young leaves plastids represent at least 15% of the leaf volume, this component has been putatively linked to the plastids. On this basis, one of the outcomes expected from the long kinetic study (chapter 1) was to observe the decrease in the intensity of the third T_2 component in very old leaves where the plastid dismantling occurs. Unexpectedly, the parameters of that T_2-component did not vary so much in old leaves, even long after the disappearance of plastids was observed on light micrographs. One hypothesis is that the proliferation of small vesicles (RCB, autophagosome…) described during senescence-associated autophagic processes (Otegui et al., 2005; Wada and Ishida, 2009) may cause the occurrence of new proton pools that may contribute to the

signal of this T_2 component. These vesicles are often surrounded by plastid-like membranes (Chen and Yu, 2013) and even if their size is smaller compare to plastids these vesicles are more numerous. The exact number of these vesicles is difficult to determinate because of their different nature and their rapid turn-over. Another hypothesis about the third T_2-component is a contribution of vascular tissues to the signal. Indeed, although the sampling procedure was made so as to avoid major veins, samples contained some of the minor ones. Vascular tissues are made of two different vessels; xylem that is a long tube of dead lignified cells and phloem made on the superposition of small punctuated cells that exchange water between each other very quickly (Turgeon and Wolf, 2009). According to micrographs, the area of the cells of the minor veins was more comparable to the area of plastids than of the palisade cell vacuole. That description let clearly think that water form these vessels contribute to the NMR signal. This hypothesis could be further tested through NMR measurement of the leaf tissue samples having different proportions of vessels. Another proton pool that can contribute to the third component of the NMR signal is the lipid fraction. There was always a degree of incertitude in the water amount-CPMG intensity correlation, and, if that small gap may be due to the measurement itself, it can also be attributed to the contribution of lipids to the signal. In young leaves lipids are mainly present in form of membrane phospho- and galactolipids (especially in plastids), but during senescence these membranes are degraded into triglycerides forming plastoglobuli (Thompson et al., 1998). It has been shown in *Arabidopsis* leaves that this lipid fraction increases five-fold during leaf senescence (Berger et al., 2001) and our own investigations revealed a high number of plastoglobuli in old leaves (see chapter 1). The impact of these cellular and metabolic changes on NMR signal and the contribution of triglycerides on this signal remain to be finely evaluated.

The **second NMR T_2 component** measured in oilseed rape leaves cannot be strictly attributed to one cell compartment. These T_2 (around 2ms) is a characteristic of water close to solid surfaces or macromolecules (in this case polysaccharides). Experiments conducted through Mn^{2+} infiltration in apple fruit parenchyma (Snaar and Van As, 1992) allowed the authors to attribute the equivalent T_2 component to the extracellular water. However, the authors of this study did not take the starch deposition into account. In the photosynthetic leaves, starch is the main stored source of C in the form of granules in the plastids. These granules are generally well hydrated and water inside starch granules has been shown to have a T_2 of a few ms (Le Grand et al., 2007). Moreover, our work demonstrated that this component disappeared when plastids changed into starch–free gerontoplast or became completely dismantled. After quantitative determination, the starch quantity measured in leaf tissues cannot explain by itself the intensity of this component. Our hypothesis is thus, that this T_2 component of the NMR signal from oilseed rape leaves may correspond to water bound to overall polysacharides, it means both apoplastic water and water of starch hydration. The apoplast, mainly made of cell wall material, is, as starch content, strongly impacted by senescence processes. We clearly observed that the cell wall became thinner with ageing and that is coherent with the reduction/disappearance of the putative corresponding T_2-component. The actual contribution and the importance of the starch water

to this component could be further investigated through a kinetic study during photoperiod since the starch deposition is strictly dependent on photosynthetic processes and cumulative over the course of the day. Insofar as we felt the potential interference of the gradual accumulation of the starch on the NMR signal, all the NMR experiments of this work were conducted in the morning. Another possibility to investigate the attribution of this component can be the use of oilseed rape/Arabidopsis mutant lines. Comparing a wild type leaf to a leaf from a mutant deficient in starch production should for instance provide reliable information. In the same way, mutant in the cell wall biosynthesis pathway could be used to determinate the contribution of polysaccharids of the cell wall to that component.

The first T_2 component with a very short T_2 (around 0,004ms) was shown to correspond to the signal from the protons of the solid part. Despite technical difficulties, quantifying the dry mass of a sample using the intensity of the first component of the NMR signal can be interesting as the dry mass is a clear marker of the remobilization status of the leaf.

2-NMR signal can be used as an accurate leaf developmental marker

As already mentioned, structure of *B. napus* leaves (size and organization of tissues and cells) has not been extendedly studied. In opposite, the leaf structure of numerous woody plants has been described (Castro-Diez et al., 2000) and several studies have been made on *Arabidopsis (Wuyts et al., 2012)*, tobacco (Radochova et al., 2000) and rice (Inada et al., 1998). Olive trees are often submitted to water deficit and their tolerance to that stress has also been studied through leaf structure (Guerfel et al., 2009; Ennajeh et al., 2010).

As described in the first chapter, T_2 distribution of the *B. napus* leaf changes during the time course of development and ageing. In young maturing leaves, this signal is made of four components, while with ageing (senescence onset) the T_2 of the last one increases leading to the split (*i. e.* appearance of a fifth component). Finally, the second signal component disappears in senescent leaves. These changes in the NMR signal are easily assessable and they have been observed in all genotypes and conditions tested, making them robust fingerprints of leaf development.

The experiment described in the second article of the first chapter revealed that the fourth NMR signal component split is an obligatory step of leaf development and that it corresponds to the onset of senescence (when the chlorophyll content begins to decrease). More, following the relative expression pattern of two senescence-related genes (Cab which is repressed and SAG12 which is over-expressed during senescence progression), already used as molecular senescence marker milestones in *B. napus* (Brunel-Muguet et al., 2013*)*, the intersection of the two curves has been shown to happen for the same leaf rank/age as the NMR split of the relaxation peak was observed. That experiment also

showed that for two plants grown under the same conditions and considered as biological repetitions, the NMR-split and the relative expression of Cab/SAG did not happen for the same leaf rank, indicating developmental differences between the two leaves considered as repetitions. Among the different indicators commonly used to determinate leaf age, Cab/SAG genes relative expression is certainly accurate but this method is destructive and difficult to carry out. All easier to handle indicators usually used for determinate the leaf developmental status present specific defaults (Lim et al., 2007) and most of them reflect the evolution of chloroplast material. The chlorophyll content, the fluorescence yield of photosystems, RGB and multi-spectral imaging are rapid and non-invasive but suffer from some inaccuracies (Guiboileau et al., 2010). In contrast, the NMR relaxation splitting was shown to be easily measurable and very precise. The NMR relaxometry signature can then be proposed as a simple and effective methodology for monitoring and phenotyping leaf tissue maturation and ageing. Determining the exact leaf development stage when these changes occur in term of hormonal balance and molecular events should be an interesting comprehensive perspective.

Despite the clear visual differentiation between palisade and spongy tissues and their different functions, these tissues were rarely studied separately. The major reason is technical as there is no rapid and easy method to access the isolated leaf tissues. The only experimental approach that has been used to study separately leaf tissues was the microscopy (Castro-Diez et al., 2000; Günthardt-Goerg et al., 2000). Most of microscopy technics require embedding and cutting the sample that is not always suitable for vegetal tissues. Indeed, embedding the sample is a time consuming and difficult process in the case of highly hydrated tissues (as senescing leaves). Further, the infiltration can modify cell structure especially for the cells with thin or damaged wall. Finally, quantitative analysis of leaf micrographs, such as estimation of compartment volumes, requires numerous replicates because of the low representativity of the small-size samples analyzed. The possibility of having access to information at the tissue level through a non-destructive NMR method is thus an important progress in studying leaf tissues separately.

In our studies performed under different conditions (optimal growth, vernalization, N and water stress…) the leaf aging was associated to the disappearance of the second NMR T_2 component. The T_2 of this component remains stable around 2-3ms in all conditions and its intensity remains constant in young leaves and decrease briefly before its complete disappearance. In some stressed plants studied, the leaf fell while the second component was still present and all other development markers indicated that the final stage of the leaf senescence was not achieved before falling. This probably indicates that senescence was accelerated by stress. The acceleration of senescence and the fall of leaves before complete senescence lead to an incomplete nutrient remobilization. This lack of remobilization is in part at the origin of the yield decrease observed in the case of stress (Munne-Bosch and Alegre, 2004; Avice and Etienne, 2014). The presence/absence of the second T_2 component, easily measurable in the

oldest leaf of a plant, can give information on the senescence status and may be a reliable indicator to discriminate the tolerance of different genotype to stress.

3-Leaf structural modification can be affected by environmental conditions

The plants used in the first set of experiments (results shown in the first chapter) belong to the Tenor genotype and were grown under controlled conditions without vernalization step. The following experiments aiming at investigating nitrogen and water stress impact (chapter 2 and 3 results) have used Aviso and Express genotypes and plants were vernalized before measurement. The vernalization step corresponds to a period of exposure to cold conditions (8 weeks at 4°C under our design) that is required to induce flowering in winter oilseed rape (Dornbusch et al., 2011). Before addressing the specific effects induced by N-depletion and water stresses it was essential to assess the genetic contribution and the cold exposure effects on the NMR signal. The measurements and comparison of the NMR signal of three leaf rank of Tenor genotype under non-vernalized conditions, and Aviso genotype under both vernalized and non-vernalized conditions were realized. No typical differences have been observed in term of number and relative intensity of the usual signal components (Figure 1).

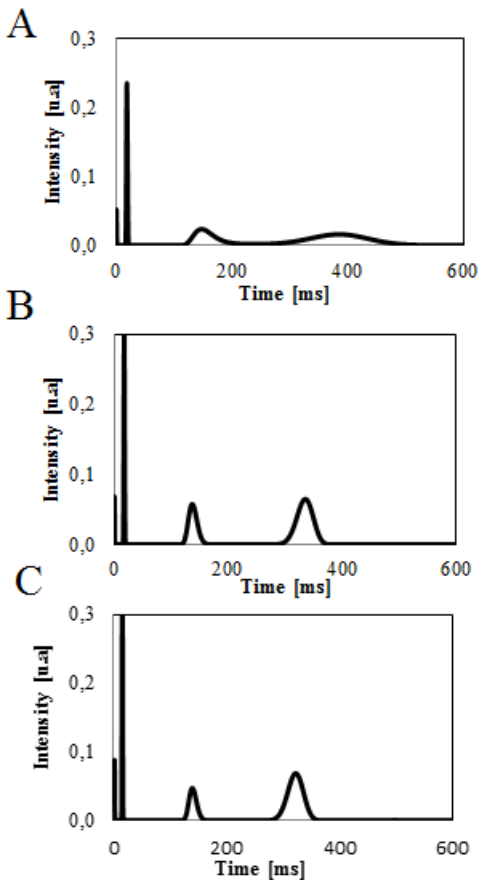

Figure 1: NMR T_2 distribution of three old leaves (leaf rank 2) of *Brassica napus*; A Aviso genotype (non-vernalized), B Tenor genotype (vernalized) and, C Aviso genotype (vernalized).

The challenge was to determine the leaves to be compared since the process of vernalization singularly affects growth and development of tissues and can be seen as a stress. As a matter of fact,

numerous ontogenic, morphological and physiological changes were observed comparing leaves of vernalized plants to leaves from non-vernalized. Vernalized leaves were smaller, as the cold period stopped or at least drastically slowed down leaf expansion (Nanda et al., 1995). Vernalized leaves were also redder due to the well-known anthocyanin accumulation in the vacuoles in response to cold stress (Chalker-Scott, 1999). During senescence, when the leaf loss its green color due to chlorophyll degradation, the anthocyanin deposition was clearly visible in vernalized leaves whereas non-vernalized leaves were fully yellow. Vernalized leaves also presented a surface that seemed waxier, certainly due to changes in the cuticle composition that is also largely described in literature (Vigh et al., 1981; Xiang et al., 2007).

At the tissue level, light micrographs revealed that palisade tissue of non-vernalized leaves was made of two cell layers (in Tenor genotype) whereas in vernalized leaves three to four layers were visible (in both Express and Aviso). If the modification of cell expansion and division in response to cold has already been reported in others species (Dornbusch et al., 2011), the hypothesis of a difference due to genotype cannot be ignored. An important increase in leaf thickness during senescence has been observed in leaves of non-vernalized plants, in contrast to vernalized leaves in which the changes were minor insofar as the process of vernalization itself is already generator of thickening (probably with different structural attributes). Cold exposition has slowed considerably phyllochron and leaf appearance; as a consequence leaf rank comparison is not a guarantee of leaf age correspondence. Taking the NMR signal splitting as a landmark, micrographs investigations pointed out that vernalized leaves were thicker (500 µm) but presented smaller palisade cells (around 0.5 mm^3) than non-vernalized ones (1.2 mm^3). In vernalized leaves, thickness of epidermal cells did not change with ageing whereas in non-vernalized ones clear changes were noticed. All these observations took into account the fact that the vernalization process shorten the leaf lifespan (Tommey and Evans, 1991; Miralles et al., 2001) and thus less structural changes (especially in water content) may be observed before the leaf fall. Leaf senescence progression after vernalization relief should be singularly different in comparison to what is observed in non-vernalized plants since developmental program is redesigned directed to rapid bolting and flowering in vernalized plants. As a matter of fact, when one compares the oldest leaves in both conditions all parameters measured in vernalized plants (whatever the age of the plant) present a less advance senescence. For example, the chlorophyll content decrease rarely reached a non-measurable value in vernalized conditions whereas leaves of non-vernalized plants fall several weeks after the complete decrease in the chlorophyll content and similar tendency were also observed on NMR results and water content. Thus, in vernalized mature leaves, water content was lower than in non-vernalized condition and despite an increase with senescence its value never reached that of the oldest non-vernalized leaves. In mature leaves the difference can be due to both cell and cuticle sizes as described above. In the case of senescing leaves the accelerated senescence avoided an important increase in water content. One of the consequences is also a less clear tissue differentiation in the vernalized leaves that corresponds with the less increase in

water content and with a constant thickness described above. Nevertheless, a differentiation of cell size was described in vernalized condition (second chapter) even if it cannot be linked to a specific tissue. Taking the NMR signal splitting as marker, the leaves presenting that differentiation are at the really beginning of the tissue differentiation observed in non-vernalized conditions.

An interesting difference between conditions is the ratio of the intensities of the vacuolar components after the split. Indeed, in the majority of leaves presenting five T_2 components the intensity of the fifth component was higher than the intensity of the fourth one. However, in plants used for water stress experiment, the intensities of the fourth and fifth signal components presented an inverse ratio. Because of the lack of micrographs in this experiment, it was difficult to determine accurately the reason of this structural modification. Nevertheless, it is interesting to note that these leaves were the only ones studied that had appeared in the middle of the vernalization period. It can thus indicate that when the leaf appearance and tissue differentiation took place during the cold period the leaf structure is modified.

Nitrogen nutrition impact on leaf development and senescence-dependent leaf structural modifications has also been studied in the present work. Nutrient remobilization during N-stress has been extensively investigated in crops including oilseed rape (Mae and Ohira, 1981; Diaz et al., 2008; Avice and Etienne, 2014) but its relation to leaf structures has never been detailed. The major structural change we have pointed out in leaf tissues in response to N-deficiency was an increase in intercellular spaces. Indeed, to our knowledge, changes in intercellular spaces amount have never been reported as a response to N-deficiency. In our study, the N-deficiency was moderate and the leaves studied were already fully expanded when the depletion was applied. The intercellular modifications observed may be due to changes in the cell adherence in response to the trophic depletion. These modifications became more visible with the senescence-induced increase in cell size. Nevertheless, studies on different crops focusing on the use of plant debris in composting, for which the cell wall polysaccharides composition was important, have revealed that N-deficiency decreased lignin contents but did not impact cellulose and hemicellulose content (Murozuka et al., 2014). The apoplast also contains numerous enzyme and signal molecules that play key role in senescence and remobilization (Martínez and Guiamet, 2014), while the impact of N-deficiency on these molecules quantity and efficiency remain unknown. In our study, the genotype presenting the highest increase in intercellular spaces was also the one with the highest decrease in yield under nitrogen deficiency. The LWW of the fourth component was lower in stressed leaves demonstrating that NMR signal can reflect the growth conditions.

Water stress is known to impact leaf structure (Wuyts et al., 2012). From assays of controlled dehydration of leaf tissues, NMR results proved that water loss was mainly assumed by the spongy parenchyma, as shown by the fourth component disappearance (chapter 2b). That is not surprising because of the well-known functions of these cells; *i.e* gas exchange (including water vapor) and

maintenance of leaf water status. In the case of water stress applied on whole plant, results were more complex to interpret due to the combined interference of leaf acclimation to vernalization, water stress and ageing on leaf structure organization. As already stated, the vernalization process provoked changes in the leaf structure (when the leaf appearance takes place during the cold period) leading do a different ratio LWW_5/LWW_4 than observed in previous studies. It seems that under these conditions, the fourth component of the NMR signal still corresponded to spongy cells vacuoles but certainly also to some vacuoles of palisade cells. At the beginning of the water stress, water content remained stable and water parameters slightly changed, indicating an acclimation of the leaf tissues. After that period, while the water stress increased, NMR signatures showed water exchange between tissues. Finally, at the end of the water stress period whenthe leaf could not maintained its water status and loss water, NMR measurement confirmed that the loss came mainly from spongy cells. Indeed, during the stress period, the LWW_4 was impacted in the same manner as water parameters (water potential, RWC). The tissue modifications provoked by water stress can thus be estimated through the NMR signal. The extend of that method to other species (with well differentiated tissues) should be very interesting for studying at the tissue level, water stress or other stress known to impact leaf structure (such as ozone for example).

4-Leaf structural modifications monitored by NMR relaxometry are linked with nutrient remobilization processes

Increasing NUE and remobilization efficiency of nutrient from vegetative to reproductive organs is a major breeding ambition in the case of oilseed rape. This means to go through the exploration of genetic variability for these traits and the effective phenotyping of numerous genotypes. Nutrient recycling performances of plant tissues are generally addressed through isotopic experiences with stable elements (^{15}N, ^{13}C, ^{34}S,…) or biochemical analyzes of metabolic attributes of remobilization processes (Malagoli et al., 2005; Albert et al., 2012). Molecular targets are also proposed as candidates to appreciate senescence-induced remobilization performance (Hirel et al., 2007). Following the leaf structure alteration as a reliable picture of organic matter recycling proposed in the present work should be strengthen but is undeniably a new approach of interest especially if the structural analysis method is easy to implement as it is the case for NMR. Despite the complex interference of environmental conditions, the T_2 distribution and its pattern of evolution in leaf tissues were homogeneous whatever growth conditions. The relaxation peak splitting and the second T_2 component disappearance with ageing were systematically observed except for Express genotype leaves that presented a decrease with ageing in the second T_2 component intensity but which was still present before the leaf fall. It is interesting to note that for Aviso genotype, this T_2 component disappearance and the split happened in the same leaf, whereas under non-vernalized conditions these

events were separate in time. This confirms that under vernalized condition of the present study, the senescence process was not only unachieved but also accelerated. That incomplete developmental phase may be partly associated with yield penalties.

The differences in term of structure, especially in term of intercellular spaces, between leaves under moderate nitrogen depletion and control conditions may be explained by differences in the apoplast composition. The apoplast has a major role in senescence and signaling (Dani et al., 2005; Martínez and Guiamet, 2014). Even though numerous clues indicate an important role of the apoplast in the nutrient remobilization process from senescing leaves, this aspect has not been detailed in the literature. Indeed loading steps in the phloem are controlled by numerous molecular actors, N-depletion induced changes in apoplast composition can thus be at the origin of a lesser export of cell constituents leading to a yield decrease.

The hydration of the leaf during senescence is a new highlight and its effect on the leaf structure has been detailed in the present work. Nevertheless, the impact of this phenomenon on the chemical aspect of remobilization remains not clear, especially those of the massive water entry during senescence on the lytic enzymes efficiency, on the nutrient export and/ or on the small vesicle trafficking.The biochemical consequence of the leaf hydration on remobilization efficiency could be thus an interesting new field of research.

Conclusions and perspectives

The results of the present study bring new highlights on fundamental comprehension of leaf senescence structural changes and also demonstrate the suitability of the NMR relaxometry method for assessment of the physiological status of the leaf. The link between nutrient remobilization efficiency and leaf structure modifications revealed opens a new field of investigation. The exact role of apoplast, cell wall components and leaf hydration in remobilization performance also remains to be investigated. These perspectives will be the next steps of the RAPSODYN project which includes a study focused on the comparison of the leaf NMR relaxation time distribution from plants grown in field under two different nitrogen supplies. The sampling of the entire canopy will be made at different typical states of development (flowering, stem elongation…) and the pattern of evolution of leaf NMR signal components of the entire canopy will be measured. These patterns will be used as indicators of leaf development for different genotypes and growth conditions. Backed by biochemical and transcriptional analyses linked to nutrient remobilization, this experiment should reinforce correlations between senescence induced leaf structure changes and remobilization efficiency. Another expected outcome would be the ability to set up a leaf NMR relaxation signal database useable in plant breeding for NRE, by associating the yield parameters with NMR signal measurements realized throughout the canopy under different environmental conditions and on different genotypes.

The present work demonstrated that the pattern of evolution of NMR T_2 components (*i. e.* split and second component disappearance) is an accurate marker of leaf senescence. This marker could be relatively simply implemented in breeding programs. It can be used to sample two leaves in the same developmental state and to determine the senescence rate. Accelerated senescence is often associated to stress (Guo and Gan, 2005; Lim et al., 2007) and yield reduction (Gregersen et al., 2008; Guiboileau et al., 2010) and thus determining and comparing senescence evolution between genotypes in response to stress is of great interest for breeding. Indeed, NMR relaxation spectrum is not only easier to measure than numerous indicators of leaf senescence; the method is also very precise and provides integrative information of leaf senescence process at the tissue level.

The next step will be to develop portable NMR devices. Despite great progress being made in the last years in the development of these apparatus, it is important to consider that the magnetic field generated by the portable instrument is inhomogeneous comparing to the highly homogeneous field of the bench top spectrometers. Consequently, the quality of the NMR signal measured with portable spectrometers does not allow accessing all information obtained by the standard measurements. Nevertheless, technical progress in this area should lead in the next years to better management of the signal quality and the possibility to carry out experiments similar to those performed in the present work and applicable to larger scale designs and field experiments.

Senescence progression is known to follow a gradient at the leaf level (Avice and Etienne, 2014) generally from the top to the bottom of the limb. Senescence-induced changes at the leaf level are usually understated, but the accuracy of NMR highlighted in the present work should allow investigations at this level. A preliminary study comparing NMR signal of different parts of the same leaf made it possible to reveal such a gradient. The results demonstrated that beside the ability of NMR relaxometry to detect differences in leaf physiological status induced by age, position in the canopy and/or environmental conditions, this method makes it also possible to reveal tissues heterogeneities among the leaf limb.

In the present work, practical test of NMR signal measurement performed on *Arabidopsis* leaves at three different development states, i. e. young, mature and senescent, showed similar results as measurements performed on *B. napus*. (Figure 2).

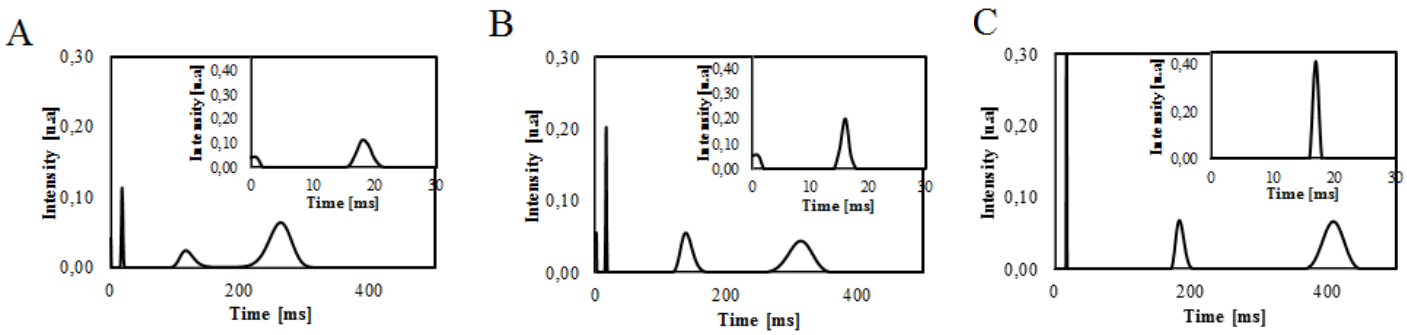

Figure 2 : NMR T_2 distribution of young (A), mature (B) and senescent (C) leaves of *Arabidopsis thaliana* (genotype Col 0).

Indeed, the NMR signal of *Arabidopsis* also presented an increase in vacuolar T_2 and a disappearance of the second T_2 component with ageing. The difference between two main parenchyma is obvious (Figure 3) on the micrograph of *Arabidopsis* found in the literature (Wuyts et al., 2010). In another study, Wuyts *et al*, (2012) have quantified cell volume in both parenchyma of *Arabidopsis* genotype Col-0 and reported that in mature leaves cell volume of palisade and spongy cell was in average 10^5 and $0.6*10^5$ μm^3, respectively. That reinforced the tissular attribution of vacuolar components in leaves and indicated that the method developed in oilseed rape may be generalized to others species. It has to be noted that the T_2 decay signal of young *Arabidopsis* leaves was already made of five components, possibly explained by differences in structure of young leaves between *Arabidopsis* and oilseed rape. It will be interesting to perform the NMR and microscopy measurements on the same leaves, like in oilseed rape experiments in order to confirm this hypothesis. Nevertheless, the continuous increase in T_2 of vacuolar compartments observed in *Arabidopsis* leaves as in oilseed rape leaves can be used to compare leaf age.

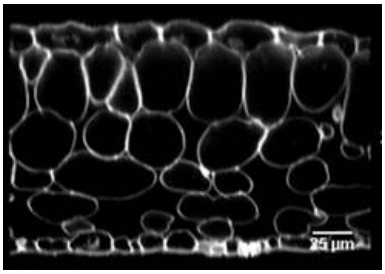

Figure 3: Typical cross section of a mature leaf of *Arabidopsis thaliana* obtain through confocal microscopy (Wuyts et al., 2010).

Moreover, as a plant model, numerous mutants of *Arabidopsis* are available, and it can be a great use to work on the attribution of the other components of the signal. For example mutant with deficiency in the starch production should help in the confirmation of the attribution of the second T_2 component of the NMR signal to the water in starch granules. In the same way, mutant deficient in autophagy process will not present the increasing number of small vesicle observed in wild type during senescence, the impact of that difference on the third T_2 component should give us new clue on the attribution of NMR T_2 components. The results in *Arabidopsis*, associated with preliminary results on different species (*hordeum, nicotinia, lactuca*) are promising on the efficiency of NMR measurement to follow leaf structural modification in others species.

REFERENCES

Litterature cited

Aasamaa K, Niinemets U, Sober A (2005) Leaf hydraulic conductance in relation to anatomical and functional traits during Populus tremula leaf ontogeny. Tree Physiology **25:** 1409-1418

Abeles FB, Dunn LJ, Morgens P, Callahan A, Dinterman RE, Schmidt J (1988) INDUCTION OF 33-KD AND 60-KD PEROXIDASES DURING ETHYLENE-INDUCED SENESCENCE OF CUCUMBER COTYLEDONS. Plant Physiology **87:** 609-615

Adam Z, Clarke AK (2002) Cutting edge of chloroplast proteolysis. Trends in Plant Science **7:** 451-456

Aharoni N, Back A, Benyehoshua S, Richmond AE (1975) EXOGENOUS GIBBERELLIC-ACID AND CYTOKININ ISOPENTENYLADENINE RETARDANTS OF SENESCENCE IN ROMAINE LETTUCE. Journal of the American Society for Horticultural Science **100:** 4-6

Al Sahli AA, Al-Muwayhi MA, Doaigey AR, Basalah MO, Ali HM, El-Zaidy M, Sakran AM (2013) Effect of Ozone and Ascorbic Acid on the Anatomical, Physiological and Biochemical Parameters of Pepper (Capsicum frutescens L.). Journal of Pure and Applied Microbiology **7:** 159-168

Albert B, Le Caherec F, Niogret MF, Faes P, Avice JC, Leport L, Bouchereau A (2012) Nitrogen availability impacts oilseed rape (Brassica napus L.) plant water status and proline production efficiency under water-limited conditions. Planta **236:** 659-676

Andersen MN, Heidmann T, Plauborg F (1996) The effects of drought and nitrogen on light interception, growth and yield of winter oilseed rape. Acta Agriculturae Scandinavica Section B-Soil and Plant Science **46:** 55-67

Austin JR, II, Frost E, Vidi P-A, Kessler F, Staehelin LA (2006) Plastoglobules are lipoprotein subcompartments of the chloroplast that are permanently coupled to thylakoid membranes and contain biosynthetic enzymes. Plant Cell **18:** 1693-1703

Avice J-C, Etienne P (2014) Leaf senescence and nitrogen remobilization efficiency in oilseed rape (Brassica napus L.). Journal of experimental botany**:** eru177

Bacic G, Ratkovic S (1984) WATER EXCHANGE IN PLANT-TISSUE STUDIED BY PROTON NMR IN THE PRESENCE OF PARAMAGNETIC CENTERS. Biophysical Journal **45:** 767-776

Back A, Richmond A (1969) An Interaction between the Effects of Kinetin and Gibberellin in Retarding Leaf Senescence. Physiologia plantarum **22:** 1207-1216

Baerenfaller K, Massonnet C, Walsh S, Baginsky S, Buehlmann P, Hennig L, Hirsch-Hoffmann M, Howell KA, Kahlau S, Radziejwoski A, Russenberger D, Rutishauser D, Small I, Stekhoven D, Sulpice R, Svozil J, Wuyts N, Stitt M, Hilson P, Granier C, Gruissem W (2012) Systems-based analysis of Arabidopsis leaf growth reveals adaptation to water deficit. Molecular Systems Biology **8**

Bartlett MK, Scoffoni C, Sack L (2012) The determinants of leaf turgor loss point and prediction of drought tolerance of species and biomes: a global meta-analysis. Ecology Letters **15:** 393-405

Berger S, Weichert H, Porzel A, Wasternack C, Kuhn H, Feussner I (2001) Enzymatic and non-enzymatic lipid peroxidation in leaf development. Biochimica Et Biophysica Acta-Molecular and Cell Biology of Lipids **1533:** 266-276

Berry P, Spink J, Foulkes M, White P (2010) The physiological basis of genotypic differences in nitrogen use efficiency in oilseed rape (< i> Brassica napus</i> L.). Field crops research **119:** 365-373

Besseau S, Li J, Palva ET (2012) WRKY54 and WRKY70 co-operate as negative regulators of leaf senescence in Arabidopsis thaliana. Journal of Experimental Botany **63:** 2667-2679

Blum A (1996) Crop responses to drought and the interpretation of adaptation. Plant Growth Regulation **20:** 135-148

Bohler S, Sergeant K, Jolivet Y, Hoffmann L, Hausman J-F, Dizengremel P, Renaut J (2013) A physiological and proteomic study of poplar leaves during ozone exposure combined with mild drought. Proteomics **13:** 1737-1754

Bouchereau A, Aziz A, Larher F, Martin-Tanguy J (1999) Polyamines and environmental challenges: recent development. Plant Science **140:** 103-125

Bouchereau A, Clossais-Besnard N, Bensaoud A, Leport L, Renard M (1996) Water stress effects on rapeseed quality. European Journal of Agronomy **5:** 19-30

Bouchet A-S, Nesi N, Bissuel C, Bregeon M, Lariepe A, Navier H, Ribière N, Orsel M, Grezes-Besset B, Renard M Genetic control of yield and yield components in winter oilseed rape (Brassica napus L.) grown under nitrogen limitation. Euphytica**:** 1-23

Brehelin C, Kessler F (2008) The Plastoglobule: A Bag Full of Lipid Biochemistry Tricks. Photochemistry and Photobiology **84:** 1388-1394

Brehelin C, Kessler F, van Wijk KJ (2007) Plastoglobules: versatile lipoprotein particles in plastids. Trends in Plant Science **12:** 260-266

Brenner WG, Romanov GA, Kollmer I, Burkle L, Schmulling T (2005) Immediate-early and delayed cytokinin response genes of Arabidopsis thaliana identified by genome-wide expression profiling reveal novel cytokinin-sensitive processes and suggest cytokinin action through transcriptional cascades. Plant Journal **44:** 314-333

Brown KM (1997) Ethylene and abscission. Physiologia Plantarum **100:** 567-576

Brunel-Muguet S, Beauclair P, Bataille M-P, Avice J-C, Trouverie J, Etienne P, Ourry A (2013) Light Restriction Delays Leaf Senescence in Winter Oilseed Rape (Brassica napus L.). Journal of Plant Growth Regulation **32:** 506-518

Buchanan-Wollaston V, Earl S, Harrison E, Mathas E, Navabpour S, Page T, Pink D (2003) The molecular analysis of leaf senescence - a genomics approach. Plant Biotechnology Journal **1:** 3-22

Buchanan-Wollaston V, Page T, Harrison E, Breeze E, Lim PO, Nam HG, Lin JF, Wu SH, Swidzinski J, Ishizaki K, Leaver CJ (2005) Comparative transcriptome analysis reveals significant differences in gene expression and signalling pathways between developmental and dark/starvation-induced senescence in Arabidopsis. Plant Journal **42:** 567-585

BuchananWollaston V (1997) The molecular biology of leaf senescence. Journal of Experimental Botany **48:** 181-199

Bush DR (1999) Sugar transporters in plant biology. Current Opinion in Plant Biology **2:** 187-191

Cameron KD, Teece MA, Smart LB (2006) Increased accumulation of cuticular wax and expression of lipid transfer protein in response to periodic drying events in leaves of tree tobacco. Plant Physiology **140:** 176-183

Capitani D, Brilli F, Mannina L, Proietti N, Loreto F (2009) In Situ Investigation of Leaf Water Status by Portable Unilateral Nuclear Magnetic Resonance. Plant Physiology **149:** 1638-1647

Castro-Diez P, Puyravaud JP, Cornelissen JHC (2000) Leaf structure and anatomy as related to leaf mass per area variation in seedlings of a wide range of woody plant species and types. Oecologia **124:** 476-486

Cattivelli L, Rizza F, Badeck F-W, Mazzucotelli E, Mastrangelo AM, Francia E, Mare C, Tondelli A, Stanca AM (2008) Drought tolerance improvement in crop plants: An integrated view from breeding to genomics. Field Crops Research **105:** 1-14

Chalker-Scott L (1999) Environmental significance of anthocyanins in plant stress responses. Photochemistry and Photobiology **70:** 1-9

Chaves MM, Maroco JP, Pereira JS (2003) Understanding plant responses to drought - from genes to the whole plant. Functional Plant Biology **30:** 239-264

Chen WQ, Provart NJ, Glazebrook J, Katagiri F, Chang HS, Eulgem T, Mauch F, Luan S, Zou GZ, Whitham SA, Budworth PR, Tao Y, Xie ZY, Chen X, Lam S, Kreps JA, Harper JF, Si-Ammour A, Mauch-Mani B, Heinlein M, Kobayashi K, Hohn T, Dangl JL, Wang X, Zhu T (2002) Expression profile matrix of Arabidopsis transcription factor genes suggests their putative functions in response to environmental stresses. Plant Cell **14:** 559-574

Chen Y, Yu L (2013) Autophagic lysosome reformation. Experimental Cell Research **319:** 142-146

Chimenti MS, Khangulov VS, Robinson AC, Heroux A, Majumdar A, Schlessman JL, Garcia-Moreno B (2012) Structural Reorganization Triggered by Charging of Lys Residues in the Hydrophobic Interior of a Protein. Structure **20:** 1071-1085

Chung T (2011) See How I Eat My Greens-Autophagy in Plant Cells. Journal of Plant Biology **54:** 339-350

Colire C, Lerumeur E, Gallier J, Decertaines J, Larher F (1988) An assessment of proton nuclear magnetic-resonance as an alternative method to describe water status of leaf tissues in wilted plants. Plant Physiology and Biochemistry **26:** 767-776

Cook ER, Seager R, Cane MA, Stahle DW (2007) North American drought: Reconstructions, causes, and consequences. Earth-Science Reviews **81:** 93-134

Correa de Souza T, Cesar Magalhaes P, Jose Pereira F, Mauro de Castro E, Netto Parentoni S (2011) Morpho-physiology and maize grain yield under periodic soil flooding in successive selection cycles. Acta Physiologiae Plantarum **33:** 1877-1885

Cosgrove DJ (1999) Enzymes and other agents that enhance cell wall extensibility. Annual Review of Plant Physiology and Plant Molecular Biology **50:** 391-417

Cosgrove DJ (2005) Growth of the plant cell wall. Nature reviews molecular cell biology **6:** 850-861

Dani V, Simon WJ, Duranti M, Croy RRD (2005) Changes in the tobacco leaf apoplast proteome in response to salt stress. Proteomics **5:** 737-745

Delannoy M, Alves G, Vertommen D, Ma J, Boutry M, Navarre C (2008) Identification of peptidases in Nicotiana tabacum leaf intercellular fluid. Proteomics **8:** 2285-2298

Desclos M, Etienne P, Coquet L, Jouenne T, Bonnefoy J, Segura R, Reze S, Ourry A, Avice J-C (2009) A combined N-15 tracing/proteomics study in Brassica napus reveals the chronology of proteomics events associated with N remobilisation during leaf senescence induced by nitrate limitation or starvation. Proteomics **9:** 3580-3608

Diaz C, Lemaitre T, Christ A, Azzopardi M, Kato Y, Sato F, Morot-Gaudry J-F, Le Dily F, Masclaux-Daubresse C (2008) Nitrogen recycling and remobilization are differentially controlled by leaf senescence and development stage in Arabidopsis under low nitrogen nutrition. Plant Physiology **147:** 1437-1449

Diepenbrock W (2000) Yield analysis of winter oilseed rape (Brassica napus L.): a review. Field Crops Research **67:** 35-49

Dornbusch T, Baccar R, Watt J, Hillier J, Bertheloot J, Fournier C, Andrieu B (2011) Plasticity of winter wheat modulated by sowing date, plant population density and nitrogen fertilisation: Dimensions and size of leaf blades, sheaths and internodes in relation to their position on a stem. Field Crops Research **121:** 116-124

Dreccer MF, Schapendonk A, Slafer GA, Rabbinge R (2000) Comparative response of wheat and oilseed rape to nitrogen supply: absorption and utilisation efficiency of radiation and nitrogen during the reproductive stages determining yield. Plant and Soil **220:** 189-205

Dreccer MF, Schapendonk AHCM, Slafer GA, Rabbinge R (2000) Comparative response of wheat and oilseed rape to nitrogen supply: absorption and utilisation efficiency of radiation and nitrogen during the reproductive stages determining yield. Plant and Soil **220:** 189-205

Duval FP, Cambert M, Mariette F (2005) NMR study of tomato pericarp tissue by spin-spin relaxation and water self-diffusion. Applied Magnetic Resonance **28:** 29-40

Ehrler WL, Idso SB, Jackson RD, Reginato RJ (1978) DIURNAL CHANGES IN PLANT WATER POTENTIAL AND CANOPY TEMPERATURE OF WHEAT AS AFFECTED BY DROUGHT. Agronomy Journal **70:** 999-1004

Ellis CM, Nagpal P, Young JC, Hagen G, Guilfoyle TJ, Reed JW (2005) AUXIN RESPONSE FACTOR1 and AUXIN RESPONSE FACTOR2 regulate senescence and floral organ abscission in Arabidopsis thaliana. Development **132:** 4563-4574

Ellis JR, Leech RM (1985) CELL-SIZE AND CHLOROPLAST SIZE IN RELATION TO CHLOROPLAST REPLICATION IN LIGHT-GROWN WHEAT LEAVES. Planta **165:** 120-125

Ennajeh M, Vadel AM, Cochard H, Khemira H (2010) Comparative impacts of water stress on the leaf anatomy of a drought-resistant and a drought-sensitive olive cultivar. Journal of Horticultural Science & Biotechnology **85:** 289-294

Etienne P, Desclos M, Le Goua L, Gombert J, Bonnefoy J, Maurel K, Le Dily F, Ourry A, Avice J-C (2007) N-protein mobilisation associated with the leaf senescence process in oilseed rape is

concomitant with the disappearance of trypsin inhibitor activity. Functional Plant Biology **34:** 895-906

Evans JR, vonCaemmerer S (1996) Carbon dioxide diffusion inside leaves. Plant Physiology **110:** 339-346

Franzaring J, Weller S, Schmid I, Fangmeier A (2011) Growth, senescence and water use efficiency of spring oilseed rape (Brassica napus L. cv. Mozart) grown in a factorial combination of nitrogen supply and elevated CO2. Environmental and Experimental Botany **72:** 284-296

Gambhir PN, Pramila RK, Nagarajan S, Joshi DK, Tiwari PN (1997) Relationship between NMR relaxation characteristics and water activity in cereal leaves. Cellular and Molecular Biology **43:** 1191-1196

Gaude N, Brehelin C, Tischendorf G, Kessler F, Doermann P (2007) Nitrogen deficiency in Arabidopsis affects galactolipid composition and gene expression and results in accumulation of fatty acid phytyl esters. Plant Journal **49:** 729-739

Ghosh S, Mahoney SR, Penterman JN, Peirson D, Dumbroff EB (2001) Ultrastructural and biochemical changes in chloroplasts during Brassica napus senescence. Plant Physiology and Biochemistry **39:** 777-784

Gibon Y, Sulpice R, Larher F (2000) Proline accumulation in canola leaf discs subjected to osmotic stress is related to the loss of chlorophylls and to the decrease of mitochondrial activity. Physiologia Plantarum **110:** 469-476

Gilroy EM, Hein I, van der Hoorn R, Boevink PC, Venter E, McLellan H, Kaffarnik F, Hrubikova K, Shaw J, Holeva M, Lopez EC, Borras-Hidalgo O, Pritchard L, Loake GJ, Lacomme C, Birch PRJ (2007) Involvement of cathepsin B in the plant disease resistance hypersensitive response. Plant Journal **52:** 1-13

Gombert J, Etienne P, Ourry A, Le Dily F (2006) The expression patterns of SAG12/Cab genes reveal the spatial and temporal progression of leaf senescence in Brassica napus L. with sensitivity to the environment. Journal of Experimental Botany **57:** 1949-1956

Gombert J, Le Dily F, Lothier J, Etienne P, Rossato L, Allirand J-M, Jullien A, Savin A, Ourry A (2010) Effect of nitrogen fertilization on nitrogen dynamics in oilseed rape using N-15-labeling field experiment. Journal of Plant Nutrition and Soil Science **173:** 875-884

Good AG, Beatty PH (2011) Biotechnological approaches to improving nitrogen use efficiency in plants: alanine aminotransferase as a case study. The Molecular and Physiological Basis of Nutrient Use Efficiency in Crops**:** 165-191

Gookin TE, Hunter DA, Reid MS (2003) Temporal analysis of alpha and beta-expansin expression during floral opening and senescence. Plant Science **164:** 769-781

Gotow K, Taylor S, Zeiger E (1988) Photosynthetic carbon fixation in guard-cell protoplasts of vicia-fabia L - evidence from radiolabel experiments. Plant Physiology **86:** 700-705

Grbic V, Bleecker AB (1995) Ethylene regulates the timing of leaf senescence in *Arabidopsis*. Plant Journal **8:** 595-602

Gregersen PL, Holm PB, Krupinska K (2008) Leaf senescence and nutrient remobilisation in barley and wheat. Plant Biology **10:** 37-49

Gubler F, Millar AA, Jacobsen JV (2005) Dormancy release, ABA and pre-harvest sprouting. Current Opinion in Plant Biology **8:** 183-187

Guerfel M, Baccouri O, Boujnah D, Chaibi W, Zarrouk M (2009) Impacts of water stress on gas exchange, water relations, chlorophyll content and leaf structure in the two main Tunisian olive (Olea europaea L.) cultivars. Scientia Horticulturae **119:** 257-263

Guiboileau A, Sormani R, Meyer C, Masclaux-Daubresse C (2010) Senescence and death of plant organs: Nutrient recycling and developmental regulation. Comptes Rendus Biologies **333:** 382-391

Guiboileau A, Yoshimoto K, Soulay F, Bataille M-P, Avice J-C, Masclaux-Daubresse C (2012) Autophagy machinery controls nitrogen remobilization at the whole-plant level under both limiting and ample nitrate conditions in Arabidopsis. The New phytologist **194:** 732-740

Günthardt-Goerg M, McQuattie C, Maurer S, Frey B (2000) Visible and microscopic injury in leaves of five deciduous tree species related to current critical ozone levels. Environmental Pollution **109:** 489-500

Guo YF, Gan SS (2005) Leaf senescence: Signals, execution, and regulation. *In* GP Schatten, ed, Current Topics in Developmental Biology, Vol 71, Vol 71, pp 83-+

Hatzig S, Zaharia LI, Abrams S, Hohmann M, Legoahec L, Bouchereau A, Nesi N, Snowdon RJ (2014) Early osmotic adjustment responses in drought-resistant and drought-sensitive oilseed rape. Journal of Integrative Plant Biology **56:** 797-809

He P, Osaki M, Takebe M, Shinano T, Wasaki J (2005) Endogenous hormones and expression of senescence-related genes in different senescent types of maize. Journal of Experimental Botany **56:** 1117-1128

He YH, Fukushige H, Hildebrand DF, Gan SS (2002) Evidence supporting a role of jasmonic acid in Arabidopsis leaf senescence. Plant Physiology **128:** 876-884

Hikosaka K (2005) Leaf canopy as a dynamic system: Ecophysiology and optimality in leaf turnover. Annals of Botany **95:** 521-533

Hills BP, Duce SL (1990) The influence of chemical and diffusive exchange on water proton transverse relaxation in plant-tissue. Magnetic Resonance Imaging **8:** 321-331

Hills BP, Nott KP (1999) NMR studies of water compartmentation in carrot parenchyma tissue during drying and freezing. Appl Magn Reson **17:** 521-535

Hills BP, Remigereau B (1997) NMR studies of changes in subcellular water compartmentation in parenchyma apple tissue during drying and freezing. International Journal of Food Science and Technology **32:** 51-61

Hills BP, Takacs SF, Belton PS (1990) A new interpretation of proton NMR relaxation-time measurements of water in food. Food Chemistry **37:** 95-111

Hirel B, Le Gouis J, Ney B, Gallais A (2007) The challenge of improving nitrogen use efficiency in crop plants: towards a more central role for genetic variability and quantitative genetics within integrated approaches. Journal of Experimental Botany **58:** 2369-2387

Hoertensteiner S (2006) Chlorophyll degradation during senescence. *In* Annual Review of Plant Biology, Vol 57, pp 55-77

Hoertensteiner S (2009) Stay-green regulates chlorophyll and chlorophyll-binding protein degradation during senescence. Trends in Plant Science **14:** 155-162

Honda SI, Hongladarom-Honda T, Kwanyuen P, Wildman SG (1971) Interpretations on chloroplast reproduction derived from correlations between cells and chloroplasts. Planta **97:** 1-15

Horie Y, Nagane T, Ito H, Kusaba M, Tanaka R, Tanaka A (2007) Characterization of an Arabidopsis stay-green mutant lacking the NYC1 gene encoding chlorophyll b reductase. Plant and Cell Physiology **48:** S131-S131

Horigome D, Satoh H, Itoh N, Mitsunaga K, Oonishi I, Nakagawa A, Uchida A (2007) Structural mechanism and photoprotective function of water-soluble chlorophyll-binding protein. Journal of Biological Chemistry **282:** 6525-6531

Horst W, Behrens T, Heuberger H, Kamh M, Reidenbach G, Wiesler F (2003) Genotypic differences in nitrogen use-efficiency in crop plants. Innovative Soil–Plant Systems for Sustainable Agricultural Production**:** 75-92

Inada N, Sakai A, Kuroiwa H, Kuroiwa T (1998) Three-dimensional analysis of the senescence program in rice (Oryza sativa L.) coleoptiles - Investigations by fluorescence microscopy and electron microscopy. Planta **206:** 585-597

Ingram J, Bartels D (1996) The molecular basis of dehydration tolerance in plants. Annual Review of Plant Physiology and Plant Molecular Biology **47:** 377-403

Izumi M, Wada S, Makino A, Ishida H (2010) The Autophagic Degradation of Chloroplasts via Rubisco-Containing Bodies Is Specifically Linked to Leaf Carbon Status But Not Nitrogen Status in Arabidopsis. Plant Physiology **154:** 1196-1209

Jaspers P, Kangasjarvi J (2010) Reactive oxygen species in abiotic stress signaling. Physiologia Plantarum **138:** 405-413

Jenks MA, Joly RJ, Peters PJ, Rich PJ, Axtell JD, Ashworth EN (1994) CHEMICALLY-INDUCED CUTICLE MUTATION AFFECTING EPIDERMAL CONDUCTANCE TO WATER-VAPOR AND DISEASE SUSCEPTIBILITY IN SORGHUM-BICOLOR (L) MOENCH. Plant Physiology **105:** 1239-1245

Jing HC, Sturre MJG, Hille J, Dijkwel PP (2002) Arabidopsis onset of leaf death mutants identify a regulatory pathway controlling leaf senescence. Plant Journal **32:** 51-63

Jongdee B, Fukai S, Cooper M (2002) Leaf water potential and osmotic adjustment as physiological traits to improve drought tolerance in rice. Field Crops Research **76:** 153-163

Jordan WR, Brown KW, Thomas JC (1975) Leaf age as a determinant in stomatal control of water-loss from cotton during water stress. Plant Physiology **56:** 595-599

Kaku S (1993) Monitoring stress sensitivity by water proton NMR relaxation-times in leaves of *Azaleas* that originated in different ecological habitats. Plant and Cell Physiology **34:** 535-541

Kaku S, Iwayainoue M (1990) Factors affecting the prolongation of NMR relaxation-times of water protons in leaves of woody-plants affected by formation of insect galls. Plant and Cell Physiology **31:** 627-637

Kaku S, Iwayainoue M, Toki K (1992) Anthocyanin influence on water proton NMR relaxation-times and water contents leaves of Evergreen woody-plants during the winter. Plant and Cell Physiology **33:** 131-137

Karim S, Lundh D, Holmstrom KO, Mandal A, Pirhonen M (2005) Structural and functional characterization of AtPTR3, a stress-induced peptide transporter of Arabidopsis. Journal of Molecular Modeling **11:** 226-236

Kato Y, Murakami S, Yamamoto Y, Chatani H, Kondo Y, Nakano T, Yokota A, Sato F (2004) The DNA-binding protease, CND41, and the degradation of ribulose-1,5-bisphosphate carboxylase/oxygenase in senescent leaves of tobacco. Planta **220:** 97-104

Kato Y, Saito N, Kakuda K, Sato F (2005) Physiological characterization of Arabidopsis CND41 homologues in senescence. Plant and Cell Physiology **46:** S226-S226

Kato Y, Yamamoto Y, Murakami S, Sato F (2005) Post-translational regulation of CND41 protease activity in senescent tobacco leaves. Planta **222:** 643-651

Kaup MT, Froese CD, Thompson JE (2002) A role for diacylglycerol acyltransferase during leaf senescence. Plant Physiology **129:** 1616-1626

Keech O (2011) The conserved mobility of mitochondria during leaf senescence reflects differential regulation of the cytoskeletal components in Arabidopsis thaliana. Plant signaling & behavior **6:** 147-150

Keech O, Pesquet E, Ahad A, Askne A, Nordvall D, Vodnala SM, Tuominen H, Hurry V, Dizengremel P, Gardestroem P (2007) The different fates of mitochondria and chloroplasts during dark-induced senescence in Arabidopsis leaves. Plant Cell and Environment **30:** 1523-1534

Kessel B, Becker H (1999) Genetic Variation of Nitrogen-Efficiency in Field Experiments with Oilseed Rape (Brassica Napus L.). *In* G Gissel-Nielsen, A Jensen, eds, Plant Nutrition — Molecular Biology and Genetics. Springer Netherlands, pp 391-395

Kichey T, Hirel B, Heumez E, Dubois F, Le Gouis J (2007) In winter wheat (Triticum aestivum L.), post-anthesis nitrogen uptake and remobilisation to the grain correlates with agronomic traits and nitrogen physiological markers. Field Crops Research **102:** 22-32

Kim HU, Wu SSH, Ratnayake C, Huang AHC (2001) Brassica rapa has three genes that encode proteins associated with different neutral lipids in plastids of specific tissues. Plant Physiology **126:** 330-341

Kim T-H, Boehmer M, Hu H, Nishimura N, Schroeder JI (2010) Guard Cell Signal Transduction Network: Advances in Understanding Abscisic Acid, CO2, and Ca2+ Signaling. Annual Review of Plant Biology, Vol 61 **61:** 561-591

KingstonSmith AH, Thomas H, Foyer CH (1997) Chlorophyll a fluorescence, enzyme and antioxidant analyses provide evidence for the operation of alternative electron sinks during leaf senescence in a stay-green mutant of Festuca pratensis. Plant Cell and Environment **20:** 1323-1337

Kosma DK, Bourdenx B, Bernard A, Parsons EP, Lue S, Joubes J, Jenks MA (2009) The Impact of Water Deficiency on Leaf Cuticle Lipids of Arabidopsis. Plant Physiology **151:** 1918-1929

Krishnan P, Chopra UK, Verma APS, Joshi DK, Chand I (2014) Nuclear magnetic resonance relaxation characterisation of water status of developing grains of maize (Zea mays L.) grown at different nitrogen levels. Journal of Bioscience and Bioengineering **117:** 512-518

Krishnan P, Joshi DK, Maheswari M, Nagarajan S, Moharir AV (2004) Characterisation of soybean and wheat seeds by nuclear magnetic resonance spectroscopy. Biologia Plantarum **48:** 117-120

Krishnan P, Joshi DK, Nagarajan S, Moharir AV (2004) Characterisation of germinating and non-germinating wheat seeds by nuclear magnetic resonance (NMR) spectroscopy. European Biophysics Journal with Biophysics Letters **33:** 76-82

Krishnan P, Singh R, Verma APS, Joshi DK, Singh S (2014) Changes in seed water status as characterized by NMR in developing soybean seed grown under moisture stress conditions. Biochemical and Biophysical Research Communications **444:** 485-490

Krupinska K, Humbeck K (2008) Senescence processes and their regulation. Plant Biology **10:** 1-3

Kusano T, Berberich T, Tateda C, Takahashi Y (2008) Polyamines: essential factors for growth and survival. Planta **228:** 367-381

Lalonde S, Wipf D, Frommer WB (2004) Transport mechanisms for organic forms of carbon and nitrogen between source and sink. Annual Review of Plant Biology **55:** 341-372

Lara MEB, Garcia MCG, Fatima T, Ehness R, Lee TK, Proels R, Tanner W, Roitsch T (2004) Extracellular invertase is an essential component of cytokinin-mediated delay of senescence. Plant Cell **16:** 1276-1287

Larher F, Leport L, Petrivalsky M, Chappart M (1993) EFFECTORS FOR THE OSMOINDUCED PROLINE RESPONSE IN HIGHER-PLANTS. Plant Physiology and Biochemistry **31:** 911-922

Larher FR, Lugan R, Gagneul D, Guyot S, Monnier C, Lespinasse Y, Bouchereau A (2009) A reassessment of the prevalent organic solutes constitutively accumulated and potentially involved in osmotic adjustment in pear leaves. Environmental and Experimental Botany **66:** 230-241

Le Grand F, Cambert M, Mariette F (2007) NMR signal analysis to characterize solid, aqueous, and lipid phases in baked cakes. Journal of Agricultural and Food Chemistry **55:** 10947-10952

Lecoeur J, Wery J, Turc O, Tardieu F (1995) EXPANSION OF PEA LEAVES SUBJECTED TO SHORT WATER-DEFICIT - CELL NUMBER AND CELL-SIZE ARE SENSITIVE TO STRESS AT DIFFERENT PERIODS OF LEAF DEVELOPMENT. Journal of Experimental Botany **46:** 1093-1101

Lee RH, Wang CH, Huang LT, Chen SCG (2001) Leaf senescence in rice plants: cloning and characterization of senescence up-regulated genes. Journal of Experimental Botany **52:** 1117-1121

Leport L, Turner NC, French RJ, Barr MD, Duda R, Daves SL, Tennant D, Siddique KHM (1999) Physiological responses of chickpea genotypes to terminal drought in a Mediterranean-type environment. European Journal of Agronomy **11:** 279-291

Levey S, Wingler A (2005) Natural variation in the regulation of leaf senescence and relation to other traits in Arabidopsis. Plant Cell and Environment **28:** 223-231

Lim PO, Kim HJ, Nam HG (2007) Leaf senescence. *In* Annual Review of Plant Biology, Vol 58, pp 115-136

Lim PO, Woo HR, Nam HG (2003) Molecular genetics of leaf senescence in Arabidopsis. Trends in Plant Science **8:** 272-278

Lin JN, Kao CH (1998) Effect of oxidative stress caused by hydrogen peroxide on senescence of rice leaves. Botanical Bulletin of Academia Sinica **39:** 161-165

Liu L, Zhou Y, Zhou G, Ye R, Zhao L, Li X, Lin Y (2008) Identification of early senescence-associated genes in rice flag leaves. Plant Molecular Biology **67:** 37-55

Lohaus G, Fischer K (2002) Intracellular and intercellular transport of nitrogen and carbon,

Lu S, Zhao H, Des Marais DL, Parsons EP, Wen X, Xu X, Bangarusamy DK, Wang G, Rowland O, Juenger T, Bressan RA, Jenks MA (2012) Arabidopsis ECERIFERUM9 Involvement in Cuticle Formation and Maintenance of Plant Water Status. Plant Physiology **159:** 930-944

Mae T, Ohira K (1981) The remobilization of Nitrogen related to leaf growth and senescence in rice *Oryza sativa* (L). Plant and Cell Physiology **22:** 1067-1074

Maheswari M, Joshi DK, Saha R, Nagarajan S, Gambhir PN (1999) Transverse relaxation time of leaf water protons and membrane injury in wheat (Triticum aestivum L.) in response to high temperature. Annals of Botany **84:** 741-745

Makino A, Osmond B (1991) Effects of Nitrogen nutrition on Nitrogen partitioning between chloroplasts and mitochondria in pea and wheat. Plant Physiology **96:** 355-362

Malagoli P, Laine P, Le Deunff E, Rossato L, Ney B, Ourry A (2004) Modeling nitrogen uptake in oilseed rape cv capitol during a growth cycle using influx kinetics of root nitrate transport systems and field experimental data. Plant Physiology **134:** 388-400

Malagoli P, Laine P, Rossato L, Ourry A (2005) Dynamics of nitrogen uptake and mobilization in field-grown winter oilseed rape (Brassica napus) from stem extension to harvest - I. Global N flows between vegetative and reproductive tissues in relation to leaf fall and their residual N. Annals of Botany **95:** 853-861

Malagoli P, Laine P, Rossato L, Ourry A (2005) Dynamics of nitrogen uptake and mobilization in field-grown winter oilseed rape (Brassica napus) from stem extension to harvest. II. An N-15-labelling-based simulation model of N partitioning between vegetative and reproductive tissues. Annals of Botany **95:** 1187-1198

Manupeerapan T, Davidson J, Pearson C, Christian K (1992) Differences in flowering responses of wheat to temperature and photoperiod. Crop and Pasture Science **43:** 575-584

Marcum KB (1998) Cell membrane thermostability and whole-plant heat tolerance of Kentucky bluegrass. Crop Science **38:** 1214-1218

Mariette F, Brannelec C, Vitrac O, Bohuon P (1999) Effet du procédé de friture sur la répartition et l'état de l'eau mesurée par RMN et IRM. *In* Les produits alimentaires et l'eau, Agoral 99. Edition Tec & Doc, Nantes, pp 411-416

Mariette F, Guillement JP, Tellier C, Marchal P (1996) Continuous Relaxation Time Distribution Decomposition by MEM. *In* DN Rutledge, ed, Signal Treatment and Signal Analysis in NMR. Elsevier, Paris, pp 218-234

Mariette F, Rodriguez S, Lucas T, Marchal P (1999) Influence de la déshydratation sur la répartition cellulaire de l'eau étudiée par relaxation RMN. *In* Les produits alimentaires et l'eau, Agoral 99. Edition Tec & Doc, Nantes, pp 417-422

Martinez DE, Bartoli CG, Grbic V, Guiamet JJ (2007) Vacuolar cysteine proteases of wheat (Triticum aestivum L.) are common to leaf senescence induced by different factors. Journal of Experimental Botany **58:** 1099-1107

Martinez DE, Costa ML, Gomez FM, Otegui MS, Guiamet JJ (2008) 'Senescence-associated vacuoles' are involved in the degradation of chloroplast proteins in tobacco leaves. Plant Journal **56:** 196-206

Martínez DE, Costa ML, Guiamet JJ (2008) Senescence-associated degradation of chloroplast proteins inside and outside the organelle. Plant Biology **10:** 15-22

Martinez DE, Guiamet JJ (2004) Distortion of the SPAD 502 chlorophyll meter readings by changes in irradiance and leaf water status. Agronomie **24:** 41-46

Martínez DE, Guiamet JJ (2014) Senescence-Related Changes in the Leaf Apoplast. Journal of Plant Growth Regulation **33:** 44-55

Martinez JP, Silva H, Ledent JF, Pinto M (2007) Effect of drought stress on the osmotic adjustment, cell wall elasticity and cell volume of six cultivars of common beans (Phaseolus vulgaris L.). European Journal of Agronomy **26:** 30-38

Masclaux-Daubresse C, Daniel-Vedele F, Dechorgnat J, Chardon F, Gaufichon L, Suzuki A (2010) Nitrogen uptake, assimilation and remobilization in plants: challenges for sustainable and productive agriculture. Annals of Botany **105:** 1141-1157

Masclaux-Daubresse C, Reisdorf-Cren M, Orsel M (2008) Leaf nitrogen remobilisation for plant development and grain filling. Plant Biology **10:** 23-36

Masclaux C, Valadier M-H, Brugière N, Morot-Gaudry J-F, Hirel B (2000) Characterization of the sink/source transition in tobacco *Nicotiana tabacum* (L.) shoots in relation to nitrogen management and leaf senescence. Planta **211:** 510-518

Matin MA, Brown JH, Ferguson H (1989) LEAF WATER POTENTIAL, RELATIVE WATER-CONTENT, AND DIFFUSIVE RESISTANCE AS SCREENING TECHNIQUES FOR DROUGHT RESISTANCE IN BARLEY. Agronomy Journal **81:** 100-105

McCain DC (1995) Nuclear-Magnetic-Resonance Study of Spin Relaxation and Magnetic-Field Gradients in Maple Leaves. Biophysical Journal **69:** 1111-1116

McCain DC, Markley JL (1989) More manganese accumulates in maple sun leaves than in shade leaves. Plant Physiology **90:** 1417-1421

McCain DC, Marsh KB, Peterson LA (1990) EXCESS MANGANESE ACCUMULATES IN THE VACUOLES OF POTATO LEAVES. Potato Research **33:** 389-397

McIntyre GI (1987) The role of water in the regulation of plant development. Canadian Journal of Botany-Revue Canadienne De Botanique **65:** 1287-1298

Miller G, Suzuki N, Ciftci-Yilmaz S, Mittler R (2010) Reactive oxygen species homeostasis and signalling during drought and salinity stresses. Plant Cell and Environment **33:** 453-467

Miralles DJ, Ferro BC, Slafer GA (2001) Developmental responses to sowing date in wheat, barley and rapeseed. Field Crops Research **71:** 211-223

Miro B (2010) Identification of traits for nitrogen use efficiency in oilseed rape (Brassica napus L.).

Mohapatra PK, Patro L, Raval MK, Ramaswamy NK, Biswal UC, Biswal B (2010) Senescence-induced loss in photosynthesis enhances cell wall beta-glucosidase activity. Physiologia plantarum **138:** 346-355

Morris K, Mackerness SAH, Page T, John CF, Murphy AM, Carr JP, Buchanan-Wollaston V (2000) Salicylic acid has a role in regulating gene expression during leaf senescence. Plant Journal **23:** 677-685

Munne-Bosch S, Alegre L (2004) Die and let live: leaf senescence contributes to plant survival under drought stress. Functional Plant Biology **31:** 203-216

Murozuka E, Laursen KH, Lindedam J, Shield IF, Bruun S, Magid J, Moller IS, Schjoerring JK (2014) Nitrogen fertilization affects silicon concentration, cell wall composition and biofuel potential of wheat straw. Biomass & Bioenergy **64:** 291-298

Musse M, Cambert M, Mariette F (2010) NMR Study of Water Distribution inside Tomato Cells: Effects of Water Stress. Applied Magnetic Resonance **38:** 455-469

Musse M, De Franceschi L, Cambert M, Sorin C, Le Caherec F, Burel A, Bouchereau A, Mariette F, Leport L (2013) Structural Changes in Senescing Oilseed Rape Leaves at Tissue and Subcellular Levels Monitored by Nuclear Magnetic Resonance Relaxometry through Water Status. Plant Physiology **163:** 392-406

Nagarajan S, Joshi DK, Ahand A, Verma APS, Pathak PC (2005) Proton NMR transverse relaxation time and membrane stability in wheat leaves exposed to high temperature shock. Indian Journal of Biochemistry & Biophysics **42:** 122-126

Naidu BP, Paleg LG, Jones GP (2000) Accumulation of proline analogues and adaptation of Melaleuca species to diverse environments in Australia. Australian Journal of Botany **48:** 611-620

Nanda R, Bhargava SC, Rawson HM (1995) Effect of sowing date on rates of leaf appearance, final leaf numbers, and aeras in *Brassica campestris*, *Brassica juncea*, *Brassica napus* and *Brassica carinata*. Field Crops Research **42:** 125-134

Nardini A, Raimondo F, Lo Gullo MA, Salleo S (2010) Leafminers help us understand leaf hydraulic design. Plant Cell and Environment **33:** 1091-1100

Netto ADA, Rodrigues JD, De Pinho SZ (2000) Growth analysis in the potato crop under different irrigation levels. Pesquisa Agropecuaria Brasileira **35:** 901-907

Nilson SE, Assmann SM (2007) The control of transpiration. Insights from Arabidopsis. Plant Physiology **143:** 19-27

Nixon PJ, Michoux F, Yu J, Boehm M, Komenda J (2010) Recent advances in understanding the assembly and repair of photosystem II. Annals of Botany **106:** 1-16

Noiraud N, Avice J, Noquet C, Malagoli P, Lainé P, Beauclair P, Henry M, Le Dantec C, Rossato L, Ourry A (2003) Contribution of the amino acid and sucrose transporters to assimilate partitioning in response to sink manipulations in oilseed rape. *In* 11th International Rapeseed Congress,

Noodén LD, ed (2004) Cell death process : Introduction. Elsevier Science

Nooden LD, Guiamet JJ, John I (1997) Senescence mechanisms. Physiologia Plantarum **101:** 746-753

Noquet C, Avice JC, Rossato L, Beauclair P, Henry MP, Ourry A (2004) Effects of altered source-sink relationships on N allocation and vegetative storage protein accumulation in Brassica napus L. Plant Science **166:** 1007-1018

Norouzi M, Toorchi M, Salekdeh GH, Mohammadi S, Neyshabouri M, Aharizad S (2008) Effect of water deficit on growth, grain yield and osmotic adjustment in rapeseed. Journal of Food Agriculture and Environment **6:** 312

Oh IS, Park AR, Bae MS, Kwon SJ, Kim YS, Lee JE, Kang NY, Lee SM, Cheong H, Park OK (2005) Secretome analysis reveals an Arabidopsis lipase involved in defense against Alternaria brassicicola. Plant Cell **17:** 2832-2847

Oh MH, Kim YJ, Lee CW (2000) Leaf senescence in a stay-green mutant of Arabidopsis thaliana: Disassembly process of photosystem I and II during dark-incubation. Journal of Biochemistry and Molecular Biology **33:** 256-262

Oh SA, Park JH, Lee GI, Paek KH, Park SK, Nam HG (1997) Identification of three genetic loci controlling leaf senescence in Arabidopsis thaliana. Plant Journal **12:** 527-535

Okumoto S, Schmidt R, Tegeder M, Fischer WN, Rentsch D, Frommer WB, Koch W (2002) High affinity amino acid transporters specifically expressed in xylem parenchyma and developing seeds of Arabidopsis. Journal of Biological Chemistry **277:** 45338-45346

Oshita S, Maeda A, Kawagoe Y, Tsuchiya H, Kuroki S, Seo Y, Makino Y (2006) Change in diffusional water permeability of spinach leaf cell membrane determined by nuclear magnetic resonance relaxation time. Biosystems Engineering **95:** 397-403

Otegui MS, Noh YS, Martinez DE, Vila Petroff MG, Andrew Staehelin L, Amasino RM, Guiamet JJ (2005) Senescence-associated vacuoles with intense proteolytic activity develop in leaves of Arabidopsis and soybean. Plant Journal **41:** 831-844

Parthier B (1988) Gerontoplasts - the yellow end in the ontogenesis of chloroplasts. International Journal on Endocytobiosis and Cell Research **5:** 163-190

Peuke AD, Windt C, Van As H (2006) Effects of cold-girdling on flows in the transport phloem in Ricinus communis: is mass flow inhibited? Plant Cell and Environment **29:** 15-25

Qiao Y, Galvosas P, Callaghan PT (2005) Diffusion correlation NMR spectroscopic study of anisotropic diffusion of water in plant tissues. Biophysical Journal **89:** 2899-2905

Quick WP, Chaves MM, Wendler R, David M, Rodrigues ML, Passaharinho JA, Pereira JS, Adcock MD, Leegood RC, Stitt M (1992) THE EFFECT OF WATER-STRESS ON PHOTOSYNTHETIC CARBON METABOLISM IN 4 SPECIES GROWN UNDER FIELD CONDITIONS. Plant Cell and Environment **15:** 25-35

Quirino BF, Noh YS, Himelblau E, Amasino RM (2000) Molecular aspects of leaf senescence. Trends in Plant Science **5:** 278-282

Radochova B, Vicankova A, Kutik J, Ticha I (2000) Leaf structure of tobacco in vitro grown plantlets as affected by saccharose and irradiance. Biologia Plantarum **43:** 633-636

Raison JK, Berry JA, Armond PA, Pike CS (1980) Membrane properties in relation to the adaptation of plants to temperature stress. Adaptation of plants to water and high temperature stress.**:** 261-273

Rampino P, Spano G, Pataleo S, Mita G, Napier JA, Di Fonzo N, Shewry PR, Perrotta C (2006) Molecular analysis of a durum wheat 'stay green' mutant: Expression pattern of photosynthesis-related genes. Journal of Cereal Science **43:** 160-168

Ratcliffe RG (1994) In-vivo nmr-studies of higher-plants and algae. Advances in Botanical Research, Vol 20 **20:** 43-123

Rathke GW, Behrens T, Diepenbrock W (2006) Integrated nitrogen management strategies to improve seed yield, oil content and nitrogen efficiency of winter oilseed rape (Brassica napus L.): A review. Agriculture Ecosystems & Environment **117:** 80-108

Redgwell RJ, MacRae E, Hallett I, Fischer M, Perry J, Harker R (1997) In vivo and in vitro swelling of cell walls during fruit ripening. Planta **203:** 162-173

Reid MS, Chen J-C (2008) 11 Flower senescence. Annual Plant Reviews, Senescence Processes in Plants **26:** 256

Riederer M, Schreiber L (2001) Protecting against water loss: analysis of the barrier properties of plant cuticles. Journal of Experimental Botany **52:** 2023-2032

Rivero RM, Kojima M, Gepstein A, Sakakibara H, Mittler R, Gepstein S, Blumwald E (2007) Delayed leaf senescence induces extreme drought tolerance in a flowering plant. Proceedings of the National Academy of Sciences of the United States of America **104:** 19631-19636

Roberts IN, Caputo C, Kade M, Criado MV, Barneix AJ (2011) Subtilisin-like serine proteases involved in N remobilization during grain filling in wheat. Acta Physiologiae Plantarum **33:** 1997-2001

Rossato L, Laine P, Ourry A (2001) Nitrogen storage and remobilization in Brassica napus L. during the growth cycle: nitrogen fluxes within the plant and changes in soluble protein patterns. Journal of Experimental Botany **52:** 1655-1663

Ruuska SA, Lewis DC, Kennedy G, Furbank RT, Jenkins CLD, Tabe LM (2008) Large scale transcriptome analysis of the effects of nitrogen nutrition on accumulation of stem carbohydrate reserves in reproductive stage wheat. Plant Molecular Biology **66:** 15-32

Sakamoto W (2006) Protein degradation machineries in plastids. *In* Annual Review of Plant Biology, Vol 57, pp 599-621

Sakr MM, Almaghrabi OA (2011) Effect of sowing dates and vernalization on Beta vulgaris L. cv. Univers C-leaf structure. Saudi Journal of Biological Sciences **18:** 267-272

Sardans J, Penuelas J, Lope-Piedrafita S (2010) Changes in water content and distribution in Quercus ilex leaves during progressive drought assessed by in vivo1H magnetic resonance imaging. BMC Plant Biology **10**

Sarwat M, Naqvi AR, Ahmad P, Ashraf M, Akram NA (2013) Phytohormones and microRNAs as sensors and regulators of leaf senescence: Assigning macro roles to small molecules. Biotechnology Advances **31:** 1153-1171

Satoh H, Uchida A, Nakayama K, Okada M (2001) Water-soluble chlorophyll protein in Brassicaceae plants is a stress-induced chlorophyll-binding protein. Plant and Cell Physiology **42:** 906-911

Sattelmacher B (2001) Tansley review no. 22 - The apoplast and its significance for plant mineral nutrition. New Phytologist **149:** 167-192

Scheible WR, Morcuende R, Czechowski T, Fritz C, Osuna D, Palacios-Rojas N, Schindelasch D, Thimm O, Udvardi MK, Stitt M (2004) Genome-wide reprogramming of primary and secondary metabolism, protein synthesis, cellular growth processes, and the regulatory infrastructure of Arabidopsis in response to nitrogen. Plant Physiology **136:** 2483-2499

Schjoerring JK, Bock JGH, Gammelvind L, Jensen CR, Mogensen VO (1995) Nitrogen incorporation and remobilization in different shoot components of field-grown winter oilseed rape (Brassica napus L) as affected by rate of nitrogen application and irrigation. Plant and Soil **177:** 255-264

Schreiber U, Berry JA (1977) HEAT-INDUCED CHANGES OF CHLOROPHYLL FLUORESCENCE IN INTACT LEAVES CORRELATED WITH DAMAGE OF PHOTOSYNTHETIC APPARATUS. Planta **136:** 233-238

Schroeder JI, Kwak JM, Allen GJ (2001) Guard cell abscisic acid signalling and engineering drought hardiness in plants. Nature **410:** 327-330

Schulte auf'm Erley G, Wijaya KA, Ulas A, Becker H, Wiesler F, Horst WJ (2007) Leaf senescence and N uptake parameters as selection traits for nitrogen efficiency of oilseed rape cultivars. Physiologia Plantarum **130:** 519-531

Schulze ED, Kelliher FM, Korner C, Lloyd J, Leuning R (1994) RELATIONSHIPS AMONG MAXIMUM STOMATAL CONDUCTANCE, ECOSYSTEM SURFACE CONDUCTANCE, CARBON ASSIMILATION RATE, AND PLANT NITROGEN NUTRITION - A GLOBAL ECOLOGY SCALING EXERCISE. Annual Review of Ecology and Systematics **25:** 629-&

Schussler MD, Alexandersson E, Bienert GP, Kichey T, Laursen KH, Johanson U, Kjellbom P, Schjoerring JK, Jahn TP (2008) The effects of the loss of TIP1;1 and TIP1;2 aquaporins in Arabidopsis thaliana. Plant Journal **56:** 756-767

Serafini-Fracassini D, Di Sandro A, Del Duca S (2010) Spermine delays leaf senescence in Lactuca sativa and prevents the decay of chloroplast photosystems. Plant Physiology and Biochemistry **48:** 602-611

Serraj R, Sinclair TR (2002) Osmolyte accumulation: can it really help increase crop yield under drought conditions? Plant Cell and Environment **25:** 333-341

Sibgatullin TA, Anisimov AV, de Jager PA, Vergeldt FJ, Gerkema E, Van As H (2007) Analysis of diffusion and relaxation behavior of water in apple parenchymal cells. Biofizika **52:** 268-276

Silva H, Martinez JP, Baginsky C, Pinto M (1999) Effect of water stress on the leaf anatomy of six cultivars of the common bean Phaseolus vulgaris. Revista Chilena De Historia Natural **72:** 219-235

Singh U (2005) Integrated nitrogen fertilization for intensive and sustainable agriculture. Journal of Crop Improvement **15:** 259-288

Smith AM, Zeeman SC (2006) Quantification of starch in plant tissues. Nature Protocols **1:** 1342-1345

Snaar JEM, Van As H (1992) A method for the simultaneous measurement of NMR spin-lattice and spin-spin relaxation times in compartmentalized systems. J Magn Reson **99:** 139-148

Snaar JEM, Van As H (1992) Probing water compartments and membrane permeability in plant cells by 1H NMR relaxation measurements. Biophysical Journal **63:** 1654-1658

Sood S, Nagar PK (2008) Post-harvest alterations in polyamines and ethylene in two diverse rose species. Acta Physiologiae Plantarum **30:** 243-248

Sorin C, Musse M, Bouchereau A, Mariette F, Leport L (2014) Nitrogen deficiency impacts cell and tissue leaf structure with consequences on senescence and nutrient remobilization efficiency in Brassica napus. Planta **accepted for publication**

Stolz J, Ludwig A, Stadler R, Biesgen C, Hagemann K, Sauer N (1999) Structural analysis of a plant sucrose carrier using monoclonal antibodies and bacteriophage lambda surface display. Febs Letters **453:** 375-379

Szegletes Z, Erdei L, Tari I, Cseuz L (2000) Accumulation of osmoprotectants in wheat cultivars of different drought tolerance. Cereal Research Communications **28:** 403-410

Takahashi T, Kakehi J-I (2010) Polyamines: ubiquitous polycations with unique roles in growth and stress responses. Annals of Botany **105:** 1-6

Taylor CB, Bariola PA, Green PJ (1993) RNS2 - A SENESCENCE-ASSOCIATED RNASE OF ARABIDOPSIS THAT DIVERGED FROM THE S-RNASES BEFORE SPECIATION. Plant Physiology **102:** 11-11

Tesfamariam EH, Annandale JG, Steyn JM (2010) Water Stress Effects on Winter Canola Growth and Yield. Agronomy Journal **102:** 658-666

Thompson J, Taylor C, Wang TW (2000) Altered membrane lipase expression delays leaf senescence. Biochemical Society Transactions **28:** 775-777

Thompson JE, Froese CD, Hong Y, Hudak KA, Smith MD (1997) Membrane deterioration during senescence. Canadian Journal of Botany-Revue Canadienne De Botanique **75:** 867-879

Thompson JE, Froese CD, Madey E, Smith MD, Hong Y (1998) Lipid metabolism during plant senescence. Progress in Lipid Research **37:** 119-141

Thompson JE, Froese CD, Madey E, Smith MD, Hong YW (1998) Lipid metabolism during plant senescence. Progress in Lipid Research **37:** 119-141

Tilsner J, Kassner N, Struck C, Lohaus G (2005) Amino acid contents and transport in oilseed rape (Brassica napus L.) under different nitrogen conditions. Planta **221:** 328-338

Tommey AM, Evans EJ (1991) TEMPERATURE AND DAYLENGTH CONTROL OF FLOWER INITIATION IN WINTER OILSEED RAPE (BRASSICA-NAPUS L). Annals of Applied Biology **118:** 201-208

Trotel P, Bouchereau A, Niogret MF, Larher F (1996) The fate of osmo-accumulated proline in leaf discs of Rape (Brassica napus L) incubated in a medium of low osmolarity. Plant Science **118:** 31-45

Tsuchisaka A, Theologis A (2004) Unique and overlapping expression patterns among the arabidopsis 1-amino-cyclopropane-1-carboxylate synthase gene family members. Plant Physiology **136:** 2982-3000

Turgeon R, Wolf S (2009) Phloem Transport: Cellular Pathways and Molecular Trafficking. *In* Annual Review of Plant Biology, Vol 60, pp 207-221

Van As H (2007) Intact plant MRI for the study of cell water relations, membrane permeability, cell-to-cell and long distance water transport. Journal of Experimental Botany **58:** 743-756

van der Graaff E, Schwacke R, Schneider A, Desimone M, Fluegge U-I, Kunze R (2006) Transcription analysis of arabidopsis membrane transporters and hormone pathways during developmental and induced leaf senescence. Plant Physiology **141:** 776-792

van der Hoorn RAL (2008) Plant proteases: From phenotypes to molecular mechanisms. *In* Annual Review of Plant Biology, Vol 59, pp 191-223

van der Weerd L, Claessens M, Ruttink T, Vergeldt FJ, Schaafsma TJ, Van As H (2001) Quantitative NMR microscopy of osmotic stress responses in maize and pearl millet. Journal of Experimental Botany **52:** 2333-2343

van Doorn WG (2005) Plant programmed cell death and the point of no return. Trends in Plant Science **10:** 478-483

Vigh L, Horvath I, Farkas T, Mustardy LA, Faludidaniel A (1981) STOMATAL BEHAVIOR AND CUTICULAR PROPERTIES OF MAIZE LEAVES OF DIFFERENT CHILLING-RESISTANCE DURING COLD TREATMENT. Physiologia Plantarum **51:** 287-290

Wada S, Ishida H (2009) Chloroplasts autophagy during senescence of individually darkened leaves. Plant signaling & behavior **4:** 565-567

Wagner R, Aigner H, Funk C (2012) FtsH proteases located in the plant chloroplast. Physiologia Plantarum **145:** 203-214

Wilson J, Mannetje Lt (1978) Senescence, digestibility and carbohydrate content of buffel grass and green panic leaves in swards. Crop and Pasture Science **29:** 503-516

Windt CW, Vergeldt FJ, De Jager PA, Van As H (2006) MRI of long-distance water transport: a comparison of the phloem and xylem flow characteristics and dynamics in poplar, castor bean, tomato and tobacco. Plant Cell and Environment **29:** 1715-1729

Wingler A, Mares M, Pourtau N (2004) Spatial patterns and metabolic regulation of photosynthetic parameters during leaf senescence. New Phytologist **161:** 781-789

Wingler A, von Schaewen A, Leegood RC, Lea PJ, Quick WP (1998) Regulation of leaf senescence by cytokinin, sugars, and light - Effects on NADH-dependent hydroxypyruvate reductase. Plant Physiology **116:** 329-335

Winter D, Vinegar B, Nahal H, Ammar R, Wilson GV, Provart NJ (2007) An "Electronic Fluorescent Pictograph" Browser for Exploring and Analyzing Large-Scale Biological Data Sets. Plos One **2**

Woo HR, Chung KM, Park JH, Oh SA, Ahn T, Hong SH, Jang SK, Nam HG (2001) ORE9, an F-box protein that regulates leaf senescence in Arabidopsis. Plant Cell **13:** 1779-1790

Wu X-Y, Kuai B-K, Jia J-Z, Jing H-C (2012) Regulation of Leaf Senescence and Crop Genetic Improvement. Journal of Integrative Plant Biology **54:** 936-952

Wuyts N, Massonnet C, Dauzat M, Granier C (2012) Structural assessment of the impact of environmental constraints on Arabidopsis thaliana leaf growth: a 3D approach. Plant Cell and Environment **35:** 1631-1646

Wuyts N, Palauqui J-C, Conejero G, Verdeil J-L, Granier C, Massonnet C (2010) High-contrast three-dimensional imaging of the Arabidopsis leaf enables the analysis of cell dimensions in the epidermis and mesophyll. Plant Methods **6**

Xiang Y, Huang Y, Xiong L (2007) Characterization of stress-responsive CIPK genes in rice for stress tolerance improvement. Plant Physiology **144:** 1416-1428

Xiao S, Dai LY, Liu FQ, Wang Z, Peng W, Xie DX (2004) COS1: An Arabidopsis Coronatine insensitive1 suppressor essential for regulation of jasmonate-mediated plant defense and senescence. Plant Cell **16:** 1132-1142

Xiao S, Gao W, Chen Q-F, Chan S-W, Zheng S-X, Ma J, Wang M, Welti R, Chye M-L (2010) Overexpression of Arabidopsis Acyl-CoA Binding Protein ACBP3 Promotes Starvation-Induced and Age-Dependent Leaf Senescence. Plant Cell **22:** 1463-1482

Yoshida S, Ito M, Nishida I, Watanabe A (2001) Isolation and RNA gel blot analysis of genes that could serve as potential molecular markers for leaf senescence in Arabidopsis thaliana. Plant and Cell Physiology **42:** 170-178

Yoshimoto K, Hanaoka H, Sato S, Kato T, Tabata S, Noda T, Ohsumi Y (2004) Processing of ATG8s, ubiquitin-like proteins, and their deconjugation by ATG4s are essential for plant autophagy. Plant Cell **16:** 2967-2983

Zeeman SC, Smith SM, Smith AM (2007) The diurnal metabolism of leaf starch. Biochem J **401:** 13-28

Zeevaart JAD, Creelman RA (1988) Metabolism and physiology of abscisic-acid. Annual Review of Plant Physiology and Plant Molecular Biology **39:** 439-473

Zelisko A, Jackowski G (2004) Senescence-dependent degradation of Lhcb3 is mediated by a thylakoid membrane-bound protease. Journal of Plant Physiology **161:** 1157-1170

Zellnig G, Perktold A, Zechmann B (2010) Fine structural quantification of drought-stressed Picea abies (L.) organelles based on 3D reconstructions. Protoplasma **243:** 129-136

Zentgraf U, Laun T, Miao Y (2010) The complex regulation of WRKY53 during leaf senescence of Arabidopsis thaliana. European Journal of Cell Biology **89:** 133-137

Zhang K, Xia X, Zhang Y, Gan S-S (2012) An ABA-regulated and Golgi-localized protein phosphatase controls water loss during leaf senescence in Arabidopsis. Plant Journal **69:** 667-678

Zhang K, Xia X, Zhang Y, Gan SS (2012) An ABA-regulated and Golgi-localized protein phosphatase controls water loss during leaf senescence in Arabidopsis. The Plant Journal **69:** 667-678

Zhang M-P, Zhang C-J, Yu G-H, Jiang Y-Z, Strasser RJ, Yuan Z-Y, Yang X-S, Chen G-X (2010) Changes in chloroplast ultrastructure, fatty acid components of thylakoid membrane and chlorophyll a fluorescence transient in flag leaves of a super-high-yield hybrid rice and its parents during the reproductive stage. Journal of plant physiology **167:** 277-285

Zhang SQ, Outlaw WH (2001) Gradual long-term water stress results in abscisic acid accumulation in the guard-cell symplast and guard-cell apoplast of intact Vicia faba L. plants. Journal of Plant Growth Regulation **20:** 300-307

Zhao FY, Wang K, Zhang SY, Ren J, Liu T, Wang X (2014) Crosstalk between ABA, auxin, MAPK signaling, and the cell cycle in cadmium-stressed rice seedlings. Acta Physiologiae Plantarum **36:** 1879-1892

Zimmermann P, Zentgraf U (2005) The correlation between oxidative stress and leaf senescence during plant development. Cellular & Molecular Biology Letters **10:** 515-534

ANNEXES

Annexe 1

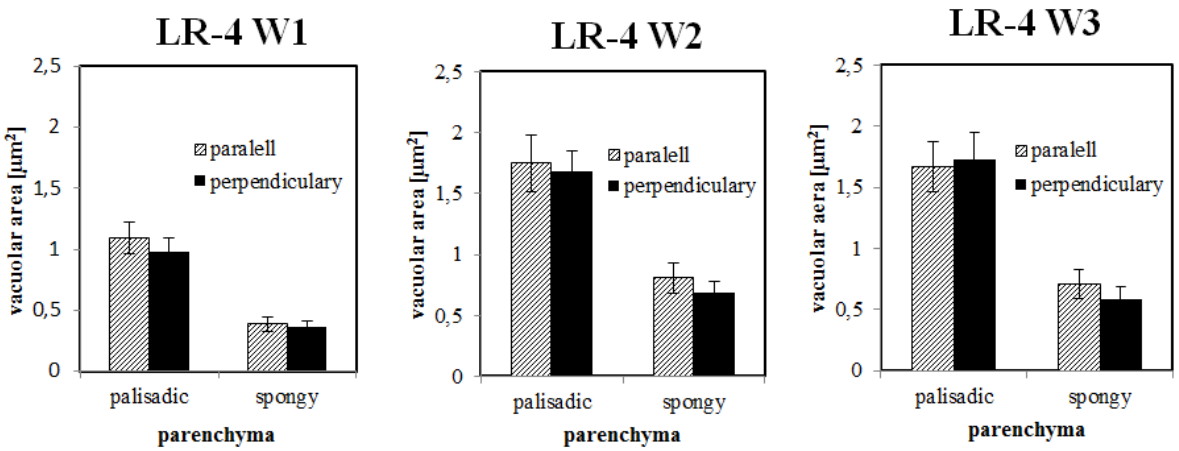

Annexe 1: Aera of the vacuole of each parenchyma, for the leaf rank four during the three first weeks of measurement. Values were calculated from micrographs cross section sampled in parallel (strip) or perpendicularly (black) to the central vein.

Annexe 2

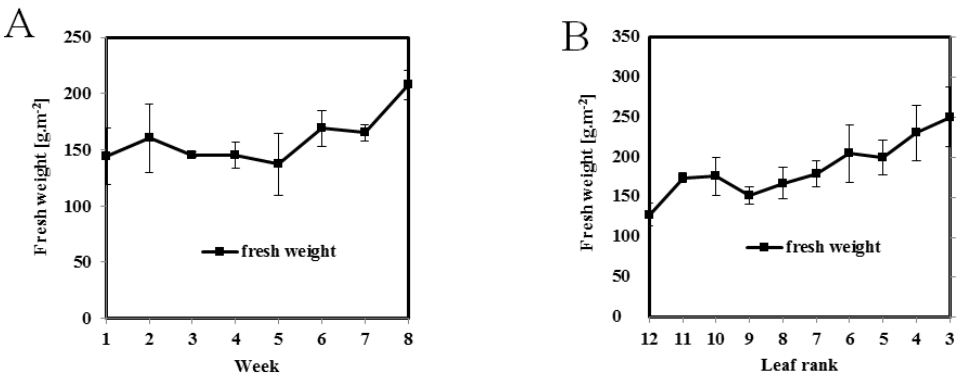

Supplementary data 1: Leaf fresh weight (in $g.m^{-2}$) of the eighth leaf over the measurement period (A) and fresh weight of all leaves from four plants at the third week of the measurement period.

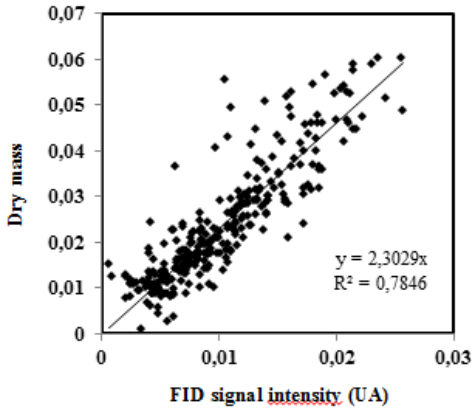

Supplementary data 2: correlation between FID signal intensity and dry mass of the sample

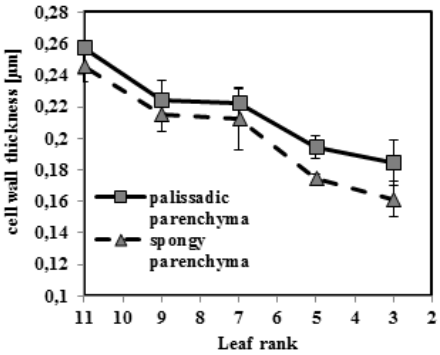

Supplementary data 3: Change in cell wall thickness for each parenchyma in relation to the leaf rank for the third week of the measurement period.

Annexe 3

VU : VU :

Le Directeur de Thèse **Le Responsable de l'École Doctorale**
(Nom et Prénom)

VU pour autorisation de soutenance

Rennes, le

Le Président de l'Université de Rennes 1

Guy CATHELINEAU

VU après soutenance pour autorisation de publication :

Le Président de Jury,
(Nom et Prénom)

Organisation subcellulaire et remobilisation métabolique durant la sénescence chez le colza : effets des stress abiotiques

Résumé

Brassica napus est une des cultures oléagineuse majeure dans le monde. En raison de sa faible efficacité d'utilisation de l'azote (NUE) comparée aux autres grandes cultures, la gestion de cette ressource présente un objectif écologique et économique majeur pour cette culture. La remobilization des nutriments des organes sources vers les organes puits est une composante de la NUE qui se déroule durant la sénescence et qui est associée aux processus de recyclages métaboliques et à des modifications de la structure foliaire. L'objectif de cette thèse était de comprendre et de quantifier ces modifications structurales afin d'évaluer à travers ces processus les capacités de remobilization du colza en fonction de son génotype et de son statut nutritionnel (eau et azote).

La structure foliaire a été étudiée grâce à la relaxométrie RMN qui donne accès au statut et à la distribution de l'eau au niveau cellulaire. Ces travaux de thèse ont mis en évidence que la distribution des temps de relaxation transversale (T_2) dépend non seulement de la structure cellulaire, mais aussi de l'organisation tissulaire. Cette étude a aussi mis en évidence le processus d'élargissement cellulaire et d'hydratation pendant la sénescence, spécifiquement dans le parenchyme palissadique. Il a été également démontré que le signal RMN reflète la déstructuration progressive se déroulant durant la sénescence au niveau subcellulaire et est un marqueur de sénescence précis permettant de suivre le développement de la feuille. De plus, le statut nutritionnel de la plante modifié par les carences azotées ou le stress hydrique, impacte grandement la sénescence séquentielle et les conséquences en termes d'efficacité de la remobilisation peuvent être suivies par RMN.

Ce travail a permis de renforcer les connaissances sur la structure et le fonctionnement de la feuille au niveau tissulaire et cellulaire. De plus, il a été démontré que le signal de relaxométrie RMN donne accès à des informations sur la structure foliaire inaccessible par des méthodes courantes. Une des principales applications de ce travail serait le phénotypage, particulièrement la sélection de génotypes caractérisés par une forte efficacité de remobilisation en particulier en cas de carence azoté ou de stress hydrique.

Mots clefs : colza, structure foliaire, remobilisation, stress hydrique, carence azote; RMN, temp de relaxation (T_2)

Subcellular modification and nutrient remobilization during *Brassica napus* leaf senescence: effects of abiotic stresses.

Abstract

Brassica napus is one of the major oil crops of the world. Due to its low NUE (Nitrogen Use Efficiency) compared to other species, Nitrogen management presents a major economic and environmental goal for improvement of that crop production. As a component of NUE, nutrient remobilization from source to sink tissues takes place mainly during the leaf senescence and is associated to metabolic recycling processes and modification of the cellular organization and structure. The aim of this work was therefore to understand and estimate the amplitude of these structural modifications with the objective to appreciate through these processes remobilization performance according to oilseed rape genotypes and nutritional status in terms of nitrogen and water supply.

The leaf structure was investigated through NMR relaxometry, providing access to cellular water status and distribution. The present work demonstrated that the transverse relaxation time (T_2) distribution depends on both leaf tissue structure and cellular compartmentalization. The study revealed a process of cell enlargement and hydration during leaf senescence, specifically in the palisade parenchyma and showed that the T_2 relaxation time was able to discriminate parenchyma tissues at an early phase of senescence induction. Moreover, the NMR relaxometry signal was shown to reflect specific chronological loss of sub-cellular structuring all along the senescence process progression and was demonstrated to be an accurate non-invasive monitoring method of leaf development. Finally, plant nutrition status experienced through nitrogen and water availability limitation has been demonstrated to strongly affect regular sequential leaf senescence. Consequences on remobilization efficiency by stress conditions have been also assessed through the NMR signal.

This work has improved the understanding of leaf structure and functioning at the cell and tissue levels after the onset and during the progression of senescence. Moreover, it was demonstrated that NMR relaxometry provides access to leaf structural information that are not accessible with currently used techniques for plant structural investigations. One of the main applications would be for plant phenotyping, especially for selecting genotypes with higher nutrient remobilization efficiency especially under environmental stresses like nitrogen and water limitations for sustainable oil and protein production.

Key words: oilseed rape, leaf structure, remobilization, water stress, nitrogen depletion; NMR, transverse relaxation (T_2)